Application of Technology to Water Measurement and Management

A USCID Workshop

Recognizing the Retirements of

John A. Replogle and Marinus G. Bos

February 25-26, 2004
Scottsdale, Arizona

SOME OBSERVATIONS ON IRRIGATION FLOW MEASUREMENTS AT THE END OF THE MILLENNIUM

J. A. Replogle

ABSTRACT. *This article provides a brief historical look at the origins of flow metering in the last millennium, touching on some of the developments we use today in open–channel and pipeline flows for irrigated agriculture. While the basic physical principals recognized as useable for measuring flows have remained basically unchanged, the range and accuracy of monitoring these physical effects have been vastly improved by collateral developments in electronics and computer technology. For example, the ultrasonic properties of a fluid medium have long been recognized, but only in the last decade have the practical and inexpensive means to exploit these properties become available. Some of the newer developments during the last quarter of the past century include long–throated flumes of many shapes for which the discharge ratings, or calibrations, are determined by computer techniques. A recent extension to the computer–calibrated flume's repertoire includes the adjustable–throat flumes that aid in placement in earthen channels because they virtually eliminate concern for vertical elevation of the throat, which can be adjusted to accommodate ditch flow conditions after installation. Other recent developments include: vortex–shedding meters; ultrasonic flow meters, of both the Doppler type and transonic types; and simplifications on construction and application of Pitot tubes for measuring flow in irrigation wells.*

Keywords. *Flow measurement, Water measurement, Irrigation, Irrigation management.*

The measurement of applied irrigation water is one of the major links in efforts to improve irrigation management to achieve effective water management. As the millennium ended, we may well consider the developments in flow measurement benefiting irrigated agriculture. Briefly discussed herein, are a few of the measurement methods that have evolved to this point in history that are of significant interest to those dealing with irrigation water management. While a few devices have come to fruition in only the last few decades, we must look back at least a century to find the origins for most of the currently used devices. An example is Clemens Herschel's version of the Venturi meter in 1886, and the pioneering canal work in France of Henri Bazin in 1865 (Chow, 1959). Yet another century is reached for the principles investigated by Venturi himself in about 1791 and to the instrumentation used by Bazin credited to Henri Pitot, who in 1730 used a bent glass tube to measure velocities in the River Seine. However, it takes more than two millenniums to encompass Archimedes' principle, which legend places at 287–212 BC, the science behind many of the hydraulic systems in use today.

While the basic physical principles used for measuring flows have remained essentially unchanged, the range and accuracy of monitoring the effects of these principles have been vastly improved by collateral developments in electronics and computer technology. For example, the behaviors of sound in a fluid medium have long been recognized, but only in the last decade have the practical means to exploit these sonic properties become available.

Irrigated agriculture uses both open channel measuring systems and pipe flow meters. Over the last several decades, industrial sources have provided most of the advances in metering technology for flow in pipes. Industrial involvement in canal flows has been much less. Thus, public agency emphasis has largely been directed to developing open–channel flow measuring systems.

This review considers some of the flow meters that are particularly important to irrigated agriculture and extends the historical perspective to recent developments and current outlooks.

FLOW METERING OVERVIEW

Traditionally, flow meters have been classified according to the physical principle or property exploited, such as those related to sound, magnetism, electricity, chemical reactions, mixing, and volume, mass and energy relations, (ASME, 1959). In order to exploit a physical property or principle, the metering system must interact with the fluid in some way. The mechanism involved in the immediate interaction is called the primary element. The mechanisms involved in detecting the effects of the interaction and converting it to an observable reading is the secondary element (ASME, 1959). Meters can broadly be grouped into flow–rate meters or quantity meters, according to the effect that is first observable. An appropriate secondary element can convert most primary elements to respond either way. Not all meters are currently practical for use in irrigated agriculture. Emphasize on the word "currently" is to be noted here because of the possibility that someone will overcome an

Article was submitted for review in April 2001; approved for publication by the Soil & Water Division of ASAE in October 2001.

Names of companies or suppliers are for the convenience of the reader and do not imply endorsement by the United States Government.

The author is **John A. Replogle, ASAE Member Engineer**, Research Hydraulic Engineer, U.S. Water Conservation Laboratory, ARS–USDA, 4331 E. Broadway Rd., Phoenix, AZ 85050; phone: 602–437–1702; fax: 602–437–5291; e–mail: Jreplogle@uswcl.ars.ag.gov.

existing restriction limiting an application, making that metering method practical for irrigation. Major restrictions to irrigation applications are often the lack of electric power at the metering site, capital cost, and poor maintenance support.

The applicability of many flow–metering methods is discussed in some detail in USBR (1997), which provides a quick overview of common meters with an indication of best applications. Meters based on viscous properties of fluids, vortex–shedding meters and some special acoustic meters are relatively new to the irrigation industry and are not listed in that work.

Canal Flow Measurements

A Brief History of Flow Measuring Flumes

Accurate water measurement with flumes has greatly aided the management of irrigation water and the development of irrigated lands in the American West. Older devices, such as weirs, required large head loss in the form of large overfall height, which was frequently not available in the flat regions around the world that are commonly associated with irrigation. Flumes provided acceptable accuracy with significantly less head loss requirement. Among the first of these that were widely used in the 20th Century was the Parshall flume.

The history of the Parshall flume begins with V. M. Cone, USDA, in Fort Collins who introduced the Venturi flume in about 1910 (Chow, 1959). While theoretically amenable, the small head–differential produced between the upstream depth and the higher speed flow in a slightly contracted section was hard to detect and thus limited its accuracy. In 1926, Ralph Leroy Parshall (1881–1959) published his work on a more practical improvement that had a contraction great enough to produce "critical flow" in a contracted throat. Chow (1959) discussed somewhat parallel developments of flumes in India, England, Italy, Switzerland, and Argentina from about 1925 though 1955. Their impact on irrigation did not reach the level enjoyed by the Parshall flume.

The advantages of Parshall's critical flow flume were soon apparent even though it required more head drop than the original Venturi flume of Cone. However, this head drop was still much less than for weirs, and accuracy was improved. It also did not need two readings like the Venturi–type usage of the Cone flume, one in the approach channel and one in the contracted section, because critical depth can be inferred from the upstream reading, to which it is uniquely related. Disadvantages, include the limitation on choice of sizes and the rectangular shape that required considerable canal work for installation into a trapezoidal canal. Calibrations, which were not practical to directly compute, were developed from careful laboratory studies for several flume sizes. These flumes were more or less the standard for irrigation flow measurements for much of the 20th Century.

Robinson and Chamberlain (1960) developed flumes that were formed by side contractions in small concrete–lined trapezoidal irrigation canals. These fumes required less canal work to make them fit into existing canals. The side contractions with a floor that matched the canal were thought at the time to be advantageous for moving bed–load sediments, an assumption that was only partly correct. These flumes also were laboratory calibrated. Their general shape concepts were later used during a period from 1969 to the present, when converging technologies between hydraulic engineering and computer science led to yet another development, the critical–flow flume. Interchangeably called the "Computable Flumes" or the "Replogle Flumes," these flume designs can be obtained through hydraulically based mathematical relations solved by computer (Replogle, 1975; Bos et al., 1991; Clemmens et al.. 2001). A broad range of shapes and sizes of flumes can be tailored to nearly any channel shape.

The computable–flume concept is now employed worldwide and the resulting flumes are becoming the preferred irrigation canal–measuring device. The primary hydraulic innovation leading to their success was to produce parallel flow in the throat rather than the curved flow as formed by the Parshall flumes. This parallel flow allowed them to be treated mathematically, because knowledge of the flow curvature, necessary for mathematical treatment, was simplified to no curvature. This parallel flow does not exist in Parshall flumes and mathematical treatment is unreliable. These flumes also have smaller head loss than the Parshall flumes.

Evolution of Flume Constructions

Various field installation techniques evolved in attempts to develop convenient constructions applicable to irrigated agriculture. The early flume versions were based on channel side contractions, much as Robinson and Chamberlain (1960) had done, and were difficult to build. A special inside mold as a concrete forming system was used. A ditch–company contractor devised that mold. Later, a broad–crested weir with an upstream ramp was designed, which could be built without the contractor's mold, using premixed concrete and two plywood forms made to fit the canal shape up to the height of the finished sill.

These flume shapes were easy to construct and have some hydraulic advantages, such as requiring only a small head loss to make them operate. Thus, they were suited to flat irrigation areas. This upstream ramp and construction method was initially intended only as an emergency, short–term installation because the prevailing thought at the time was that the contraction had to be made from the sides with no raised floor in order to let sediments pass. These conditions are not necessarily true in all cases. Sometimes sediments ruin the side contraction flume measurements anyway, and sometimes they pass over a raised sill. Sediments still are a problem and account for most of the needed maintenance. Many flow criteria govern sediment deposition and movement, besides the flume floor profile.

A variety of sizes were designed and built. A large flume near Phoenix, Arizona, was constructed on the Arizona canal heading of the Salt River Project (fig. 1). The flow rate was about 40 m^3/s (1400 cfs). At the other extreme, small sizes for experiments on irrigation furrows were fashioned that could measure less than 1 L/s (16 gpm).

Constructions in Small Concrete Canals

Eventually, the mold–formed method was replaced, first with the wooden forms, but later, with an even simpler process that used a small metal frame for the important throat section. The frame helped produce a known width and aided in producing a level top. This metal–frame method works

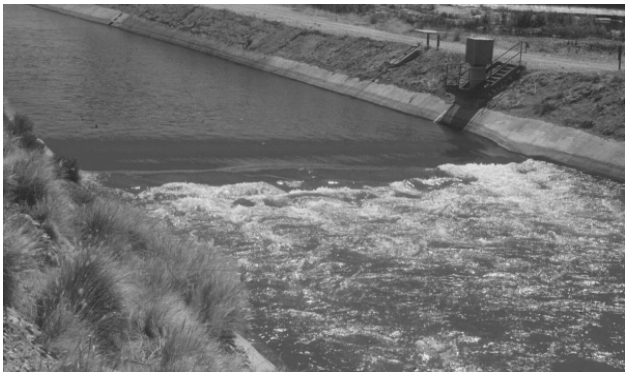

Figure 1. Flume in large canal. Note stilling well and the region of wavy water surface. Sill crest is located about midway between these two features. Canal flow depth is about 2.4 m (8 ft) and sill crest is about 1.4 m (4.5 ft) high.

Figure 2. Flume in small concrete–lined canal.

well in existing concrete lined canals (fig. 2). Field soil formed the support for the 5– to 10–cm (2– to 4–in.) concrete veneer used. It is quick and easy and works well in existing concrete lined canals. The process is illustrated in figure 3. This supporting under–structure of soil was allowed to wash away.

Sedimentation Problems

Sediment movement and deposition in channels is a complicated function of the sediment composition, sediment concentration, flow velocity, and channel shape. In general, erosive velocities for most sediments start at about 1 m/s (3 ft/s) depending on the sediment material (Chow, 1959). In small flumes with flows of less that about 500 L/s (20 cfs), the velocities may be too slow in the upstream section and the stilling well may not function because of sediment accumulations. In larger flumes with flows in excess of 1 m^3/s, the flume shape can usually be selected to cause increased velocities in the flume approach section so that the flume stilling well area remains free of sediments. One of these methods is to use a raised floor in the approach channel that will increase the flow velocities in the approach section of the flume. The concept is illustrated in figure 4.

The flume design criteria suggest that velocities in the approach section be such that the Froude Number, F_n, is less than 0.5. (The Froude Number is a dimensionless ratio of the dynamic (velocity related) forces, *V*, in a channel to the gravity forces, *g*, or $F_n = V/\sqrt{gD}$, where *D* = Channel cross–sectional area divided by the channel top width.) In small flumes, this limit on F_n may not produce the necessary flow velocity needed to transport sediment. Because, trapezoidal shapes have decreasing F_n (and velocities) with decreasing flow, sediment handling is usually best at design maximum flow. On the other hand, rectangular shapes with side contractions tend to maintain the same $F_{n.}$ throughout their flow range, particularly if no raised sill is used, and this can sometimes be used to improve sediment passage over a relatively wide flow range. (Bos et al., 1991).

Portable Flumes

The flume design concepts were applied in many formats around the world, including portable devices in semicircular channels in Morocco. A simple portable system was needed for flow surveys. The result was a portable system consisting of a broad–crested weir sill made from flat sheet metal, with a width equal to about 80% of the channel diameter (this matches a sill height of 0.2 times the diameter), and a ramp that was cut as part of an ellipse to fit the channel bottom (fig. 5). A point gage was used to sense the depth of water above the top of the weir crest using the translocated stilling well system described in Replogle (1997) (fig. 6).

Adjustable Flume

Small earthen canals are common in both the United States and abroad. On an irrigation evaluation project in Nepal, irrigation consultants attempted to measure water with Cutthroat flumes, but were not very successful because most of the earthen channels had less than 3 cm (1 in.) of freeboard. The flow backup required by these existing devices usually caused the canal to breach.

That experience in Nepal led to what has become an adjustable flume. It can be placed in these types of channels and gradually raised to cause only about 10 mm (0.5 in.) of backwater and survive the limited freeboard. This idea has been commercialized in the United States as the Adjust–A–Flume (Nu–Way Flume and Equipment Co., Delta, Colo.).

The Adjust–A–Flume is sold in many sizes, from about 12 to 1000 L/s (200 gpm to 35 cfs). It is easy to install and usually avoids the problem of being too deep or too shallow and needing to be reinstalled. It effectively deals with the problem encountered when trying to vertically relocate a flume after flow is started. Resealing a flume in this flowing situation is usually difficult. Thus, the advantages of simply lowering or raising the sill while the water is flowing are a distinct advantage. Figure 7 shows the flume being checked for level with a carpenter's level and sealing against bypass flow with field soil.

The adjustable flume has a sidewall gage that is marked to indicate discharge rate. No discharge tables need to be carried by the user. The largest version, shown as it was being installed (fig. 8) has a capacity of 1000 L/s (35 cfs). Vertical adjustments are by use of a lifting mechanism in the covered box shown mounted over the flume. Four threaded rods with nuts can be substituted, if adjustments are seldom necessary after initial installation.

Ultrasonic Metering of Open Channels

Ultrasonic stream gauging is based on detecting stream flow velocity by using the difference in time for sound

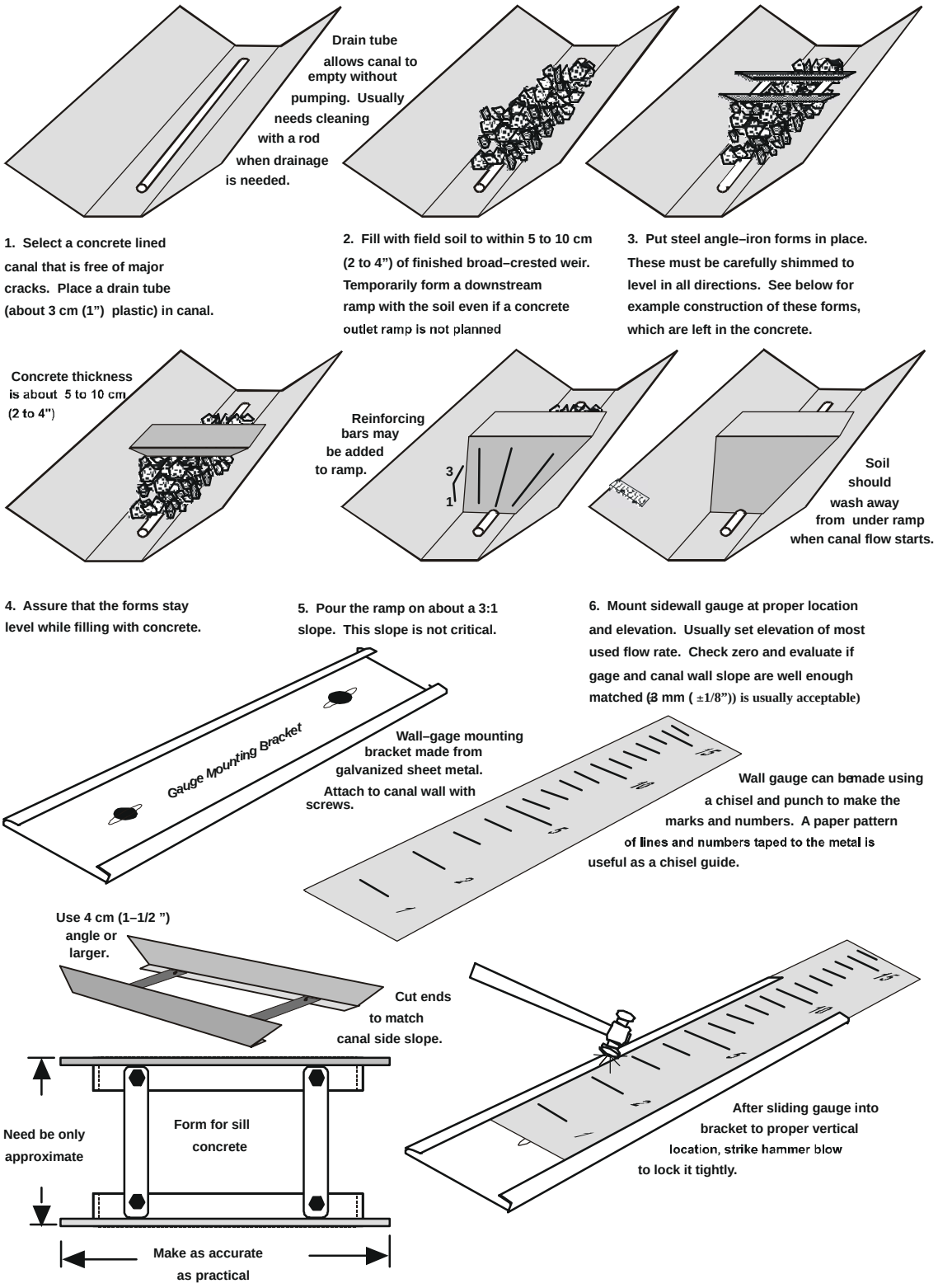

Figure 3. Construction process for small concrete–lined canals.

transmissions sent obliquely across the stream in opposite directions. Because of the flow movement, the sound propagates at a higher velocity in the direction of flow than against the direction of flow. This difference is translated into average velocity in the sound path that was sampled. This principle will be discussed further in the section dealing on pipe flows (Herschy, 1985). In channel flows, several paths are often used, particularly on rivers that may have irregular boundaries. Single path installations are approaching the economics that have interested large irrigation districts. The application has not been without difficulties. Movable bed channels require special monitoring of the sand dune movement through the metering section. Also, if a single path is to be monitored, the relationship of the chosen path to the flow profile needs to be known.

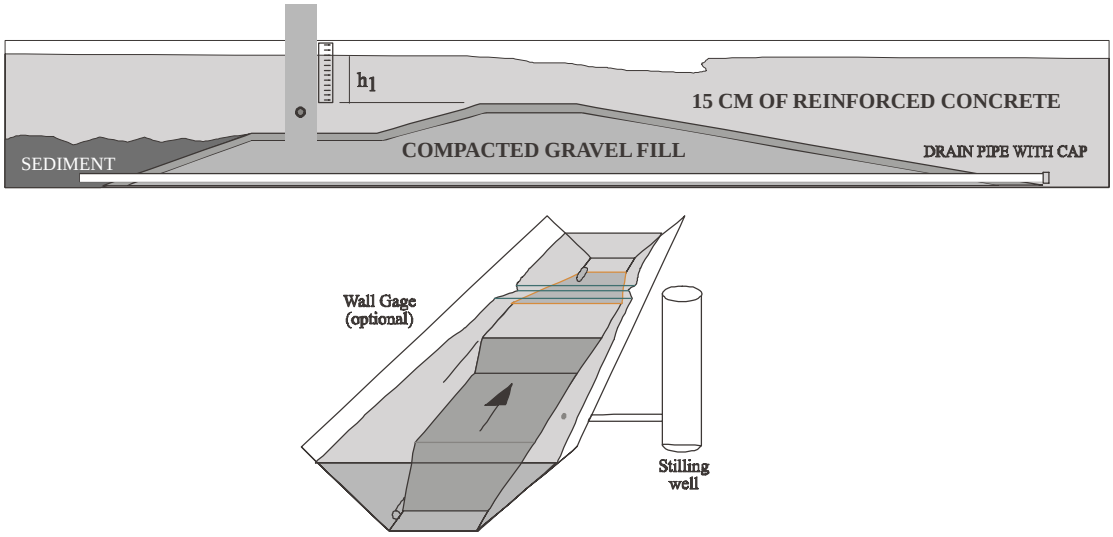

Figure 4. Designing for sediment transport through flumes.

To partly address some of these difficulties, it is recommended that a channel section be constructed to increase the local velocities to the point that bed load movement as dunes is discouraged through the section being sampled by the sonic paths. This channel section may take the form of a raised sill much like a long–throated flume, but not to the severity of causing critical flow, thus causing only negligible head loss. Depending on the sediment concentrations, this "constructed" velocity may be as low as 1 m/s (3 ft/s). If the flow depth fluctuates significantly, it appears that the 0.6 depth path across the channel, often recommended for propeller–type current metering would be desirable. The construction mentioned above could provide an opportunity to always sample this path level if the section is made rectangular with the transducers that are mounted on an adjustable mechanism.

(a) **(b)**

Figure 5. Portable flume system (Morocco). (a) System parts: static tube, level sensing cup and wooden mount, flume ramp, and flume sill. (b) System installed in semicircular channel.

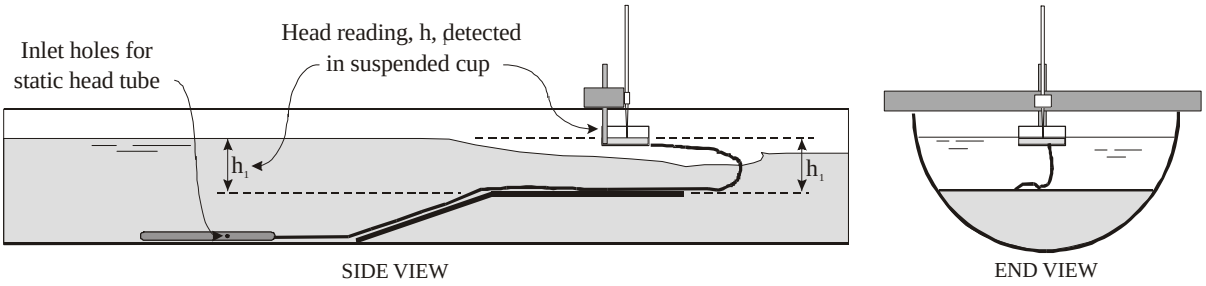

Figure 6. Point gage used with portable flume in semicircular channel (Morocco).

MEASUREMENTS IN IRRIGATION PIPELINES

While advances in canal flow measurements have significantly aided irrigation water management worldwide, there have nevertheless been developments in pipe flow measurements that also significantly impact irrigation flow measurements. Most of these advances have been through the introduction of modern electronics to detect and report the flow measurement information from otherwise well–established techniques, for example, the differential pressure across a Venturi meter or orifice meter, or the speed of sonic waves across a pipe. These electronic advances are resulting in lower–cost metering systems, often with improved accuracy. Many metering techniques depend heavily on these advances such as the vortex–shedding meter, the ultrasonic Doppler flow meter, and the ultrasonic transit–time flow meter. Many of the standard meters such as the propeller meters, Venturi meters, orifice meters, etc. are described in a number of references (Miller, 1996) and only newer methods and some special applications of older methods that are particularly interesting for irrigation management applications are described below.

VORTEX–SHEDDING FLOW METERS

Vortex–shedding flow meters have only recently been introduced to irrigation in a configuration that makes them competitive with orifice meters (Miller, 1996), although they have been around since at least the 1960s. They generally cause less head loss than orifice meters and can cover a wider discharge range for a particular installation, but require electric power. They are now offered routinely to the irrigation industry for pipe flow measurements. Open–channel applications in this format are not considered practical.

Figure 7. Adjustable flume being installed while channel continues to flow. Capacity: 56 L/s (2 cfs).

Vortex–shedding flow meters operate by using the viscous fluid principles that form alternating eddies downstream from a bluff body held in a liquid flow. The formation frequency of these eddies is related to the flow velocity. The detection and conversion of the signal were expensive a few decades ago. Again advances in electronics and frequency monitoring have joined to make these meters practical for irrigation wells and center pivot systems (fig. 9). For volumetric flow rate, the meters are accurate to within ±0.7% over a maximum to minimum flow range of 30:1. The meters are offered as insertion probes to be placed through the wall of an existing pipe, or mounted in a section of pipe called a "spool" as to be inserted as a part of the pipeline. The accuracy of the meter can be as good as ±0.5% for the spool versions over a 20:1 range of flows. The insertion probes are slightly less accurate because of their dependence on the manufactured pipe into which they are inserted. A wider flow range can be used, but with increased error.

ULTRASONIC FLOW METERS

A desirable meter could be described as one that can be installed on the outside of a pipe, but can give the performance of the best flow meters installed inside the pipe. Ultrasonic time–of–flight meters are slowly developing toward these apparently conflicting but demanding criteria.

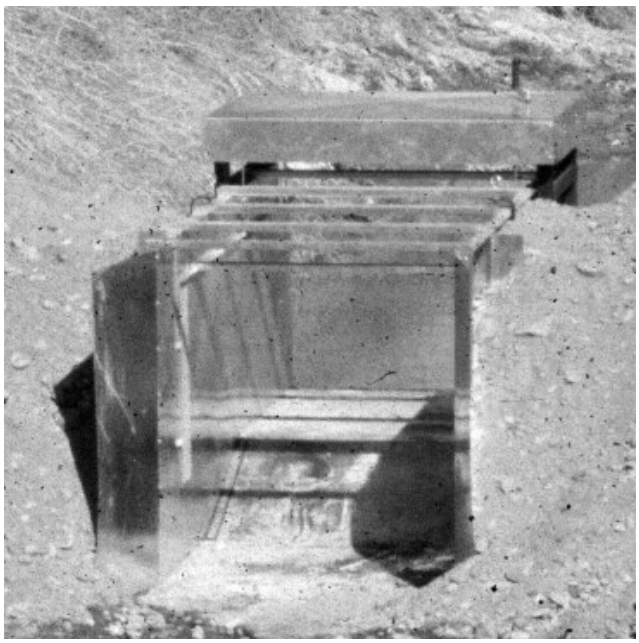

Figure 8. Large Adjust–A–Flume with hoisting mechanism. Capacity: 1000 L/s (35 cfs).

Figure 9. V–Bar™ Insertion Vortex Meter (after EMCO)[2].

Multiple beam systems have been installed on many pipelines. There are two basic types of ultrasonic flow meters that are used in liquid flows (Miller, 1996). One type is based on the time of flight of an ultrasonic wave, usually of a frequency of about 1 MHz, across the pipe at an angle (fig. 10). Depending on the flow direction, with or against the liquid flow, the travel times will differ. The readout is the average velocity in an axial plane from wall to wall through the pipe center. These meters operate best in liquids without suspended particles. A second style, the Doppler type, operates much like a radar return system and requires particles moving with the general flow to return sonic echoes that are interpreted for local velocities. The velocities are usually those near the wall, so the flow rate depends on successful inference of the total velocity profile from the velocities near the wall. The profile is assumed to be a form of flat–nosed "bullet shape" that is symmetrical in all radial planes and changes its shape as a function of velocity and pipe roughness.

The time–of–flight meters are not immune to profile shape either. For example, if the profile is a square fronted "piston" and the ultrasonic meter averages an axial slice across the pipe, then this piston shape directly represents the complete pipe flow. On the other extreme, if a pointed cone represents the flow profile, then the meter detects the average of a triangular shape (one–half of the peak velocity) as the equivalent piston, but to represent a cone, it should be one–third of the detected value. Fortunately, symmetrical flow profiles can usually be predicted with suitable accuracy. Of greater concern is non–symmetrical profiles caused by pipe bends, valves and other fittings. Thus, it is important to follow the manufacturer's recommendations on upstream straight–pipe length requirements.

The modern clamp–on transit–time meter in a good mounting location can indicate a flow rate accurate to within ±2% of flow reading, depending on design, compared to Doppler meters that usually indicate no better than ±5% of full scale reading. Field accuracies are variable, but can be expected to add at least 2 to 3% to these error values, which were determined under controlled conditions. A major advantage of ultrasonic methods is the negligible head loss and the ability to install either portable or dedicated systems without a pipeline shutdown. A disadvantage is the need to determine the effective pipe wall thickness and the velocity of sound in the pipe material being used. This velocity of sound in the pipe material can vary from about 2300 m/s (7500 ft/s) for some plastic pipes to 4900 m/s (16,000 ft/s) for steel pipe, and over 6000 m/s (20,000 ft/s) for some aluminum alloys.

Figure 10. Portable ultrasonic flow meter on outlet pipe of an irrigation well. Sensors are usually mounted on the side of pipe to avoid air bubbles that may be in the pipe.

New Primary Device for Channels and Pipelines

In about 1997 a relatively new acoustic Doppler–based flow meter, entered the marketplace called the ADFM Velocity Profiler™ (Acoustic Doppler Flow Meter, MGD Technologies, San Diego, Calif.). The ADFM is able to sample the velocity at many discrete points along several ultrasonic paths in the depth of flow in a channel or pipe cross section. These point velocities then are combined to determine a velocity profile and thus a flow rate for the channel or pipe (fig. 11).

These multiple paths allows the ADFM to be installed in large channels that can have complex hydraulic conditions and still obtain suitable flow rate data. The technology usually removes the need for an *in–situ* calibration, making system installation relatively simple and safe. Because it appears to be simple to install, it may be thought of as somewhat portable, or at least amenable to reinstallation at various locations within canal systems.

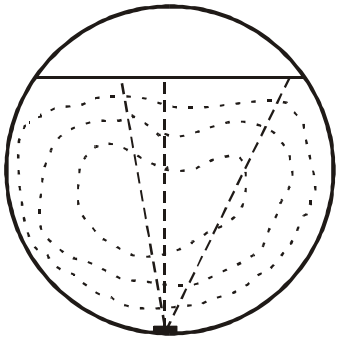

Figure 11. Doppler–based acoustic velocity profiler.

Improvements of Existing Methodology

Well–known flow measuring techniques are sometimes incorporated in new ways to make flow measurements more convenient and economical. For example, Pitot–tube systems have long been used in pipe flows. Most require that special holes be drilled in the outflow pipe of the well through which the Pitot tube can be inserted. Special double walled, double–tube constructions, sometimes called Prandtl–type Pitot tubes (Daugherty and Ingersoll, 1954), have been used at the outlet of pumping systems discharging directly into a canal (fig. 12). These Prandtl tubes are difficult to build with simple machine shop procedures and are relatively expensive.

The advantage of the Pitot tube method is that it can measure flows with a distorted velocity profile and may be a practical way to measure flows when upstream elbows, the pump head, or other pipe fittings produce a distorted flow profile that is detrimental to the proper installation and operation of commonly available pipe meters, such as the propeller meter illustrated. A damaged or corroded pipe end makes it difficult to attach such devices as portable end–cap orifices. Clinging flow, with a partial vacuum at the outlet, may become unstable as soon as a velocity probe is inserted and can oscillate between a partly filled pipe flow and a full pipe flow. Sometimes, it is desirable to know how distorted the flow profile really is before attempting to condition the flow with longer discharge piping or straightening vanes. If this information can be provided, the meter technician may be able to determine whether a correction in the meter coefficient will suffice, or if flow–conditioning equipment is needed. Lastly, a partly filled pipe will cause errors in meters that require full pipe flow, including the Pitot–tube method.

Replogle (1999) developed an economical method to construct and use a special Pitot–tube system to field evaluate the operation of an installed meter in these compromising situations. A specially constructed Pitot–tube system is clamped near the outlet of the pump discharge pipe. It is used to detect the velocity at several points across the pipe diameter at the usual 10 points recommended for classical Pitot traverses. Recommendations for special point locations across the pipe to reduce the number of points from the 10 to only two are given. Distorted profiles can be detected and measured.

To overcome the difficult construction methods needed for the Prandl tube, the system was separated into two tubes, a simple Pitot impact tube, with a companion, but separate static–pressure tube. Both can be constructed using common shop techniques and standard small pipe fittings (fig. 13).

Description of Equipment Features

Referring to figure 13, the Pitot–static system consists of a Pitot tube, or impact pressure sensing probe, and a static pressure sensing probe, with pressure sensing holes. Rubber end dams and C–clamps are used to produce sufficient back pressure to maintain full pipe flow at the measurement plane, thus preventing partial pipe flow while still maintain minimum back pressure on the well pump. The probes are made from standard 1/8–in. galvanized steel pipe, with an outside diameter of about 10 mm. Construction details are to be found in Replogle (1999), and laboratory studies are reported in Replogle and Wahlin (2000). Errors for a 10–point traverse are within ±3% and for a special two–point process it is within about ±5%.

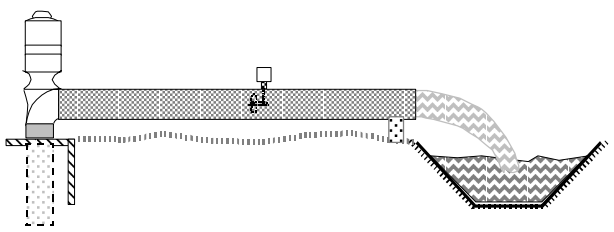

Figure 12. Typical installation for irrigation wells that discharge into canals.

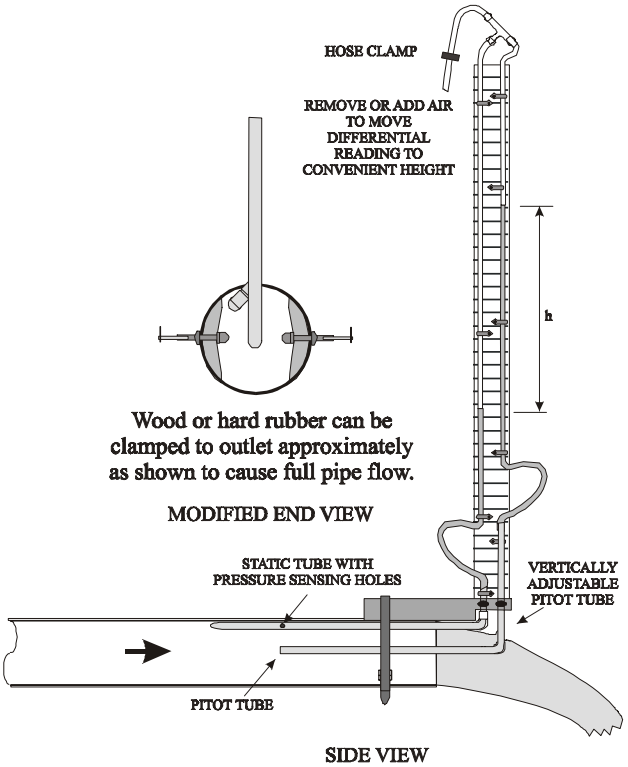

Figure 13. Pitot system used to evaluate irrigation well discharge (Replogle, 1999).

Summary and Outlook

Making predictions is usually a hazardous pursuit. Risk is reduced if predictions follow a line of need, for indeed "necessity is the mother of invention." With that in mind, there is great demand for noninvasive measuring technology at affordable costs. Ultrasonic meters are beginning to meet these criteria, at least in pipe flows. They are most easily applied where electric power is available. Electric power is usually available in irrigation well applications because of the dominance of electric motor driven pumps near the measuring site. In open channel applications, the expense of providing power to the site is a major consideration. For accurate information, the site usually should be modified with a lined section designed to carry sediments through in a way that does not change the flow section area. This cost may rival the cost of constructing a long–throated flume, and while not in the category of noninvasive measurements, long–throated flumes still will offer a solution to channel flow measurements for at least a decade or more. Research efforts should continue to investigate not only novel new

methods, but also novel applications of existing methodology.

REFERENCES

ASME. 1959. *Fluid Meters, Their Theory and Application*, Fifth Ed. Report of ASME Research Committee on fluid meters. New York: The American Society of Mechanical Engineers.

Bos, M. G., J. A. Replogle, and A. J. Clemmens. 1991. *Flow Measuring Flumes for Open Channel Systems*. St. Joseph, Mich.: ASAE. (Republication of book by same title, originally by John Wiley and Sons, New York. 1984.)

Chow, V. T. 1959. *Open Channel Hydraulics.* New York: McGraw–Hill Book Co., Inc.

Clemmens, A. J., T. L. Wahl, M. G. Bos, and J. A. Replogle. 2001. *Water Measurement with Flumes and Weirs.* Publication 58. Wageningen, The Netherlands: International Institute for Land Reclamation and Improvement / ILRI.

Daugherty, R. L., and A. C. Ingersoll. 1954. *Fluid Mechanics.* New York: McGraw–Hill Book Co., Inc.

Herschy, R. W. 1985. *Streamflow Measurement.* New York: Elsevier Applied Science Publishers.

Miller, R. W. 1996. *Flow Measurement Engineering Handbook.* Third Ed. New York: McGraw–Hill Book.

Replogle, J. A. 1975. Critical–flow flumes with complex cross–section. In *Irrigation and Drainage in an Age of Competition for Resources, Conference Proceedings of the Irrigation and Drainage Division*, 366–388. Reston, Va.: Amer. Soc. Civil Engineers.

_____. 1997. Practical technologies for irrigation flow control and measurement. *J. of Irrig. and Drainage Systems* 11(3): 241–259.

_____. 1999. Measuring irrigation well discharges. *J. of Irrig. and Drainage Eng.* 125(4): 223–229.

Replogle, J. A., and B. T. Wahlin. 1998. Portable and permanent flumes with adjustable throats. *Irrigation and Drainage Systems* 12: 23–34.

Replogle, J., and B. Wahlin. 2000. Pitot–static tube system to measure discharges from wells. *J. of Hydraulic Eng.* 126(5): 335–346.

Robinson, A. R., and A. R. Chamberlain. 1960. Trapezoidal flumes for open–channel flow measurements. *Transactions of the ASAE* 3(3): 120–24, 128.

USBR. 1997. *Water Measurement Manual*, Third Ed. U.S. Department of Interior, Bureau of Reclamation. Superintendent of Documents, Washington, D.C.: U.S. Government Printing Office.

Water Measurement for Improved Irrigation Performance: Where, How, When?

Prof Dr Marinus G. BOS
International Institute for Geo-Information Science and Earth Observation
www.itc.nl

Water management in future irrigation schemes could be improved if systems were designed in such a way that their proper management would be as easy as the mismanagement of existing systems.

Where?

How?

When?

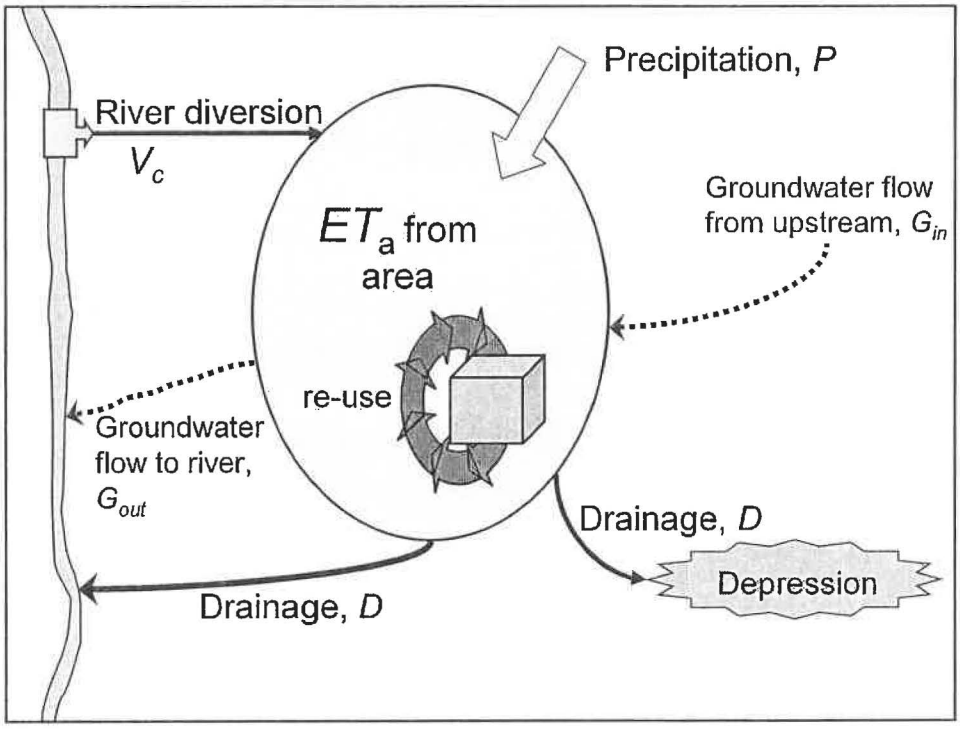

Depleted Fraction

The *Depleted Fraction* quantifies the fraction of water evapo-transpired by the crops in the water balance of the irrigated area. Assuming negligible non-irrigation water deliveries, the ratio is defined as:

$$\frac{\text{Actual Evapotranspiration}}{\text{Total Water Supply}} = \frac{ET_{actual}}{P_{gross} + V_c}$$

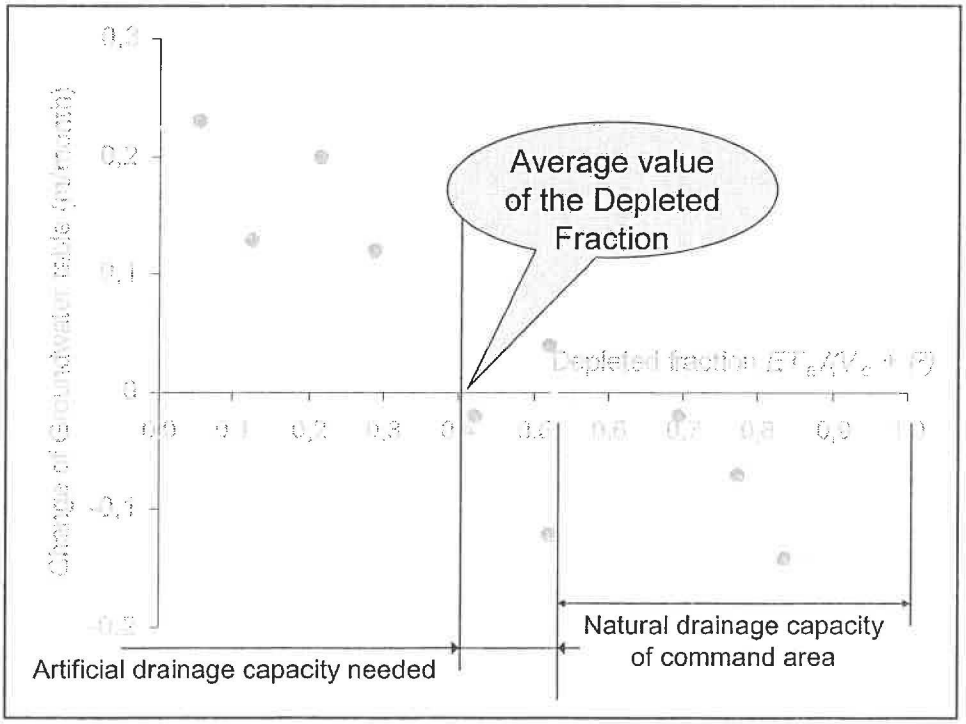

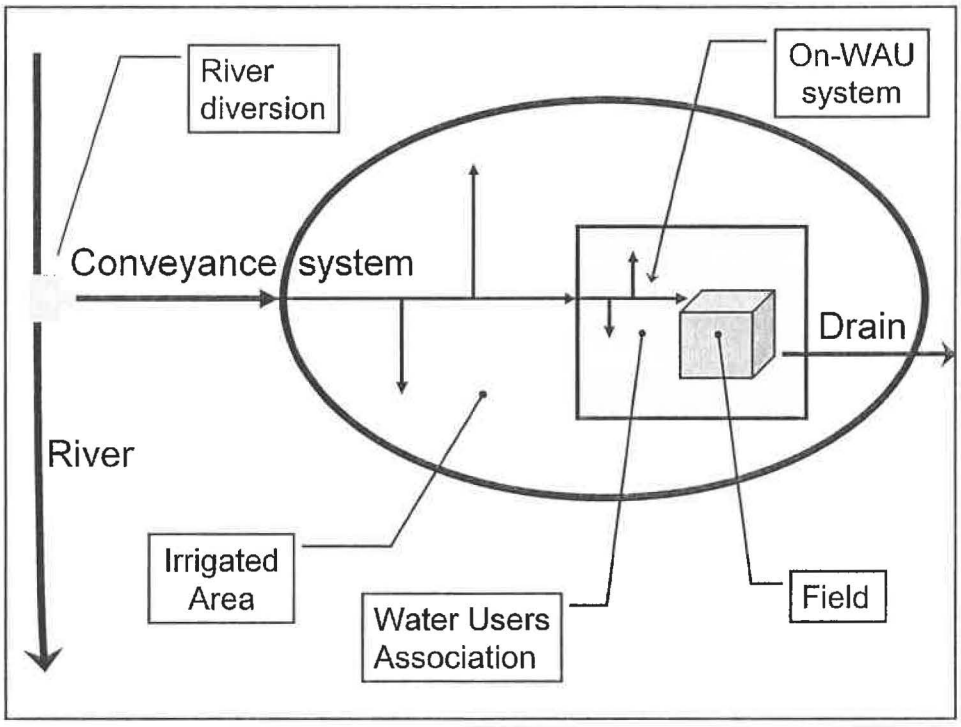
River diversion
On-WAU system
Conveyance system
Drain
River
Irrigated Area
Water Users Association
Field

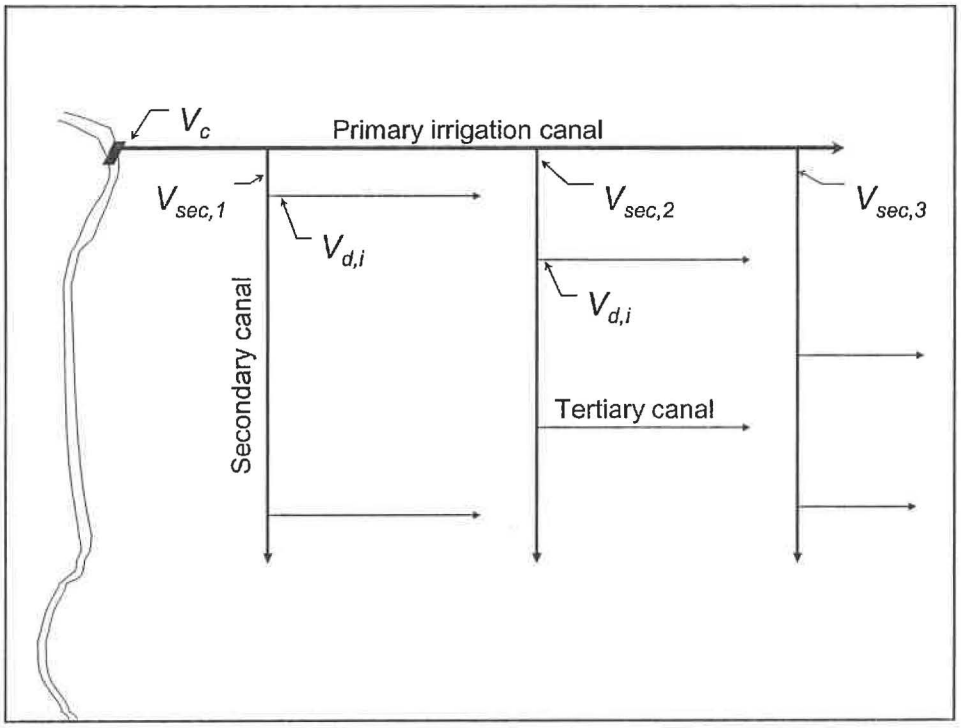
V_c
Primary irrigation canal
$V_{sec,1}$
$V_{sec,2}$
$V_{sec,3}$
$V_{d,i}$
$V_{d,i}$
Secondary canal
Tertiary canal

Where?

How?

When?

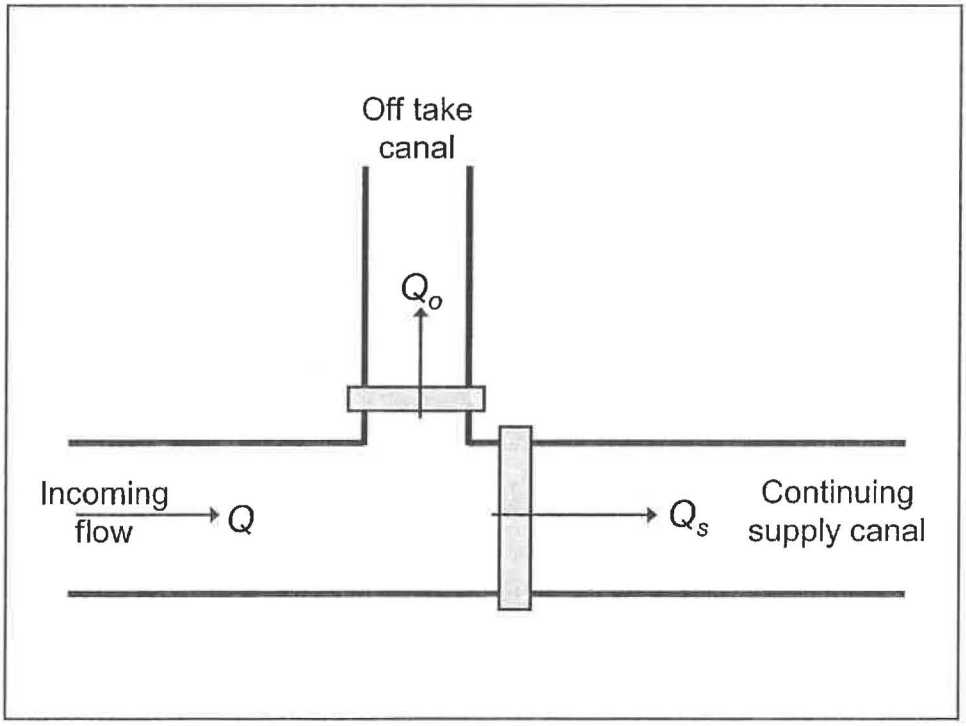

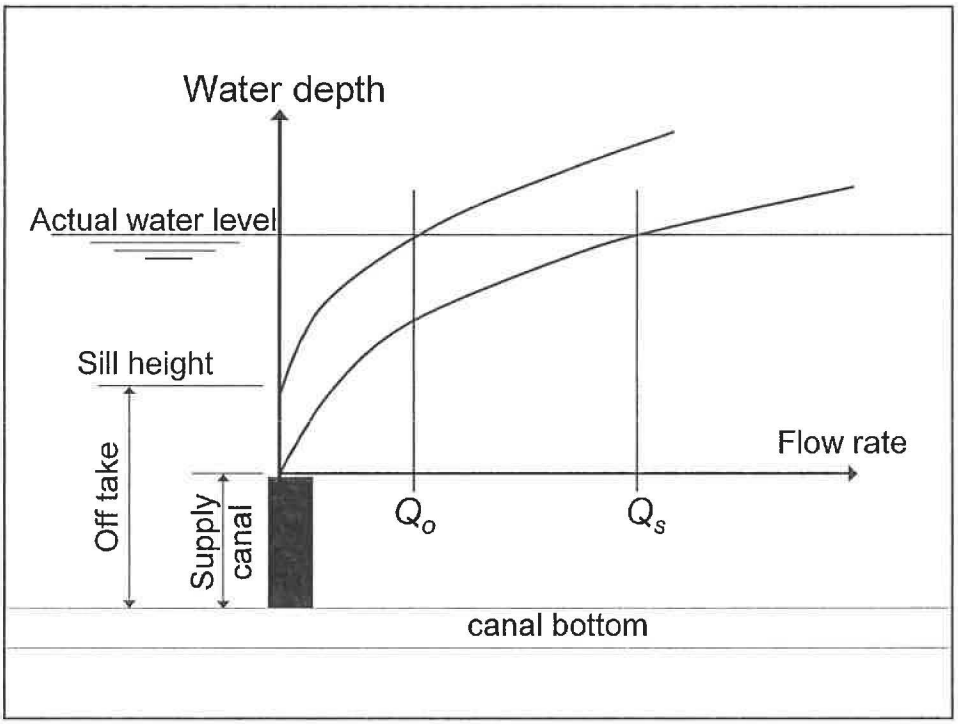
Water depth
Actual water level
Sill height
Off take
Supply canal
Flow rate
Q_o
Q_s
canal bottom

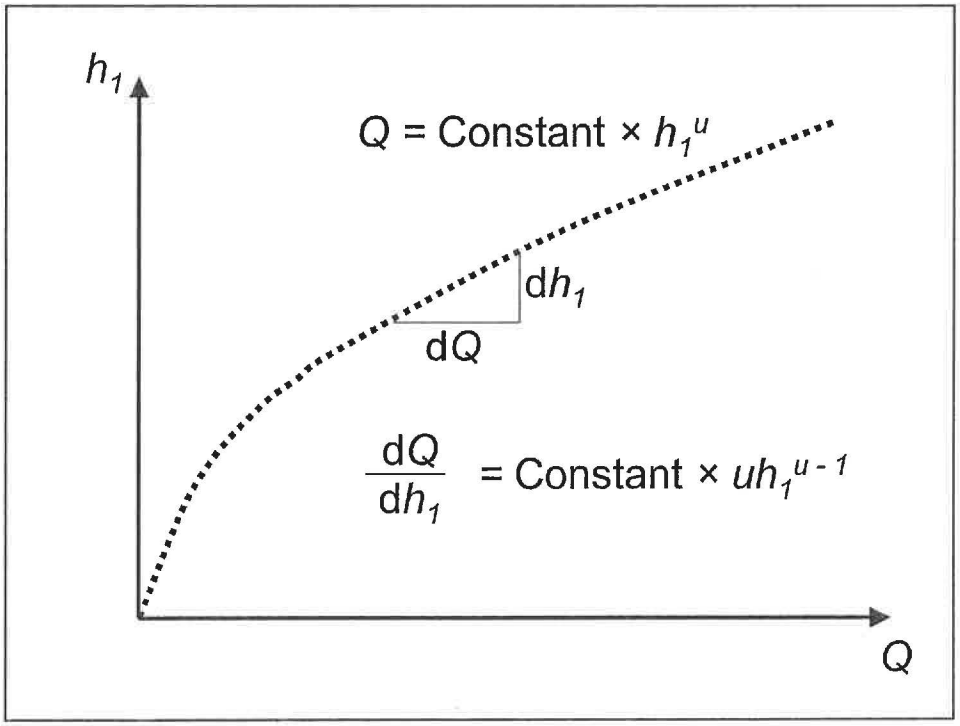
h_1
Q = Constant × h_1^u
dh_1
dQ
$\frac{dQ}{dh_1}$ = Constant × uh_1^{u-1}
Q

The sensitivity of a structure is defined as the fractional change of flow rate through the structure that is caused by the unit rise (usually $\Delta h_1 = 0.01$m) of the upstream water level.

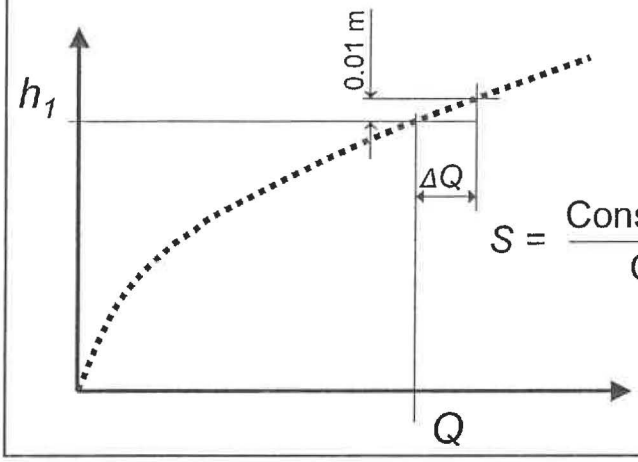

$$S = \frac{\Delta Q}{Q}$$

$$S = \frac{\text{Constant} \times u h_1^{u-1} \Delta h_1}{\text{Constant} \times h_1^{u}}$$

$$S = \frac{u}{h_1} \Delta h_1$$

Sensitivity of a structure is: $S = \frac{u}{h_1} \Delta h_1$

Shape	*U –value*
Orifice	*0.5*
Rectangular	*1.5*
Parabolic	*2.0*
Triangular	*2.5*

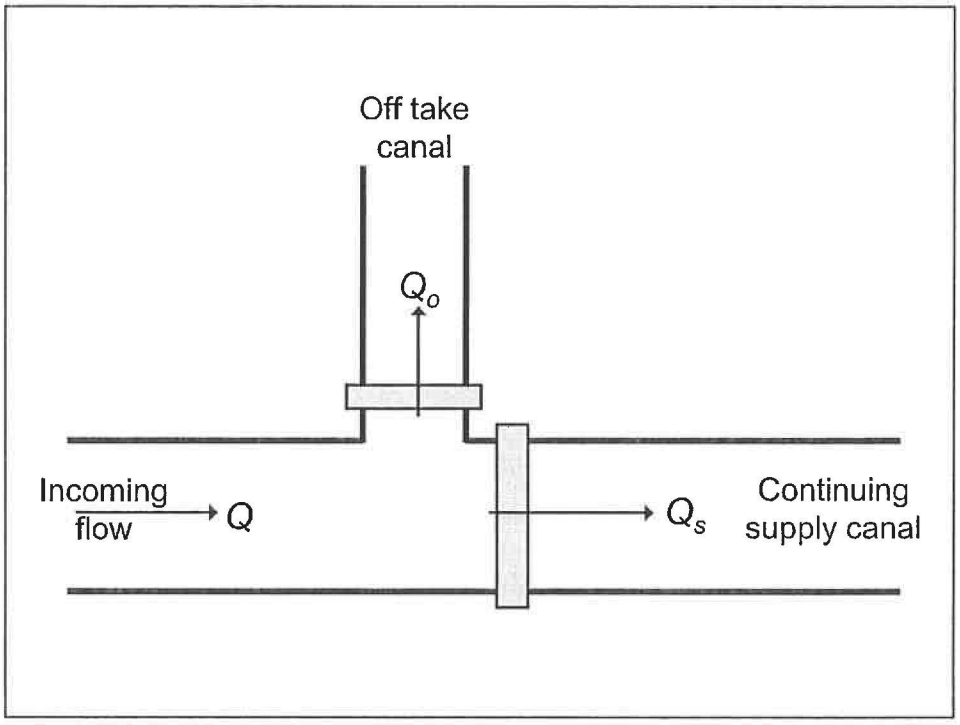

Relative Sensitivity of Canal Bifurcation

$$F = \frac{S_{\text{off take}}}{S_{\text{supply}}} = \frac{u_{\text{off take}} \times h_{1,\text{supply}}}{u_{\text{supply}} \times h_{1,\text{off take}}}$$

$$F = \frac{\Delta Q_{\text{off take}} / Q_{\text{off take}}}{\Delta Q_{\text{supply}} / Q_{,\text{supply}}}$$

$$Q_{incoming} = Q_{supply} + Q_{off\ take}$$

2 equations
Q_s and Q_o unknown

Relative sensitivity = 1.0

weir in supply canal

weir in off take

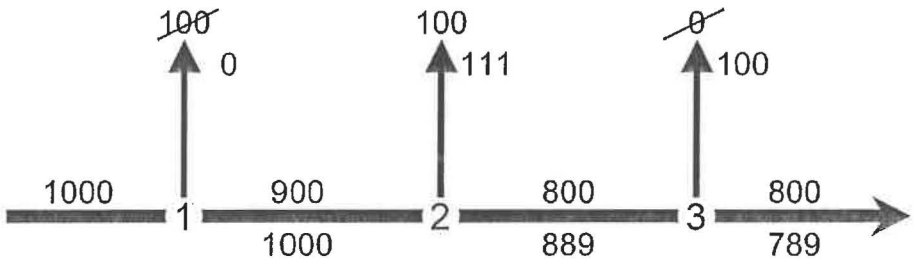

Relative sensitivity = 0.1

weir in supply canal

orifice in off take

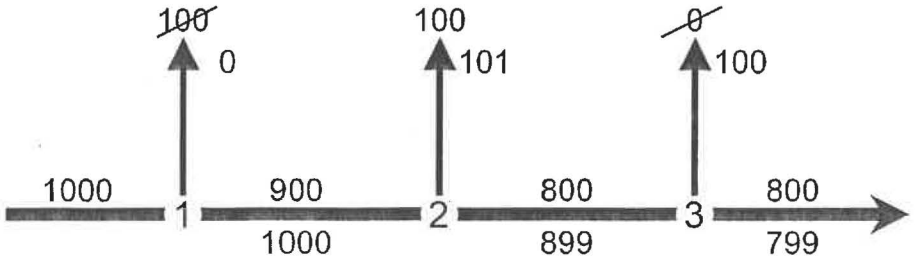

Relative sensitivity = 10.0

undershot gate (orifice) in supply canal

weir in off take

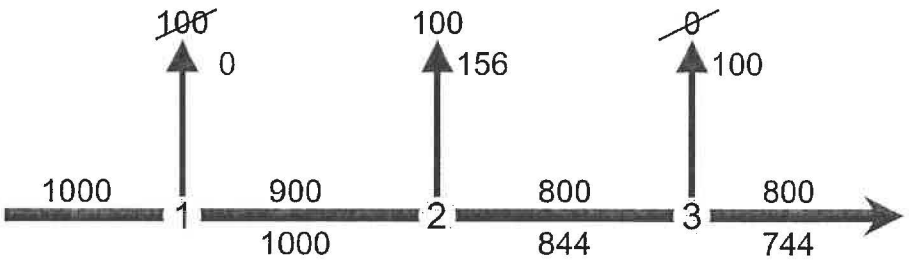

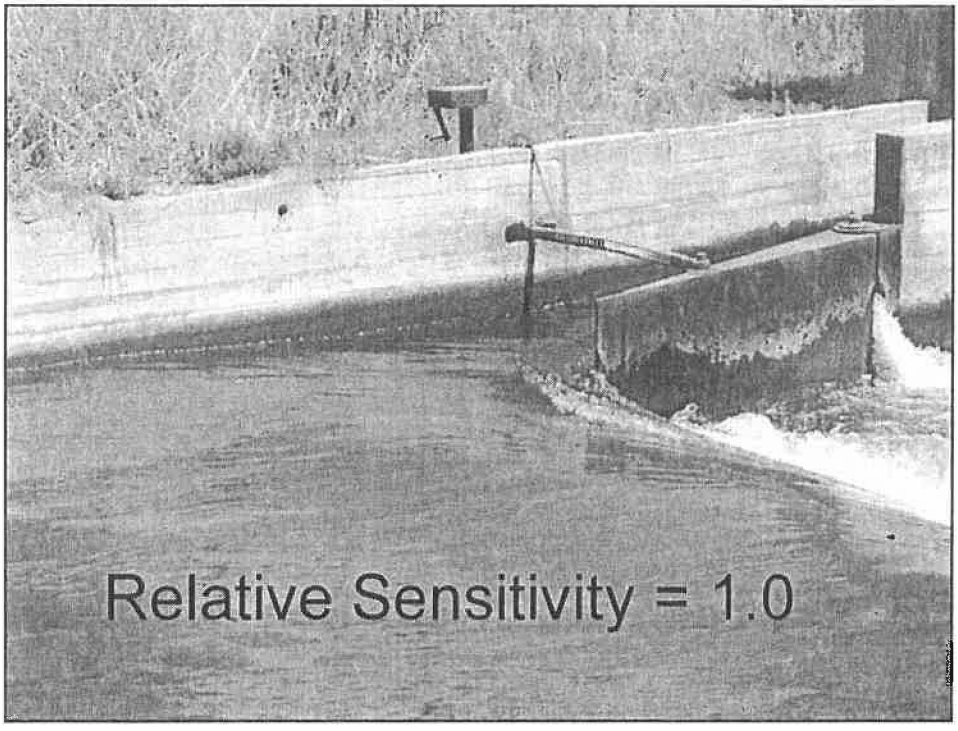

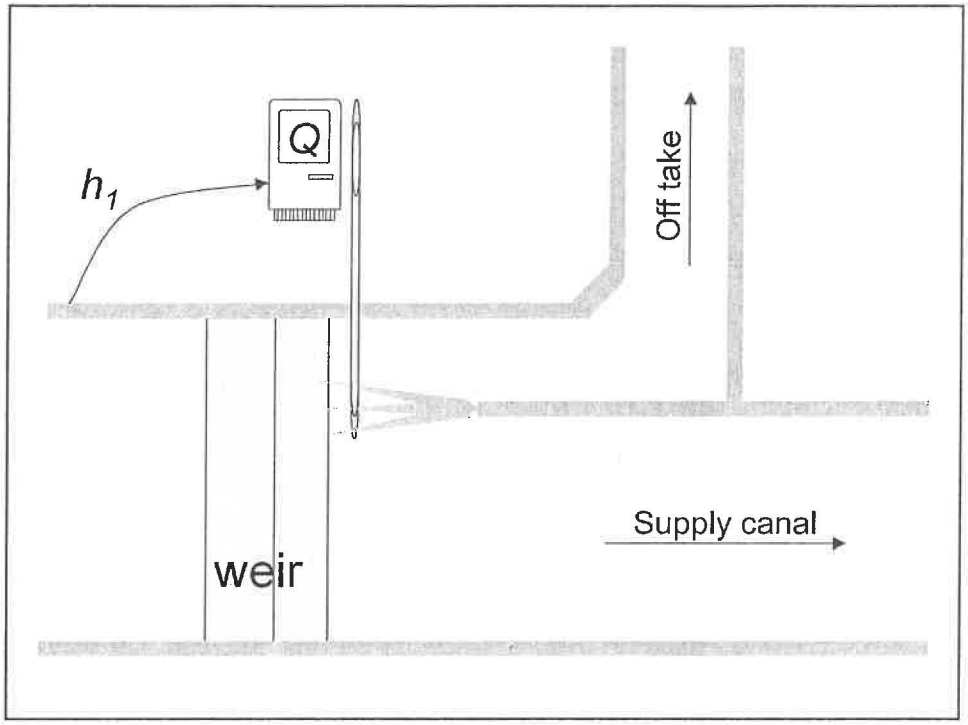
Q
h_1
Off take
Supply canal
weir

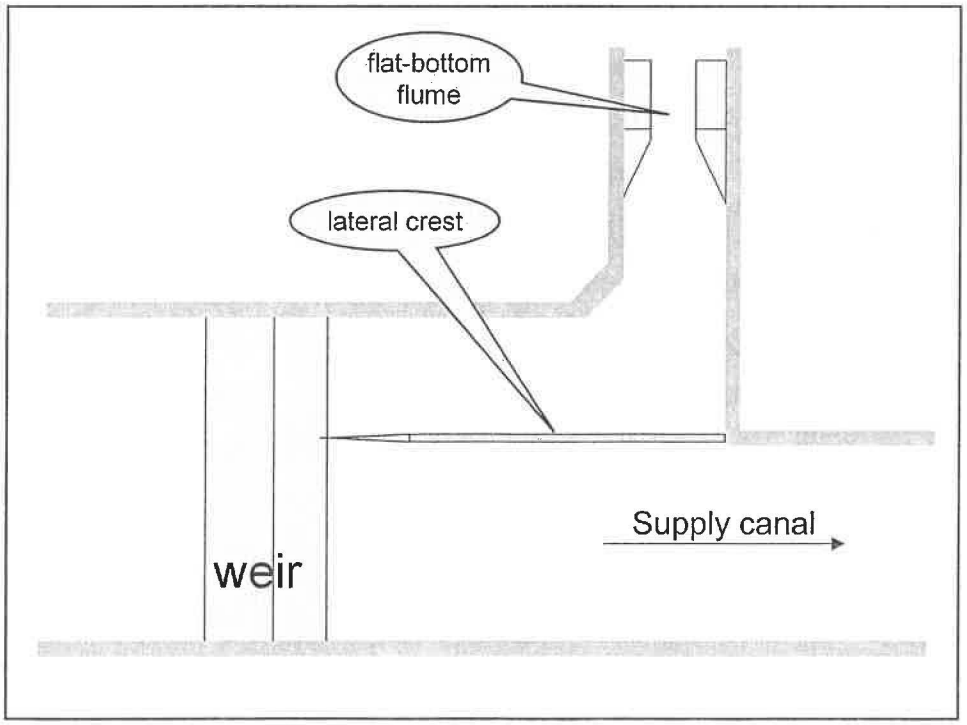
flat-bottom flume
lateral crest
Supply canal
weir

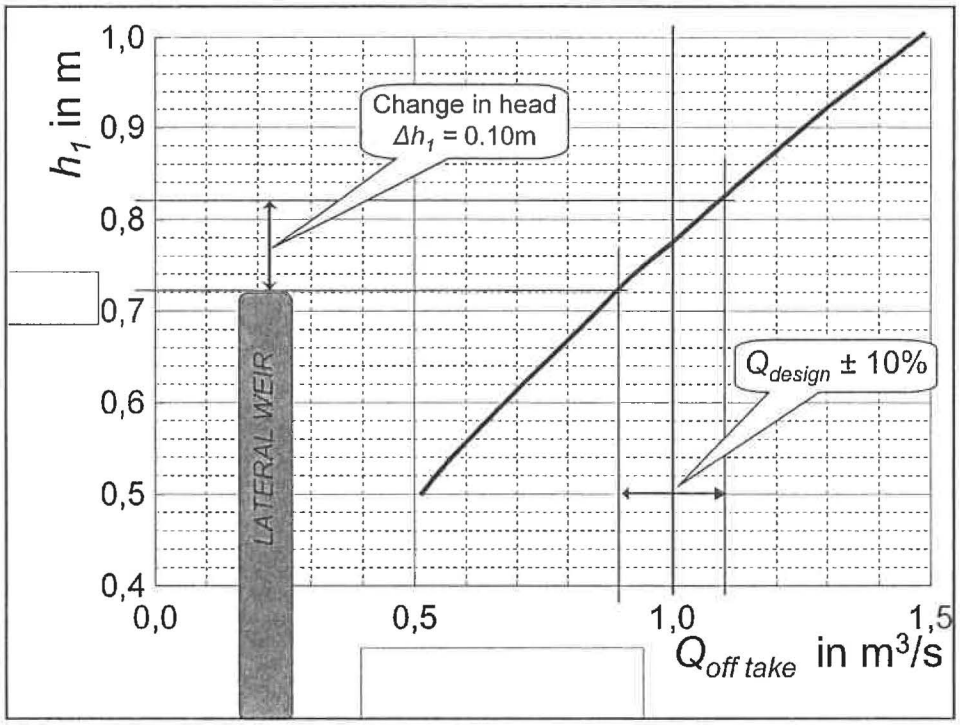
h_1 in m
1,0
0,9
0,8
0,7
0,6
0,5
0,4
Change in head
Δh_1 = 0.10m
LATERAL WEIR
Q_{design} ± 10%
0,0
0,5
1,0
1,5
$Q_{off\ take}$ in m³/s

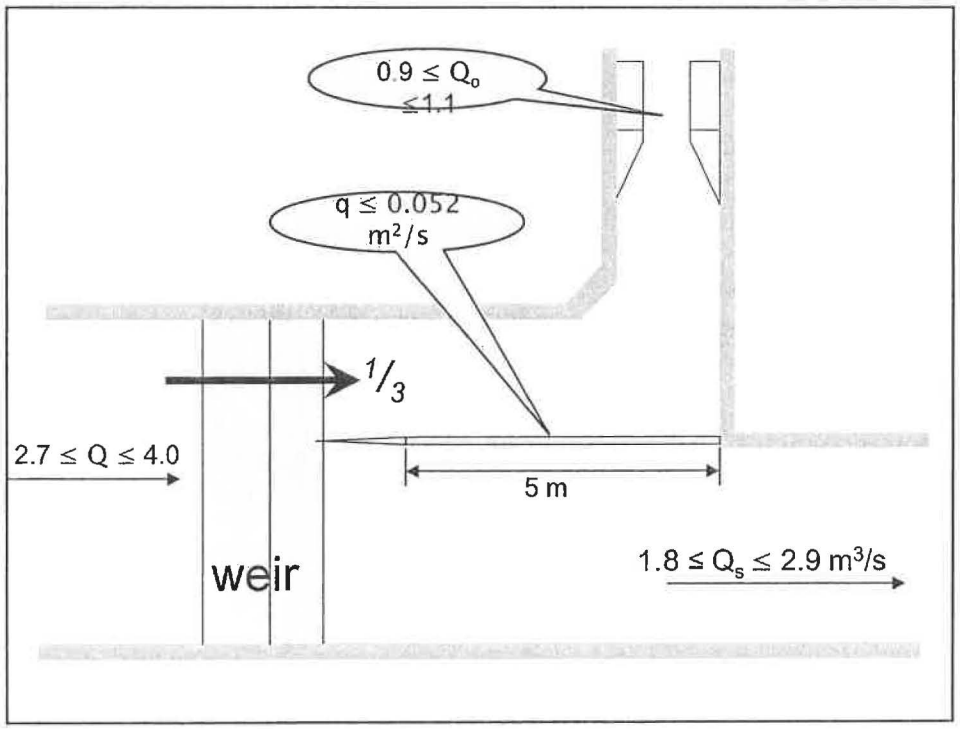
0.9 ≤ Q_o ≤1.1
q ≤ 0.052 m²/s
1/3
2.7 ≤ Q ≤ 4.0
5 m
weir
1.8 ≤ Q_s ≤ 2.9 m³/s

Where?

How?

When?

Measured Data during Canal System Operation

Only Time is Measured

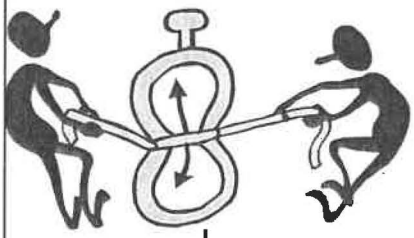

Actual length of Period / Intended length of Period

Flow Rate is Measured

Actual Flow during Period / Intended Flow during Period

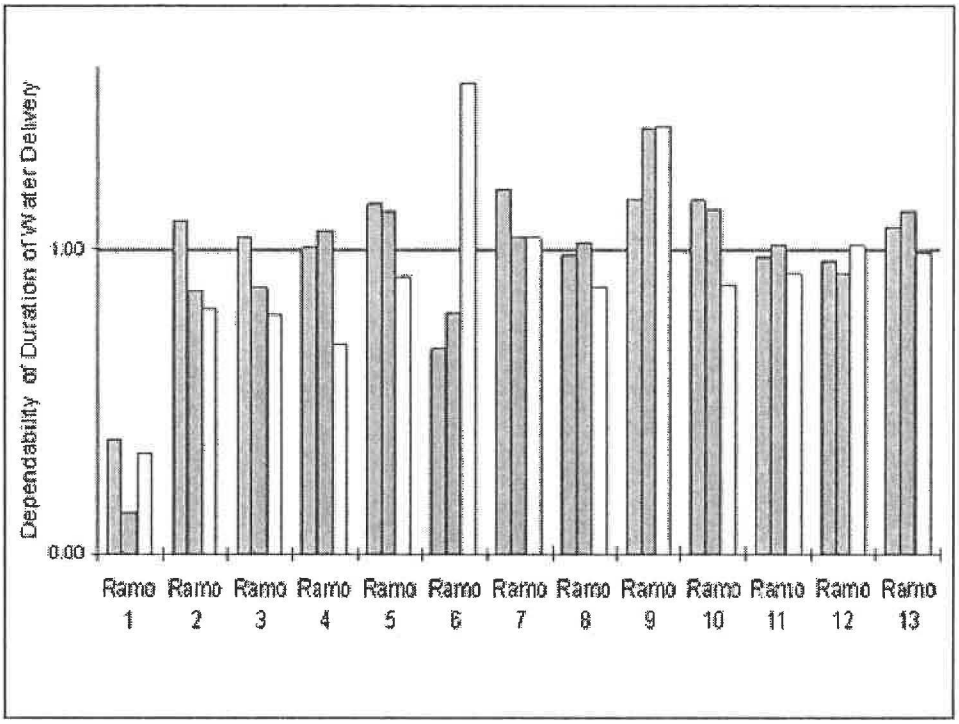

When do we start measuring flow?

Incentives:

Shortage of water

Environmental problems

Labor shortage (automation)

Research

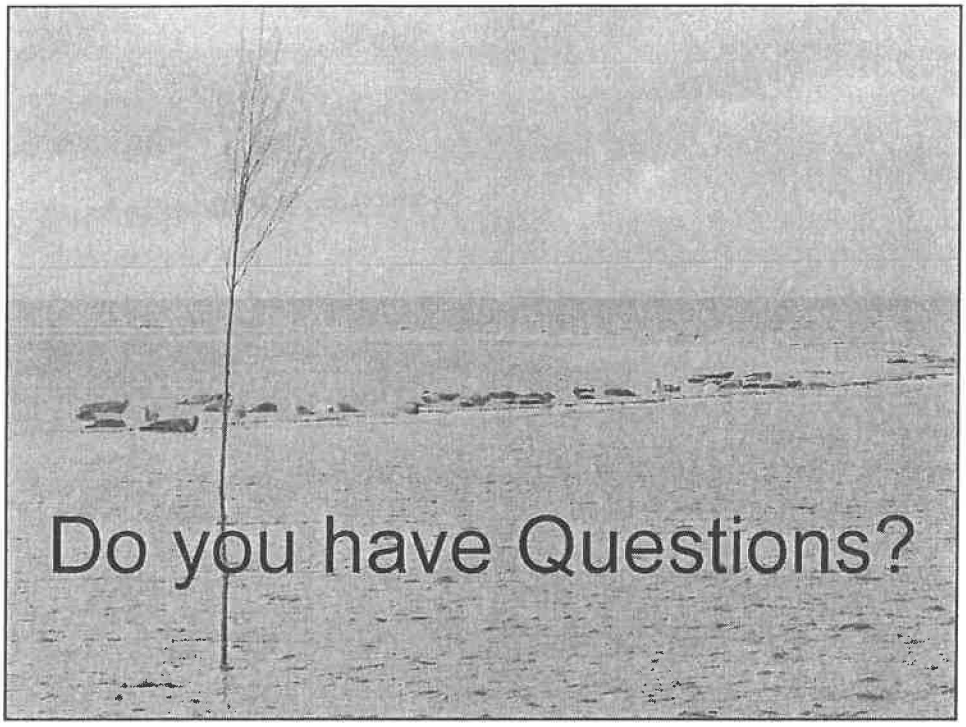

Correspondence to:

Prof Dr M. (Rien) G. Bos

ITC
P. O. Box 6
7500 AA Enschede
The Netherlands
bos@itc.nl
MarinusGBos@cs.com

Canal Velocity Indexing at Colorado River Indian Tribes (CRIT) Irrigation Project in Parker, Arizona using the SonTek Argonaut SL

Authors: Dr. Stuart Styles P.E., Mark Niblack, Beau Freeman

Abstract

An index velocity rating was developed for a SonTek/YSI Argonaut Side-Looking (SL) ultrasonic Doppler flow meter installed in the Main Canal of the Colorado River Indian Tribes (CRIT) Irrigation Project in Parker, Arizona. Velocity data collected concurrently with the ultrasonic flow meter and conventional current meter were compared using linear regression techniques. The rating equation for this installation provides a reasonably accurate means of computing discharge. This project was completed by the Irrigation Training and Research Center (ITRC), California Polytechnic State University, San Luis Obispo, working under a technical assistance contract for the Water Conservation Office, United States Bureau of Reclamation (USBR), Yuma, Arizona and the California Energy Commission (CEC).

The procedure used in the evaluation included multiple measurements over a range of low, medium, and high flows. This approach verified the validity of discharge measurement through analysis of coefficients of determination and by comparison of discharges computed from the ratings to measured discharges.

Introduction

This paper is a summary of an application of the Index Velocity Rating Procedure for a SonTek/YSI Argonaut™ Side-Looking (SL) 1.5-MHz acoustic Doppler current meter. The Argonaut SL has the ability to perform internal discharge computations as the product of mean channel velocity and cross-sectional area. The index coefficients for establishing the empirical velocity relationship in a channel are determined through regression analysis. Computing flow with the internal flow algorithm requires the user to input a specific velocity equation and the channel geometry defined by up to 20 cross-sectional points (x-y pairs).

The discharge and velocity measurements presented in this paper were collected in the Colorado River Indian Tribes (CRIT) Main Canal. Current metering was done following procedures established by the USBR in their Water Measurement Manual (USBR 2001). The actual Argonaut SL measured velocity values are used to illustrate the index velocity rating technique and the development of an equation to accurately produce discharge records using hydroacoustic instruments. The process discussed in this paper is a modification of the procedure outlined by the USGS for indexing (USGS 2002).

Utilizing electronic flow rate measurement equipment that can cost less than 10 percent of a large concrete flume is attractive economically. However prior to the use of this indexing procedure, there was much uncertainty of the overall accuracy in the use of a flow meter such as the Argonaut SL in some irrigation canal applications.

Basic Operation Principle

The SonTek/YSI Argonaut SL measures 2-dimensional horizontal water velocity in an adjustable location and size of the sampling volume using the physical principle termed the Doppler shift. The Argonaut transducers measure the change in frequency of a narrow beam of acoustic signals in order to compute along-beam velocity data. Beam velocities are converted to XYZ (Cartesian) velocities using the known beam geometry of 25° off the instrument axis.

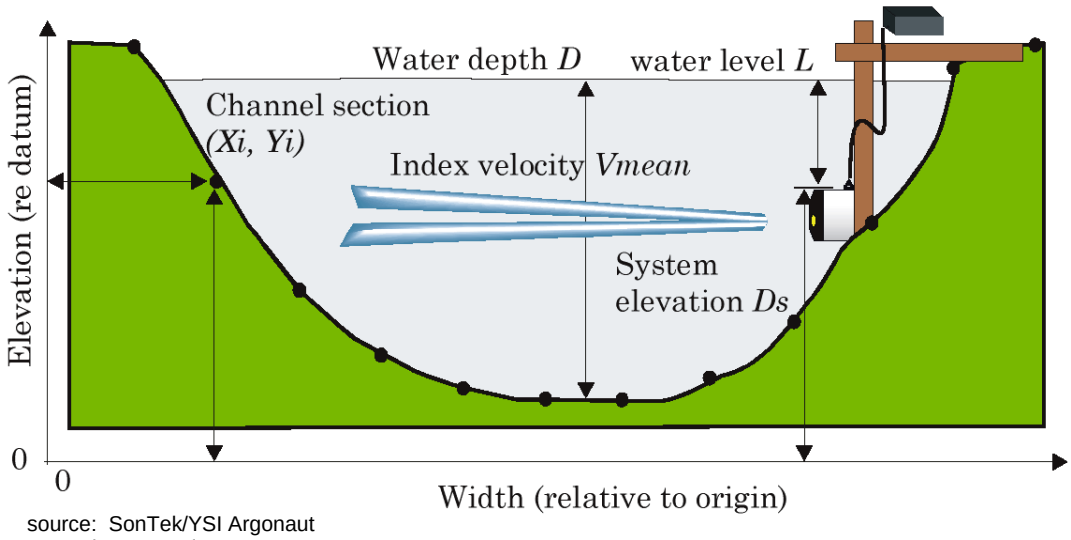

source: SonTek/YSI Argonaut Operation Manual

Figure 1. SonTek/YSI Argonaut SL channel geometry for internal flow computations

Basic Deployment Instructions

Before deployment of the Argonaut SL, the site must be prepared to achieve a high level of accuracy of the device. The following guidelines outline the required characteristics of a site for the Argonaut SL.

1. The location of the device must be ten widths of the canal away from bends or turbulences as to have good horizontal velocity distribution.

2. The device must be located at a concrete-lined section of the canal that is well surveyed.

3. The device must be installed on a removable arm for easy removal of the device for maintenance.

4. A moss deflector must be installed around the device to prevent trash or organic matter from collecting on or around the device.

5. A calibration procedure, like the one discussed in this paper, must be completed.

To determine an index velocity rating, concurrent mean channel velocity and Argonaut SL measured velocities are required. The following steps outline the basic procedures one follows in collecting velocity and stage data

for developing an index velocity rating. The result is a dataset comprised of i) a mean velocity, ii) average Argonaut SL velocity, and iii) average stage.

1. An Argonaut SL is installed with the appropriate deployment settings and mounting bracket. Site selection is an important consideration and the diagnostic guidelines provided in the manufacturer's technical documentation should be carefully observed. These diagnostic parameters include an assessment of the signal strength and standard deviation for a given set of operating conditions.

2. The channel is accurately surveyed and a stage-area rating is developed. Elevations for the cross-section points are in terms of stage referenced to the station datum.

3. Discharge measurements (Price AA current metering or comparable device) are made near the Argonaut SL site while the instrument is sampling velocity.

4. The average stage during the discharge-measurement period is recorded.

5. Mean channel velocity is derived for each individual discharge measurement by dividing the measured discharge by the channel area computed from the stage-area rating.

6. For each discharge measurement, Argonaut SL measured velocities are averaged for the discharge-measurement period. For the Argonaut SL, the velocity x-component or the computed velocity vector can be used for the measured velocity.

7. Each discharge measurement yields a computed mean channel velocity and an average Argonaut SL velocity.

8. The index velocity rating procedure recommended by the ITRC requires a wide spread in the measured discharge (a 2:1 ratio), usually at least 10 measurement values over the entire range of flows. The regression coefficient (r^2) must be better than 0.96 to assure confidence in the results.

This discussion does not attempt to provide a detailed description of all the technical issues involved with the deployment of the instrument for a desired level of accuracy. The performance of the Argonaut SL depends on considerations such as the influence of boundary interference, proper alignment with the flow, appropriate settings of the averaging and sampling intervals, and cell size. A further limitation in the operation of the Argonaut SL is the aspect ratio, which is defined as the ratio of the measurement range to height. Range is horizontal distance from the instrument and height is the vertical distance to the surface or bottom. It is strongly recommended to use the Argonaut SL for aspect ratios greater than 5:1. It is not recommended for aspect ratios less then 5:1. A bottom-mounted unit looking toward the water surface is recommended for those applications.

Measurement Results

A total of eight discharge measurements were collected in the CRIT Main Canal. The measured stage, computed mean channel velocity determined by current meter, and the Argonaut SL measured velocity are summarized in **Table 1.**

Table 1. CRIT Main Canal Current Meter and Argonaut SL Velocity Measurements

No.	Stage, feet	Current Meter Velocity, fps	Argonaut SL Velocity, fps
1	11.80	1.19	1.29
2	12.20	1.19	1.39
3	11.30	2.05	2.08
4	11.30	1.97	2.09
5	11.80	3.00	2.95
6	11.80	2.97	3.06
7	10.50	1.48	1.42
8	10.50	1.47	1.42

Index Velocity Rating Development

An index velocity rating is developed in this section to relate the mean channel velocity to the velocity measured by the Argonaut SL in the CRIT Main Canal. For some operating conditions, the index velocity relation may be linear, while in other situations the relation may be best expressed as curvilinear or a compound curve (USGS 2002). In each instance, the user should assume that stage might be a significant factor in the accurate prediction of mean channel velocity. This situation where the relationship between mean velocity and Argonaut measured velocity is affected by stage is handled by performing a multiple linear regression.

If the relation between the mean channel velocity and the measured Argonaut SL velocity is linear, it can be represented by a linear equation as follows:

$$V_m = xV_{SL} + C$$

where,

V_m = computed mean velocity
V_{SL} = average measured Argonaut SL velocity during one measurement period
x = velocity coefficient
C = constant

The first step in determining whether a linear relation exists is to plot mean velocity (y-axis) and Argonaut SL velocity (x-axis). **Figure 2** is a graph of the velocity dataset for the CRIT Main Canal in **Table 1**.

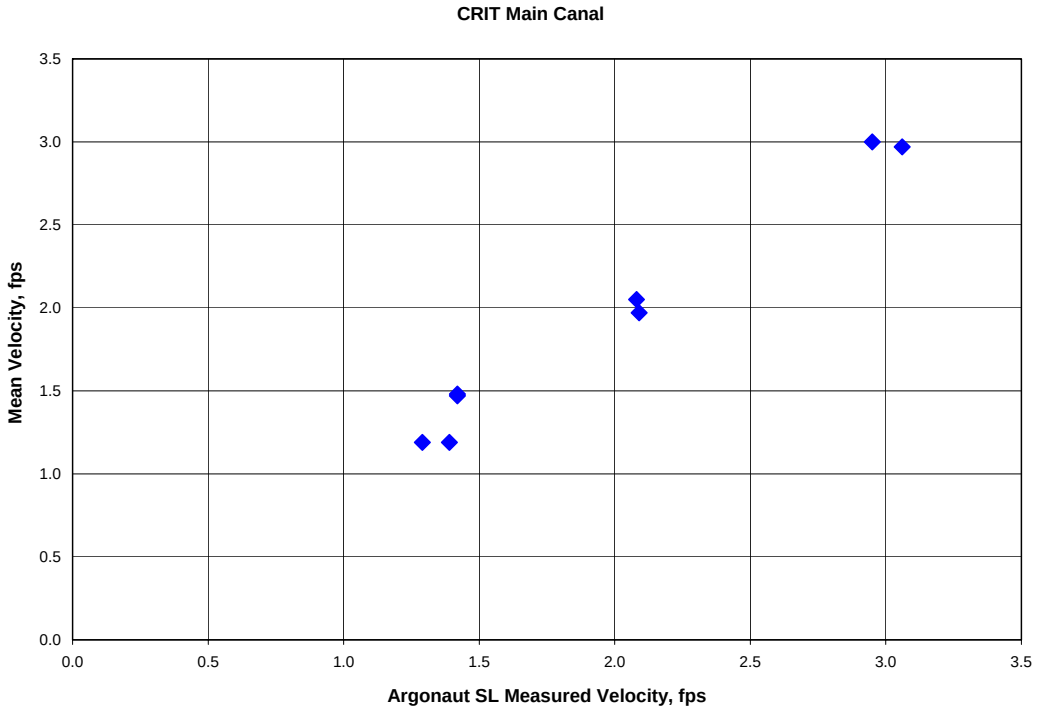

Figure 2. Mean velocity and Argonaut SL velocity from discharge measurements in the CRIT Main Canal

The next step is to derive the linear equation and compute the coefficient of determination (r^2). The r^2 value indicates what percentage of the variation in mean velocity can be explained by the variation of Argonaut SL velocity.

A simple method for determining the equation coefficient and constant along with the r^2 value is the linear regression tool in Excel® spreadsheets.

The linear index velocity rating equation determined for the CRIT Main Canal dataset in **Table 1** is shown below:

$$V_m = 1.015V_{SL} - 0.077$$

Figure 3 shows the index velocity rating from least-squares regression. The r^2 value of 0.98 indicates that 98 percent of the variation in the mean velocity can be explained by the variation in the Argonaut SL velocity.

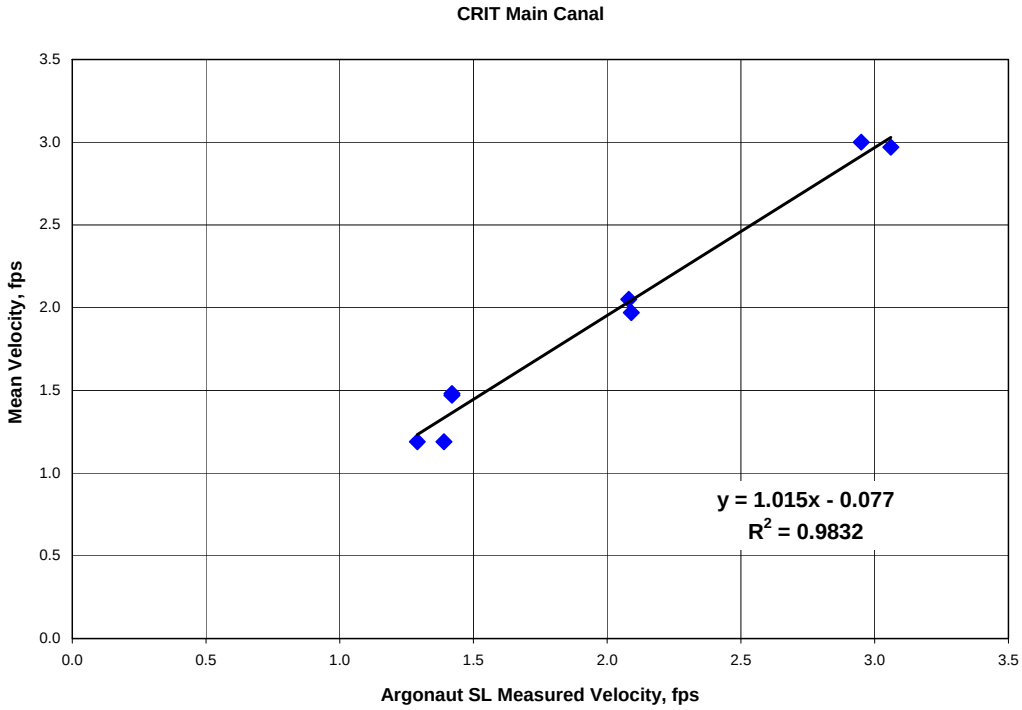

Figure 3. Index velocity rating using simple linear equation (r^2 = 0.98)

The above analysis assumed that the Argonaut SL measured velocity is the only parameter to consider when determining the index velocity rating. However depending on the site's hydraulic conditions, stage may be a significant factor in the prediction of mean channel velocity using a side-looking acoustic Doppler velocity instrument.

An equation that relates both the Argonaut SL velocity and stage to mean velocity is:

$$V_m = V_{SL}(x + yH) + C$$

where,

V_m = computed mean velocity
V_{SL} = average measured Argonaut SL velocity during one measurement period
x = velocity coefficient
y = stage coefficient
H = stage
C = constant

The values of the coefficients and constant in the index velocity equation can be determined from the multiple linear regression analysis where mean velocity is the dependent variable and the independent variables are the Argonaut SL measured velocity and the product of measured velocity and stage.

Using multiple regression analysis, the equation and r^2 value determined for the CRIT Main Canal dataset in **Table 1** assuming that stage is a factor is:

$$V_m = V_{SL}(1.995 - 0.080H) - 0.192$$
$$r^2 = 0.99$$

Figure 4 shows the relationship between the mean velocity and the computed index velocity using multiple linear regression.

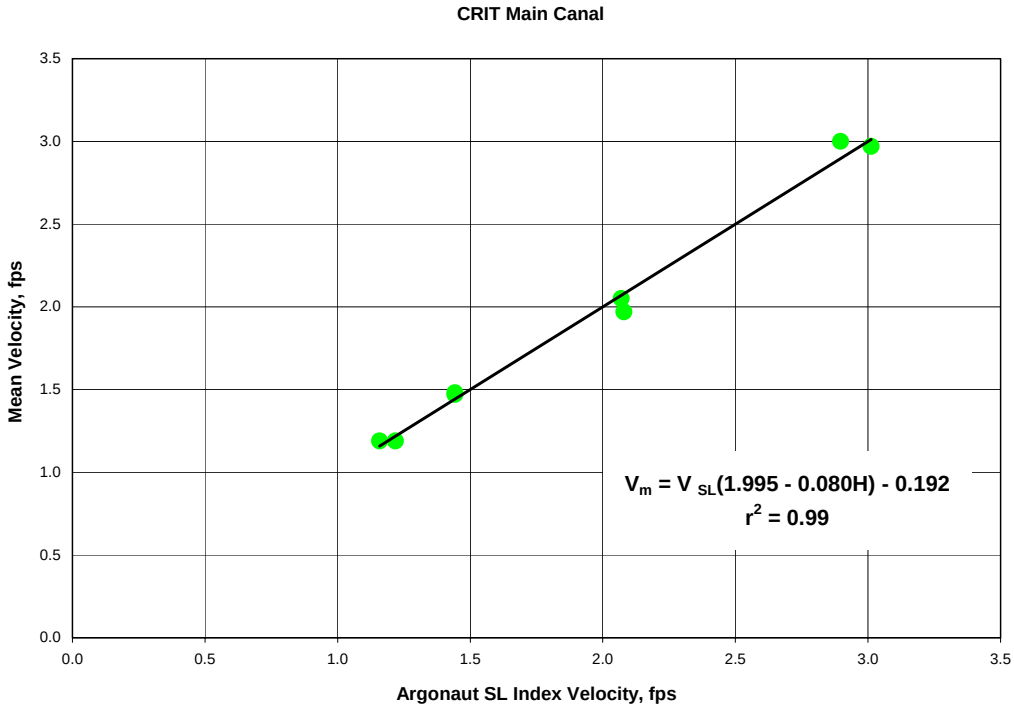

Figure 4. Index velocity rating using multiple regression equation

Results

Table 2 summarizes the computed discharge using both index velocity equations and the percent error relative to the current meter measurements. The flow rate (Q = VA) was computed using the index velocity and channel area based on the measured stage and a bottom width of 25 ft and side slope of 1:1.

Table 2. Discharge (cfs) and percent error using simple linear regression and multiple regression with stage

No.	Current meter discharge, cfs	Simple linear equation no stage		Multiple regression with stage	
		cfs	% error	cfs	% error
1	514	535	4.1%	503	-2.1%
2	540	605	12.1%	553	2.4%
3	841	834	-0.8%	849	0.9%
4	805	839	4.2%	853	6.0%
5	1318	1267	-3.9%	1258	-4.6%
6	1304	1315	0.9%	1308	0.3%
7	562	509	-9.5%	538	-4.3%
8	547	509	-7.0%	538	-1.7%

Conclusion

The index velocity rating determined using the multiple linear regression analysis with stage is generally closer to the discharge measured with a current meter. The percent error of the index velocity for the simple linear equation and the multiple linear regression equation is approximately ±10% and ±6%, respectively. In other words, the inclusion of stage as a factor in determining the index velocity rating for this particular dataset improved the accuracy by about ±4%. It is recommended to always include stage in the development of an Index Velocity Rating Procedure. The final equation can be readily programmed into the instrument for use with the internal flow computations option.

Figure 4. SonTek/YSI Argonaut SL installed in a canal

Due to the inherent problems in using current metering as the reference flow rate, future evaluations will be done using other rapid measurement techniques. The issues with current meters include; poorly defined cross-sections, fluctuating flow rates, moss hanging on meter, etc. Potential technologies include using the portable Doppler meters that can be mounted to boats and rapidly determine the flow rate in a canal.

References

USBR - Bureau of Reclamation. 2001. Water Measurement Manual – A Guide to Effective Water Measurement Practices for Better Water Management. United States Department of the Interior. Bureau of Reclamation. Third Edition. Denver, Colorado.

USGS - Morlock, S.E., H.T. Nguyen, and J.H. Ross. 2002. Feasibility of Acoustic Doppler Velocity Meters for the Production of Discharge Records from U.S. Geological Survey Streamflow-Gaging Stations. U.S. Geological Survey, Water-resources Investigations Report 01-4157. Denver, Colorado.

Disclaimer

ACCURACY OF IRRIGATION EFFICIENCY ESTIMATES

By A. J. Clemmens[1] and C. M. Burt,[2] Members, ASCE

ABSTRACT: Evaluation of actual irrigation system performance should rely on an accurate hydrologic water balance over the area considered. In a companion paper, water uses are categorized as consumptive or nonconsumptive, and beneficial or nonbeneficial. Real performance is based on water uses over a specified period of time, rather than observation of a single irrigation event (with associate potential, but not yet actual, consumptive and/or beneficial uses). Once the components in the water balance have been determined, it is shown that the accuracy of irrigation performance parameters can be determined from the accuracy of the components in the water balance, using standard statistical procedures. Accuracy is expressed in terms of confidence intervals. Equations, procedures, and examples are provided for making these calculations. It is recommended that confidence intervals be included in all reporting of irrigation system performance parameters.

INTRODUCTION

The ASCE Task Committee on Describing Irrigation Efficiency and Uniformity has attempted to define irrigation performance measures from a hydrologic standpoint (Burt et al. 1997). For any system the lateral and vertical boundaries are precisely defined. The areal extent of the system can be on any scale (e.g., field, farm, district, or project), depending on the intent of the evaluation. Similarly, the vertical extent can include only the crop root zone, or may also include a shallow ground water aquifer or the entire ground water aquifer, depending on the intent or the hydrologic setting. Then, a water balance is applied to the inflows and outflows from the system (Fig. 1). Irrigation performance measures are defined in terms of the ultimate destination (i.e., use) of the applied irrigation water. Irrigation water that enters and leaves the boundaries (i.e., representing a particular use) is separated from the other inflows and outflows (e.g., the amount of precipitation, other surface water flow, and ground water flow, etc.).

Another important consideration of the ASCE Task Committee in viewing irrigation system performance was separating consumptive use from beneficial use. Some water is consumed nonbeneficially, whereas some water that is beneficially used is not consumed (i.e., it remains within the hydrologic system as a liquid). This suggests the development of terms or symbols for describing the hydrologic balance (i.e., consumed versus nonconsumed) that are different from those for describing irrigation performance (i.e., beneficially versus nonbeneficially used). Furthermore, one can also define terms that describe proper management of both irrigation water and precipitation, or terms that describe proper management of any other portion of the water balance of interest.

Because of the large amount of water consumed by irrigated agriculture and the potential environmental degradation resulting from its drainage, there is considerable interest in defining the performance of such systems, with the hope that this will lead to improvements in overall water management. Once irrigation water is applied to a field, it becomes part of a new hydrologic system and its ultimate destination is difficult to trace. Precise measurement of the actual amount of irrigation water used by crops over a large area is difficult. Burt et al. (1997) discuss many of the difficulties in making estimates of this water use. Furthermore, deep percolation and/or shallow ground water flow in or out of the field root zone is very difficult to measure. Separating rainfall contributions from irrigation contributions further compounds the difficulty in determining the fate of the applied irrigation water. Because irrigation system performance is so tied to the hydrologic system in most cases, our knowledge of actual irrigation system performance is imprecise.

In this paper we focus on the accuracies of the estimates of the various components in the water balance and their influence on the accuracy of the resulting performance measures. Equations and procedures are presented for computing confidence intervals for the irrigation performance measures defined by the ASCE Task Committee. The same methodology can also be applied to performance measures based on other components of the water balance. This paper amplifies many of the concepts presented in the task committee report.

HYDROLOGIC WATER BALANCE

The definition of boundaries is extremely important to this hydrologic-balance approach for defining system performance. The lateral boundaries are often easy to define for a particular political entity (e.g., an irrigation district). However, such political boundaries may not be convenient for defining a hydrologic water balance. Often a water balance based on geographic boundaries is more feasible, even though more complexity is involved in separating the political entities within such boundaries. The difficulty is defining the flow of

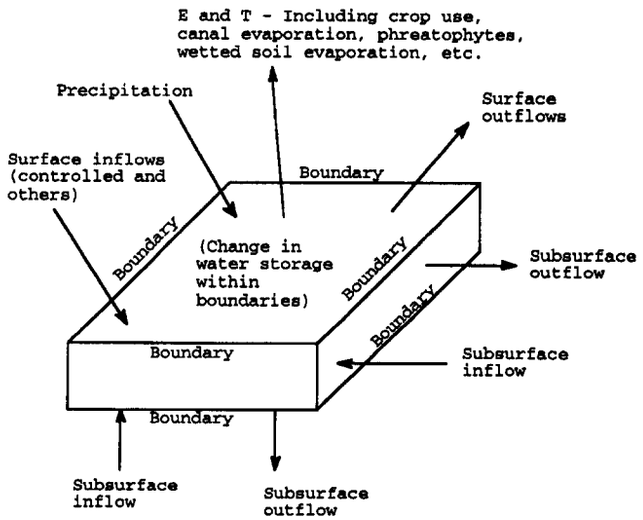

FIG. 1. Components of Simplified Water Balance within Defined Boundaries

[1]Res. Hydr. Engr., U.S. Water Conservation Lab., USDA/ARS, 4331 E. Broadway, Phoenix, AZ 85040.

[2]Dir., Irrig. Training and Res. Ctr., California Polytechnic State Univ., San Luis Obispo, CA 93407.

Note. Discussion open until May 1, 1998. Separate discussion should be submitted for the individual papers in this symposium. To extend the closing date one month, a written request must be filed with the ASCE Manager of Journals. The manuscript for this paper was submitted for review and possible publication on October 21, 1996. This paper is part of the ***Journal of Irrigation and Drainage Engineering***, Vol. 123, No. 6, November/December, 1997. ©ASCE, ISSN 0733-9437/97/0006-0443–0453/$4.00 + $.50 per page. Paper No. 11972.

water across political boundaries when there is no natural geographic boundary that restricts the flow so that it can be conveniently measured (e.g., measuring ground water flow between neighboring irrigation districts sharing the same aquifer may be very difficult and expensive).

The vertical boundaries are often more difficult to establish. For measurements on a field scale, the bottom of the root zone is generally used as the lower boundary. However, there may be extreme difficulty in estimating the amount of deep percolation. The presence of a shallow water table complicates the situation since water can be taken up from the ground water by the plant roots, and since shallow water inflow and outflow are very difficult to determine on a small scale such as a field.

The ASCE Task Committee determines performance in terms of water leaving the boundaries of the system. That is, when the water leaves, it is grouped into a category of use (consumed or nonconsumed and beneficial or nonbeneficial), but not before. For larger scale systems (i.e., larger than field scale), water is often recirculated within the boundaries of the system. Such water should not be double-counted in a water balance for determining performance measures. It is simply considered recirculating or in storage. Changes in storage must be taken into account when inflow and outflows over a specified period of time do not match.

Where ground water is pumped for irrigation and irrigation deep percolation returns to the same ground water aquifer, the ground water aquifer should be included within the boundaries of the system. For some geographic settings, this makes determination of a hydrologic balance very difficult, since natural ground water recharge and ground water inflow may be very difficult to estimate. Ground water systems with multiple aquifers that are partially connected may further complicate the hydrologic balance.

Such difficult studies are often outside the interest of agriculturalists. A common alternative to actual measurement is to use deep percolation or ground water flow as the remainder (closure term) in the water balance calculations. This is feasible, in many cases, but requires that more accurate estimates be made of consumptive uses, which can also be difficult in a diverse landscape.

UNCERTAINTY AND CONFIDENCE INTERVALS

Every measurement of a nondiscrete quantity, such as water volume, contains an element of uncertainty, regardless of the variable and the method of measurement. This applies to all methods for estimating the water sources and destinations in the water-balance diagrams. Confidence intervals are a standard statistical approach for describing the uncertainty associated with the value of each water quantity. The 95% confidence interval is commonly used in statistics to represent the degree of certainty for a variable of interest. It represents the range within which we are 95% certain that the true value of that variable lies. For a normal distribution of measurements, the 95% confidence interval represents approximately ±2 standard deviations (Fig. 2). Here, we define the confidence interval (CI) as ±2 standard deviations, regardless of the distribution type. For other distributions (e.g., log-normal, beta, etc.), this confidence interval may represent a percentage slightly different from 95%.

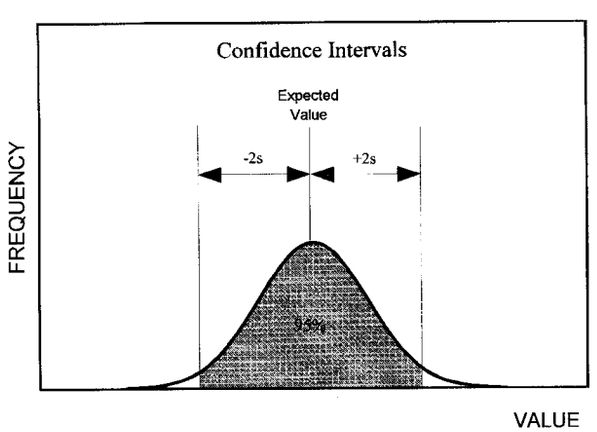

FIG. 2. Normal Distribution of Values Showing 95% Confidence Interval

Errors in measurements include errors in the device calibration, errors in reading, errors in installation or zeroing, and so forth, and can be either systematic or random. Random errors are typically normally distributed. Repeated measurements at a given site can reduce the impact of random errors, since for a very large sample these random errors approach 0. The accuracy of a water volume determined from multiple flow rate measurements can be improved by more frequent measurement (i.e., it is related to number of samples), if the measurement error is random. However, repeated measurements of a given flow or water quantity do not remove systematic errors, and the inaccuracy caused by systematic errors is not related to the number of samples taken. Systematic errors, for example, from installation, are constant for one installation but may vary randomly from installation to installation. Such errors may be unknown for any given installation, but when considering the combined influence of installations at many sites, they are often treated as random errors, again normally distributed. However, the average value for measurements at many similar sites may still contain a systematic error.

For many quantities of interest, more than one measurement is needed to determine a numerical value; for example, a quantity of interest may consist of two other components that are added, subtracted, multiplied, or divided. Standard statistical equations are given subsequently for determining the uncertainty of the result, given the uncertainty of the individual measurements. The associated statistics can also be used to determine which quantities contribute most to the uncertainty of the desired performance measure and to guide efforts to reduce uncertainty.

Statistical Relationships

In this context we are trying to estimate the one true value of some variable (i.e., a water volume) that might be estimated by summing (e.g., integrating) several measurements or that might have several individual estimates (or a distribution of possible values). Classical statistics typically deal with the distribution of a population and measures of that population such as the mean. Here we are interested in the expected value of a variable, which, in reality, has one true value, and its distribution of possible values. It does not matter how this variable is estimated for other statistics (i.e., it could be a sum, a mean, a product, a quotient, the result of integration, etc.). The statistical relationships and equations for dealing with the expected value of a variable and the mean of a population are identical. Thus, when we refer to the expected value, we use m in the notation to conform to the standard statistical notation.

The standard deviation, s, is a standard statistical measure of variability. It describes the spread of the distribution of values. The variance is the square of the standard deviation. The variance for the variable y, for example, can be estimated from a sample of size n with

$$s_y^2 = \frac{\sum_{i=1}^{n} (y_i - m_y)^2}{n - 1} \quad (1)$$

The coefficient of variation of y, CV_y, is the standard deviation s_y divided by the expected value, m_y

$$CV_y = \frac{s_y}{m_y} \tag{2}$$

Formally, the confidence interval for the true value of y is defined here as

$$m_y - 2s_y \leq y \leq m_y + 2s_y \tag{3}$$

However, the confidence interval is often expressed in terms of the variation around the expected value, either in terms of the standard deviation or in terms of the coefficient of variation

$$CI = \pm 2s \quad \text{or} \quad CI = \pm 2CV \tag{4}$$

The latter gives a measure of relative accuracy and has no units (i.e., CI relative to the magnitude of the expected value). The CV and CI are often expressed as a percent, particularly when they represent an accuracy of measurement.

Combination of Variance Equations

When several component parameters contribute to the variation of a parameter of interest, we use the notation y_0 for the combined result and y_1, y_2, y_3, ... to represent the components. For simplicity the symbol y is dropped from the subscripts for m, s, CV, and so on, so that m_0, for example, represents the expected value of y_0. The following combination of variance equations can be found in Mood et al. (1974). These equations assume only that the variables are random; the variables need not be normally distributed (i.e., one equation might follow a log-normal distribution while another follows a beta distribution).

Addition

When adding several quantities of interest, for example, $y_0 = y_1 + y_2$, the expected value of the sum is just the sum of the component expected values

$$m_0 = m_1 + m_2 \tag{5}$$

The variance is found from

$$s_0^2 = s_1^2 + s_2^2 + 2s_{12}^2 \tag{6}$$

where s_{12}^2 = covariance of y_1 and y_2, defined as

$$s_{12}^2 = \frac{\sum_{i=1}^{n} (y_{1_i} - m_1)(y_{2_i} - m_2)}{n - 1} \tag{7}$$

If the quantities are independent, the covariance is 0, the last term in (6) is eliminated, and the coefficient of variation is found from

$$CV_0^2 = \frac{m_1^2}{m_0^2} CV_1^2 + \frac{m_2^2}{m_0^2} CV_2^2 \tag{8}$$

Multiplication

We can also combine the influences of several factors that are multiplied to obtain the combination (e.g., $y_0 = y_1 y_2$). The expected value of y_0 can be found from

$$m_0 = m_1 m_2 + s_{12}^2 \tag{9}$$

Note that if y_1 and y_2 are not independent, then the expected value is not the product of the component expected values. That is, $m_0 = m_1 m_2$ only if y_1 and y_2 are independent.

The variance of the product can be found from

$$s_0^2 = m_2^2 s_1^2 + m_1^2 s_2^2 + s_1^2 s_2^2 + 2m_1 m_2 s_{12}^2 \tag{10}$$

in which higher-order terms have been ignored. If y_1 and y_2 are independent, the coefficient of variation for y_0 is

$$CV_0^2 = CV_1^2 + CV_2^2 + CV_1^2 CV_2^2 \tag{11}$$

Division

The expected value and variance of a quotient of two variables, each with its own distribution, for example, $y_0 = y_1/y_2$, cannot be computed exactly, even if the correlation between y_1 and y_2 is known. Approximate equations (Mood et al. 1974) are

$$m_0 \approx \frac{m_1}{m_2}\left(1 + \frac{s_2^2}{m_2^2} - \frac{s_{12}^2}{m_1 m_2}\right) \tag{12}$$

$$s_0^2 \approx \frac{m_1}{m_2}\left(\frac{s_1^2}{m_1^2} + \frac{s_2^2}{m_2^2} - \frac{2s_{12}^2}{m_1 m_2}\right) \tag{13}$$

Note that for division, the expected value of the quotient is not the quotient of the expected values, even if y_1 and y_2 are independent, due to the term s_2^2/m_2^2. However, this term is usually quite small. If y_1 and y_2 are independent and this term is ignored, a conservative estimate for the coefficient of variation for y_0 can be found from

$$CV_0^2 \approx CV_1^2 + CV_2^2 \tag{14}$$

IRRIGATION PERFORMANCE MEASURES

Having a firm understanding of the hydrologic water balance is an important first step in assessing irrigation performance. Once the components of the water balance are quantified, one can make rational decisions about the appropriateness of the water uses and whether they have a positive or negative effect on crop production, the economic health of the region, the environment, or any other issues of importance. Any number of performance measures can be constructed from these water-balance components. For illustrative purposes this paper deals with the main performance measures associated with irrigation. More specifically, two irrigation system performance indicators proposed by the ASCE Task Committee are discussed.

The first indicator, irrigation efficiency, IE, deals with water that was beneficial for crop production

$$IE = \frac{\text{volume of irrigation water beneficially used}}{\text{volume of irrigation water applied} - \Delta\text{storage of irrigation water}} \times 100\% \tag{15}$$

where Δstorage refers to change in storage of the irrigation water within the boundaries. This change in storage represents irrigation water inflow that has not left the boundaries and is therefore neutral with regard to beneficial or nonbeneficial use. (Irrigation water that was initially in storage and later leaves the boundaries also represents a change in storage.) The numerator is really the sum of the beneficial uses, whereas the denominator is the sum of the beneficial uses plus the sum of the nonbeneficial uses.

The second indicator, irrigation consumptive use coefficient, $ICUC$, deals with the fraction of water actually consumed (i.e., no longer liquid water)

$$ICUC = \frac{\text{volume of irrigation water consumptively used}}{\text{volume of irrigation water applied} - \Delta\text{storage of irrigation water}} \times 100\% \tag{16}$$

The denominator is the sum of the water consumed beneficially plus the sum of the water consumed nonbeneficially. Determining numerical values for these two indicators requires

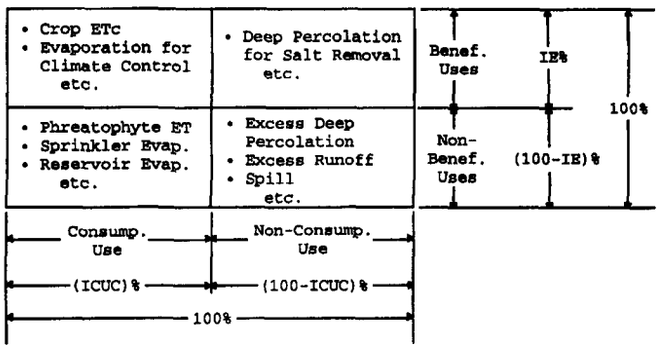

FIG. 3. Division between Consumptive and Nonconsumptive Uses Is Distinct from Division between Beneficial and Nonbeneficial Uses

estimates for each component in the water balance. The difference between *IE* and *ICUC* is demonstrated in Fig. 3.

ESTIMATING WATER USES

For the purposes of this discussion, water uses are grouped into four categories—representing combinations of consumptive/nonconsumptive and beneficial/nonbeneficial. For each quantity of interest, three methods can be used to estimate its numerical value

- Direct measurement—for example, with an accumulating water meter
- Indirect measurement—for example, estimates of evapotranspiration (*ET*) from weather data and crop coefficients
- Mass balance closure—that is, the remainder in a water or ion balance

Direct measurements are usually preferred, but not always feasible. Indirect measurements require some assumptions that may require field verification. For a water balance there can only be one closure term (or a group of related quantities). Obtaining an accurate estimate of the closure term requires good estimates of all other terms in the water balance. The accuracy of the remainder can be estimated from the accuracy of the other terms with the preceding equations, as will be demonstrated subsequently.

Quantifying Consumptive Beneficial Uses

In many irrigated areas crop consumptive use is the largest consumptive use and the largest beneficial use of water. Crop consumptive use is primarily crop evapotranspiration, ET_c. Thus, ET_c usually receives the primary focus of attention in any water-balance study. A major problem with determining ET_c over large areas is that it can be highly variable, not only from differences in vegetation type but also from variations in ET_c within one field.

There are several ways to estimate crop consumption. The primary ones, however, are the following.

Direct Measurement. There are a few specialized procedures for measuring evapotranspiration, more or less, directly. For example, the eddy-correlation method measures the flux of vapor above the surface. The Bowen-ratio approach combines this measurement with other atmospheric measurements and an energy balance. Such methods require significant instrumentation to obtain essentially a point measurement in space and time. Such point measurements may be difficult to extrapolate to large areas where evapotranspiration is highly variable and to an irrigation season.

Indirect Measurement. Weather-based methods are the most common approach for estimating crop evapotranspiration. First, atmospheric measurements are used to determine hourly or daily reference evapotranspiration, ET_r. Then crop coefficients are applied to account for differences in crop properties and growth stages. These crop coefficients are ideally a combination of basal crop coefficients derived from field experiments during relatively dry soil surface conditions, modified for the moisture content at the soil surface and in the root zone. Different approaches to estimating ET_r produce estimates that may differ by more than 10% (Jensen et al. 1990; Ley et al. 1994). Crop coefficients depend on the method for computing reference evapotranspiration. These crop coefficients, even with the same reference, can vary with climatic conditions. Relatively accurate crop coefficients are available for the major crops such as wheat, corn, and cotton, but for many crops they are either nonexistent or based on very limited data. Furthermore, this approach generally assumes that crop *ET* is uniform over the entire field and not limited by soil moisture, salinity, insect damage, and so forth (e.g., no local plant stress). The result is that these methods are not precise and can contain significant error. Other indirect measurement methods and their associated difficulties are discussed in Burt et al. (1997).

Mass Balance Closure. A water balance can be used to estimate the unmeasured water uses, which can be done at a field, farm, district, or project scale. If estimates of surface and subsurface inflow and outflow and change in storage are made, the remainder in the water balance is the total evapotranspiration from the area, one component of which is the crop *ET*. To determine only the portion of *ET* for the crop and for the irrigation water, estimates of *ET* for all the other *ET* components must be made. These might include crop *ET* from rainfall, weed *ET*, canal and reservoir evaporation, soil evaporation, windbreak and phreatophyte *ET*, etc. Estimating the aerial extent and *ET* rate from such areas on a district scale can be quite difficult. More details on problems with applying any of these methods are given in the ASCE Task Committee paper (Burt et al. 1997).

Quantifying Nonconsumptive Beneficial Uses

The main nonconsumptive beneficial use is deep percolation water that is needed to leach salts from the soil. Water for leaching is needed in arid areas even after initial reclamation of the soil since salts dissolved in the irrigation water are left behind when the water evapotranspires. The leaching requirement, *LR*, is defined as

$$LR = \frac{\text{volume of irrigation water needed for leaching}}{\text{volume of irrigation water needed for } ET_c \text{ and leaching}} \tag{17}$$

The volume of water that is potentially beneficial for leaching (required-beneficial-deep percolation) is then

$$V_{rbdp} = \frac{LR \times ET_{c_{iw}}}{1 - LR} \tag{18}$$

where $ET_{c_{iw}}$ is the ET_c of the irrigation water, expressed as a volume.

The leaching requirement varies with the quality of the irrigation water and the sensitivity of the particular crop to soil salinity. Several equations have been suggested for determining the leaching requirement (e.g., Rhodes 1974). These equations typically define the amount of deep percolation water needed to maintain soil salinity at a given level. They regularly do not include reclamation leaching and often ignore the contribution of rainfall to leaching. These equations are beyond the scope of the current paper, except to say that this is a very inexact science. Thus, the volume of water that was actually beneficial for leaching salts for a given field cannot be precisely determined. Also, because of soil nonuniformity and

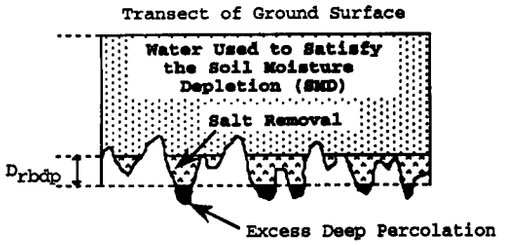

FIG. 4. Deficit Irrigation with Nonbeneficial Deep Percolation (D_{rbdp} = Depth of Required Beneficial Deep Percolation)

preferential flow, even if the irrigation system applies water with perfect uniformity, all of the leaching water likely will not be beneficial, even if the average leaching depth is less than the required leaching depth, as shown in Fig. 4 [see Burt et al. (1997) for further discussion].

Other beneficial uses include water for the following:

- Crop cooling (e.g., for quality or to alter dormancy and growth stages)
- Frost protection
- Soil preparation
- Disease and pest control
- Germination
- Maintenance of cover crops and windbreaks

Some of this water is consumed, whereas some is not. Clearly not all the water used for these purposes is justified as beneficial (e.g., applying a 100-mm irrigation for frost control when only 30 mm is needed). Estimating how much of the water applied for these uses is beneficial is very difficult to determine accurately. Yet, these are real needs of crop production, and some amount of water for these purposes is essential.

Quantifying Consumptive Nonbeneficial Uses

Consumptive nonbeneficial uses are primarily excess evaporation from free water surfaces and wet soil and transpiration by plant that are nonbeneficial for crop production. This is not to say that this use of water is not beneficial for other purposes (e.g., wildlife). However, this partitioning of water separates the agricultural uses from other uses. Evaporation from supply reservoirs and irrigation canals can be estimated with energy balance approaches with reasonable accuracy. Transpiration from other vegetation within the boundaries can be difficult —both in terms of accurately knowing the area of various plants and in knowing their transpiration rates. Examples include weeds, grasses and trees along canals and drains, and so on.

Quantifying Nonconsumptive Nonbeneficial Uses

Nonconsumptive nonbeneficial uses are represented by water that leaves the boundaries of the system, but which cannot be assigned as a beneficial use. In some cases, whether the use is consumptive or nonconsumptive depends on how you draw the boundaries of the system (e.g., whether drainage channels containing phreatophytes are included or not). Water leaving the system as surface flow can be relatively easy to measure accurately, whereas deep percolation or subsurface flows are much more difficult to estimate.

Quantifying Water Sources

Surface water supplies include water from reservoirs, river diversions, or canal deliveries, and water pumped from rivers or ground water. Such water sources are generally easier to measure than the water uses. However, in many projects measurement and records are not sufficient to provide these volumes within the desired accuracy. Oftentimes flow measurement devices are either improperly installed or calibrated, nonfunctional, or missing entirely. Records of water deliveries are not always accurately maintained. In most states measurement of ground water pumping is not required and wells are simply not metered. Depending on site specific conditions, quantifying the water supply can be as difficult and expensive as measurement of the water uses.

ESTIMATING CONFIDENCE INTERVALS

For many water quantities or uses, estimates of measurement error can be made from evaluation of the methods and instruments in use. Meter specifications often give only the precision of the reading, which can be much smaller than the accuracy and does not take into account errors associated with a specific installation. Some meters provide an accuracy for a single reading but do not separate the systematic and random error components, which are needed to determine the error associated with repeated measurements. Furthermore, the accuracy of secondary devices, which translate the primary measurement device into a useful reading, can add error to the overall measurement that is often not included in the published accuracy of the primary device. In some cases periodic readings from a measuring device that measures flow rate are used to determine volume over time. This is typically done in a systematic fashion (e.g., each morning), which can also add a systematic error. Even for well-documented water measurement devices, some engineering analysis and judgment may be required to estimate the confidence interval of the measured water volume.

For many of the quantities or uses in the water balance, the values chosen are no better than educated guesses. For such uses determining the accuracy or confidence interval is very difficult. Also, for some instruments and equipment, errors are often one-sided. Examples include pyranometers and radiometers whose lenses get dirty (and thus read low), or propeller meters that turn slower as the bearings wear.

The confidence interval reflects a best estimate of the range of likely values for the quantity of interest. For quantities with limited available data, we can estimate the largest value we think is possible, and the lowest value we think is possible. That is, rather than defining the expected value and standard deviation, we define a range over which we are confident the true value will lie. This is commonly done in simulation studies, where a triangular distribution is defined based on minimum, maximum, and most likely value (Pritsker 1986). For our purposes we suggest using this range as the confidence interval. If this range is ± 2 standard deviations, then the standard deviation is one-fourth the range.

The calculation of standard deviation and confidence interval range do not assume anything about the probability distribution. However, for different distribution types (e.g., other than Gaussian), the probability of being within ± 2 standard deviations may not be 95% and the expected value may not be in the center of the *CI* range. If the most likely value of one quantity is not centered on the range, then we have no way of easily determining where the confidence interval for the final value is relative to the expected value. For example, if the confidence interval range is 4 (± 2) and the expected value is 10, then if it is centered, the confidence interval is 8–12. However, it may also be 9–13 or 7.5–11.5. For now we recommend assuming that the most likely value is in the middle of the range. In reality the confidence intervals provided with this methodology are simply an estimate.

The statistical procedures demonstrated in the following examples allow us to determine the influence of the accuracy of

any particular quantity on the accuracy of the final result. For some of the smaller quantities in the water balance, whether the confidence interval is very wide or very narrow has little influence on the accuracy of the final result, and a reasonable guess is sufficient. The larger quantities typically need to be determined very accurately.

EXAMPLES

Example 1. Simplified Example for Estimating *IE* Confidence Intervals

Consider a seasonal evaluation of a field with inflows and beneficial uses, and their associated accuracies as given in Table 1. The beneficial leaching for salt removal in Table 1 was based on a leaching requirement of 0.07, knowledge that there was no underirrigation, and the assumption that no rainfall ended up as deep percolation. The volume of leaching water is found from (18). The confidence interval for the volume of beneficial leaching was assumed to be ±30%. The coefficient of variation of the ratio $LR/(1 - LR)$ can be taken as

$$CV_{\text{ratio}} = \left(1 + \frac{LR}{1 - LR}\right) CV_{LR} \tag{19}$$

which can be derived from (7) and (13), assuming that *LR* and $(1 - LR)$ are 100% correlated and are a simplified form of (12). With $CV_{LR} = 0.15$ and $LR/(1 - LR) = 0.075$, (19) gives $CV_{\text{ratio}} = 0.161$. Since the volume of beneficial leaching is obtained by multiplying this ratio by the beneficial *ET*, (11) is used to compute the *CV* for the beneficial leaching, which is 0.166. This gives a confidence interval of ±0.333 or ±33.3%, as shown in Table 1.

The other beneficial uses were assumed to range from 0 to 2% of the beneficial *ET*. This was assumed to represent the confidence interval, giving an expected value of 1% and a *CI* = ±100%. The accuracies given in Table 1 are typical of engineering studies of actual beneficial uses, based on careful inflow and outflow measurements [see Burt et al. (1997) for further discussion].

Find. The volume of beneficial use and *IE*, and their associated *CI*s. First assume that these volumes are all independently measured, then assume that all beneficial uses are related to beneficial *ET*.

Solution with Independent Estimates. The volume of beneficial use is 6,000 + 450 + 60 = 6,510 m^3. The variance of beneficial uses is found from (6), assuming these uses were independently estimated

$$s_{BU}^2 = 240^2 + 75^2 + 30^2 \tag{20}$$

which gives $s_{BU}^2 = 64{,}125$ m^6, or $s_{BU} = 253$ m^3, resulting in a confidence interval of $\pm 2s_{BU} = \pm 507$ m^3, or a range of 6,005–7,019 m^3. The confidence interval expressed in terms of the coefficient of variation is ±7.8%. The variances in column 4 of Table 1 indicate the relative influence of the different beneficial use components on the variance of the total beneficial use. Note that the large uncertainties associated with the smaller volumes do not have much influence on the confidence interval of the total. Also, when several independent random numbers are summed, the accuracy of the total can be better than any of the components (i.e., the *CI* for beneficial *ET* was ±8.0%, and for total beneficial use was ±7.8%).

TABLE 1. Example Data for Computing Confidence Intervals for *IE*

Measured variable (1)	Volume estimate (m^3) (2)	Standard deviation (m^3) (3)	Variance (m^6) (4)	Confidence interval (±2*CV*) (%) (5)
Sum of irrigation water uses	10,000	250	62,500	±5.0
Beneficial *ET*	6,000	240	57,600	±8.0
Beneficial leaching for salt removal	452	75	5,641	±33.3
Other beneficial uses	60	30	907	±100.0
Total beneficial uses	6,512	253	64,148	±7.8

If the beneficial uses and net irrigation water uses are estimated independently, the expected value of *IE* is computed from (12), giving

$$m_{IE} = \frac{6{,}512}{10{,}000}\left(1 + \frac{250^2}{10{,}000^2}\right) \times 100\% \tag{21}$$

or 65.2%. (For division the expected value is actually affected by the accuracy of the denominator because the influence of the denominator on the value of the quotient is highly nonlinear.) The variance and standard deviation are found from (13), or

$$s_{IE}^2 = \left(\frac{6{,}512}{10{,}000}\right)^2 \left[\left(\frac{253}{6{,}512}\right)^2 + \left(\frac{250}{10{,}000}\right)^2\right] \times 100\% \tag{22}$$

which gives $s_{IE} = 3.0\%$. The confidence interval for the estimated irrigation efficiency is thus ±6.0%, for a range of 59–71%. This wide range is typical of attempts at trying to precisely define *IE* under field conditions.

Solution with Dependent Estimates. If all three beneficial uses are directly related to ET_{c-iw}, then an estimate of the *CI* of the total cannot be made by (6) unless the covariances are known. In this case the total beneficial uses are

$$BU_{\text{Total}} = ET_{c_{iw}}\left(1 + \frac{LR}{1 - LR} + \frac{BU_{\text{other}}}{ET_{c_{iw}}}\right) \tag{23}$$

To avoid computing covariances, we can evaluate the *CI* for the sum inside the parentheses with (6) and then evaluate the *CI* for the product of $ET_{c_{iw}}$ and this sum with (11).

The sum in the parentheses of (23) is 1.085. The *CV* for this sum is computed from the standard deviation of the total

$$s^2 = 0^2 + (0.161 \times 0.075)^2 + (0.50 \times 0.01)^2 \tag{24}$$

giving $s = 0.013$ and $CV = 0.013/1.085 = 0.0121$. Combining this with the *CV* for the beneficial uses of 0.04 with (11) gives $CV_{BU} = 0.042$, or a confidence interval of 8.4%, rather than the 7.8% computed with independent components. Using the foregoing procedures gives a confidence interval for *IE* of ±6.4%, rather than 6.0% when estimates were assumed to be independent.

Example 2. Detailed Example of Project Water Budged

Data for this example were taken from Styles (1993) and are based on a study done for the Imperial Irrigation District, located in southern California. Styles made estimates of all the major components for a hydrologic water balance for the years 1987–92. In this example we use Styles's estimates of these water-balance components for the year 1987. This example is for illustrative purposes and no attempt was made to correct errors or omissions from that report. We have assigned rough estimates for the accuracy of the various water volumes reported (Styles 1993). These are considered potential systematic errors (most quantities were based on a large number of measurements such that the effects of random errors were minimized) and are not meant to be definitive. For this example we only consider the division between consumptive and non-

consumptive uses of irrigation water and do not attempt to determine beneficial and/or reasonable uses. Furthermore, this example is intended to demonstrate the procedures rather than to determine definitive performance values.

Styles (1993) performed a water balance on the entire valley, including the underlying ground water aquifers. The major inflows and outflows are measured, and the change in storage was assumed to be negligible due to the unique hydrologic conditions. Table 2 shows the estimated volume of inflow for the year 1987. Canal inflow represents the flow into the irrigated area from the All-American Canal. Colorado River water diverted into the canal and delivered to other users or lost to seepage and evaporation along the way is not included (i.e., Table 2 includes only the water that reaches the irrigated area). The accuracy of this volume is based on details not shown here and which have a minor influence on these results. Details of the other inflows are given in Styles (1993). These other inflows have a minor influence on the accuracy of the total inflow, as can be seen by comparing the magnitudes of the variance in column 5 of Table 2.

The major outflows from the valley are the Alamo and New River flows to the Salton Sea, a saline lake whose surface is approximately 70 m below mean sea level. The sea has risen over the past several decades such that most of the irrigated land that is adjacent to the sea is below the Salton Sea level and below the local river levels. Local drainage flow in this area must be pumped into the sea or into one of the two rivers. Much of the soil in this area is very heavy clay, such that very little subsurface flow passes the boundary between the sea and the local aquifer (Table 3). With very heavy soil underlying most of the valley, subsurface flow into and out of the other boundaries is also minimal; there is no conjunctive use.

High water tables exist throughout most of the valley and tile drainage is used to remove excess water. Deep surface drains carry away tile drainage, tailwater runoff, and canal spills into the two rivers. Very little change in long-term aquifer storage exists, such that on a year to year basis overall district storage changes are minimal. Several surface reservoirs exist in the valley, but their changes in storage were not considered by Styles's water budget because their volumes are insignificant. The results of the water budget are given in Table 4, where total consumption (primarily *ET*) for the entire valley is the remainder.

In Table 5 water consumption is divided among the various uses, with total water consumption on irrigated land as the remainder. This consumption is further divided (Table 6) be-

TABLE 2. Surface and Subsurface Water Inflows, Example 2

Category (1)	Volume (1,000 dam³) (2)	Confidence interval (%) (3)	Standard deviation (1,000 dam³) (4)	Variance (1,000 dam³)² (5)
Canal inflow	2,159	±3.6	39	1,545
River inflows from Mexico	205	±10	10	105
Total rainfall	102	±30	15	235
Other surface inflows	2	±30	0	0
Subsurface inflow	16	±30	2	6
Total inflow	2,485	±3.5	43	1,891

TABLE 3. Surface and Subsurface Water Outflows, Example 2

Category (1)	Volume (1,000 dam³) (2)	Confidence interval (%) (3)	Standard deviation (1,000 dam³) (4)	Variance (1,000 dam³)² (5)
Alamo River outflow	415	±8	17	276
New River outflow	400	±8	16	256
Direct flow to Salton Sea	80	±10	4	16
Subsurface outflow	2	±40	0	0
Total outflow	897	± 5.2	23	548

TABLE 4. Total Consumption (Primarily *ET*) for Area as Remainder, Example 2

Category (1)	Volume (1,000 dam³) (2)	Confidence interval (%) (3)	Standard deviation (1,000 dam³) (4)	Variance (1,000 dam³)² (5)
Total inflow	2,485	±3.5	43	1,891
Total outflow	−897	±5.2	23	1,548
Change in storage	−0	undefined	4	16
Total water consumption	1,588	±6.2	50	2,455

TABLE 5. Determining Irrigated Farm Consumptive Use by Subtracting Nonfarm Consumptive Use from Total Consumptive Use, Example 2

Category (1)	Volume (1,000 dam³) (2)	Confidence interval (%) (3)	Standard deviation (1,000 dam³) (4)	Variance (1,000 dam³)² (5)
Total water consumption	1,588	±6.2	49	2,455
Canal and reservoir evaporation	−24	±20	2	6
Consumption by M&I users	−40	±20	4	16
ET from rivers, drains, and phreatophytes	−73	±20	7	53
Rainfall evaporation from nonirrigated land	−13	±20	1	2
Total water consumption on irrigated land	1,439	±7.0	50	2,531

TABLE 6. Calculations for Irrigation Water Consumption on Irrigated Lands, Example 2

Category (1)	Volume (1,000 dam³) (2)	Confidence interval (%) (3)	Standard deviation (1,000 dam³) (4)	Variance (1,000 dam³)² (5)
Total water consumption on irrigated land	1,439	±7.0	50	2,531
Effective precipitation	−52	±20	5	27
Noneffective rainfall evaporation	−23	±20	2	5
Total irrigation-water consumption on irrigated land	1,364	±7.4	51	2,563

TABLE 7. Calculations for Dividing Canal Water into Irrigation and Municipal and Industrial Uses, Example 2

Category (1)	Volume (1,000 dam³) (2)	Confidence interval (%) (3)	Standard deviation (1,000 dam³) (4)	Variance (1,000 dam³)² (5)
Canal inflow	2,159	±3.6	39	1,545
M&I deliveries	52	±5	1	2
Canal inflow for irrigation	2,107	±3.7	39	1,546

tween rainfall and irrigation water. In Table 7 canal inflow is divided among irrigation uses and municipal and industrial (M&I) uses. Since M&I uses are such a small percentage, we assigned all canal seepage, evaporation, and spills to the irrigation water supply.

For Tables 2–9, and 13 variance of the total, sum, or remainder (shown in column 5) is the sum of the component variances, since all components were independently estimated [i.e., this is the solution of (6) extended to many components with a covariance of 0]. This variance is then used to determine the confidence interval of the result.

There are many sources of water that end up as flow in the two river systems. These river flows have two destinations: (1) Flow to the Salton Sea; and (2) evaporation from open water surfaces and evapotranspiration of phreatophytes (called the *ET* component subsequently for simplicity). In the latter case the surface drains are included as part of the river system. An estimate for the total river inflow is given in Table 8.

Table 9 divides the irrigation water into its destinations, with the remainder representing the amount of irrigation water contributing to total river flow. With this and the other quantities estimated by Styles (1993), there is sufficient information to determine the breakdown of water inflows that contribute to the various water outflows, as shown in Table 10.

Still remaining is the partitioning of the irrigation water contributing to total river flow into *ET* and flow to the Salton Sea. Here it is assumed that all sources of total river flow are partitioned into *ET* and flow to the sea with the same percentages. The *ET* portion is 73/887 = 8.2%. Then the irrigation water contribution to the *ET* portion is 8.2% of 629 dam^3, or 52 dam^3. The calculation of the variance of this result is more complicated. Eqs. (14) and (11) are used to determine the coefficient of variation of the quotient (73/887) and the product (0.082 × 639), respectively, assuming the terms are independent. The results of these calculations are given in Table 11. Unfortunately, the components in these calculations are not independently estimated, since the river *ET* component is used to estimate the total river inflow. Fortunately, this *ET* component has a small impact on the variance of the total river inflow (Table 8, column 5), and the coefficient of variation of total river inflow has a small impact on the total coefficient of variation. Thus, the lack of independence in this case should have a small impact on the results and can be safely ignored. This may not always be the case, as was shown in Example 1. Applying this procedure to the remaining water inflows results in the distribution of river flows given in Table 12.

Table 13 summarizes the consumptive uses of irrigation water inflows. Finally, the irrigation consumptive use coefficient is computed in Table 14. Eq. (14) is used to determine the coefficient of variation for the expected value of *ICUC*, assuming that the numerator and denominator in (14) are independent. To avoid confusion, the *CI*s in Table 14 are expressed as decimals rather than percentages. The expected value of *ICUC* is 68.3%, the confidence interval is ±0.080 × *ICUC* or from 0.92 × *ICUC* to 1.08 × *ICUC*. This translates to a confidence interval of ±5.5% (0.080 × 68.3%), or 63% < *ICUC* < 74%, a range of more than 10%. (Note: values in the tables for this example may contain roundoff errors.)

However, the two quantities shown in Table 14 for computing *ICUC* are both determined from the canal inflow given in Table 2, and thus are not independent. The equation for *ICUC* can be modified in an attempt to reduce the dependence

$$ICUC = \frac{A - B + C}{A - D} \times 100\% = \left(1 + \frac{-B + C + D}{A - D}\right) \times 100\% \tag{25}$$

where A, B, C, D, E = different water volumes. In this case, A = canal inflow (Table 2) and D = M&I deliveries (Table 7). Since D is extremely small relative to A, the interdependence of the numerator and denominator is minimized. This right-hand side numerator is really the (negative) volume of irrigation water not consumed. Table 15 shows the terms that make up the numerator of the quotient in the far right-hand term of (25). (These are taken directly from calculations in

TABLE 8. Total River Inflows Based on Total Outflows, Example 2

Category (1)	Volume (1,000 dam^3) (2)	Confidence interval (%) (3)	Standard deviation (1,000 dam^3) (4)	Variance (1,000 dam^3)^2 (5)
Alamo River outflow	415	±8	17	276
New River outflow	400	±8	16	256
ET from rivers, drains, and phreatophytes	73	±20	7	53
Total river inflow	887	±5.4	24	584

TABLE 9. Determining Amount of Irrigation Water Contributing to Total River Flow, Example 2

Category (1)	Volume (1,000 dam^3) (2)	Confidence interval (%) (3)	Standard deviation (1,000 dam^3) (4)	Variance (1,000 dam^3)^2 (5)
Canal water for irrigation	2,107	±3.7	39	1,546
Total irrigation water consumption on irrigated land	1,364	±7.4	51	2,563
Canal and reservoir evaporation	24	±20	2	6
Direct irrigation water flow to Salton Sea	80	±10	4	16
Irrigation water contribution to total river inflow	639	±20.1	64	4,131

TABLE 10. Disposition of Inflows and Outflows (1,000 dam^3), Example 2

Category (1)	Inflow (2)	Outflow					
		ET from irrigated land (3)	Canal and reservoir *ET* (4)	Noneffective soil evaporation (5)	Other consumption (6)	Direct flows to Salton Sea (7)	Total river inflows (8)
Canal inflow for irrigation	2,107	1,364	24			80	639
Canal inflow for M&I use	52				40		11
River inflows from Mexico	205						205
Rainfall on irrigated land	83	52		23			9
Rainfall on nonirrigated land	19			13			6
Other surface inflows	2						2
Subsurface inflows	16					2	15
Total	2,485	1,416	24	36	40	82	887

TABLE 11. Calculations for Partitioning Total River Flow into *ET* and Flow to Salton Sea, Example 2

Category (1)	Volume (1,000 dam³) (2)	Confidence interval (%) (3)	Coefficient of variation (4)	Coefficient of variation squared (5)
ET from rivers, drains, and phreatophytes	73	±20	0.10	0.0100
Irrigation water contribution to total river inflow	639	±20.1	0.10	0.0101
Total river inflow	887	±5.4	0.03	0.0007
Irrigation water contribution to *ET* from rivers, and so on	52	±29.0	0.014	0.0210

TABLE 12. Disposition of Inflows with Respect to Alamo and New River Flows (1,000 dam³), Example 2

Category (1)	Total river inflows (2)	Outflow: *ET* from rivers, drains, and phreatophytes (3)	Outflow: River flow to Salton Sea (4)
Canal inflow for irrigation	639	52	587
Canal inflow for M&I use	11	1	10
River inflows from Mexico	205	17	188
Rainfall on irrigated land	9	1	8
Rainfall on nonirrigated land	6	1	6
Other surface inflows	2	0	2
Subsurface inflows	15	1	13
Total	887	73	815

TABLE 13. Total Irrigation Water Consumption, Example 2

Category (1)	Volume (1,000 dam³) (2)	Confidence interval (%) (3)	Standard deviation (1,000 dam³) (4)	Variance (1,000 dam³)² (5)
Irrigation water consumption on irrigated land	1,364	±7.4	51	2,563
Canal and reservoir *ET*	24	±20	2	6
Irrigation water contribution to *ET* from rivers, and so on	52	±29.0	8	57
Total irrigation water consumption	1,440	±7.1	51	2,626

TABLE 14. Calculations for Irrigation Consumptive Use Coefficient, *ICUC*, Example 2

Category (1)	Volume (1,000 dam³) (2)	Relative confidence interval (±2*CV*) (3)	Coefficient of variation (4)	Coefficient of variation squared (5)
Total irrigation water consumed	1,440	±0.071	0.036	0.0013
Total irrigation water supply	2,107	±0.037	0.019	0.0003
ICUC	0.683	±0.080	0.040	0.0016

Tables 2–13.) Note that in the calculations, canal and reservoir ET is first subtracted and then added. Thus its variance really should not add to the variance of the result. Also, M&I deliveries and M&I consumption are offsetting, leaving the much smaller M&I return flows, with a much smaller variance. The last column in Table 15 gives the variances used in the calculations.

Table 16 shows the calculations for the confidence interval of the fraction not consumed. The confidence interval for this quantity is ±0.032 (0.317 × 0.104). Since taking 1 minus this quantity does not influence the confidence interval (when expressed in terms of 2*s*), *ICUC* has the same confidence interval, which translates to 65% < *ICUC* < 72%, a much narrower range than computed in the foregoing.

DISCUSSION

This detailed example is meant to show a general procedure and is not intended to reflect all possible methods to achieve a water balance or to estimate performance parameters. We do, however, intend to show how various volumes and their accuracies influence the accuracy of the final performance parameter estimates. We believe that the accuracies of water uses used in this example are typical of, and in many cases better than, the accuracies available in most irrigation districts. Furthermore, in many cases the accuracy for *IE* may be less than that for *ICUC*, since quantifying beneficial water uses is often quite difficult (e.g., beneficial leaching and distinguishing between beneficial *ET* and nonbeneficial evaporation). The confidence interval for *ICUC* in this example was about 7%. Thus, reporting of more than two significant figures for irrigation performance parameters is clearly inappropriate without careful analysis of potential errors.

One of the most powerful features of this approach is the ability to determine the relative importance of the accuracy of the variables that contribute to the estimate of these performance parameters. The variance, s^2, and relative variance, CV^2, of the components gives a general indication of the importance of the accuracy of that component on the accuracy of the final estimate. Take, for example, the estimate of the accuracy of the total irrigation water consumption on irrigated land in Table 6. The variance is dominated by one component, total water consumption on irrigated land. In Table 5 total water consumption dominates this variance (2,455 out of 2,531). Continuing to trace these back to their sources through Tables 4, 3, and 2, we find that four components dominate the variance of irrigation water consumption on irrigated land: canal inflow (1,545), Alamo River outflow (276), New River outflow (256), and total rainfall (235), as shown in Fig. 5. These variances reflect the importance of the accuracies of these measurements on the accuracy of the final result.

When the components in the water balance and performance parameter equations are independent, the statistics presented here are straightforward to apply. However, often we do not have independent estimates of the various quantities. This can greatly increase the complexity of the analysis. When quanti-

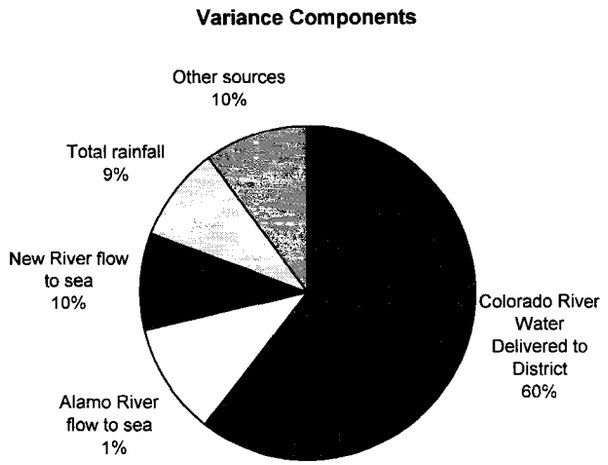

FIG. 5. Variance Components for Consumption of Irrigation Water on Irrigated Land (See Tables 2–6)

TABLE 15. Quantities Used to Determine Irrigation Water Not Consumed, Example 2

Category (1)	Volume (1,000 dam³) (2)	Confidence interval (%) (3)	Standard deviation (1,000 dam³) (4)	Variance (1,000 dam³)² (5)	Variance used (1,000 dam³)² (6)
River inflows from Mexico	205	±10	10	105	105
Total rainfall	102	±30	15	235	235
Other surface inflows	2	±30	0	0	0
Subsurface inflow	16	±30	2	6	6
Alamo River outflow	−415	±8	17	276	276
New River outflow	−400	±8	16	256	256
Direct flow to Salton Sea	−80	±10	4	16	16
Subsurface outflow	−2	±40	0	0	0
Canal and reservoir evaporation	−24	±20	2	6	
Consumption by M&I users	−40	±20	4	16	
ET from rivers, drains, and phreatophytes	−73	±20	7	53	53
Rainfall evaporation from nonirrigated land	−13	±20	1	2	2
Effective precipitation	−52	±20	5	27	27
Noneffective rainfall evaporation	−23	±20	2	5	5
Canal and reservoir *ET*	24	±20	2	6	
Irrigation water contribution to *ET* from rivers, and so on	52	±29.0	8	57	57
M&I deliveries	52	±5	1	2	1
Total	−667	±9.7	32		1,038

TABLE 16. Calculations for Fraction of Irrigation Water Not Consumed, (1 − *ICUC*), Example 2

Category (1)	Volume (1,000 dam³) (2)	Relative confidence interval (±2*CV*) (3)	Coefficient of variation (4)	Coefficient of variation squared (5)
Unconsumed irrigation water	667	±0.097	0.048	0.0023
Total irrigation water supply	2,107	±0.037	0.019	0.0003
1 − *ICUC*	0.317	±0.104	0.052	0.0027

ties are directly related, accounting for the dependence may be easy, as was the case for the beneficial uses in Example 1. However, in other cases, the interdependence is not as straightforward. Further examples on the influence of component interdependence are given in Appendix I.

Furthermore, independent components typically lead to narrower confidence intervals when components are added, as shown by Example 1, where the confidence interval went from ±8.0 to ±8.6% when the dependence of components was considered. Thus, we recommend that independent estimates of each component in the water balance be made, if possible. In some cases multiple independent estimates of a water use of water-balance component may be available. However, for calculating the confidence interval of the performance parameters, dependence may actually improve the estimate, as shown in Example 2. The statistical procedures for dealing with these situations may still need improvement.

CONCLUSIONS

This paper underscores the importance of properly defining the components in a water balance when attempting to arrive at irrigation performance measures. The equations provided herein can be used to determine the accuracy of these irrigation performance measure estimates, based on the accuracy of the water-balance components. The examples given provide some practical guidance on the use of these procedures. In addition, it is shown that the component variances can be used to determine which measured volumes need closer attention. Improving the accuracy of those components with the highest variances will have the greatest impact on improving the accuracy of the performance measures. Finally, we recommended that studies that report irrigation performance measures also provide estimates of the confidence intervals of these parameters so that inappropriate conclusions are not drawn.

ACKNOWLEDGMENTS

The writers would like to gratefully acknowledge the contributions of the Technical Working Group for the Water Use Assessment of the Coachella Valley Water District and the Imperial Irrigation District organized by the Lower Colorado Region of the Bureau of Reclamation. The writers would also like to express appreciation for the funding provided by the districts and the Bureau. The members of the group in addition to the writers were Steve Jones, U.S. Bureau of Reclamation, Boulder City, Nev.; Marvin Jensen, Consultant, Fort Collins, Colo.; Ken Solomon, Professor and Head, BioResource and Agricultural Engineering Department, California Polytechnic State University, San Luis Obispo, Calif.; and Joe Lord, Consultant, Fresno, Calif.

APPENDIX I. INFLUENCE OF DEPENDENCE ON VARIANCE ESTIMATES

It is well known that random errors in measurement can be reduced by repeated sampling. For example, if a single measurement has a random error of 10%, then averaging five measurements reduces the error to $10\%/\sqrt{5}$, or 4.5%. The same principle applies to components in the volume balance; the more independent measurements that are needed to estimate the volume for a component, the smaller is the variance of the estimate. Suppose we have two independent variables (y_1 and y_2) that add (or subtract) to determine another (y_0). Suppose $y_1 = 50$, $y_2 = 50$, and $y_0 = 100$. If the standard deviations of y_1 and y_2 are both 5, then by (6), the standard deviation of y_0 is $5 \times \sqrt{2} = 7.07$. The coefficients of variation for y_1 and y_2 are both 10%, while $CV_0 = 7.07\%$. Note that the value of s_0 does not depend on whether the components are added or subtracted; however, the value of CV_0 does [i.e., it depends on m_0; (8)].

If two parameters are dependent, it is necessary to estimate the covariance, s_{12}^2. The covariance indicates how well the two parameters are correlated. It can be estimated from

$$s_{12}^2 = \rho^2 s_1 s_2 \tag{26}$$

where ρ^2 = correlation coefficient (e.g., R^2 from linear regression with 0 intercept). Note that we have ignored higher-order terms in these equations (e.g., higher-order terms in polynomial regression). Suppose that in the above example, y_1 and y_2 are perfectly correlated, or $\rho^2 = 1$. Then $s_{12}^2 = s_1 \times s_2$. Applying (6), we find that $s_0^2 = 5^2 + 5^2 + 2 \times 1^2 \times 5 \times 5$

= 100. This gives $s_0 = 10$ and $CV_0 = 10\%$. Now the accuracy of the sum is not influenced by the fact that two correlated variables were used to determine its value.

Clearly, many of the components in the volume balance influence each other. But, here, we are dealing not with whether or not the variables are dependent on one another, but whether the estimate for one variable is dependent on the estimate for another. Even so, estimating this dependence is tricky. One might expect that $ET_{c_{iw}}$ is well correlated with the net project irrigation water supply due to the volume balance procedure (Table 5). However, if the latter increases by 10% (61.3 m^3), the former increases by 61.3 over 390, or 15.7%. An estimate for ρ^2 was obtained by solving for project *IE* (Table 16) and its *CI* without the intermediate calculation of $ET_{c_{iw}}$ (i.e., *CI* was ±13.7%). Ignoring the correlation gave *CI* = ±15.6%. To obtain the same estimate for the *CI* (i.e., ±13.7%) from (13) and (26) required $\rho^2 = 0.45$. (This is close to the ratio of the values squared.)

APPENDIX II. REFERENCES

Burt, C. M., et al. (1997). "Irrigation performance measures: efficiency and uniformity." *J. Irrig. and Drain. Engrg.*, ASCE, 123(6), 423–442.

Jensen, M. E., Burman, R. D., and Allen, R. G., eds. (1990). "Evapotranspiration and irrigation water requirements." *ASCE Manuals and Reports on Engineering Practice*, American Society of Civil Engineers, New York, N.Y., No. 70.

Ley, T. W., Hill, R. W., and Jensen, D. T. (1994). "Errors in Penman-Wright alfalfa reference evapotranspiration estimates. I: Model sensitivity analysis." *Trans. ASAE*, 37(6), 1853–1861.

Mood, A. M., Graybill, F. A., and Boes, D. C. (1974). *Introduction to the theory of statistics*, McGraw-Hill Inc., New York, N.Y.

Pritsker, A. A. B. (1986). *Introduction to simulation and slam II*, 3rd Ed., John Wiley & Sons, Inc., New York, N.Y.

Rhoades, J. D. (1974). "Drainage for salinity control." Chap. 16 in *Drainage for agriculture*, Agronomy Monograph No. 17, American Society of Agronomy, Madison, Wisc.

Styles, S. W. (1993). "On-farm irrigation efficiency." *Spec. Tech. Rep. for Imperial Irrigation District*, Boyle Engineering Corp., Imperial, Calif.

IMPACT OF WATER MEASUREMENT ACCURACY AND WATER BALANCE ANALYSIS ON WATER DUTIES AND ALLOCATIONS

Albert J. Clemmens
Director
U.S. Water Conservation Laboratory
USDA – Agricultural Research Service
4331 E. Broadway
Phoenix, AZ 85040 USA
1-602-379-4356 x269
1-602-379-4355 Fax
bclemmens@uswcl.ars.ag.gov
www.uswcl.ars.ag.gov/

ABSTRACT

When the total demand for water exceeds the available supply, as is the situation in the Western United States, our ability to determine the fate of irrigation water diverted and applied becomes crucial. On-farm water management is more concerned with the health and vigor of the crop than in whether water applied is consumed, runs off, or percolates to groundwater. However, management of the water resource requires reasonable knowledge of the ultimate fate of all water diverted. Such a water balance for an irrigated region is extremely difficult to obtain. While often the major surface inflows and outflows can be measured, many of the other inputs and outputs can only be estimated. The accuracy of these measurements and estimates becomes increasingly important as water management decisions are based on these results. In the U.S., water transfers, state water diversions, and (ultimately) water rights or duties are being influenced by water balances and our ability to accurately determine these water quantities. Several case studies from the southwestern U.S. are discussed in this paper.

INTRODUCTION

Competition for water is becoming intense in many arid areas of the world. Quantifying water use for an irrigated area is a difficult task. Once applied to the land, irrigation water become part of the natural hydrologic system and is difficult to track. This makes it difficult to quantify irrigation water use to a high degree of accuracy. Inaccurate estimates of water use by agriculture and other water users complicate the determination of water duties and whether or not water use is within those duties. The purpose of this paper is to discuss the accuracy of water use estimates and how this influences the management of water supplies.

WATER BALANCE

It is difficult to get an accurate picture of irrigation water use within an agricultural area without a good water balance. Water purveyors may have records of irrigation water delivered, but actual crop consumption and return flows are often less accurately known. Irrigation return flows and water reuse complicate the value of such records. The mixing of rainfall with irrigation water in drainage flows, surface streams, and groundwater further complicates the issue. Methods for estimating crop ET have been useful for irrigation scheduling and management, but their accuracy and usefulness for quantifying water uses has not been well documented.

Application of a water balance to the estimation of irrigation system performance is essential, as are determining the accuracy of associated performance parameters (Burt et al. 1997). One important contribution to our understanding of performance assessments by Burt et al. (1997) was inclusion of storage changes in the definition of irrigation efficiency. Essentially, water is not considered "used", beneficially or otherwise, while it is still in storage (i.e., irrigation water must leave the boundaries of the system before it can be considered in irrigation efficiency calculations). Solomon and Davidoff (1999) capture the essence of this by defining how irrigation efficiency is influenced by water reuse within a project, watershed, or river basin.

Use of a water balance requires careful consideration of the boundaries of the system. For any system, the lateral and vertical boundaries must be well defined. The aerial extent of the system can be on any scale (e.g., field, farm, district, or project), depending on the area of interest. The upper boundary is typically the top of the crop canopy. The lower boundary can be the bottom of the root zone, or may also include a shallow

groundwater aquifer or the entire groundwater aquifer, depending on the intent or the hydrologic setting. Then, a water balance is applied with the inflows, outflows, and changes in storage from the system. Figure 1 shows typical water balance components. Once all these quantities are known, judgements regarding the use of irrigation water can be made.

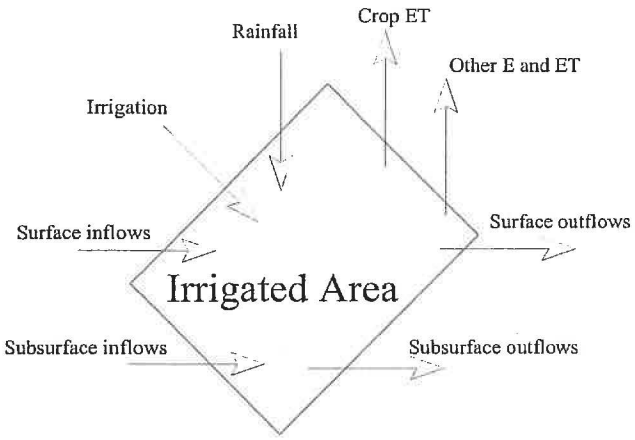

Figure 1. Water balance components.

ACCURACY OF MEASURED AND COMPUTED QUANTITIES

Statistical Equations

In a water balance, the inflows minus the outflows must theoretically equal the change in storage. In practice, all quantities in the water balance are not known with sufficient accuracy such that this relationship holds. Each quantity is estimated from some measurements – each measurement containing some degree of accuracy. The issue here is how we can estimate the accuracy of various water balance quantities from the raw measurements. Fortunately, standard statistical methods are available.

When two quantities are added together, the accuracy of the sum is related to the accuracy of the individual values through their variances (standard deviation squared), whereby

$$s_0^2 = s_1^2 + s_2^2 + s_{12}^2 \qquad (1)$$

where the subscripts $_1$, $_2$, and $_0$ refer to quantities 1 and 2 and the total, respectively, and s_{12}^2 is the covariance. If the two quantities are estimated independently, then the covariance is zero. Equation 1 does not require a normal distribution of values and is applicable regardless of sign (i.e., addition or subtraction). This equation can be extended to any number of quantities.

When two quantities are multiplied together, the influence of the variability of each quantity on the variability of the result is related to their relative size. If the two quantities are independent, then the variability of their product can be found from

$$CV_0^2 = CV_1^2 + CV_2^2 + CV_1^2 CV_2^2 \qquad (2)$$

where *CV* is the coefficient of variation, or the standard deviation divided by the mean. This can be extended to any number of quantities multiplied together. Even when the quantities are correlated, exact solutions to the variance and coefficient of variation can be computed.

Determining the accuracy of ratios is more difficult to handle statistically. No exact solutions are available. This is not surprising since quotients are not very symmetrical (e.g., a 25% increase is the inverse of a 20% decrease). Still, statistics are able to give us approximate equations that provide reasonable results. A conservative estimate of the CV for the quotient of two independent quantities can be found from

$$CV_0^2 \approx CV_1^2 + CV_2^2 \qquad (3)$$

Further details can be found in Clemmens and Burt (1997).

Accuracy is often expressed as a percentage of value. Generally, the 95% Confidence Interval is used to define this accuracy – where 95% of the readings are expected to fall within this range. For a normal distribution of values, this confidence interval is approximately ± two standard deviations (or in relative terms two times the coefficient of variation). For simplicity, I use ± two standard deviations as the confidence interval (CI). If the distribution is other than normal (Gaussian), then the CI may represent some percentage other than 95%. When I refer to accuracy in what follows, I mean CI.

Accuracy of Discharge Measurements

Errors in discharge measurements can be categorized as systematic or random. Random errors are much easier to deal with, since their effects can be reduced by repeated measurements. Systematic errors for an individual device are not reduced by repeated measurements. However, when many devices each have a systematic error, part of that systematic error can be random from device to device. Thus summing the measurements from many devices or structures can reduce the effect of the systematic error.

The most common discharge measurements for irrigation flows are

- current metering in large channels and rivers
- flumes and weirs in canals,
- and various meters in pipelines (e.g., propeller meters).

Few individual discharge measurements made with most of these methods are better than ±5%. Estimating volumes from discharge rate measurements requires integration over time. Since irrigation flows are rarely steady, converting measured discharge rates to volumes introduces additional error into the volume estimate. However, use of many discharge rate measurements reduces the contribution of random errors on the accuracy of the water volume.

Wahlin et al. (1997 and errata 1999) examined the accuracy of discharge measurements for the major inflows and outflows to the Imperial Valley of California (All American Canal, Coachella Canal, and Alamo and New Rivers). For sites with weekly current metering and continuous stage recording, the accuracy of individual current-meter discharge measurements ranged from ±6 to ±9%. The accuracy of average daily flow rates based on stage ranged from ±6 to ±16%. However, because most of the errors were random and measurements were taken frequently, the accuracy for annual volumes were ±2.3 to ±2.6% -- in some cases a 5:1 difference between daily and annual volume accuracy. However, for the large Parshall flume on the Coachella canal that had been calibrated with current metering, the accuracy of the average daily flow was ±3.2%, while the accuracy of the annual volume was ±2.5%. This small difference between daily and annual accuracy resulted from the relatively large systematic error of the flume rating.

Table 1. Summary of measurement accuracy for major Imperial Valley inflows and outflows (Wahlin et al., 1997 and errata 1999).

Site	95% CI for Individual Current Metering	95% CI for Average Daily Flow Rate Based on Stage	95% CI for Annual Volume
All-American Canal at Pilot Knob	± 6.6%	± 6.6%	± 2.3%
Coachella Canal	Not applicable	± 3.2%	± 2.5%
New River at Mexican boundary	± 8.5%	± 8.7%	± 2.3%
Alamo River at Salton Sea	± 6.3%	± 15.5%	± 2.6%
New River at Salton Sea	± 7.3%	± 10.1%	± 2.3%

Bos et al. (1984) claim ±2% accuracy for long-throated flume and broad-crested weir computer calibrated ratings. Much of the error in an actual discharge measurement, especially for small flumes, is in the zero-setting and reading of the flume head. This often produces an instantaneous discharge reading accuracy of ±5%. For long-term volumes, the accuracy improves, provided that a sufficient number of measurements are taken relative to the amount of flow-rate variation that occurs. Most other weirs, flumes and orifices require field calibration to attain high accuracy, as was performed for the Coachella Canal Parshall flume.

For irrigation districts with a large number of similar devices at delivery turnouts or spill sites, the integration of volume over a large number of sites will also reduce the random error associated with these structures, for example due to random errors in zero setting or in constructed dimensions. However, such a large number of sites will not remove the systematic error or bias in the basic device calibration.

District records of water delivered can be inaccurate because of methods used to measure and accumulate flows and because of accounting procedures. Some districts maintain different records of water delivered and water billed because they differ for a variety of reasons (e.g., poor service, free water during times of excess, etc.). Some districts intentionally deliver more water than what they bill users. This leaves users with little room to complain and allows the flow rate to fluctuate without dropping below the requested and billed rate. This intentional over delivery may or may not show up in district records. Other districts do not monitor delivery gates frequently enough when flows fluctuate and thus do not accurately accumulate volume.

Careful examination of measurement and volume accumulation procedures and flow conditions at turnouts are necessary in order to get an accurate picture of the accuracy of district water delivery records. Internal water balances are also useful for verifying district records (e.g. volumes delivered to and from lateral canals).

Accuracy of *ET* Estimates

Evapotranspiration is one of the most difficult quantities to measure accurately over an extended period of time and over a large geographic area. Point in time and single aerial location estimates are useful, but large errors can occur when these are extrapolated over space and time. Methods are available for determining the consumptive use of crops from weather data and crop coefficients. There are many uncertainties in applying this approach to large geographic areas. First, the exact cropped acreage and planting and harvest dates must be known. Few irrigation projects keep detailed records of this. Second, there must be a sufficient number of weather stations to cover the geographic diversity. Next, this method assumes that an entire field has crops using water at the rate of a non-stressed crop, whereas because of soil spatial variability and irrigation nonuniformity there are usually significant areas of a field that are consuming less water than other areas. Varietal and cultural variations cause standard crop coefficient curves to be biased. One must also consider *ET* from noncropped areas that are wetted during irrigation, plants that use water along canals and drains, canal and reservoir evaporation, dormant season *ET*, etc. Without extreme care, the accuracy of *ET* estimates with this procedure can easily exceed ±30%.

Subsurface flows are very difficult to quantify, thus having a closed basin reduces the complexity of dealing with that issue. For some geologically closed basins, it is possible to estimate total evapotransiration as the remainder in the water balance. However, the accuracy of a remainder in a water balance is always much less than the accuracy of the measured quantities. Just for example, if one measures 100 units into the system with ±10% accuracy (2s=10 units) and measures 50 units out with perfect accuracy, the remainder is 50 units with ±20% accuracy (10 units/50 units = 20%). Even where inflows and outflow are accurately measured, uncertain rainfall volumes can greatly reduce the accuracy of the remainder.

Accuracy of Beneficial Leaching

The leaching requirement is often used to define the amount of additional water that needs to be leached through the soil to maintain root-zone salinity below acceptable levels for various crops. Because of the spatial variability of soil properties, the preferential flow of water through soils, variations in climate, and variations in crop sensitivity to different types of soil salinity, estimates of leaching requirements are by their nature inexact. The determination of leaching requirements usually assumes that the soil salinity is in a state of equilibrium, whereas often it is not. Further, there are significant questions about how to determine the leaching requirements for crops in rotation with significantly different leaching requirements. The contributions of rainfall to leaching must also be considered. And while theoretical leaching requirements can be computed, it is quite another matter to actually measure the amount of leaching that occurred and was beneficial. For small areas, often *ET* is computed from weather data and crop coefficients with deep percolation computed as the remainder in the water balance. Without extensive soil water measurements over time, this method for estimating deep percolation can be highly inaccurate.

Accuracy of Other Beneficial Uses

Irrigation and farming are as much art as they are science. Supplying water for ET is only one aspect of beneficial use of irrigation water. Water is often used as a management tool, for example to prepare the soil for tillage or seedbed preparation. Water is also used for improving crop quality. Frost protection, cooling, etc. are extremely useful and beneficial. However, these applications of water end up as soil or crop ET, tailwater runoff, or deep percolation. Thus they are already included in the overall water balance and cannot be included twice. The only real difference is whether such water is considered beneficial in calculation of irrigation efficiency. These uses of water are generally quite small (e.g., on the order of 1 or 2%), and often within the accuracy of other estimates.

EXAMPLES

Water-Balance Example

The Lower Colorado River Accounting System (LCRAS) of the U.S. Bureau of Reclamation uses a water balance on the main stem of the lower Colorado River. This method is being proposed to replace the current decree accounting procedure for determining water consumption by state and by category of use (USBR

1998). Measurements are made at various stations along the river, for major diversion outside the river basin, and for major surface inflows. This is a multi-agency effort. Consumptive uses along the river are estimated using a weather-based reference-ET, crop-coefficient approach.

System inflow and outflows for 1996 taken from USBR (1998) are shown in Table 2, excluding consumption. These components are all based on physical measurements of flow or hydraulic estimates (e.g., groundwater flow, ungauged streams, etc.). The remainder in this water balance is the consumption along the river's main-stem, (2.78 km^3). This calculation was not made in USBR (1998). I made very rough estimates of the accuracy of these various estimates (based on experience with similar measurements, not from in-depth evaluation), which are also shown in Table 2. The accuracy of the estimated consumption can be determined from equation 1. These calculations are shown in Table 2, which results in an accuracy of the estimated consumption of ± 21%.

Table 2. Inflows and outflow to lower Colorado River main-stem for 1996, and estimates of accuracy, used to estimate consumption from a water balance. (Raw data from USBR, 1998).

Component	Value	Accuracy+	Standard Deviation.	Variance
	Km^3		Km^3	$(Km^3)^2$
River inflow	12.30	4%	0.25	0.0605
River outflow	-1.96	5%	0.05	0.0024
Exports	-7.74	4%	0.15	0.0240
Other inflows	0.12	50%	0.03	0.0010
Storage change	0.06	50%	0.01	0.0002
Consumption	*2.78	21%	0.30	*0.0880

+ Rough estimates * Sum

Table 3. Estimated consumption of water on the lower Colorado River main-stem for 1996 and estimates of accuracy. (Raw data from USBR, 1998).

Component	Value	Accuracy+	Standard Deviation	variance
	Km^3		Km^3	$(Km^3)^2$
Evaporation from open water surfaces	0.44	30%	0.07	0.0043
Domestic consumption	0.09	50%	0.02	0.0005
Crop ET	1.54	20%	0.15	0.0236
Phreatophyte ET	0.84	30%	0.13	0.0159
Consumption	*2.90	14%	0.21	*0.0443

+ Rough estimates * Sum

Main-stem consumption was also estimated from weather-based approaches. The values from USBR (1998) are given in Table 3, along with my very subjective estimates of the accuracy of those estimates. The result (2.90 km^3) is within 5% of the water balance estimate. The accuracy of this value is estimated to be ± 14%. These two estimates are within less than one standard deviation from each other, which is good agreement. (However, there is some question regarding whether the river water balance was used to adjust coefficients for the consumptive use estimates). Note that this analysis assumes that the quantities in Table 3 are independently estimated. If all these estimates were based on common reference ET numbers or even a common reference ET method, then a systematic error would have to be considered. This would increase the inaccuracy of the estimated consumption. Clemmens and Burt (1997) discuss methods for dealing with non-independent estimates. Tables 2 and 3 (last column) also demonstrate that the major contributors to variance of consumption are the river inflow measurement and the crop and phreatophyte ET estimates.

The issue for management along the river is how to assign consumptive use to various users along the river when the total consumption isn't even known to within ½ km^3 (out of roughly 3 km^3). The U.S. Bureau of Reclamation is considering a detailed analysis of the accuracy of water consumption along the river.

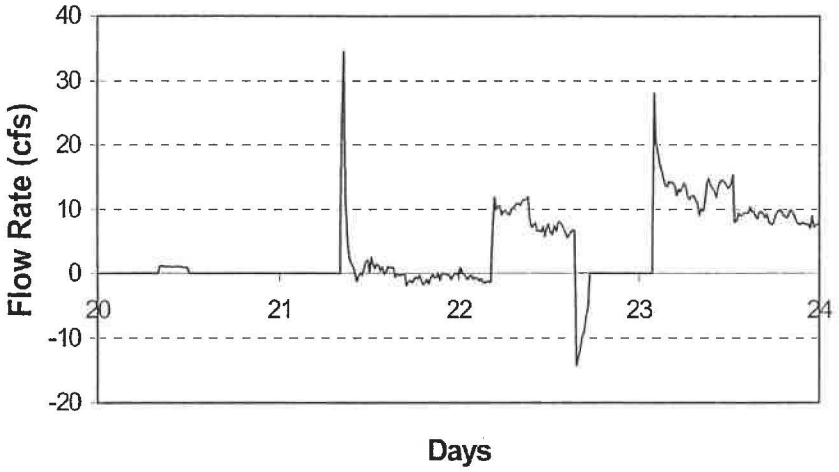

Fig. 2. Example of flow-balance graph for lateral canal (from Palmer et al. 1991).

Subsystem Water Balance Example

Palmer et al. (1991) extensively monitored two lateral canals within the Wellton Mohawk Irrigation and Drainage District in southeastern Arizona. All inflows to these lateral canals were continuously monitored (15 minute interval) with long-throated flumes and broad-crested weirs. Water balance graphs were prepared to assure that inflow and outflow balanced during non-transient periods. An example is shown in Figure 2. Note that changes in flow are obvious, as are periods of time when one or more recorders were not functioning. (In some cases, a few outflows were not measured, but instead estimated from the flow-balance graphs). Record keeping was rather lax in this district. Figure 3 shows that roughly 17% of the deliveries on these two laterals were not billed.

Ordered and actual flow rates often differed by as much as 20% (Fig. 4), while durations were often closer. Differences in actual and billed deliveries were also evident (Fig. 5). Contrary to typical expectations, the median delivered flow rates and durations were slightly less than what was ordered -- 2% and 4%, respectively. The median bill based on volume was for roughly 3% less than that actually delivered.

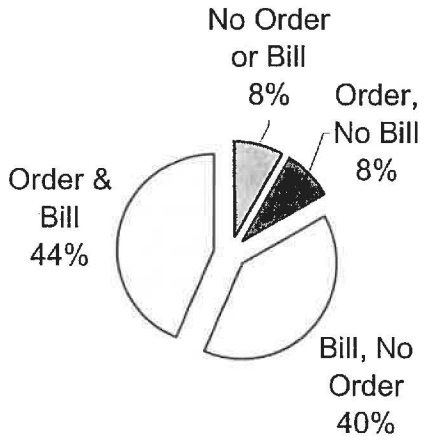

Fig. 3. Portion of measured deliveries from two monitored lateral canals with corresponding orders and/or bills (from Palmer et al. 1991).

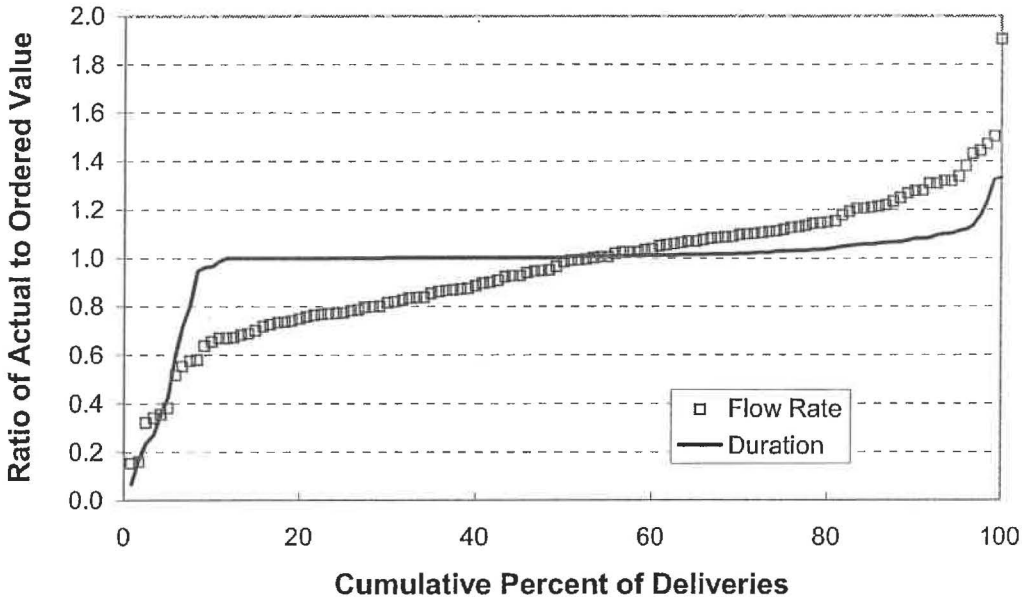

Fig. 4. Frequency distribution of the ratio of actual (measured) to ordered flow rate and durations for two monitored lateral canals (from Palmer et al. 1991).

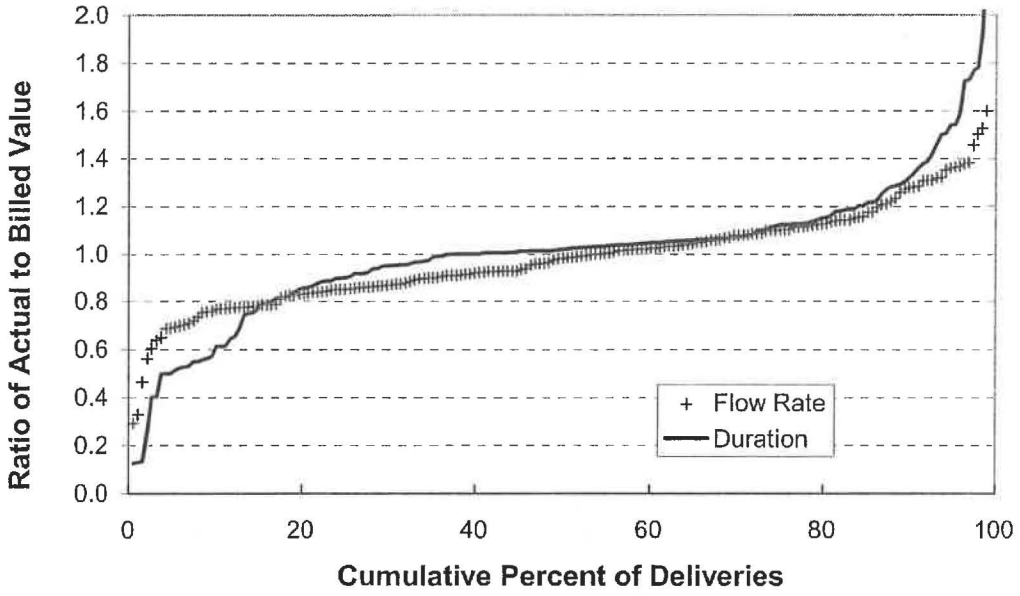

Fig. 5. Frequency distribution of the ratio of actual (measured) to billed flow rate and durations for two monitored lateral canals (from Palmer et al. 1991).

Soil Water Balance Example

Hunsaker (1999) measured water applied and changes in soil water content over time on small plots of cotton. He used his data to determine both basal crop ET and the additional soil evaporation following irrigation. He also computed both basal crop ET and soil E with the revised FAO procedure (Allen et al. 1998). This allows one to determine the magnitude of the differences in irrigation efficiency when one includes or excludes this soil evaporation. Differences between measured and computed total evapotranspiration are plotted in Figure 6. The time intervals for data points are approximately 3 to 6 days. Differences in evaporation are typically 1 to 2 mm per day. The low values early in the season are likely due to deep percolation that was not measured. A few high values late in the season were caused by rainfall. Except for the values noted, differences appear random and centered around zero. Note that this does not imply that there are no systematic errors when applying these procedures to larger fields and geographic areas, since the basal crop coefficients were matched to the measured data. Systematic errors from reference ET calculations and crop coefficients can easily be as much as 1 mm/d or larger. Care also needs to be taken to assure that effective precipitation is removed from crop ET to reflect crop ET of only the irrigation water. In climatic regions, where precipitation contributes a substantial portion of crop ET, separating out effective precipitation is difficult and inaccurate.

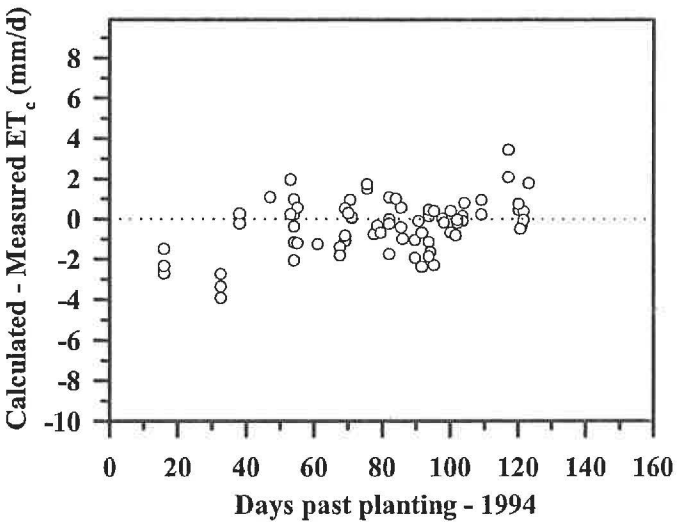

Figure 6. Comparison between measured and estimated total evapotranspiration (from Hunsaker 1999).

Accuracy of Leaching as Water Balance Remainder Example

Suppose that for an irrigation season the inflow and outflow are measured, soil moisture storage changes are measured, and the evapotranspiration is estimated with the crop-coefficient-reference-ET approach. Assume the following measurement or estimates

- measured inflow volume = 100 units with an accuracy of ±5%, or ±5 units,
- ET is estimated to be 67 units ±20% or ±13.4 units,
- measured outflow = 15 units with an accuracy of ±5%, or ±0.75 units, and
- storage changes is measured as 0 ±1 units.

The resulting deep percolation volume is 100 – 67 – 15 – 0 = 18 units. The accuracy is computed from equation 1, where the standard deviations are one half the values given above. Assuming these measurements are independent, the variance is

$$s_0^2 = (5/2)^2 + (13.4/2)^2 + (0.75/2)^2 + (1/2)^2 = 51.5 units^2 \qquad (4)$$

The standard deviation is ±7.2 units. The confidence interval is two standard deviations, or ±14.4 units, or ±80%, or 3.6 < deep percolation < 32.4 units. This is a very wide confidence interval.

Accuracy of Performance Parameters

Consider any one of the performance parameters, such as irrigation efficiency. If the numerator is estimated with 15% accuracy and the denominator with 5% accuracy. The result is accurate to within 15.8% of value (from equation 3, square root of $15^2 + 5^2$). If the value of the performance parameter (ratio) is 0.7, the 95% confidence interval becomes 0.7 ±0.11 (0.7 times 15.8%), or 0.59 < ratio < 0.81. This wide range is typical of what one might expect for many estimates of irrigation performance parameters, particularly irrigation efficiency, unless extensive measurements are made and detailed analyses are conducted. Presenting such performance measures to more than two significant digits is not appropriate, particularly when accuracy considerations suggest confidence to only one significant digit.

Policy Implication Example

The Arizona Department of Water Resources (ADWR) established water duties as a result of the Arizona groundwater management act of 1980. The water duties restrict the amount of groundwater pumped in Active Management Areas (i.e., hydrologic basins considered to be at risk of severe overdraft). Cropped acreage for each farm during the years 1975-1979 was used to establish the right for water. The consumptive use of crops grown for each acre of land were taken from Erie et al. (1982). The computed volume (land area times crop ET) was divided by 0.85 to establish the water duty for each farm. This was based on the assumption that 85% seasonal irrigation efficiency could be achieved with modern irrigation methods. This ratio was reduced to 0.75 for "problem soils." No additional water was allowed for salinity control unless the irrigation-water salinity exceeds 1000 ppm.

The consumptive use curves of Erie et al. (1982) were determined from field measurements of soil water depletion from roughly three days after an irrigation event to just prior to the next irrigation event. The data from several seasons were plotted and a smooth line drawn through the scatter of data. Since the data did not include ET for several days after each irrigation event, the consumptive use curves approximately represent basal ET – averaged over several seasons.

Table 4. Water consumption in mm for grower's cotton field during 1994 (from Hunsaker et al. 1999).

	Irrigation Water	In season precip.	Pre-season precip.	Total
Basal ET	996	48	13	1057
Soil E	78	27	n/a	105
Total Crop ET	1074	75	13	1162

ADWR's approach was over-simplified and did not properly consider all components of a water balance. They did not consider effective precipitation, additional soil evaporation, or potential use of off-season soil moisture. To examine the implications of ADWR's approach, the data presented by Hunsaker et al. (1999) on a grower's farm in central Arizona is compared to ADWR water duties. The consumptive-use value for cotton from Erie et al. (1982) is 1046 mm, divided by 0.85 gives 1231 mm for the water duty. The values of consumptive water use measured for this field are given in Table 4. Basal ET (1057 mm) was slightly higher than Erie's average (basal) number (1046 mm). Total irrigation water consumption was 1074 mm. Effective precipitation and water taken from soil storage almost canceled soil evaporation of irrigation water. In order to stay within ADWR's water duty would require an aggregate AE, or seasonal IE with soil evaporation considered beneficial, of 1074/1231 = 87.2% -- only slightly higher than that determined with ADWR assumptions.

Central Arizona now receives a significant portion of its water from the Colorado River through the Central Arizona project. The electrical conductivity for this Colorado River water (840 ppm) is roughly 1.3 dS/m. For cotton, the threshold value is 7.7 dS/m, suggesting roughly a 3% leaching fraction (Hoffman et al. 1990, Table 18.1 and Figure 18.9). Thus seasonal irrigation efficiency (assuming all soil evaporation is beneficial) must exceed 90% to stay within ADWR's water duty and maintain soil salinity. This is relatively difficult for any irrigation method and generally requires a high degree of management. For more salt sensitive crops, even higher efficiencies would be required. To date, growers have gotten around the water duty limitations through set-aside programs, fallowing land, using a shorter cotton season, and changing their cropping patterns. The removal of government set-aside programs, the need to keep land in production, and the desire to further diversify may cause difficulties for growers to meet these water duties in the future.

SUMMARY

It has been shown that a careful water balance is needed to characterize the use of irrigation water within an agricultural area. Methods are available for estimating the accuracy of various water measurements, estimates, and computed quantities (e.g., remainder in water balance). The accuracy with which these water quantities can be determined is extremely important to the application of water duties and water management practices in an area. Errors in the water balance or its application can lead to erroneous conclusions about water use and therefore water policies. A statistical analysis of errors can be used to determine which quantities contribute most to the water balance erros, and thus measurements to focus on for improving water balance accuracy.

REFERENCES

Allen, R.G., Pereira, L.S., Raes, D., and Smith, M. (1998) *Crop Evapotranspiration*. Irrigation and Drainage Paper No. 56, FAO, Rome, Italy.

Bos, M.G., Replogle, J.A. and Clemmens, A.J. (1984) Flow Measuring Flumes for Open Channel Systems. John Wiley & Sons, NY. 321 pp. (republished by ASAE, St. Joseph, MI 1991).

Burt, C.M., A.J. Clemmens, T.S. Strelkoff, K.H. Solomon, L. Hardy, T. Howell, D. Eisenhauer, R. Bleisner. (1997) Irrigation performance measures -- Efficiency and uniformity. *J. Irrigation And Drainage Eng*ineering 123(6): 423-442.

Clemmens, A.J. and Burt, C.M. (1997) Accuracy of irrigation efficiency estimates. . *J. Irrigation And Drainage Engineering*. 123(6): 443-453.

Erie, L.J., French, O.F., Bucks, D.A., and Harris, K. (1982) *Consumptive Use of Water by Major Crops in the Southwestern United States*. Conservation Research Report No. 29, USDA/ARS, Washington, DC. 40 p.

Hoffman, G.J., Howell, T.A., and Solomon, K.H. (eds.) (1990) *Management of Farm Irrigation Systems*, ASAE, St Joseph, MI.

Hunsaker, D.J. (1999) Basal crop coefficients and water use for early maturing cotton. *Trans. of ASAE*, 42(4):927-936.

Hunsaker, D.J., Clemmens, A.J., Rice, R.C., and Adamsen, F.J. (1999) *Effects of management practices on water use and irrigation efficiency in cotton furrow irrigation*. ASAE paper 992091. Presented at the 1999 ASAE/CSAE Annual International Meeting, ASAE, St. Joseph, MI.

Palmer, J.D., A.J. Clemmens, and A.R. Dedrick. (1991) Field study on irrigation delivery performance. *J. Irrigation and Drainage Engineering* 117(4):567-577.

Solomon, K.H. and Davidoff, B. (1999) On the relationship between unit and subunit irrigation performance, *Trans. of ASAE*, 42(1):115-122.

USBR (1998) *Lower Colorado River Accounting System – Demonstration of Technology. Calendar Year 1996.* Lower Colorado Region, U.S. Bureau of Reclamation, Boulder City, NV, July.

Wahlin, B. T., Replogle, J.A. and Clemmens, A.J. (1997) *Measurement Accuracy for Major Surface-Water flows entering and Leaving the Imperial Valley.* WCL Report #23, U.S. Water Conservation Laboratory, Phoenix, AZ. (and Errata to Report #23, March 30, 1999).

Published in Irrigation Australia 2000, Melbourne, Australia, May, 2000 – pp 240-249.

U.S. Department of the Interior
Bureau of Reclamation

WinFlume for Experts

An Interactive Working Session on the Use of WinFlume

Design and calibration of long-throated flumes and broad-crested weirs

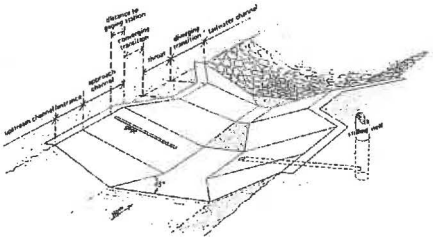

Tony L. Wahl

Water Resources Research Laboratory
Denver, Colorado

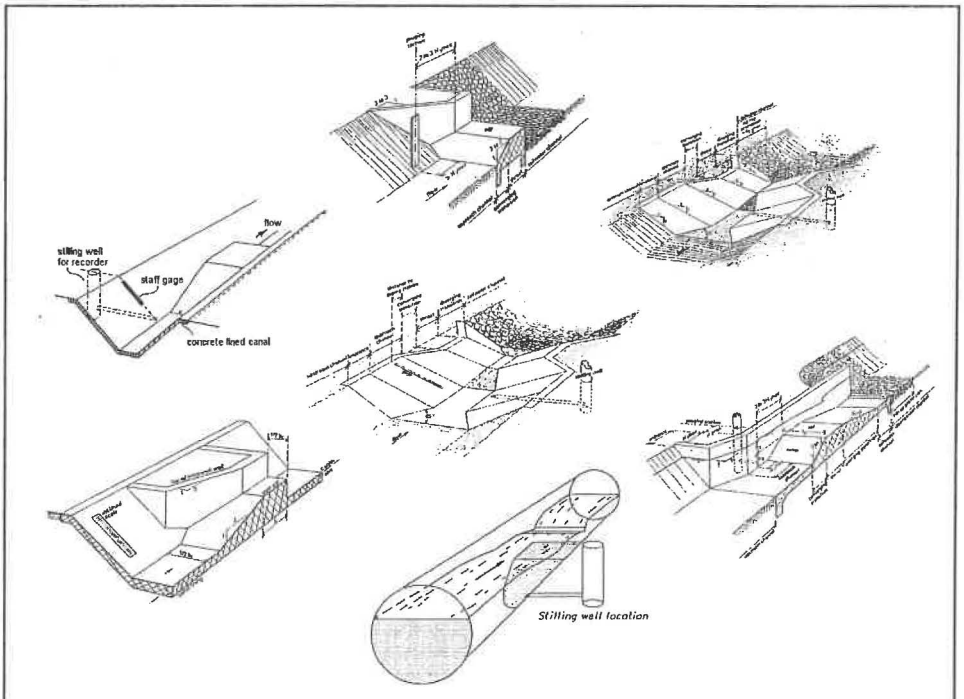

Traditional Critical-Flow Devices

- Traditional critical-flow devices have curved, three-dimensional flow fields in the control section
  - Parshall flumes, cutthroat flumes, H-flumes, etc.
  - V-notch weirs, Cipoletti weirs, rectangular weirs
- Traditional broad-crested weirs lacked an adequate transition and had 3D flow and/or non-hydrostatic pressure distributions at the control section
- All such devices require laboratory calibration

Modern Long-Throated Flumes and Broad-Crested Weirs

- Converging transition and length of throat or sill create one-dimensional flow at the control section
- ***Long-throated*** *means long enough to eliminate lateral and vertical contraction of the flow at the critical section, so streamlines are essentially parallel*
- Can be calibrated using well-established hydraulic theory
  - **No laboratory testing needed**
  - **Accurate calibration of as-built structures is possible**
  - **Custom designs can be easily calibrated**
- Calculations are iterative
- Computer models that do the calculations have made long-throated flumes reasonable to implement in recent years

Submergence of Flumes and Weirs

- Sharp-crested weirs
  - NO SUBMERGENCE ALLOWED

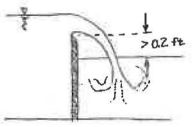

- Parshall flume
  - Some submergence allowed

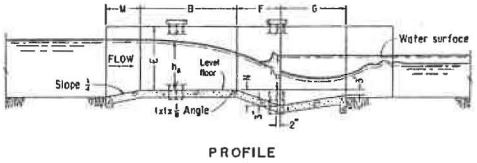

- Long-throated flume and broad-crested weir
  - Most submergence allowed
  - Lowest head loss

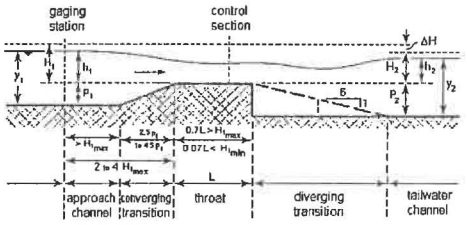

Throat Section Shape Selection

- Constructability
- Range of Flows to be Measured

Shape	Q_{max}/Q_{min} ±2% uncertainty	Q_{max}/Q_{min} ±4% uncertainty
Rectangular	35	100
Triangular	350	1970
Trapezoidal – wide at top	55	180
Trapezoidal – narrow at top	210	1080
Parabolic	105	440
Complex – wide at top	> 100	> 200
Complex – narrow at top	> 250	> 2000

Typical Flume/Weir Configurations

- Sill in a concrete-lined canal
- Rectangular-throated flumes for earthen canals
- Triangular-throated flumes for natural channels
- Flumes in circular pipes
- Portable and temporary flumes

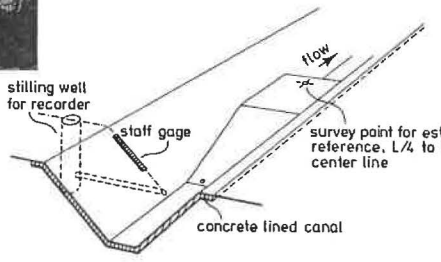

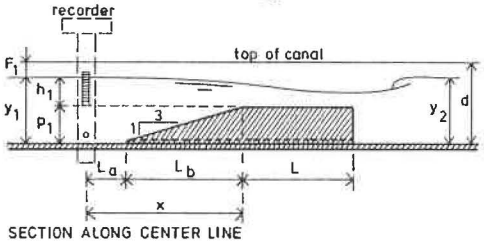

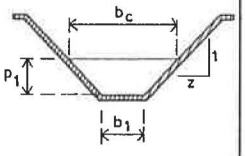

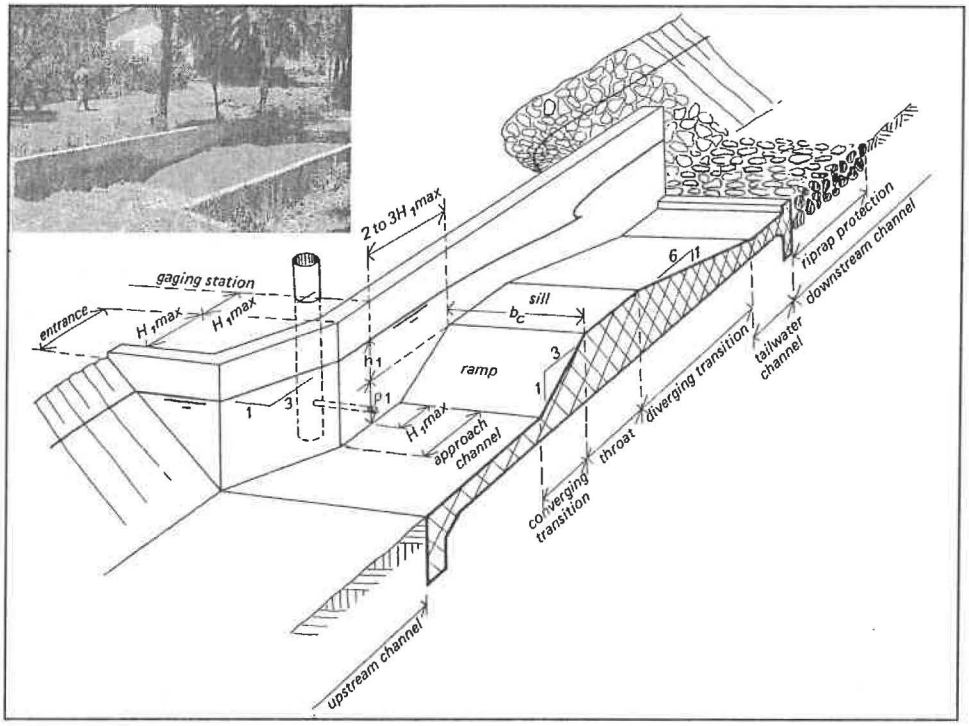

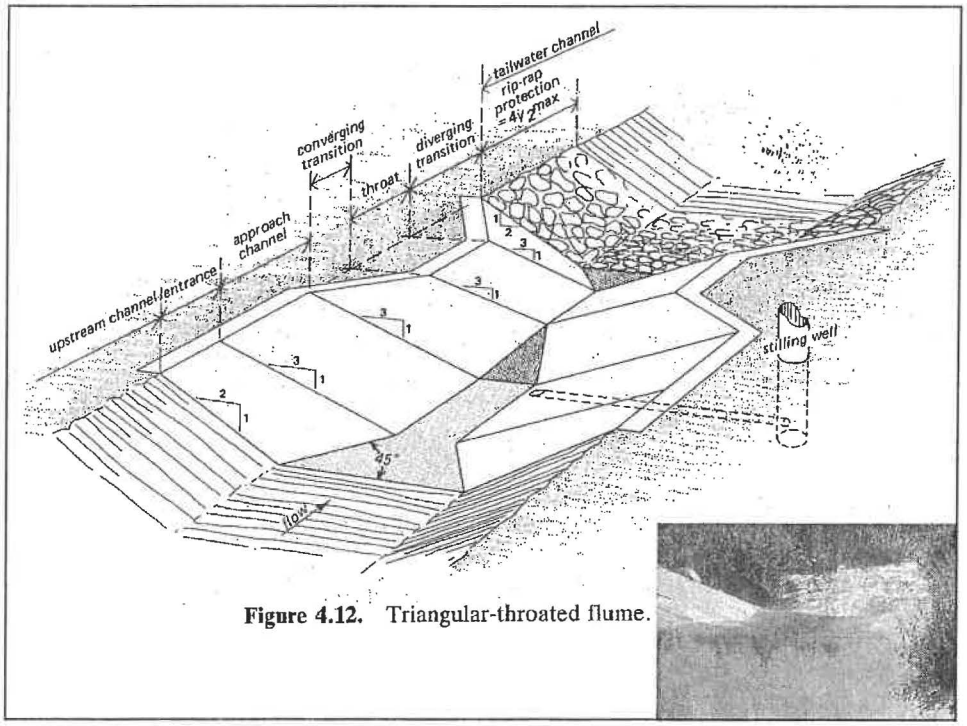

Figure 4.12. Triangular-throated flume.

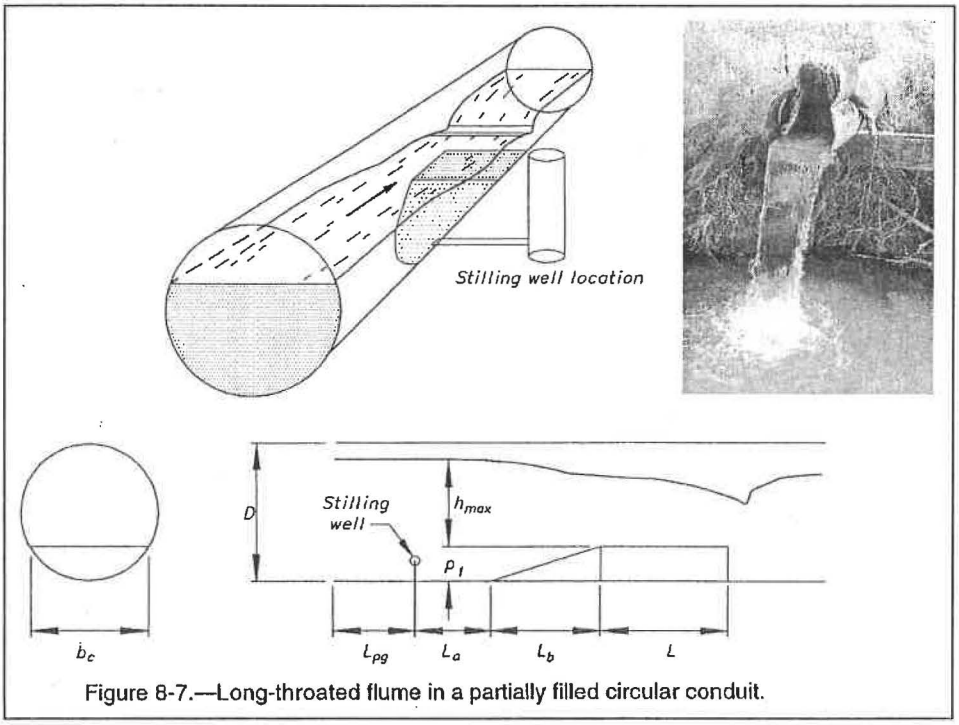

Figure 8-7.—Long-throated flume in a partially filled circular conduit.

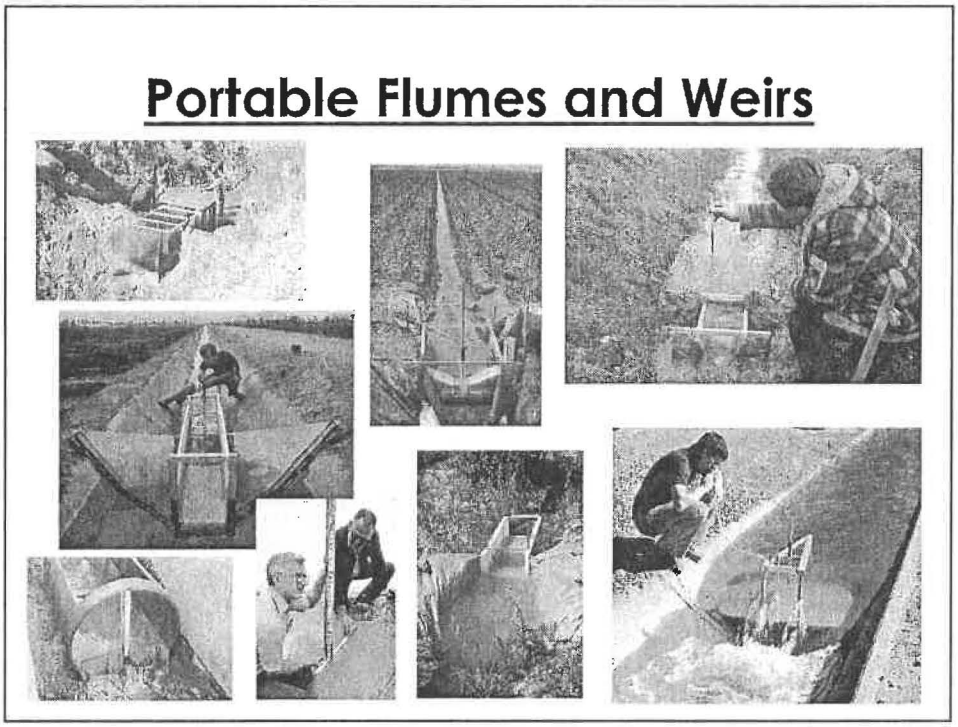

Calibrating an Existing Structure

- Define geometry of canal and flume
- Provide hydraulic data and other properties
  - Construction material
  - Tailwater conditions
- Generate output
  - Rating tables and curves
  - Curve-fit equation for data logger
  - Wall gage data and/or plot

Designing a New Structure

- Define canal geometry and initial flume control section
- Provide hydraulic data, canal/flume properties, design requirements
  - Construction material
  - Tailwater conditions
  - **Water level measurement method and required flow measurement accuracy**
  - **Required freeboard in upstream channel**
- Size and set control section
- Refine lengths of flume components
- Generate output

Principal Design Issues

- Site
  - Uniform, fully-developed flow conditions approaching structure so that hydraulic theory is applicable
- Flume control section
  - Ensure that flume is not submerged by tailwater (contraction must be enough to force critical depth)
  - Ensure structure ponds water deep enough to stabilize upstream water surface for accurate measurement ($Fr < 0.5$)
  - Ensure that flume does not create a "lack of freeboard" problem at maximum flow
  - Ensure that contraction produces enough head to make an accurate flow measurement
- Component lengths must meet "long-throated" criteria

Control Section Adjustment Methods

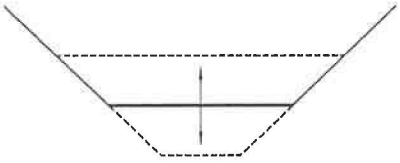

Raise or Lower Height of Sill

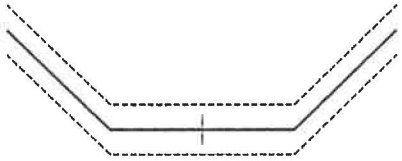

Raise or Lower Entire Section

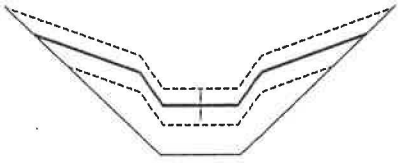

Raise or Lower Inner Section

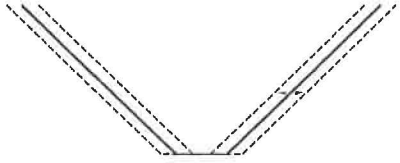

Vary Side Contraction

Lengths of Flume Components

- Throat section length, L
  - $0.07<H_1/L<0.7$ for ±2% uncertainty
  - $0.05<H_1/L<1.0$ for ±4% uncertainty
- Floor and sidewalls of converging transition
  - 2.5 to 4.5:1 transition slope
- Diverging transition
  - No flatter than 10:1
- Gaging station location (approach channel length)
  - $> H_1$ upstream of start of converging transition
  - (2 to 3) * H_{1max} from start of throat

Flume Design & Selection

- Pre-computed flume designs can be chosen using tables provided in several references
  - Water Measurement Manual
  - Water Measurement with Flumes & Weirs
- Designs can be developed using the WinFlume computer program
  - Allows for customization
  - Provides best rating table accuracy
  - Simplifies checking of design

WinFlume

SOFTWARE FOR THE DESIGN AND CALIBRATION OF
LONG-THROATED FLUMES AND BROAD-CRESTED WEIRS

Water Resources Research Laboratory
Denver, Colorado

USDA ars

U.S. Water Conservation Laboratory
Phoenix, Arizona

International Institute for Land
Reclamation & Improvement
Wageningen, The Netherlands

HOW TO OBTAIN WINFLUME

- WinFlume is available on the World Wide Web at:

  http://www.usbr.gov/pmts/hydraulics_lab/winflume

- The program operates on all Windows-based computers

This work has been funded by the U.S. Bureau of Reclamation's Water Conservation Field Services Program.

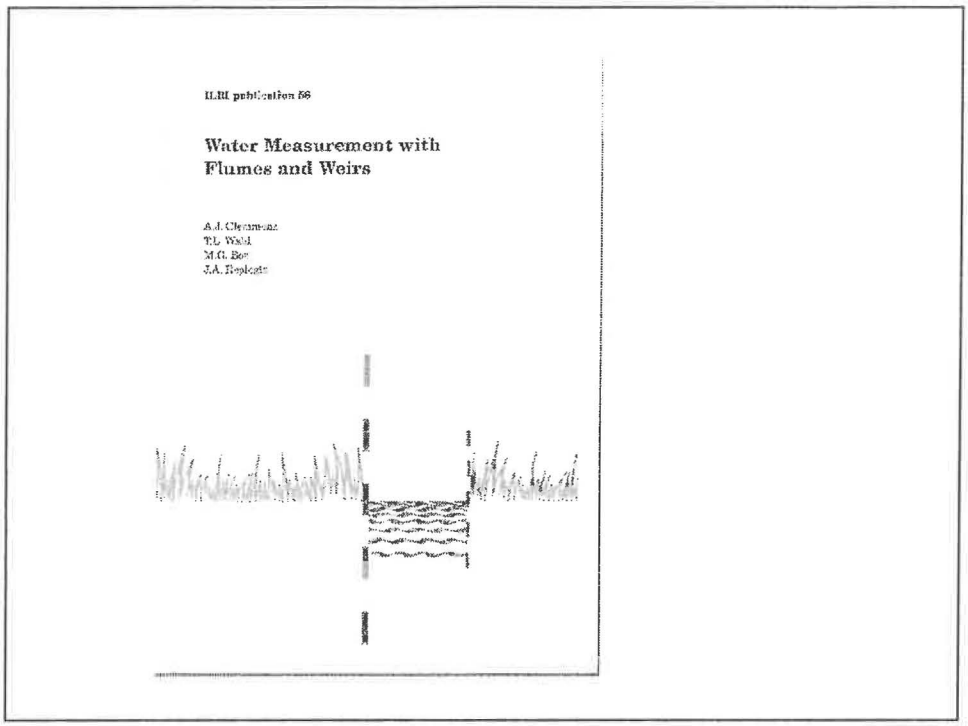

Design Examples

- Calibrating an existing structure
  - Entering data
  - Generating rating tables, equations, wall gages
- Trial and error design
- Design using WinFlume's automated tools
- Designing a flume with tight constraints

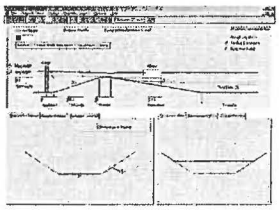

Calibrate This Structure...

Channel:	Trapezoidal, 0.3 m base width, 1:1 side slopes, 0.55 m deep
Sill Height:	0.3 m
Approach Length:	0.2 m
Upstream Ramp:	3:1 slope (0.9 m long)
Throat Length:	0.35 m
Construction Material:	Smooth concrete
Tailwater Conditions:	Normal Depth Manning's n = 0.015 S_{bed} = 0.00050 (0.5 m/km)
Discharge Range:	0.05 to 0.15 m^3/s

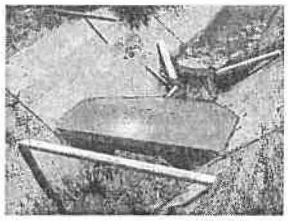

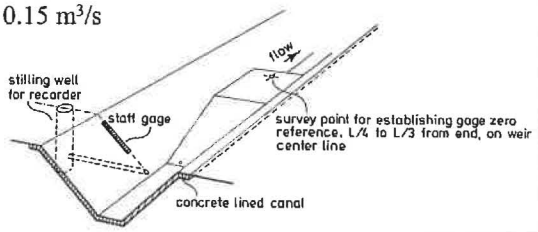

Design by Trial...

- Find appropriate sill height given that:
  - We must maintain freeboard of at least 20% of head on weir
  - We will measure upstream head with a staff gage in a stilling well
  - Allowable measurement errors are 5% at maximum flow and 8% at minimum flow

p_1=0.4 m overtops upstream channel
p_1=0.35 m violates freeboard requirement
p_1=0.3 m is not sufficiently accurate at Q_{min}
p_1=0.25 m is acceptable
p_1=0.2 m is submerged at Q_{max}

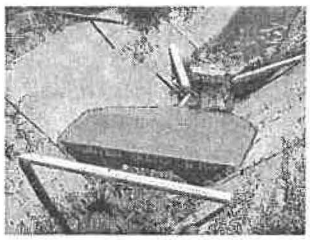

WinFlume's Design Module

- User chooses a method of contraction change and an increment at which to evaluate designs (e.g. evaluate designs at sill height increments of 0.1 ft).
- WinFlume brackets the range of possible designs by evaluating flume performance at the maximum design flow:
  - The maximum possible throat-section contraction is that needed to produce a maximum upstream water level equal to channel depth.
  - The minimum contraction is that which produces an upstream Froude number of 0.5 at maximum discharge, and an upstream water level that is at least as high as the downstream tailwater at maximum discharge.
- WinFlume builds and evaluates designs of "virtual" flumes between the lower and upper contraction limits at the interval specified by the user.

Design Module Results

- Results are presented to the user, who may choose to accept any one of the designs or discard the results.
  - Only designs meeting the four primary design criteria (freeboard, Froude number, no submergence at minimum and maximum flow) are presented, unless there are no acceptable designs.
  - Designs that meet the four primary criteria, but do not meet measurement precision requirements may be improved by specifying a better water level measurement method.
- Acceptable designs that have minimum head loss, maximum head loss, intermediate head loss, or head loss matching the bed drop at the site are highlighted in the output
- The user can choose the design that best meets their needs. A throat section with more contraction than the minimum required will provide protection against excessive submergence of the structure if tailwater levels prove to be higher than expected.

If An Acceptable Design Is Not Found On The First Trial

- If the contraction increment is too large, or if design criteria are too limiting, no acceptable design will be found. Is an acceptable design possible?
- WinFlume searches for two adjacent designs for which the unsatisfied criteria in each design are satisfied in the adjacent design.
  - An acceptable design may exist between those two designs
  - Analysis is repeated using a smaller increment of contraction change within that range.
- If no region of acceptable designs is found, then all results are presented to the user, with suggestions for how to relax the design criteria or change the initial design so that an acceptable design can be found.

Results from Design Module...

- Vary the sill height in increments of 0.05 m
- Sill heights between 0.24 m and 0.333 m are acceptable
- Sill heights above 0.286 m do not meet accuracy requirement at minimum flow
  - Could be fixed by using more accurate head measurement method

Now Let's Make Things Tougher

(example 5.6.6 from *Water Measurement with Flumes & Weirs*)

- Canal operators insist on using a staff gage in the canal, and want to meet accuracy requirements as before:
  ± 5% at Q_{max}
  ± 8% at Q_{min}

- Changing the sill height does not work
- Try raising the entire control section as a unit, making the throat identical to the canal shape (0.3 m base width)

- Sill heights from 0.153 m to 0.189 m will work
- This style of structure is more difficult to build

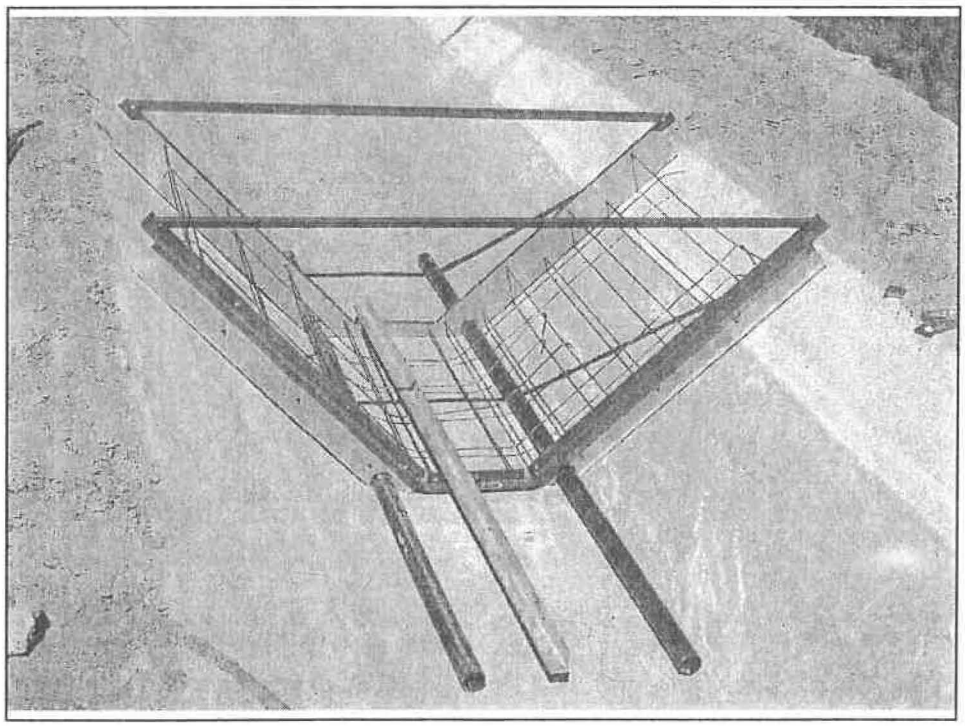

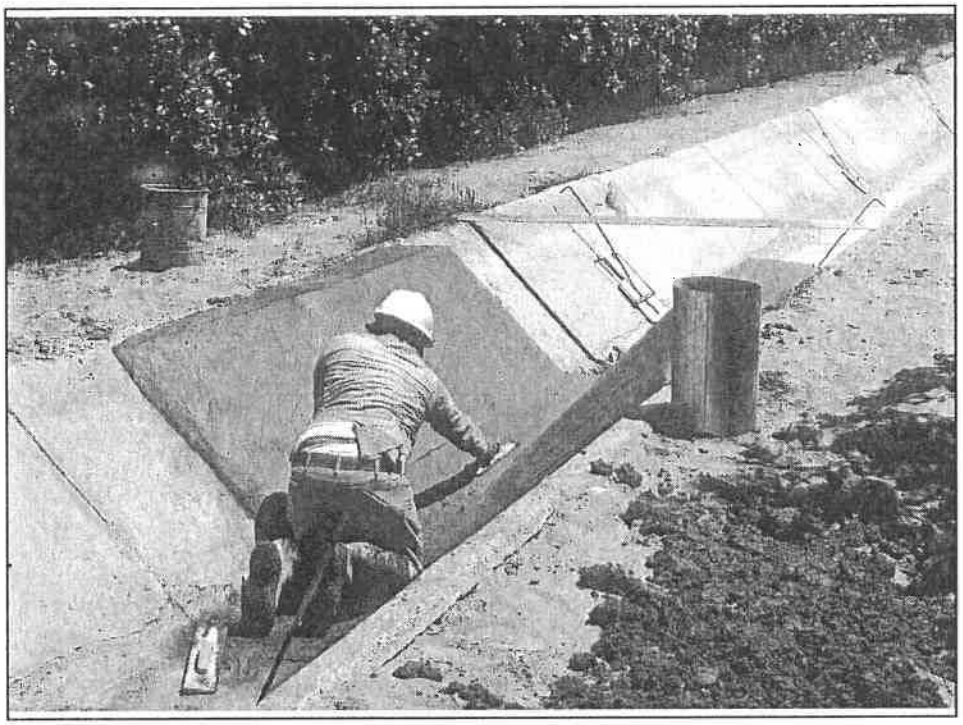

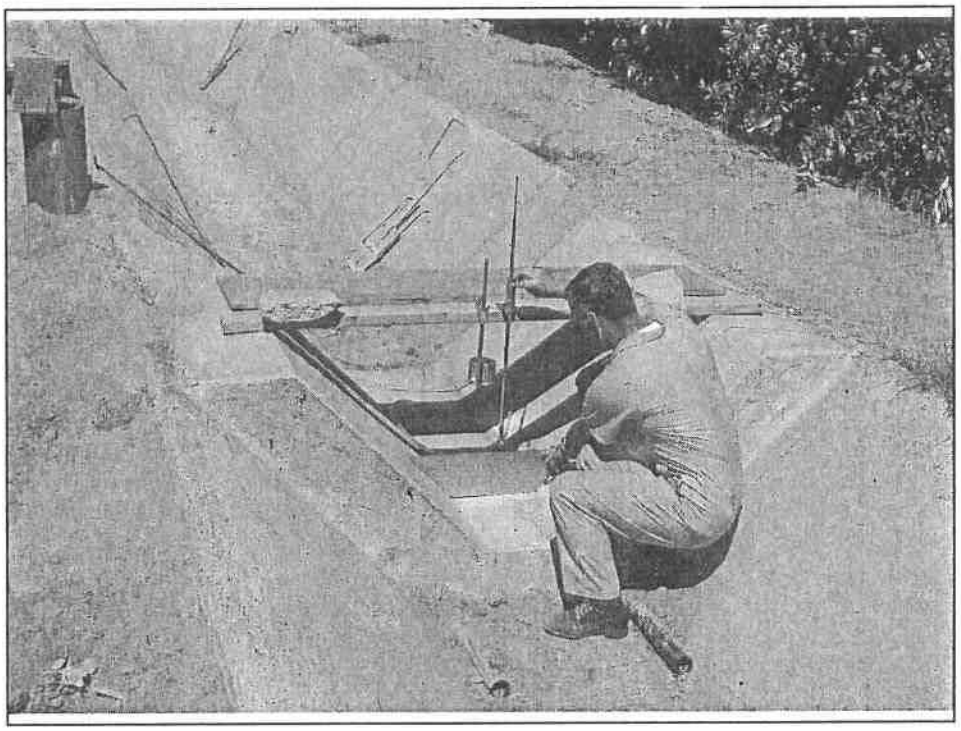

Tougher Yet...

- Canal depth is now 0.5 m !
- Freeboard problem and submergence problem at Q_{max} overlap one another
- What can we do? Change throat shape, but how?
- Main problem right now is freeboard vs. submergence...don't worry about accuracy yet
- Wider, shallower flow in the throat will...
  - Reduce upstream head, thereby increasing freeboard
  - Require less head loss (ΔH is proportional to H_1)
  - Reduces freeboard requirement (20% of head)

Let's Try It...

- Choose a trial sill height and let WinFlume determine the throat width
- A few trials show that this solves the freeboard vs. submergence problem, but there is no solution to the accuracy problem
- Throat width must be 0.36 m or less to satisfy accuracy requirements, but then freeboard is a problem
- Note that throat length can affect evaluation of accuracy criteria. If $H_1/L<0.07$ or $H_1/L > 0.7$, WinFlume penalizes accuracy

One More Thing to Try...

- A diverging transition would reduce required head loss and might give us more design freedom
- Go back to the design that used the 0.3 m base width. Add a 6:1 downstream ramp and try varying the throat section elevation again
- A sill height of 0.14 m (±3 mm) is acceptable

Design Example Summary

- Essential tradeoffs demonstrated
  - Freeboard vs. submergence at Q_{max} is most common issue, and sometimes accuracy is also a factor
  - Sometimes Froude number will control rather than submergence
  - Submergence at Q_{min} is very rarely a problem
- Changing throat section shape is sometimes necessary and requires user intervention
- Refinement of flume component lengths can come after throat section is sized and set (but throat length sometimes affects accuracy, so keep an eye on it)
- Designs for existing canals are often tightly constrained
- Flumes for new canals are much easier – required head loss can be incorporated into canal design

Special Topics

- Non-symmetric sections
- Analyzing "imperfect" as-built flumes
  - Cross-slope of a "flat" sill
  - Longitudinal slope of sill
- Warning messages regarding converging transition length
- Flumes with compound control sections

Non-Symmetric Sections

- Not an ideal situation, but tolerable if Z_1 and Z_2 are not dramatically different
- Model with a symmetric section using $Z=(Z_1+Z_2)/2$
- Mathematically, this produces correct cross-sectional area and top width, but wrong wetted perimeter
  - Slightly distorts tailwater and frictional head loss calculations

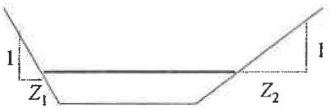

Analyzing Flume with Cross-Slope

- Cross-slope of a "flat" sill
  - Determine "average" sill height and model as a flat sill at that sill height
  - Or, model with a complex shape (a V-section in bottom of throat) with cross slope that is double actual slope.

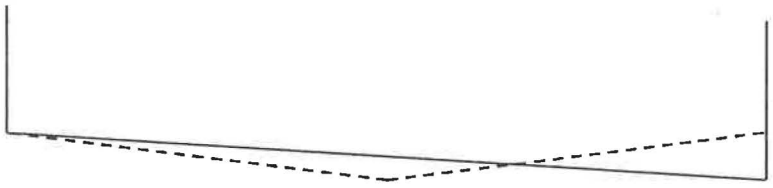

Flume with Longitudinal Slope

- Most difficult problem to correct for
- Slope moves critical section toward a zone with streamline curvature
  - Increases discharge coefficient
- If sloped uphill in the flow direction, reference head measurement to downstream end of sill
- If sloped downhill, reference head to leading edge of the sill
- If slope is 3° or more…REPAIR THE FLUME

Warning Messages Regarding Converging Section Length

- 2.5:1 to 4.5:1 transition is desired
  - Steeper than 2.5:1 causes flow separation at start of throat…affects transition to critical depth
  - Flatter than 4.5:1 yields uneconomical structure and increases friction loss between gage and control section
- WinFlume evaluates:
  - Vertical contraction of flow due to raised sill
  - Horizontal contraction of flow due to narrowed throat
- Warning messages can be difficult to overcome when aspect ratio of approach and throat sections are dramatically different
- Better to make the converging transition too long rather than too short. (Too short could cause flow separation at entrance to throat and affect flow at critical section)

Length of Converging Transition

- Throat Section Narrow at Base -

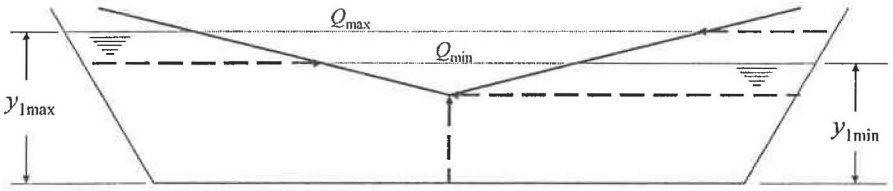

- Range of acceptable lengths is 2.5 to 4.5 times the maximum of the "contraction distances" shown
  - Evaluated separately at Q_{min} and Q_{max}
- Large horizontal contraction at the sill elevation requires long converging section
- Horizontal contraction at sill is large if base width is small or zero (V-shaped)

Flumes with V-Shaped or Compound Control Sections

- Often difficult to obtain "acceptable" length of converging transition, or acceptable length seems unreasonably long
  - Better to make the converging transition too long rather than too short. (Too short would cause flow separation at entrance to throat and affect flow at critical section)
- Compound shapes have reduced accuracy in transition zone from inner shape to outer shape
  - First, consider a triangular shape when Q_{max}/Q_{min} is large

Length of Converging Transition

- Rectangular Throat -

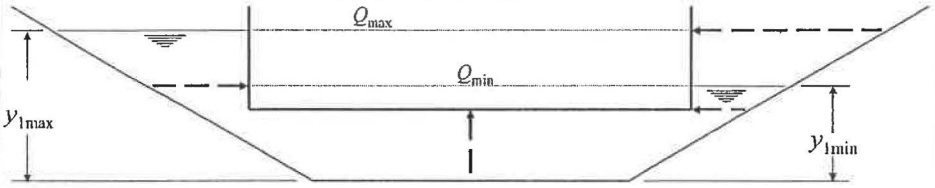

- Controlling (maximum) contraction length may be dramatically different at minimum and maximum flow
- Can lead to "contradictory" warning messages that converging section is both too short at Q_{max} (more abrupt than 2.5:1) and too long at Q_{min} (flatter than 4.5:1)
- Solutions:
  - Choose the longer recommended length. Gradual transition is best
  - Use a trapezoidal throat (similar to approach channel shape)
  - Use different transition lengths for sides and floor

D:\WinFlume\Workshops\Exercise Flumes\Converging Section Length Paradox Example.Flm

Using "Different" Transition Lengths for Sides and Floor

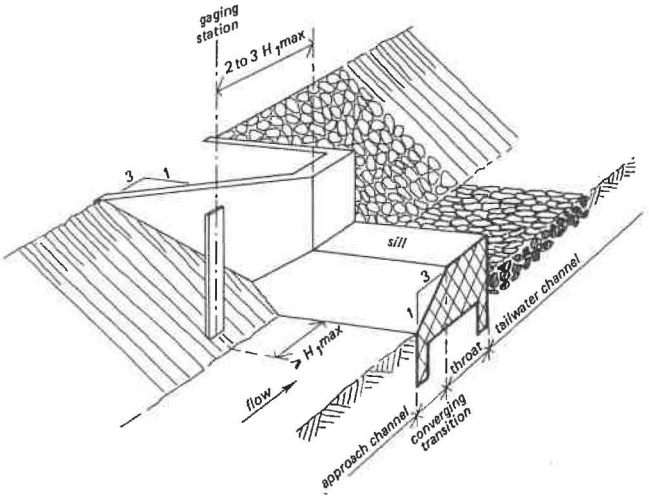

Laboratory Evaluation of a SonTek Argonaut-SW Flowmeter

by

Tracy B. Vermeyen, P.E. and Jennifer Rupp
Water Resources Research Laboratory

Acknowledgments

This evaluation was funded by Reclamation's Science and Technology program (project X0845). This evaluation was conducted in support of a research project on canal seepage reduction managed by Jay Swihart (D-8180). Joe Kubitschek, hydraulic engineer, peer reviewed this report. Craig Huhta from Sontek/YSI provided technical assistance.

Disclaimer: This evaluation was intended for internal use only and does not constitute acceptance or rejection of the product tested. The information contained in this report regarding commercial products or companies may not be used for advertising or promotional purposes and is not to be construed as endorsement of any product or company by the Bureau of Reclamation.

Purpose

The purpose of this laboratory evaluation was to determine if a newly developed acoustic Doppler flowmeter could accurately measure seepage losses from a section of unlined canal. A set of tests were designed to determine the minimum amount of seepage losses the flowmeter could accurately measure. The scope of this evaluation did not include a verification of the vertical velocity profile measurements or the algorithms used by the Argonaut-SW for the discharge computations for open channels or closed-conduits.

Introduction

The Argonaut-SW (shallow water) is a pulsed Doppler current profiling system designed for measuring water velocity profiles and level that are used to compute volumetric flow rate in natural channels, canals, culverts, or pipes. The goal of this laboratory evaluation was to determine the Argonaut-SW's flow measurement accuracy in a flume and pipe in a controlled setting.

Doppler-based Velocity Measurement Technique

The Argonaut-SW is a pulsed Doppler current meter. It uses a monostatic transceiver configuration, where the acoustic transducers transmit and receive the acoustic signals. The Argonaut-SW has three acoustic beams (figure 1). When correctly placed on the channel bottom, one of these beams is facing straight up, and the other two point

upstream and downstream at a 45-degree angle. The upward-looking beam measures water depth. For a bottom mount application, the two diverging beams measure the flow velocities in two dimensions (streamwise and vertical). The manufacturer reports the velocity range, resolution, and accuracy to be ±16 ft/sec, 0.003 ft/sec, and the larger of ±1% of the measured velocity or ±0.016 ft/sec, respectively (Sontek 2003).

A key technical feature of the Argonaut-SW, which separates it from other Doppler sensors, is that velocity measurements are made to the water surface (in open channels) without any of the contamination normally associated with side-lobe interference. This enables the SW to take full advantage of the vertically-integrated velocity in its internal flow calculations.

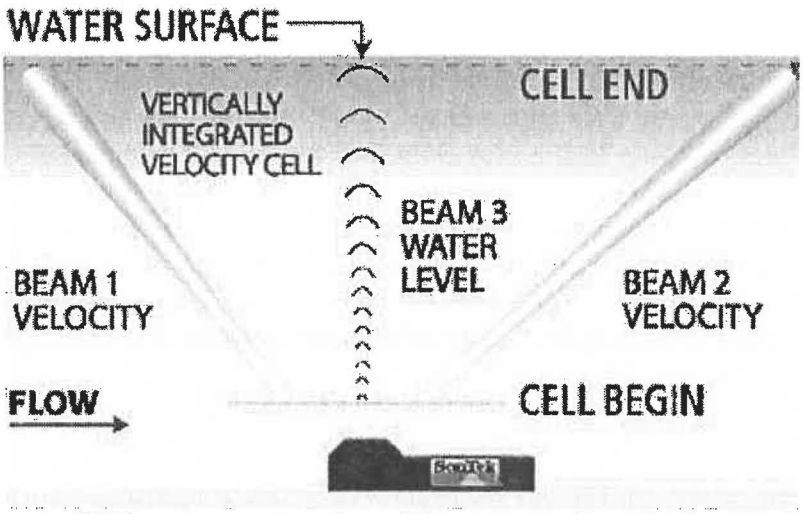

Figure 1. Argonaut–SW beam pattern and profiling extents (Sontek, System Manual, 2003).

Acoustic Water Level Measurement

A vertical beam is used to measure water level. The vertical beam sends an acoustic pulse and listens for the reflected pulse from the surface. To find the surface range from the reflection travel-time the SW uses an internal temperature sensor and user-defined salinity to calculate the speed of sound in water for the site. The SW uses the water level data for dynamic boundary adjustment which changes the velocity profile range to account for changes in depth. The manufacturer reports the water level range to be 0.6 to 16 ft, and the accuracy to be the larger of ± 0.01 ft or ±0.1% of measured depth. The minimum distance to the first velocity measurement ("cell begin" in figure 1) is about 0.3 ft above the top of the transducer.

Discharge Computations

The cross-sectional dimensions for an open channel or closed conduit are user-programmed into the flowmeter before it is deployed. The SW uses the water depth measurement and a depth-area relationship to compute the area of the flow section for each sampling period. The flow rate is computed by multiplying the area by the

computed mean channel velocity for each sample. The mean channel velocity is computed from the vertically integrated velocity using an algorithm based on the 1/6th power velocity distribution model (Chen 1991). In addition, the SW has the option to use an index-velocity relationship for discharge computations. Where the index velocity is calculated from an empirical relationship between an independent measurement of the mean channel velocities and the SW-measured velocities and depths.

Laboratory Evaluation

The Facilities – Two Argonaut-SW flowmeters were tested in a large laboratory flume that is located at the Bureau of Reclamation's Water Resources Research Laboratory, located in Denver, Colorado. The glass-walled flume is 4 feet wide, 8 feet tall and 80 feet long (figure 2). The flume has a 10-ft-long headbox which contains a baffle structure to condition the flow entering the flume. The pumped flow capacity to the flume is about 20 ft^3/sec. The depth in the flume is controlled by a tailgate located at the end of flume.

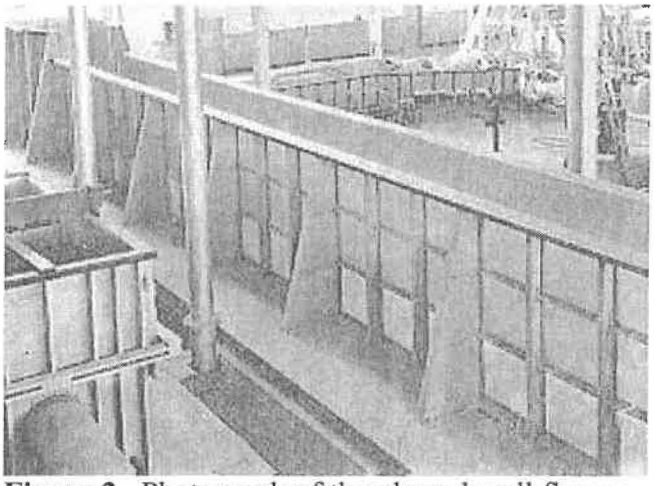

Figure 2. Photograph of the glassed-wall flume. Flow is from left to right.

The first Argonaut-SW instrument was installed 25 ft downstream from the headbox baffle and was positioned 5 ft upstream from a 1.67-ft-high labyrinth weir. The weir was being studied in the flume and was left in place with the intention of generating non-uniform vertical velocity profiles, especially at higher discharges. The non-uniform profiles would allow evaluation of the SW's theoretical discharge computation algorithm for distorted flow profiles. A staff gage mounted to the flume wall across from the SW transducer was used to measure water depth to the nearest 0.02 ft. Figure 3 is a photograph of the Argonaut-SW flowmeter installed in the flume. A 4-ft-high and 4-ft-wide channel geometry was programmed into the SW. The system elevation for this installation (offset from the flume bottom) was 0.243 ft.

A second Argonaut-SW was placed in a 9-ft-long plastic pipe located 20 ft downstream from the open channel SW. The 18-inch diameter pipe was placed in the last third of the flume and its entrance was isolated by a 4-ft-high marine grade plywood bulkhead. The bulkhead was sealed to the pipe and flume to force all the flow through the pipe. The tailgate was used to keep the water depth below the top of the pipe inlet bulkhead. The tailgate was about 15 ft downstream from the 18-in-diameter pipe outlet. Figure 4 is a photograph of the SW flowmeter installed in the pipe. Notice that the SW within the pipe was situated about 5 pipe diameters from the pipe entrance. A 1.5 ft diameter pipe description was programmed into the SW. The system elevation for this installation (offset from the pipe invert) was 0.312 ft.

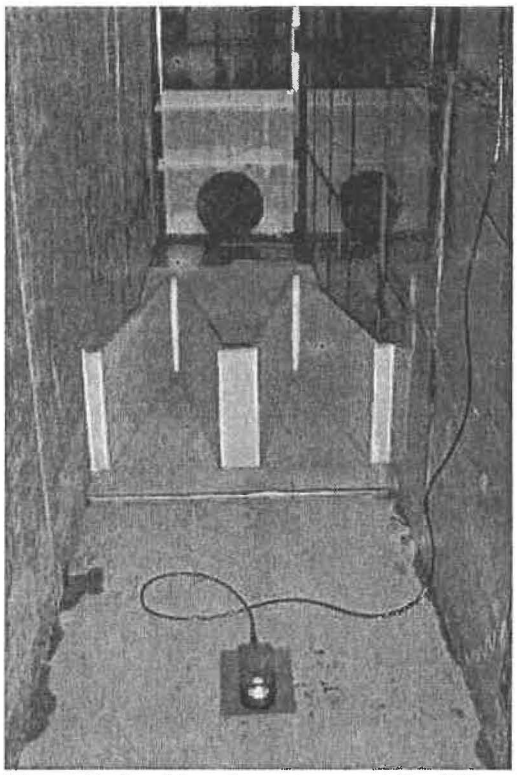

Figure 3. Looking downstream at the SW and the 1.67-ft-high laybyrinth weir in the open channel section. The bulkhead entrance to the 18-inch pipe can be seen beyond the labyrinth weir. A staff gage is visible on the steel wall across from the SW transducer.

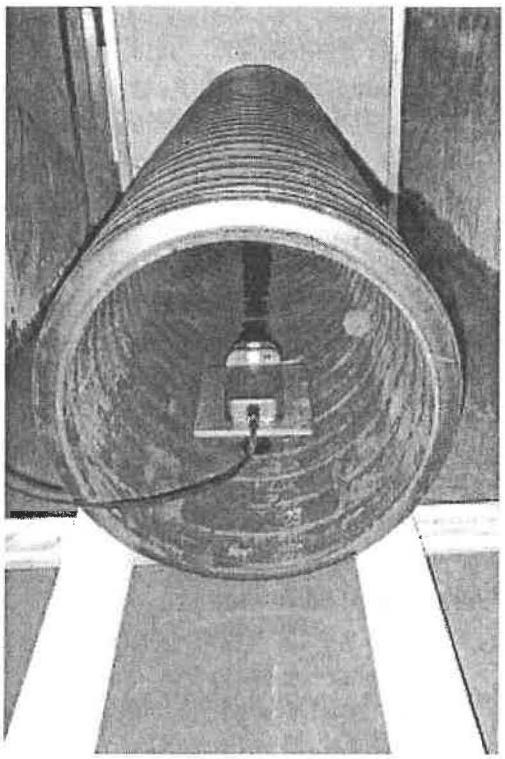

Figure 4. Looking upstream at the SW in plastic pipe section. The SW was positioned 7.5 ft downstream from the pipe entrance.

Test Procedures - Steady flows pumped from the laboratory reservoir were discharged in to the flume headbox. Inside the headbox is an 8-inch diameter drain pipe which was used to allow a portion of the inflow to bypass the flume. A series of 1 hour tests were conducted for bypass flows ranging from 0 to 10 percent of the flow supplied to the flume. Both Argonaut-SW flowmeters were programmed to store a data set every 2 minutes. During the 2 minute averaging interval, the SW collected 120 velocity profiles and depth measurements that were internally averaged prior to logging the data.

Flow supplied to the flume was measured independently using a 12-inch Venturi meter. The Venturi meter was calibrated in the laboratory calibration facility and has an uncertainty of ±0.3% of the volumetric flowrate. A laboratory control system was used to maintain a constant discharge into the flume. A strap-on acoustic flowmeter was installed on the bypass pipe to make an independent measurement of bypass flow. This flowmeter has a manufacturer reported uncertainty of about ±1 to 2 percent. A calibration test for the bypass flowmeter was not performed for this evaluation. As a result, an uncertainty of ±2 percent was used in the uncertainty analyses for the strap-on flowmeter. For most tests, the bypass flowmeter stored an average flowrate every one minute for the duration of the tests. However, for some tests the data logger memory was

filled and some data were lost. For these tests, the bypass flows were observed every 15 minutes to ensure they remained constant. Typically, the mean bypass flows were very stable and the standard error was less than ±0.01 ft^3/sec for a 30-minute test.

A staff gage was used to make an independent measurement of water depth at the flowmeter location in the flume. The staff gage was read to the nearest 0.02 ft with an uncertainty of ±0.01 ft. A tailgate located at the end of the flume was adjusted to keep the pipe completely submerged during each test and to maintain a stable depth at the open channel SW location.

Tests - Two SW units were tested for 1 hour intervals at various flowrates. At each interval, the bypass flow was adjusted to represent leakage. Tests were conducted with flume flows of 1, 5, and 7 ft^3/sec with the bypass flow adjusted once every hour. For the 1 ft^3/sec test, data were collected for target bypass flows of 0, 0.05 and 0.10 ft^3/sec. For the 5 ft^3/sec test, data were collected at target bypass flows of 0, 0.20, 0.25, 0.30, 0.40 and 0.50 ft^3/sec. For the 7 ft^3/sec test, data were taken at target bypass flows of 0.25, 0.30, 0.35, 0.50, 0.60 and 0.70 ft^3/sec.

Table 1. Depth Measurement Results for the Four-Foot Channel

Test Setup	SW Measured Depth (±dy, ft)	Staff Gage (dy=± 0.01 ft)	Discrepancy (y_{flume}-y_{sw}) (ft)	Within Specs (±0.01 ft)
1 ft^3/sec - 0.00bypass	2.297±0.063	2.30	0.00	Meets
1 ft^3/sec - 0.05 bypass	3.038±0.071	3.06	0.02	Exceeds
1 ft^3/sec - 0.10 bypass	3.130±0.000	3.10	-0.03	Exceeds
5 ft^3/sec - 0.00 bypass	2.141±0.006	2.14	0.00	Meets
5 ft^3/sec - 0.20 bypass	2.013±0.000	2.00	-0.01	Meets
5 ft^3/sec - 0.25 bypass	2.619±0.000	2.58	-0.04	Exceeds
5 ft^3/sec - 0.30 bypass	2.583±0.000	2.58	0.00	Meets
5 ft^3/sec - 0.40 bypass	2.482±0.000	2.48	0.00	Meets
5 ft^3/sec - 0.50 bypass	2.417±0.000	2.40	-0.02	Exceeds
7 ft^3/sec - 0.25 bypass	3.022±0.014	2.98	-0.04	Exceeds
7 ft^3/sec - 0.30 bypass	2.916±0.000	2.90	-0.02	Exceeds
7 ft^3/sec - 0.35 bypass	3.169±0.000	3.14	-0.03	Exceeds
7 ft^3/sec - 0.50 bypass	3.069±0.001	3.08	0.01	Meets
7 ft^3/sec - 0.60 bypass	2.971±0.000	2.96	-0.01	Meets
7 ft^3/sec - 0.70 bypass	2.809±0.001	2.78	-0.03	Exceeds

Test Results - Table 1 contains a summary of the depth measurements collected by the SW in the 4-ft flume. The SW depth values are the mean and standard error (±dy) of 30 or more samples. Depth observed using a staff gage was used to evaluate the accuracy of the SW depth measurements. Table 1 also includes the discrepancy (difference) between the two depth values and whether this discrepancy meets or exceeds the water level measurement accuracy specifications, ± 0.01 ft. The width to flow depth ratios for these tests ranged from 1.3 to 2.0.

Tables 2 and 3 contain a comparison of SW mean channel velocity to the computed mean flow velocity using the continuity equation (**V=Q/A**). Where **Q** is the volumetric flowrate and **A** is the test section cross-sectional area. To compute the mean channel velocities, the actual flow was divided by the cross sectional area of the flume or pipe:

$$A_{flume} = 4d;\ where\ d \equiv staff\ gage\ depth\ reading,\ ft^2$$

$$A_{pipe} = \frac{\pi D^2}{4};\ where\ D \equiv pipe\ diameter,\ ft^2$$

These tables also include the discrepancy between the two mean velocity values and whether this discrepancy was with the manufacturers water velocity measurement accuracy specifications, ±0.016 ft/sec. For pipe tests with flows of 5 and 7 ft^3/sec, the water velocity measurement accuracy specifications is ±1 percent of the measured velocity. Using the manufacturers velocity specification in this evaluation was especially strict because it includes uncertainty contributions from mean channel velocity computations, as well as the cross sectional area. The uncertainties (dV) in the mean channel velocity computations were computed using the general formula for error propagation as described by Taylor (1997). The uncertainties (dV) in SW mean channel velocities were computed as the standard error of the vertical velocities measured for the duration of the test which was the combined uncertainty attributed to velocity fluctuations (turbulence) and instrument noise.

Table 2. Comparison of Mean Channel Velocity to SW Mean Velocity for Flume Tests

Test Setup	Calculated Flume Velocity (±dV, ft/sec)	SW Mean Velocity (±dV, ft/sec)	Discrepancy (ft/sec) (V_{flume}-V_{sw})	Within Specs (±0.016 ft/sec)
1 ft^3/sec - 0.00 bypass	0.109±0.002	0.103±0.012	0.006	Meets
1 ft^3/sec - 0.05 bypass	0.078±0.002	0.085±0.007	-0.007	Meets
1 ft^3/sec - 0.10 bypass	0.073±0.001	0.073±0.008	0.000	Meets
5 ft^3/sec - 0.00 bypass	0.584±0.012	0.573±0.012	0.011	Meets
5 ft^3/sec - 0.20 bypass	0.598±0.012	0.576±0.010	0.022	Exceeds
5 ft^3/sec - 0.25 bypass	0.459±0.009	0.456±0.009	0.003	Meets
5 ft^3/sec - 0.30 bypass	0.456±0.009	0.460±0.009	-0.004	Meets
5 ft^3/sec - 0.40 bypass	0.477±0.010	0.470±0.010	0.007	Meets
5 ft^3/sec - 0.50 bypass	0.476±0.010	0.453±0.007	0.023	Exceeds
7 ft^3/sec - 0.25 bypass	0.566±0.012	0.567±0.009	-0.001	Meets
7 ft^3/sec - 0.30 bypass	0.578±0.012	0.584±0.008	-0.006	Meets
7 ft^3/sec - 0.35 bypass	0.529±0.011	0.527±0.004	0.002	Meets
7 ft^3/sec - 0.50 bypass	0.528±0.011	0.542±0.006	-0.014	Meets
7 ft^3/sec - 0.60 bypass	0.541±0.011	0.549±0.006	-0.008	Meets
7 ft^3/sec - 0.70 bypass	0.567±0.012	0.547±0.016	0.020	Exceeds

Table 3. Comparison of Mean Pipe Velocity to SW Mean Velocity for 18-inch Pipe Tests

Test Setup	Calculated Pipe Velocity (±dV, ft/sec)	SW Mean Velocity (±dV, ft/sec)	Discrepancy (ft/sec) (V_{pipe} -V_{sw})	Within Specs (±0.016 ft/sec or ±1% of V_{sw})
1 ft^3/sec - 0.00 bypass	0.566±0.004	0.582±0.022	-0.016	Meets
1 ft^3/sec - 0.05 bypass	0.538±0.004	0.539±0.033	-0.001	Meets
1 ft^3/sec - 0.10 bypass	0.509±0.004	0.521±0.018	-0.012	Meets
5 ft^3/sec - 0.00 bypass	2.829±0.021	2.936±0.016	-0.106	Exceeds
5 ft^3/sec - 0.20 bypass	2.705±0.021	2.820±0.014	-0.115	Exceeds
5 ft^3/sec - 0.25 bypass	2.683±0.022	2.821±0.015	-0.138	Exceeds
5 ft^3/sec - 0.30 bypass	2.666±0.022	2.800±0.019	-0.134	Exceeds
5 ft^3/sec - 0.40 bypass	2.677±0.022	2.728±0.015	-0.051	Exceeds
5 ft^3/sec - 0.50 bypass	2.586±0.022	2.682±0.016	-0.096	Exceeds
7 ft^3/sec - 0.25 bypass	3.820±0.030	3.837±0.014	-0.017	Meets
7 ft^3/sec - 0.30 bypass	3.892±0.030	3.852±0.017	-0.060	Exceeds
7 ft^3/sec - 0.35 bypass	3.763±0.030	3.708±0.014	0.055	Exceeds
7 ft^3/sec - 0.50 bypass	3.684±0.030	3.672±0.016	0.012	Meets
7 ft^3/sec - 0.60 bypass	3.622±0.031	3.661±0.013	-0.039	Exceeds
7 ft^3/sec - 0.70 bypass	3.577±0.031	3.535±0.023	0.042	Exceeds

Tables 4 and 5 summarize the temporal mean and uncertainty (dQ) in the flow computations for the 4-ft flume and 18-inch diameter pipe tests. The uncertainty in the flow computations was computed using the general formula for error propagation as described by Taylor (1997). The actual flume flow was computed as the difference between the laboratory flow and the mean bypass flow as measured with the strap-on acoustic flowmeter.

Discussion of Results

Depth Measurements – Measurement of flow depth using the staff gage was often difficult because of small waves in the flume. The staff gage readings shown in table 1 are averages of the observations at the beginning and end of the test. The uncertainty in the staff gage readings was ±0.01 ft which was selected to be half of the staff gage resolution, ±0.02 ft. Tests were conducted under a near-constant depth, but for some tests it was difficult to achieve this condition, especially for the 1 ft^3/s test. Periodic tailgate adjustments had to be made to keep the pipe submerged during those tests. For 1 ft^3/s tests, the staff gage readings at the end of the test were compared to measurements logged by the SW at the same time.

Table 4. Flow Measurement Results for the 4-ft Flume Tests

Test Setup	Target Flume Flow (±dQ, ft^3/sec)	Actual Flume Flow (±dQ, ft^3/sec)	SW Computed Flume Flow (± dQ, ft^3/sec)	Percent Difference
1 ft^3/sec - 0.00 bypass	1.000±0.003	n/a	0.994±0.147	0.6
1 ft^3/sec - 0.05 bypass	0.950±0.003	n/a	0.941±0.194	0.9
1 ft^3/sec - 0.10 bypass	0.900±0.003	n/a	0.920±0.200	-2.2
5 ft^3/sec - 0.00 bypass	5.000±0.015	5.00±0.015	4.912±0.139	1.8
5 ft^3/sec - 0.20 bypass	4.800±0.014	4.78±0.016	4.641±0.131	2.9
5 ft^3/sec - 0.25 bypass	4.750±0.014	4.74±0.016	4.774±0.169	-0.7
5 ft^3/sec - 0.30 bypass	4.700±0.014	4.71±0.016	4.754±0.166	-0.9
5 ft^3/sec - 0.40 bypass	4.600±0.014	4.73±0.016	4.664±0.160	1.4
5 ft^3/sec - 0.50 bypass	4.500±0.014	4.57±0.017	4.379±0.156	4.2
7 ft^3/sec - 0.25 bypass	6.750±0.020	n/a	6.851±0.195	-1.5
7 ft^3/sec - 0.30 bypass	6.700±0.020	n/a	6.809±0.188	-1.6
7 ft^3/sec - 0.35 bypass	6.650±0.020	6.65±0.022	6.683±0.204	-0.5
7 ft^3/sec - 0.50 bypass	6.500±0.020	6.51±0.023	6.655±0.198	-2.2
7 ft^3/sec - 0.60 bypass	6.400±0.019	n/a	6.517±0.192	-1.8
7 ft^3/sec - 0.70 bypass	6.300±0.019	6.31±0.025	6.145±0.181	2.6

n/a – time series of bypass flowmeter data not available for this test

Table 5. Flow Measurement Results for the 18-inch Pipe Tests

Test Setup	Target Pipe Flow (±dQ, ft^3/sec)	Actual Pipe Flow (±dQ, ft^3/sec)	SW Computed Pipe Flow (±dQ, ft^3/sec)	Percent Difference
1 ft^3/sec - 0.00 bypass	1.000±0.003	n/a	1.041±0.029	-4.1
1 ft^3/sec - 0.05 bypass	0.950±0.003	n/a	0.964±0.029	-1.5
1 ft^3/sec - 0.10 bypass	0.900±0.003	n/a	0.931±0.029	-3.4
5 ft^3/sec - 0.00 bypass	5.000±0.015	5.00±0.015	5.248±0.063	-5.0
5 ft^3/sec - 0.20 bypass	4.800±0.014	4.78±0.016	5.045±0.060	-5.5
5 ft^3/sec - 0.25 bypass	4.750±0.014	4.74±0.016	5.044±0.060	-6.4
5 ft^3/sec - 0.30 bypass	4.700±0.014	4.71±0.016	5.002±0.060	-6.2
5 ft^3/sec - 0.40 bypass	4.600±0.014	4.73±0.016	4.878±0.058	-3.1
5 ft^3/sec - 0.50 bypass	4.500±0.014	4.57±0.017	4.795±0.057	-4.9
7 ft^3/sec - 0.25 bypass	6.750±0.020	n/a	6.860±0.082	-1.6
7 ft^3/sec - 0.30 bypass	6.700±0.020	n/a	6.886±0.082	-2.8
7 ft^3/sec - 0.35 bypass	6.650±0.020	6.65±0.022	6.630±0.079	0.3
7 ft^3/sec - 0.50 bypass	6.500±0.020	6.51±0.023	6.565±0.078	-0.8
7 ft^3/sec - 0.60 bypass	6.400±0.019	n/a	6.544±0.078	-2.2
7 ft^3/sec - 0.70 bypass	6.300±0.019	6.31±0.025	6.320±0.076	0.2

n/a – time series of bypass flowmeter data not available for this test

The discrepancies between the depths measured by the SW and the staff gage ranged from -0.04 to 0.02 ft for this evaluation (Table 1). The manufacturer specifies the accuracy of the of the instrument's water level measurements as the larger of ±0.1% of the measured value, or ±0.01 ft. Since all of the tests were conducted for depths less than 10 ft the ±0.01 ft criterion applies. Of the 15 tests, 7 depth measurements were within the manufacturers specifications (figure 5). The mean of all 15 discrepancies in depth were within the manufacturers specification of ±0.01 ft. This result was good considering the staff gage was read to the nearest 0.02 ft and the difficulties in maintaining a constant depth for the duration of each test.

In the case of the pipe section, the mean of the SW depth measurements was 1.496 ft. Although the resolution of depth measurements was not reported in the specifications it appears to be 0.003 ft. All other depth readings were within ±0.33% of that value. As mentioned previously, the 18-inch pipe was kept submerged for the duration of all tests with the exception of the 1 ft^3/s test with a bypass flow of 0.05 ft^3/s. During this test the depth was observed to have dropped so that the pipe was no longer completely submerged. The tailgate at the end of the flume was adjusted to correct this. The time was noted and data collected during the period in which the pipe was not fully submerged were excluded from the data analysis.

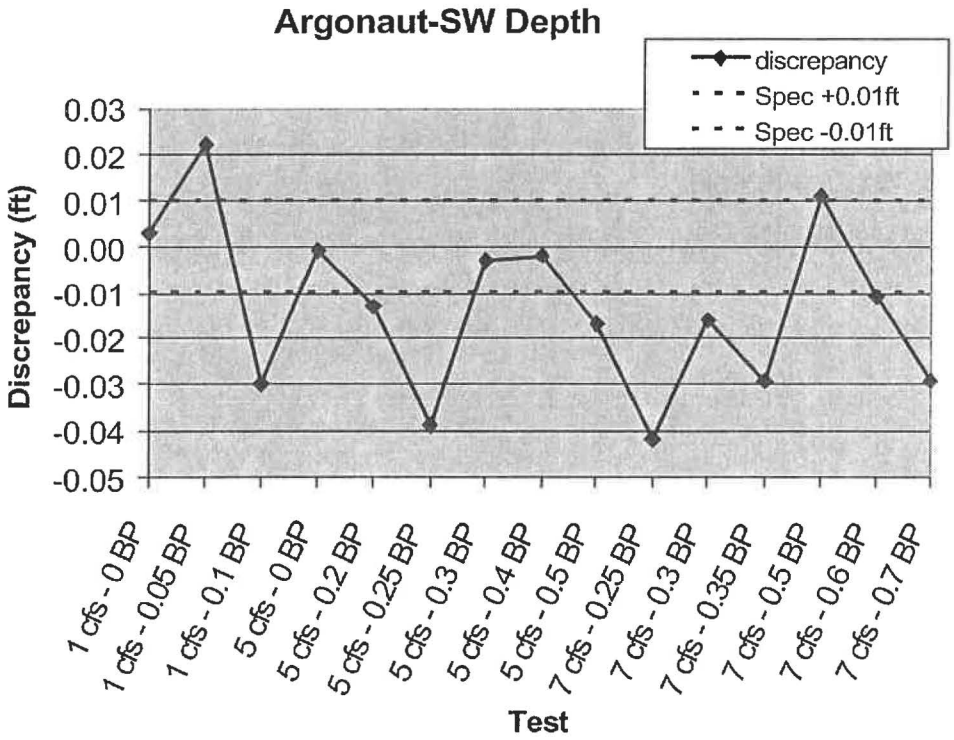

Figure 5. Discrepancies between SW and staff gage depth measurements for 15 flume tests.

Velocity Measurements - For the flume tests, computed mean channel velocities were compared to the SW computed mean velocities (Table 2). The discrepancies between these velocities ranged from -0.014 to 0.023 ft/sec for this evaluation. For the velocities measured in all 15 flume tests the ±0.016 ft/sec specification applies. In general, the

performance of the SW for the flume tests was within the "strict" specifications used for this evaluation. Figure 6 shows the discrepancies for each test and the agreement with the accuracy specification. Only three tests exceeded the accuracy specification and by less than +0.008 ft/sec. A review of the individual (120 second average) SW velocity readings for each test did not reveal any unusual readings. In fact, for all flume tests the standard errors (dV) in SW mean velocity were less than or equal to the 0.016 ft/sec specification (Table 2). This result indicates that for a 60 minute long test in a nearly constant flow field the SW collected enough velocity readings to describe the mean channel velocities within the manufacturer's accuracy specifications. The discrepancies between computed mean channel velocities probably result from errors associated with the mean velocity calculation performed by the SW and/or that the cross sectional velocity distribution in the flume is not fully developed. An error in the depth measurement could also affect the mean channel velocity uncertainty.

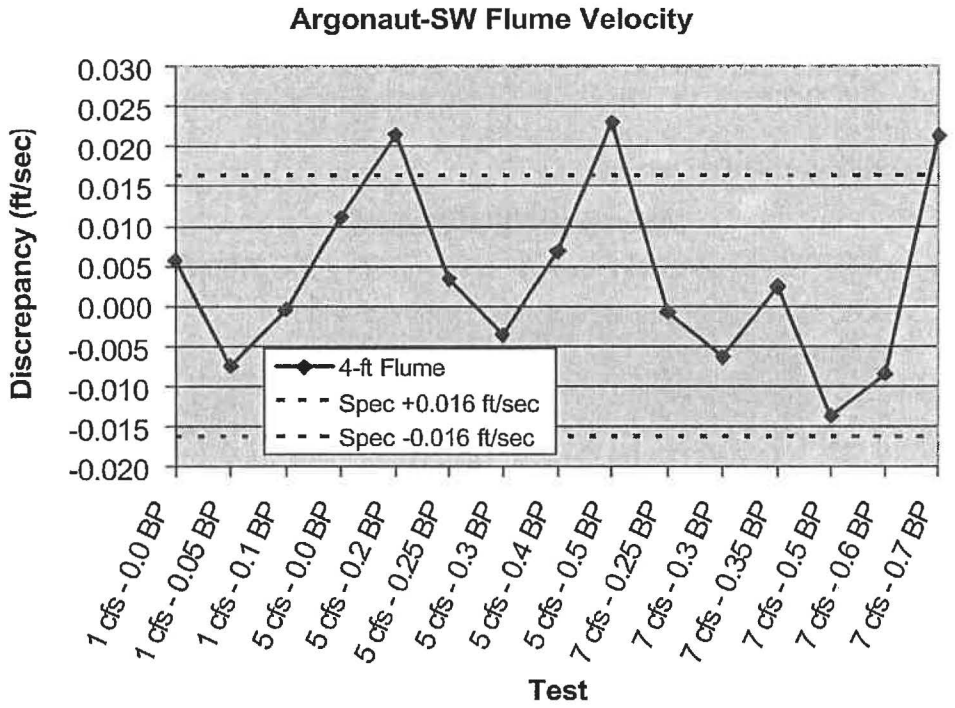

Figure 6. Discrepancy between mean channel velocities for 15 flume tests.

The SW has the capability to apply an index-velocity equation to compute the mean channel velocity using the SW-computed mean velocity and stage. For the flume tests, SW stage and velocity data were processed using multiple linear regression analysis to determine the coefficients for the index-velocity equation:

$$V_{flume} = V_{const} + V_{SW}\left(V_{coeff} + \left(Stage_{coeff} \times Stage\right)\right) \quad \text{.....Index-velocity equation}$$

Where,

V_{flume} = computed mean channel velocity, (ft/sec)
V_{const} = regression constant, (ft/sec)

V_{SW} = SW mean velocity for period of V_{flume} measurement, (ft/sec)
V_{coeff} = velocity regression coefficient, (dimensionless)
$Stage_{coeff}$ = stage regression coefficient, (1/ft)
$Stage$ = SW measured stage, (ft)

For the flume tests, the multiple linear regression was performed with V_{flume} the dependent variable and the independent variables were V_{SW} and the product of V_{SW} and stage. Multiple linear regression resulted in this best-fit equation:

$$V_{flume} = -0.00089 + V_{SW}(1.124 - 0.0405(Stage)) \ with\ an\ R^2 = 0.998$$

Where R^2 is the coefficient of determination. R^2 is a parameter which means that 99.8 percent of the variation in the mean flume velocity was described by the variables V_{SW} and stage, with a 95 percent confidence level. This is a small improvement over a simple linear regression with V_{flume} the dependent variable and V_{SW} the independent variable. Linear regression resulted in the following best-fit equation:

$$V_{flume} = -0.0008 + 1.014(V_{SW}) \ with\ an\ R^2 = 0.996$$

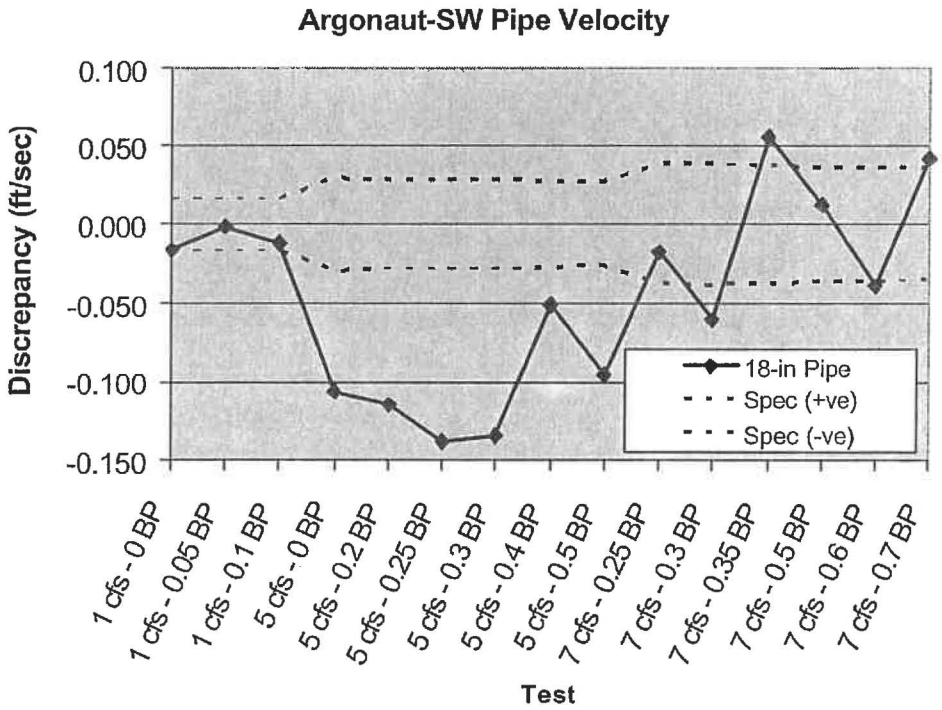

Figure 7. Discrepancy between mean velocities for 15 pipe tests.

For the pipe tests, mean pipe velocities were compared with the SW computed mean velocities. For the 1 ft^3/sec tests, the ±0.016 ft/sec specification applies. For the 5 and 7 ft^3/sec tests the ±1 percent of the measured velocity specification applies. The discrepancies between velocities ranged from -0.138 to 0.055 ft/sec for this evaluation (see Table 3). In general, the velocity discrepancies for 18-inch pipe tests exceeded the

velocity specifications. Figure 7 shows the discrepancies for each test and their relationship to the accuracy specification. Ten of 15 tests exceeded the velocity accuracy specification. It is interesting that all the 1 ft^3/sec tests were within specs, all the 5 ft^3/sec tests were outside specs, and the 7 ft^3/sec tests were close to the specs. A review of the individual SW velocity readings for each test did not reveal any unusual readings as illustrated by the small standard errors in the SW mean velocities shown in Table 3. In fact, for the 5 and 7 ft^3/sec pipe tests the standard error in SW mean velocities were less than the ±1 percent velocity specification. The discrepancies between computed mean channel velocities probably result from errors associated with the mean velocity calculation performed by the SW and/or that the cross sectional velocity distribution in the pipe is not fully developed. In contrast to the flume tests, stage measurements do not enter in to the uncertainty because the pipe was kept full.

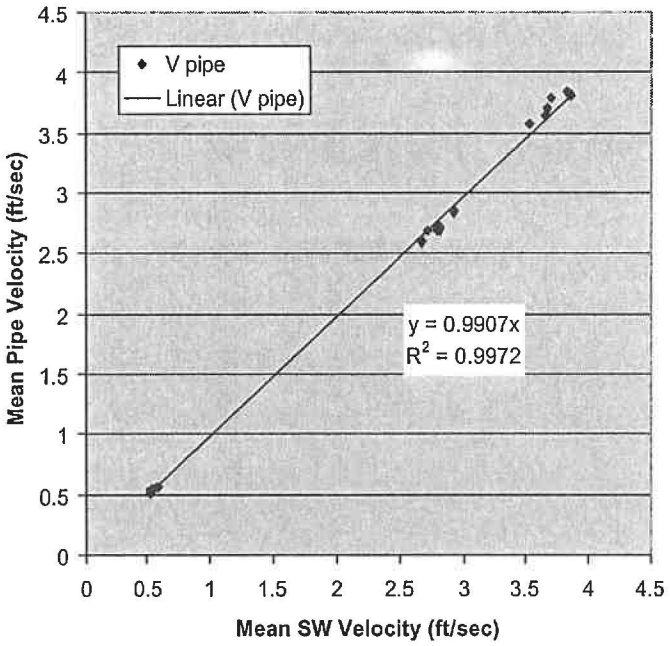

Figure 8. Linear regression relationship between SW mean velocities and the mean pipe velocity.

In an effort to describe the apparent systematic error in pipe velocities a linear regression was performed on the mean pipe velocity data. Figure 8 shows the linear regression results of all tests comparing the SW computed mean pipe velocity (V_{mean}) and the computed mean pipe velocity (V_{pipe}). For this application, the coefficient of determination (R^2) of 0.997 indicates that SW mean velocities can be adjusted to reduce the discrepancies and improve the discharge computation accuracy. This systematic error is most likely attributed to the algorithm used to convert V_x to V_{mean}. Another important factor that likely affects the velocity accuracy is the small diameter pipe used in this evaluation. In an 18-in diameter pipe the velocity measurement is determined from velocities profiled from about one half the pipe diameter because of the blanking distance

above the SW transducer and the exclusion of velocity data collected near the top of the pipe because of side-lobe interference. Sontek reports that the last 20 percent of the velocity profile in a pipe may include side-lobe interference and that their algorithm automatically excludes this data (Sontek 2003).

Flow Measurement - Tables 4 and 5 present the target, actual, and SW computed flows for the flume and pipe tests. Actual flows were computed by subtracting the average flow measured in the bypass pipe from the flow supplied to the headbox. The uncertainties in the flowrate (±dQ) are included in the tables and were computed using error propagation techniques (Taylor 1997). The percent differences in Tables 4 and 5 were calculated using the SW computed flow and the actual flow when possible; otherwise the target flow was used in place of the actual flow. The equation used to compute the percent difference is: $(Q_{flume}-Q_{SW}) / Q_{flume} \times 100\%$.

Figure 9 shows the percent differences in flow measurements for the 15 tests conducted in the flume and pipe sections. For flume tests, all the average SW computed flowrates were within ±5 percent of the laboratory flowrate. The mean percent difference for the 15 flume tests was - 0.2 percent. The SW computes flowrate using velocity and area (computed from a programmed depth-area relationship) measurements. As a result, discrepancies in velocity and depth will factor into the uncertainty in the computed flowrate. However, since the flow depth was held nearly constant throughout each test, the majority of the variation in flowrate should be attributed to velocity.

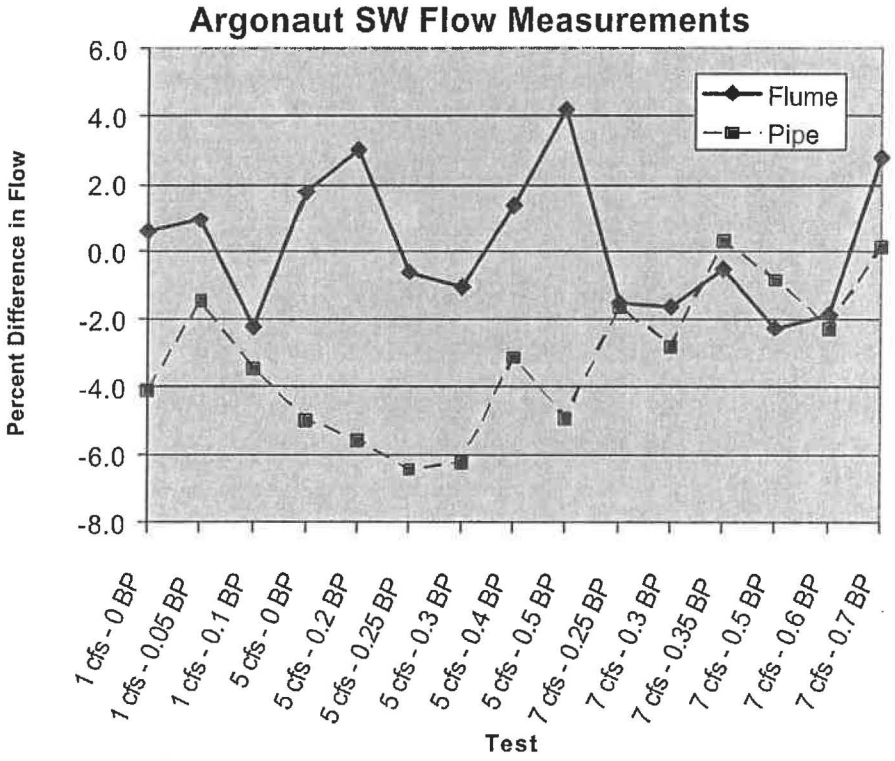

Figure 9. Percent difference of SW computed flowrates from known flowrates for flume and pipe tests.

For pipe tests, 12 of 15 tests were within ±5 percent of the laboratory flowrate. The mean percent difference for the 15 pipe tests was 3.1 percent greater than the known pipe flow. In 13 of the 15 pipe tests, the Argonaut-SW measured a flowrate greater than the flume flowrate. This systematic error in discharge seems to be related to the computation of mean pipe velocity, as described earlier.

An analysis was performed to determine the minimum averaging interval required to reduce instrument uncertainty in discharge computation to below ±5 percent. Figure 10 shows the relationship between the standard error in a series of discharge computations for a 5 ft^3/sec test and a range of averaging intervals. For the flume test, a 12 minute averaging interval was required to reduce the standard error in the SW discharge to below ±5 percent. It is important to note that this result was for steady flow conditions which may not be duplicated in a field application. Selecting an appropriate averaging interval for a field application should balance the need to capture varying flow conditions with the data storage or power requirements for the deployment. A similar analysis was done for full pipe flow and a 4 minute averaging interval was adequate to reduce the standard error in the SW discharge computation to below ±5 percent. This improved performance is likely attributed to removing the uncertainty in depth measurement (full pipe) from the discharge computations and pipe velocities that were 5 times larger than the flume velocities. Note that this analysis does not take into account uncertainties associated with the mean velocity computation (converting V_x to V_{mean}) or the discharge calculations.

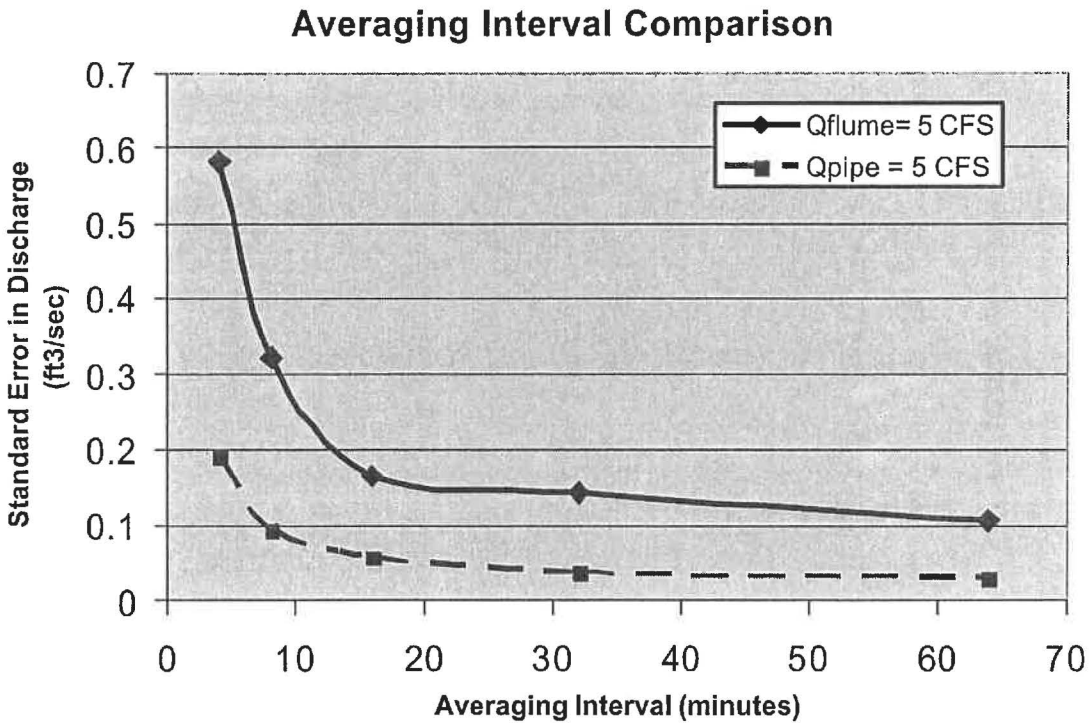

Figure 10. Standard error in SW discharges versus averaging interval for a comparable set of flume and pipe discharge measurements.

Conclusions

- Two Argonaut-SW flowmeters performed well in this laboratory evaluation for a wide range of flows. The SW-computed discharges were, on average, within +0.2 percent of the known flume discharges. For pipe tests, the SW-computed discharges were, on average, within +3.1 percent of the known pipe discharges.

- SW discharge measurement accuracy should be sufficient to quantify seepage in a canal reach provided the seepage is greater than 5 percent of the total flow and the flow conditions are steady for 30 minute intervals.

- For the majority of flume tests, the SW performed within the accuracy specifications for mean channel velocity and depth measurements. These results were notable considering the potential for a non-standard velocity profile generated from the weir located downstream. Likewise, the withdrawal of the bypass flows may have skewed the cross sectional velocity distribution.

- For the majority of pipe tests, discrepancies between computed mean pipe velocities did not meet the accuracy specifications for velocity measurements. This can most likely be attributed to the small pipe size and the algorithm (mean velocity calculation method) used by the SW to convert V_x to V_{mean}. The SW depth measurements in the pipe were within the accuracy specifications for all tests.

- For flume flow an averaging interval of 12 minutes was sufficient to reduce the instruments standard error in discharge to below ±5 percent. It is important to note that this result was for steady flow conditions which may not be duplicated in a field application. As a result, the averaging interval selected for a field application should be short enough to capture varying flow conditions.

- For full pipe flow an averaging interval of 4 minutes was sufficient to reduce the instruments standard error in discharge to below ±5 percent. The reduction in uncertainty is most likely a result of the higher velocities in the pipe as compared to the flume velocities. However, this analysis doesn't account for systematic errors attributed to the mean velocity calculation method used in the discharge computation.

References

Chen, C.L. "Unified theory on power laws for flow resistance," Journal of Hydraulic Engineering, ASCE, Vol. 117, No. 3, March 1991, pp. 371-389.

Sontek/YSI, Inc., 2003, Argonaut-SW System Manual, firmware version 9.3.

Taylor, J. R., *An Introduction to Error Analysis –the study of uncertainties in physical measurements, 2nd* edition (University Science Books, 1997).

Avoiding submergence transition zone for radial gates in parallel

A.J. Clemmens[1]

[1]U.S. Water Conservation Laboratory, USDA-ARS, 4331 E. Broadway Rd., Phoenix, AZ 85040; PH (602) 437-1702; FAX (602) 437-5291; email bclemmens@uswcl.ars.ag.gov fstrelkoff@uswcl.ars.ag.gov
Keywords. Radial gates, flow measurement, submerged flow, calibration

Abstract

The calibration of partially submerged radial and vertical-sluice gates has proven difficult to determine under field conditions. In a recent paper, the author and colleagues developed a method for determining the calibration of radial gates from free flow to submerged flow, continuously through the transition. The method uses the energy equation on the upstream side of the vena contracta and the momentum equation on the downstream side, and thus has been named the energy-momentum or EM method. Because of the nature of the partially submerged jet, an empirical energy correction is needed during partial submergence. One advantage of the method is the ability to account for a wide variety of downstream conditions, including channels that are significantly wider than the gates. It was anticipated that the method would allow estimation of discharge based only on gate openings and upstream and downstream water levels, even for multiple gates with different openings. However, if one gate is free-flowing and another in the transition zone, estimation of discharge is complicated by lateral flow, and may become intractable. One solution is to measure the downstream pressure in the vena contracta. With the energy correction term, this measurement avoids the need for use of the momentum equation downstream. However, such measurements are difficult in the field. Another solution is to move all gates to the same position, so that the EM-method can be used in the transition. This option is not suitable where operators prefer to move only one of several gates to obtain finer resolution. An alternative is to determine the position of the gates such that each is either free-flowing or fully submerged. The purpose of this paper is to explore the feasibility of options for avoiding the transition zone for multiple radial gates in parallel while still allowing the operator to adjust one gate to vary discharge. The approach is demonstrated on the Salt River Project's Arizona Canal.

Introduction

Calibration of radial gates continues to be a difficult problem under operational conditions, even though a significant amount of laboratory and theoretical work has been published. Most theoretical and laboratory studies have been conducted with upstream and downstream channels that are essentially the same width as the gate being calibrated. For given upstream and downstream water levels, the velocity in the channel, both upstream and downstream, is then related only to the settings and hydraulic characteristics of that gate. For a gate under free-flowing conditions, the velocity head in the approach channel is small relative to the total head, so differences in the upstream approach velocity have a minor influence on the calibration. However, Clemmens et al. (2003) show that the downstream channel conditions can have a significant influence on the downstream water level under which the gate becomes submerged and on the calibration under submerged conditions, as shown in Figure 1.

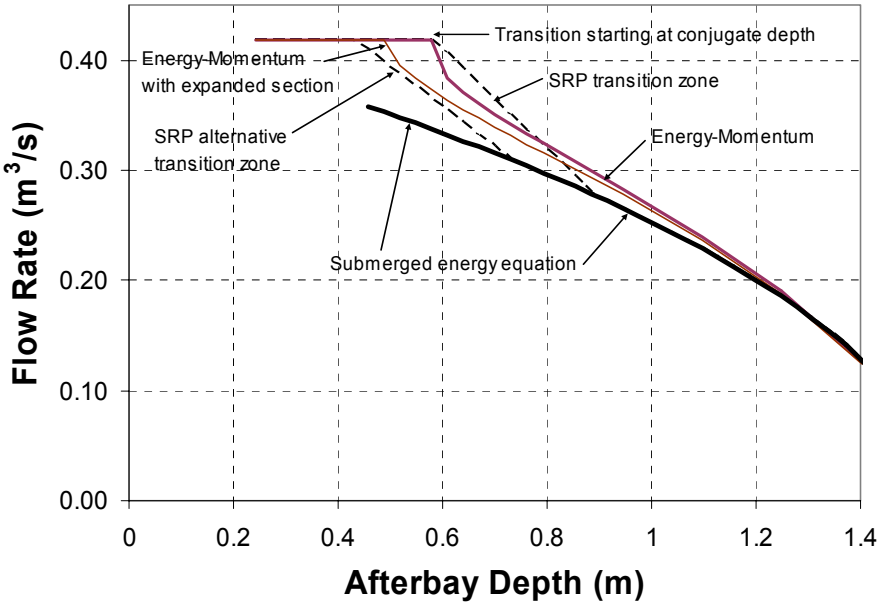

Figure 1. Radial-gate flow rates computed with energy equation (as used by SRP) and the EM method. (Fixed gate opening and upstream depth). From Clemmens et al. (2003).

The influence of downstream conditions on radial gate calibrations is particularly problematic when a canal check structure has several gates in parallel. A typical operational response to this calibration complexity has been to construct all gates with similar radial dimensions and to set all gates at the same gate opening. Once field calibrated, this configuration can provide good flow measurement accuracy. For canal headgates, this is often a viable option. However for many situations, keeping all gates at a check structure in the same position is not feasible. First, setting the gates to the same position takes more effort than moving one of the gates. For field personnel operating many check structures, this is not feasible. Second, for low flow conditions,

this may require the gates to have a very small opening. This tends to trap debris and makes operation difficult. A more common option is to only open a limited number of gates when the flow is low, the rest remaining closed. Finally, a convenient operational procedure is to make gross adjustments with several of the gates and to use one gate for fine adjustments, sometimes even under automation controls.

Under these typical operational conditions, the published relationships for submerged radial gate calibrations are often inappropriate, particularly near the transition from free to submerged flow. The purpose of this paper is to use the recently developed Energy-Momentum (EM) radial gate calibration method of Clemmens et al. (2003) to examine the ability of this method to deal with radial gates in parallel near the transition between free and submerged flow. In particular, the paper examines conditions under which one or more gates are submerged while other gates are free flowing. Finally recommendations are provided for avoiding the transition zone between free and submerged flow, where accuracy is typically much worse.

Background

Calibration relationships for radial gates have been available for decades (e.g., Bos 1989, Buyalski 1983). Under free-flow conditions, these calibrations have proven to be adequate. However, under submerged conditions they have often not provided adequate predictions under field conditions. Clemmens et al. (2003) have shown that these procedures do not adequately deal with changes in the jet nappe during the transition from free to submerged flow and they do not deal with variations in downstream flow conditions. The Energy-Momentum (EM) method is presented here briefly. The basic layout is shown in Figure 2.

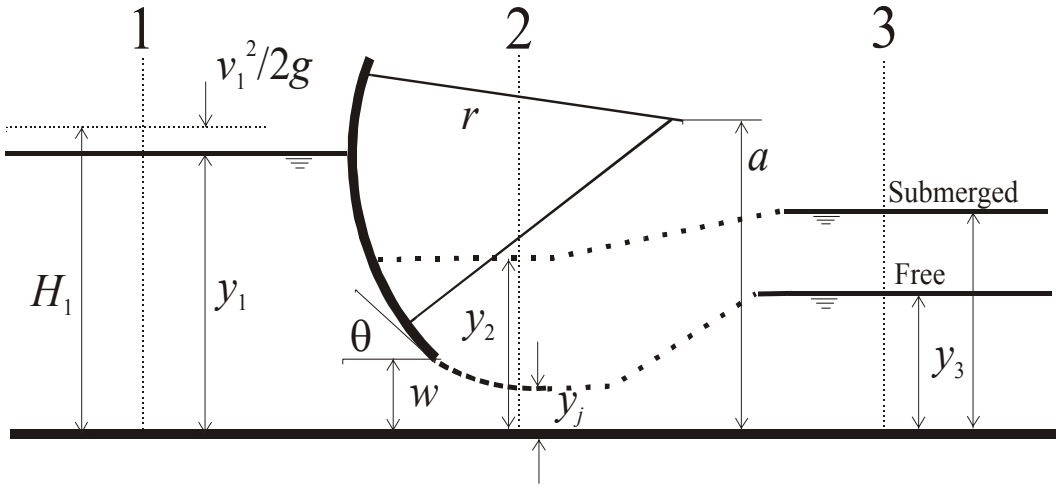

Figure 2. Definition sketch for radial-gate.

Under free flow conditions, the discharge for a given gate opening (and configuration) and a given upstream energy level can be found from

$$Q = \delta w b_c \sqrt{\frac{2g(H_1 - \delta w)}{1+\xi}} \tag{1}$$

where Q is the discharge, H_1 is the upstream energy head, b_c is the width of the gate, δ is the contraction coefficient (ratio of minimum depth y_j to gate opening w), g is the acceleration of gravity, and ξ is the energy loss coefficient. Simple equations for the contraction coefficient and energy loss coefficient are found in Clemmens et al. (2003). This expression provides a refinement on prior equations for free flow.

For submerged flow conditions, the EM method uses the energy equation on the upstream side of the gate, and the momentum equation on the downstream side. Clemmens et al. (2003) show that the jet velocity changes during initial submergence. This alters the energy relationship. They propose an energy correction term, E_{corr}, to account for this change in velocity. The resulting expression for discharge is

$$Q = \delta w b_c \sqrt{\frac{2g(H_1 - y_2 + E_{corr})}{1+\xi}} \tag{2}$$

where y_2 is the depth at the vena contracta during submerged flow conditions. The energy correction term published in Clemmens et al. (2003) was in error. It should have been

$$E_{Corr} = (y_2 - y_j)\left(0.52 - 0.34 \arctan\left\{7.89\left[\frac{y_2 - y_j}{y_j} - 0.83\right]\right\}\right) \tag{3}$$

Wahl (2004) has provided alternative expressions for this energy correction term based on the ratio of gate opening to upstream energy head.

The momentum equation is applied from the vena contracta to a point downstream from the hydraulic jump. (See Figure 2).

$$Qv_e + b_c g \frac{{y_2}^2}{2} + \frac{F_w}{\rho} = Qv_3 + \frac{F_3}{\rho} + \frac{F_{drag}}{\rho} \tag{4}$$

where v_e is the effective velocity in the jet (discussed below), v_3 is the downstream velocity, ρ is the density of water (mass per unit volume), F_3 is the hydrostatic-pressure force exerted by the downstream water depth, F_w is the component of the force on the water from all surfaces between Sections 2 and 3 opposite to the direction of flow, including hydrostatic forces on all walls, and F_{drag} is the frictional force of the channel bed and sidewalls on the water. These surfaces can be determined by taking the downstream area and projecting it back to Section 2 (assuming the section only expands from Section 2 to Section 3). Projected surfaces include the edges of the piers that separate the individual gates, closed gates, weir overfall sections, and the canal walls where the cross section expands. For rectangular cross sections, the force terms reduce to $bgy^2/2$, with subscripts 3 or w on b and y. Clemmens et al. (2003) ignored channel friction and bed slope effects.

The effective velocity in the jet is found from

$$\frac{v_e^{\,2}}{2g} = \frac{v_j^{\,2}}{2g} - E_{Corr} \tag{5}$$

where v_j is the theoretical velocity in the jet, $Q/(\delta w b_c)$. In the earlier work of Clemmens et al. (2003), the drag force caused by friction was ignored since we were not fully applying the momentum equation for the free-flow case. With multiple gates, we need to determine the force-momentum balance for all gates in total, not just individually. So, if we have one gate submerged and one free, we need to determine the frictional force associated with free-flowing gates. This force can be computed with one of several frictional resistance formulas. For a unit width channel where the wetted perimeter equals the bottom width, the force term is

$$\frac{F_{drag}}{\rho} = \frac{v^2 g b_c L}{C^2} = \frac{n^2 v^2 g b_c L}{C_u y^{1/3}} = \frac{C_F v^2 b_c L}{2} \tag{6}$$

where L is the channel length considered, v is the velocity of the live stream acting on the bed, C is the Chezy coefficient, n is the roughness factor in the Manning equation with units coefficient C_u, and C_F is the drag coefficient. In the vena contracta, the velocity distribution is nearly uniform, suggesting the use of a drag coefficient would be most appropriate. Here for simplicity we use a drag coefficient of 0.003. (see Clemmens et al. 2001 for justification and calculation methods).

Application to Multiple Gates

The EM method has been tested, to a limited degree, on check structure 1-08 on the Arizona Canal. The check structure is shown in Figure 3 has three radial gates and a weir, with widths from right to left; 4.87 m gate 1, 1.83 m gate 2, 1.52 m weir, and 6.09 m gate 3. The weir will not be considered in this analysis. The other gate dimensions are trunnion-pin height, a = 1.53 m and radius, r = 1.94 m. The approach and tailwater channels are 0.06 m above the invert of the gate structure. As a starting point for this analysis, the data collected on May 22, 2002 was used, for which the upstream water level was 1.774 m above the gate structure invert and the downstream water level was 0.934 m above the invert. The gate openings for these three gates were 0.273 m, 0.608 m, and 0.198 m, respectively. The free-flow discharge was calculated based on the assumption that these gates were completely independent of one another (i.e., each had a separate approach velocity), as one would get from the standard textbook equation. The results are shown in Table 1. Note that the velocities in the approach and tailwater channels are different for each gate, as if the gates were completely isolated. Results are shown in terms of the force plus momentum (F+M) at sections 2 and 3.

From Table 1, we see that gates 1 and 2 are free flowing, since the force+momentum at section 2 is greater than the force+momentum at section 3. The difference in F+M is made up by the force caused by the frictional resistance of the channel bed and walls. This resistance slows down the water until the change in momentum is in

Figure 3. Multi-gate check structure 1-08 of the Salt River Project, Phoenix, AZ. Structures numbered from right to left.

balance with the sum of the forces, and there a hydraulic jump forms. For gate 3, we see that F+M at section 3 exceeds that at section 2. Thus under free flow, there is not enough F+M to avoid submergence, and a reduced discharge results. Note that when F+M is balanced (last row in Table 1), that the depth at the vena contracta has increased due to the submergence (0.530 m, rather than 0.141 m) and the discharge has dropped from 4.87 to 4.25 m^3/s, a 13% decrease. Total discharge changed from 13.97 to 13.36 m^3/s, a 4% decrease.

Table 1. Results of EM method for individual gates.

Gate	v_1	y_2	Q	F+M Section 2	v_3	F+M Section 3	F+M Gain	Condition
	m/s	m	m^3/s	m^4/s^2	m/s	m^4/s^2		
1	0.62	0.190	5.21	30.06	1.22	27.23	-9.4%	Free
2	1.24	0.399	3.90	22.25	2.44	17.34	-22.0%	Free
3	0.47	0.141	4.87	28.24	0.92	30.53	8.1%	As if free
3	0.41	0.530	4.25	29.48	0.80	29.48	0.0%	Submerged

The scenario depicted in Table 1 does not adequately describe the situation since, in fact, these gates have common fore and after bays. The approximation would probably be acceptable if the walls between the gates extended 5 to 10 m upstream and say, 30 m downstream. This rarely occurs in practice. If we assume the channels upstream and downstream are rectangular with a width equal to the sum of the three gate widths and a common velocity in the forebay and a common velocity in the after bay, we get the results shown in Table 2. Gate 2 has a much larger vertical gate opening than the others, and is much narrower. Note how the velocity downstream from Gate 2 significantly decreases as the result of combining the downstream flow.

One might erroneously conclude from Table 2 that gate 3 will prove more submerged when the flow is combined downstream than if separate. However this is not the case. First, one must consider the total F+M for all three gates when considering gate

submergence. In the above calculations, we are balancing force and momentum for each gate with combined velocities, but still with a balance for each gate. In reality, there is lateral momentum transfer through turbulent shear and mixing of streams as a result of large differences in water depths downstream from these gates. Unfortunately, it is not enough to simply take the values of F+M calculated here to establish whether or not all gates are free or not. The friction on the bed must also be included, since those gates that are free flowing will have significant drag forces. (Otherwise they would never jump).

Table 2. Results of EM method with common upstream and downstream velocities. (Total channel width same as Table 1).

Gate	v_1	y_2	Q	F+M Section 2	v_3	F+M Section 3	F+M Gain	Condition
	m/s	M	m^3/s	m^4/s^2	m/s	m^4/s^2		
1	0.63	0.190	5.21	30.08	1.24	27.34	-9.1%	Free
2	0.63	0.399	3.82	21.41	1.24	12.58	-41.2%	Free
3	0.63	0.141	4.88	28.40	1.24	32.16	13.2%	As if free
Total			13.91	79.89		72.08	-9.7%	

To get an estimate of the length of channel required to obtain a F+M balance, a direct-step method was used to solve the momentum equation, assuming each gate is independent. Starting with the depth of the free jet in the vena contracta, the depth was incremented. F+M at each depth was calculated, and equation 6 was used to solve for the length, L, for which equation 4 was in balance, using the average velocity. This was continued at successively deeper depths until the momentum equation balanced. For gate one, with $C_F = 0.003$ the distance was 13.4 m and the resulting depth was 0.212 m, only 11% greater than the vena contracta depth. For gate 2, use of the drag coefficient gave 89 m, at a depth 45% greater. (For comparison, a Manning $n = 0.015$ gave 5.3 m and 47 m for gates 1 and 2, respectively. Selection of the appropriate frictional-resistance formula will be the subject of future work.)

The issue remains that we have to balance the force and momentum for the sum of all gates. For this example, the gate sidewalls end about 2 meters downstream from the vena contracta. Beyond that, the flow for all gates mix and the depths increase significantly, even though one particular gate may indicate a higher velocity and lower depth. From Table 1, note the depths at the vena contracta for the three gates, with gate 3 submerged; 0.19, 0.40, and 0.53 m for these three gates, respectively. Once the sidewalls have ended, it is not possible to maintain these differences in flow depth downstream from individual gates (Figure 4). This then influences the length over which we need to consider frictional forces. For a simple first cut, it is assumed that all gates incurred frictional resistance for 2 m downstream, and free-flowing gates incur frictional resistance for a distance of $b_c/2$ downstream, since flow under a very wide gate may encounter some resistance over part of its width. (Note, this is just a rough calculation to get a sense of the magnitude of this effect.) In addition, the force of frictional resistance was computed for a total distance of 30 m downstream from the vena contracta, approximately where downstream water level was measured, with a depth, and associated velocity, equal to the measured tailwater depth. The

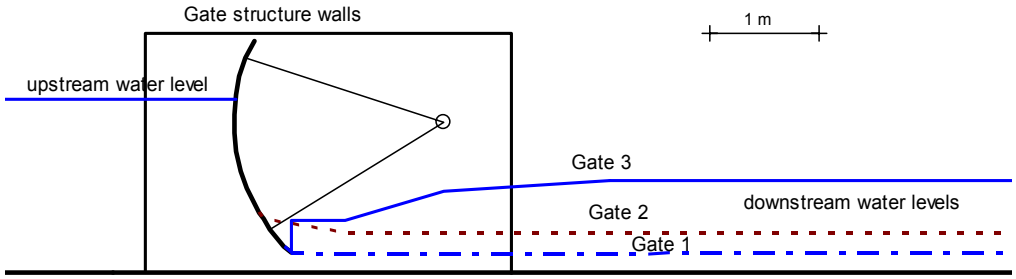

Figure 4. Profile of gate structures with different downstream water levels.

results are shown in Table 3. The momentum balances shown are the difference between the momentum at section 3 and that at section 2, with the additional momentum from the two friction terms added to the values for section 3 in Table 2. Note that even when considering this frictional resistance, the total momentum balance is still negative, indicating that all gates are still free flowing. While these calculations are approximate, they do indicate that a free flowing gate will help to keep a neighboring gate from becoming submerged. The effects of frictional resistance changed the overall momentum balance by about 4%.

Table 3. Additions to EM method from force of frictional resistance.

Gate	Jet length	Friction of jet	Downstream length	Friction downstream	Momentum balance	Momentum balance	Condition
	m	m^4/s^2	m	m^4/s^2	m^4/s^2		
1	7.44	1.71	22.56	0.26	-0.77	-2.6%	Free
2	5.91	0.44	24.09	0.10	-8.28	-38.7%	Free
3	2.00	0.59	28.00	0.40	4.74	16.7%	As if free
Total					-4.31	-5.4%	All Free!

Field measurements under these conditions showed static pressures in the vena contractas for these three gates of 0.335, 0.485, and 0.712 m, respectively. Visual observations suggested that gate 2 was clearly free flowing, gate 1 was either free flowing or just starting to submerge and gate 3 was clearly submerged. At least qualitatively, the relative submergence of these gates is in line. The above calculations used the contraction coefficient used by the Salt River Project, which may not match that determined by Wahl (2004) for gates with a J-seal. Also, the channel was much wider than the three gates, adding further to submergence, and there was flow over the side weir.

Avoiding Submergence Transition

As a practical matter, the calibration of radial gates seems to be sufficiently accurate with the EM method if the gates are either free-flowing or fully submerged. It is when the gates are in the transition zone that calibration is highly inaccurate. Wahl (2004) suggests that the range of the transition zone is highly dependent upon the relative gate opening, w/H_1. For large values, where the gate is open wide compared to the

upstream energy head, the transition zone can become very wide. However, when the head on the gate is large with respect to the opening, the transition zone is sufficiently narrow that it may be worth developing logic to avoid it. Adjusting gates to avoid the transition zone could improve measurement accuracy. This might be accomplished by positioning all gates to the same opening so that all are in free flow. When that is not feasible or when that produces transition zone flow, one could open some gates to ensure that they are in free flow and close others to increase the submergence upon them. This will require further investigation over a wider range of conditions before substantial recommendations can be made.

The exercise given here attempts to determine the feasibility of avoiding the submergence transition zone. As an example, we start with the same check structure as above, with all gates set to 0.404 m and with the same fore and after bay water levels. The results are shown in Table 4. Note that all gates are free flowing, while as previously set, it gave the appearance of one being submerged. With all gates set at the same position, the momentum balance is more negative indicating that the gates are farther from being submerged. Based on rough calculations, a momentum balance is obtained with a jump roughly 12 m downstream.

Table 4. Results of EM method with all gates in same position with free flow.

Gate	v_1	y_2	Q	Momentum Section 2	v_3	Momentum Section 3	Momentum Difference	Condition
	m/s	m	m^3/s	m^4/s^2	m/s	m^4/s^2		
1	0.63	0.194	5.29	30.52	1.24	27.43	-10.1%	Free
2	0.63	0.194	1.98	11.45	1.24	10.29	-10.1%	Free
3	0.63	0.194	6.61	38.16	1.24	34.29	10.1%	Free
Total			13.88	80.14		72.01	-10.1%	Free

Now, the after bay water level is artificially raised to 1.01 m, at which momentum is just balanced (actually -0.9%). Raising the after bay level to 1.02 m puts all gates into the transition zone, as reflected by the relative value of energy correction, $E_{corr}/(y_2-y_j)$ = 0.51 (Clemmens et al. (2003). The result of these conditions is shown in Table 5. The discharge in this case has been decreased from 13.88 to 13.53, or only 2.5%. The downstream velocity has decreased both due to decreased discharge and increased water depth. Note that the depth in the vena contracta has nearly doubled, $(y_2-y_j)/y_j$ = 0.83.

Table 5. Results of EM method with all gates in same position with transition flow.

Gate	v_1	y_2	Q	Momentum Section 2	v_3	Momentum Section 3	Momentum Difference	Condition
	m/s	m	m^3/s	m^4/s^2	m/s	m^4/s^2		
1	0.62	0.355	5.15	30.38	1.11	30.38	0.0%	Transition
2	0.62	0.355	1.93	11.40	1.11	11.40	0.0%	Transition
3	0.62	0.355	6.44	37.98	1.11	37.98	0.0%	Transition
Total			13.53	79.77		79.77	0.0%	Transition

To provide the same flow rate with two gates free and one submerged, the positions of the three gates were moved from 0.404 m to 0.500, 0.500, and 0.313 m,

respectively. This provides the results shown in Table 6. This table does not show the momentum contribution from frictional resistance along the floor. Depending on the choice for the length of the jet considered to be free flowing, we can get the net momentum to be 1% or so on either side of 0.0%. In this case, we do not compute a momentum balance for the submerged gate 3, which would result in a much higher depth in the vena contracta. The depth there is already more than three times the vena-contracta depth.

Table 6. Results of EM method with one gate fully submerged.

Gate	v_1	y_2	Q	Momentum Section 2	v_3	Momentum Section 3	Momentum Difference	Condition
	m/s	m	m^3/s	m^4/s^2	m/s	m^4/s^2		
1	0.62	0.242	6.50	37.25	1.11	31.88	-14.4%	Free
2	0.62	0.242	2.44	13.98	1.11	11.96	-14.4%	Free
3	0.62	0.490	4.59	30.38	1.11	35.94	18.3%	Submerged
Total			13.53	81.61		79.77	-2.3%	

Summary

This evaluation of radial gate submergence shows that the EM method is able to deal with the issue of multiple radial gates, even when the gates are not open by the same amount. The method can also deal with the case of one or more free-flowing and one submerged gate. However, the influence of friction on the bed under free flow needs to be dealt with more rigorously to make this a practical approach. The two-dimensional aspect of the gate structure plays a role in determining the appropriate frictional force. Further studies are also needed to examine methods for dealing with the combination of multiple submerged gates with one or more free-flowing gates. This analysis also did not examine the errors in flow measurement prediction from making various assumptions.

References

Bos, M. G. (Editor) 1989. Discharge measurement structures. 3rd Edition. Publication 20. International Institute for Land Reclamation and Improvement/ILRI, Wageningen, The Netherlands. 401 pp

Buyalski, C.P. 1983. Discharge Algorithms for Canal Radial Gates. REC-ERC-83-9, Engineering and Research Center, U.S. Bureau of Reclamation, Denver, CO. 232 pp.

Clemmens, A. J., Wahl, T. L., Bos, M. G., and Replogle, J. A. 2001. Water Measurement with Flumes and Weirs, Publication #58. International Institute for Land Reclamation and Improvement, Wageningen, The Netherlands. 382 pp.

Clemmens, A.J., Strelkoff, T.S., and Replogle, J.A. 2003. Calibration of submerged radial gates. J. Hydraulic Engr. 129(9):680-687.

Wahl, T.L. 2004. Energy correction for calibration of submerged radial gates. J. Hydraulic Engr. (draft under journal review).

In Search of Easy-to-Use Methods for Calibrating ADCP's for Velocity and Discharge Measurements

Kevin Oberg[1]

[1]U.S. Geological Survey, Office of Surface Water, 221 N. Broadway Ave., Urbana, IL 61801; PH (217) 344-0037; email: kaoberg@usgs.gov

Abstract

Acoustic Doppler current profilers[2] (ADCP's) have become a common tool for measuring streamflow and profiles of water velocity. Despite their widespread use, no standard procedure has been adopted or accepted for calibration of ADCP's. Limitations of existing facilities for testing point-velocity meters, the complexity of ADCP instruments, and rapid changes in ADCP technology are some of the reasons that a standard procedure has not been adopted. This paper outlines various methods for calibrating ADCP's, discusses the advantages and disadvantages of these methods, and presents a simple, cost-effective procedure for calibrating an ADCP in the field.

Standard methods for the calibration of current meters involve towing a meter in a tow tank at various known speeds. This method has also been used to calibrate ADCP's. Disadvantages to this method include lack of adequate and uniform backscattering material, lack of flowing water in the testing facility, and inability to use the ADCP's internal flux-gate compass. Use of flumes for ADCP calibration is not practical for many ADCP's due to width and depth restrictions associated with the instruments. ADCP's and conventional methods for measuring velocity and discharge have also been compared. However, these field comparisons are costly and conventional velocity and discharge measurements may be subject to relatively large uncertainties.

The USGS is investigating a new method for ADCP calibration. This method requires the use of differential global positioning system (DPGS) with sub-meter accuracy and standard software for collecting ADCP data. The method involves traversing a long (400 – 800 meter) course at a constant compass heading and speed, while collecting simultaneous DGPS and ADCP data. This process is repeated several times and the ratio of the course length measured by means of the ADCP to the course length measured by means of DGPS is computed. When this ratio is less than 0.995, measurements made with RD Instruments' Rio Grande ADCP most likely have a negative bias error and when it is greater than 1.003 the ADCP most likely has a positive bias error. It is estimated that this procedure can be completed in 2 hours or less, and can be done by anyone with access to a sub-meter DGPS.

Introduction

Acoustic Doppler current profilers (ADCP's) have become a common tool for measuring water velocity and discharge. At present (2002), the U.S. Geological Survey (USGS) operates

[2] In this paper, the use of the term acoustic Doppler current profiler is intended to refer to a class of instruments rather than any particular brand or model.

approximately 130 ADCP's for measurement of velocity and discharge in streams and estuaries throughout the United States. Many more ADCP's are used throughout the world, especially for the measurement of ocean currents and flows in estuaries. Despite their widespread use, no standard procedure yet has been accepted for calibration of ADCP's. No standard procedure has been accepted because of limitations of existing facilities for testing current meters, the complexity of the instrument, and rapid changes in the technology. Many of the facilities used for testing devices for measuring currents in streams were not designed for use with ADCP's, but rather for mechanical, point velocity current meters. Often physical features of these facilities, such as the width of a tow tank, limit its use for ADCP calibration. When making ADCP measurements, consideration must be given to factors such as adequate backscattering material in the water, interference from sidewalls and the bottom, and the presence of variable magnetic fields. When calibrating mechanical current meters, most of these factors are not important. Much more data are collected during ADCP measurements as compared to mechanical current meters. Interpretation of ADCP data is sometimes challenging and more difficult than data collected with mechanical current meters. Finally, the functionality of ADCP's has changed rapidly over the past 10 years. Scientists and engineers often spend considerable effort to keep abreast of these technological developments, which limits time available for detailed calibration and testing.

The purpose of this paper is to (1) discuss various methods for calibrating ADCP's and advantages and disadvantages of these methods, (2) present results from tow tank tests made by the USGS, and (3) propose a simple method for calibrating an ADCP in the field. The scope of this paper does not allow for a detailed discussion of each of the methods, nor a detailed presentation of the results of such methods as tow tank testing. A more comprehensive report is planned for detailed presentation of these results.

Methods for Calibrating Acoustic Doppler Current Profilers

Engineers and oceanographers have considered various methods and/or facilities for calibrating ADCP's. Not all of these methods and facilities will be discussed in detail. Rather, only the more promising methods are discussed here along with method advantages and disadvantages.

Instrument Comparisons

A common method for evaluating or calibrating new instruments is to conduct measurements with that instrument and compare the results to measurements made simultaneously or nearly simultaneously with other well-calibrated instruments. For example, Lohrmann and others (1994) and Voulgaris and Trowbridge (1998) both compared measurements made with an acoustic Doppler velocimeter (ADV) to measurements made with a laser Doppler velocimeter (LDV). Voulgaris and Trowbridge (1998) found that mean flows and Reynolds stress values from the ADV were within 1 percent of measurements made with the LDV. These comparisons were made in a laboratory setting without using an ADCP. Few comparisons have been made in a laboratory flume, using commercially available ADCP's. Nystrom and others (2002) showed that mean velocities from ADCP measurements were within 1 cm/s of ADV measured velocities. Furthermore, they found that turbulence statistics that were computed based on ADCP measurements usually were biased. Nystrom and others made their comparisons in a 1.8 m wide

laboratory flume in 0.9 m deep flow. The advantages of such comparisons are that flow rates and instrument settings can be controlled precisely in a laboratory flume. In addition, it is not difficult to keep enough backscattering material suspended in the flow such that the ADCP will function. However, acoustic interference, caused by reflections from sidewalls and the bottom of the flume, can result in erroneous measurements. Although flow rates can be changed in the laboratory, it is difficult to obtain high velocity measurements because typically the water depths for higher flow rates are such that there is inadequate depth to allow for proper ADCP operation. Furthermore, instrument comparisons must be carefully made because often the instruments being compared do not measure the same volume of water at the same time. The question often arises when making such comparisons, "Which instrument is correct"?

Bos (1991), Lemmin and Rolland (1997) and Appell and others (1985) all have made field comparisons of ADCP's with other instruments or other ADCP's. Simpson and Oltmann (1993) made many detailed velocity profile measurements with mechanical current meters and compared the profiles to those obtained from an ADCP. Many other researchers have made comparisons that are not cited here. Appell's (1985, p. 726) remarks aptly summarize some field comparisons issues. Appell states, "This experiment highlights the difficulty of trying to determine from field intercomparisons. …. It is difficult to estimate uncertainty with any field intercomparison without adequate measurements from reliable, calibrated instruments strategically place at the experiment site." As a result, field comparisons typically are costly and cannot be made with the same degree of reliability as in a controlled laboratory.

Tow Tanks

Tow tanks have been used to calibrate current meters for many years. Many detailed studies have been done in tow tanks, and experience and expertise in the use of such facilities is well developed. Experience has shown that tow tanks are a reliable method for calibrating many types of current meters, especially mechanical meters. It is therefore not unusual that one of the first methods considered for calibration of ADCP's is a tow tank. Appell and others (1988), Lemmin and Rolland (1997), and Shih and others (2000), among others, all have made use of a tow tank to calibrate or evaluate ADCP's.

Tow tanks offer the advantage of providing a very accurate reference velocity. The tow cart velocity can be measured precisely and even be referenced to known standards, such as the National Institute of Standards. The speeds used in tow tank tests also more closely match the range of velocities that will be measured in the field. For example the tow cart at the USGS Hydraulics Lab is capable of obtaining speeds from 0.08 m/s to 3.6 m/s. The primary disadvantage of tow tanks is that the water in the tank has a zero or very small velocity (small currents induced by thermal gradients are not uncommon). As a result backscattering material, essential to ADCP operation, does not stay suspended in the water column and artificial seeding of the water becomes necessary. However, this seeding usually does not result in a uniform distribution of the backscattering material. Other disadvantages of tow-tank facilities are boundary interferences, lack of any shear in the water column, and the presence of large magnetic or electromagnetic fields that cause fluctuations in the heading measured by the ADCP.

Distance Course

Appell and others (1988) others describe the layout and application of a distance course for calibrating ADCP's. Two courses, one 200 meters long and the other, 1000 meters long, were surveyed and established on a lake for the purpose of testing ADCP's. With this method, the ADCP is mounted on a boat and driven over the course at a constant speed and using a constant heading. Usually, two passes with the boat and ADCP are made on reciprocal courses. The distance traveled as measured by the ADCP using bottom tracking then is compared to the known distance. This method can be quickly used to determine whether any bias errors are present and commonly is used by ADCP manufacturers to check for beam alignment errors. It also is possible to use water tracking, by selecting a layer of water at a user-specified depth, as a reference for the boat speed. Use of a water layer as a reference for testing an ADCP is appropriate as long as any ambient currents in the lake are constant while the two passes (on reciprocal headings) are made. There are various disadvantages in using a distance course including, (1) the startup cost of surveying in a distance course at locations convenient to users throughout the U.S. and (2) this method does not test all aspects of ADCP operation.

Discharge Measurement Comparisons

The USGS has made comparisons of discharges measured by the ADCP to discharges as measured by other commonly used equipment, such as Price AA current meters. Morlock (1995) made comparison discharge measurements at 11 locations throughout the U.S. and found that most of the ADCP measured discharges typically were within 5 percent of the discharge measured by Price AA current meters. Mueller (2002) repeated this work using profilers that were not available to Morlock. Such comparisons are important to the USGS because discharge records are the primary product of the USGS national streamgaging program. Furthermore, almost all the ADCP sensors are used in making a discharge measurement and therefore the errors associated with that measurement reflect the performance of these sensors.

However, there are several major disadvantages to such comparisons. A typical mechanical current meter measurement will only sample a small percentage of the flow area (< 3%), whereas an ADCP will sample between 20 – 60% of the flow area. The time period used when making discharge measurements is often significantly different for both kinds of measurements. Furthermore, mechanical current meter measurements are subject to both instrument and human errors. This makes it difficult to accurately determine measurement errors, without resorting to many such comparisons. Finally, discharge measurement comparisons are quite expensive to make.

USGS Tow-Tank Tests

As a part of a joint effort by the USGS and the South Florida Water Management District to evaluate the accuracy of ADCP measurements, the USGS arranged to conduct ADCP testing at the Naval Center for Surface Warfare in the David Taylor Model Basin, in West Bethesda, Maryland. This facility is used regularly by personnel from the National Oceanographic and Atmospheric Administration (NOAA) to calibrate ADCP's used by NOAA. The USGS contracted to use this facility for ADCP testing for the period March 13-16, 2000. The goal of these tests was to evaluate the feasibility of using such a facility to calibrate ADCP's. If these

tests were successful and could be done cost-effectively, the procedures used could become an essential part of the USGS streamflow quality-assurance and quality control program.

David Taylor Model Basin

The David Taylor Model Basin consists of several hydraulic facilities, including two towing basins and a circulating water channel (http://www50.dt.navy.mil/facilities/Carriages.html). The towing basins are 760 m long, of which one is 15 m wide and the other is 8 m wide. The 15-m wide basin has been divided into two sections, one section which is 260 m long and the other section is approximately 500 m long. The tests described herein were conducted in the 260-m long section of the 15-m wide basin.

Testing Procedure

The testing procedure for each instrument consisted of the following steps:

1. Mount the ADCP to be tested in dry dock of the towing basin.
2. Seed the tank with powdered limestone.
3. Make calibration runs at specified tow cart speeds. Two measurements were made at various speed, one in an easterly direction and one in a westerly direction. Two passes in opposite directions were made so that any residual current in the basin would cancel out.

Both ADCP data and tow cart velocities were simultaneously recorded on a computer.

When testing acoustic Doppler velocity meters in a towing basin, it is necessary to seed the tank with a backscattering material. Adequate backscattering material is essential to Doppler measurements. If the concentration of backscattering material is too low (< 35 db), the size of the backscattering particles is too small, or the concentration of the backscattering material is highly variable, significant errors in the measured velocities may result. Various approaches to seeding were used during the 4 days of testing. Initially, seeding consisted of broadcasting powdered limestone from the tow cart. This seeding worked fairly well but required a lot of lime and did not provide good backscatter uniformity. Subsequently, a lime slurry was sprayed into the towing basin prior to the commencement of testing. It was hoped that this method would result in more uniform backscatter in the towing basin.

Five ADCP's were tested at the David Taylor Model Basin, a SonTek[3] Argonaut SL ADP, a 3 mHz SonTek ADP, a RD Instruments Rio Grande 600 kHz ADCP, a RD Instruments Broadband 1200 kHz ADCP, and a prototype 3-beam horizontal 600 khz ADCP made by RD Instruments. Only the results from the Rio Grande and Broadband ADCP were available for inclusion in this paper. Data for the other instruments presently are being analyzed and the data and corresponding analyses are planned to be published later. The test results summarized below are for the Rio Grande 600 kHz ADCP, serial number 1189 with firmware version 16.03 and the Broadband 1200 kHz ADCP, serial number 1330, using firmware version 5.47. The Rio Grande ADCP firmware used (version 16.03) is actually firmware from the Workhorse series of ADCP's. This firmware was being used in this instrument as a part of a separate evaluation of new firmware features. Two independent velocity measurements were obtained, the bottom

[3] The use of firm, trade, and brand names in this report is for identification purposes only and does not constitute endorsement by the U.S. Geological Survey.

track velocity and the water track velocity. The bottom track velocity, or the velocity of the ADCP over the bed, is measured by the ADCP using a long acoustic pulse that is independent of water velocity measurements. A single velocity is recorded for each sample (known as an ensemble). Water-track velocities are measured using a different technique than bottom tracking (Simpson, 2002) that involves the use of short, phase-encoded acoustic pulses.

Test Results

The means of two tow-cart runs, one in the easterly direction and one in the westerly direction, with one exception are shown in table 1. Tow cart velocities were not available for the 1200 kHz ADCP run in the westerly direction at a speed of 41 cm/s. Therefore, only the results from the single run in the easterly direction are shown. All ADCP velocity measurements shown in table 1 were obtained by computing the depth-averaged velocity for all valid velocity measurements over the entire time span of each run. Tow cart velocities were obtained by averaging the speeds from a speed log provided by the David Taylor Model Basin staff.

Table 1.--Selected results of tow tank tests at the David Taylor Model Basin, West Bethesda, Maryland, March 13-16, 2000

[cm/s, centimeter per second; %, percent; kHz, kilohertz; --, not applicable; bottom track, velocity as measured by the ADCP using a bottom track pulse; water track, velocity as measured by the ADCP using a water track pulse]

	ADCP						
	Mean measured velocity			Mean velocity difference			
	Tow Cart	Bottom Track	Water Track	Bottom Track		Water Track	
ADCP Type	(cm/s)	(cm/s)	(cm/s)	(cm/s)	(%)	(cm/s)	(%)
1200 kHz	7.74	8.20	7.65	0.46	5.9	-0.09	-1.2
1200 kHz	14.9	15.0	14.7	0.09	0.6	-0.16	-1.1
1200 kHz	22.8	22.8	22.6	-0.03	-0.1	-0.19	-0.8
1200 kHz	41.1	41.0	40.9	-0.09	-0.2	-0.21	-0.5
1200 kHz	61.8	61.8	61.5	0.00	0.0	-0.30	-0.5
1200 kHz	123	123	123	-0.28	-0.2	-0.51	-0.4
				0.62	--	0.00	--
600 kHz	0.00	0.62	0.00	-0.50	-6.6	0.00	0.0
600 kHz	7.61	7.10	7.60	-0.77	-5.2	-0.25	-1.7
600 kHz	15.0	14.2	14.7	-0.62	-2.7	-0.42	-1.9
600 kHz	22.8	22.1	22.3	-0.06	-0.1	-0.35	-0.6
600 kHz	61.8	61.8	61.5	-1.13	-0.9	-0.21	-0.2
600 kHz	123	122	123	-0.16	-0.1	-0.76	-0.4
600 kHz	185	185	185	-0.43	-0.2	0.30	0.1
600 kHz	258	257	258	0.46	5.9	-0.09	-1.2

The mean difference between the tow-cart velocity and the measured ADCP velocity was -0.21 cm/s and -0.23 cm/s for bottom track and water track respectively. The mean percent difference was -0.8% and -0.7% for bottom track and water track respectively. These differences are close to the expected error from such instrument. ADCP's will tend to report a measured velocity that is somewhat less than the true velocity due to a number of instrument factors. The average errors described above are about what would be expected for a well-calibrated system (Gary Murdock, RD Instruments, personal communication, 2002). Some versions of firmware (< 10.09 for Rio Grande ADCPs) had bottom tracking errors of about this magnitude. However, it is noticeable that differences between tow cart and bottom-track velocities at slow speeds (15 cm/s or less) are larger than those for water-track velocities. This may be indicative of undetected interference and needs to be investigated further.

For the 600 kHz ADCP, various tests were conducted in which the tow carriage was not moved while both tow cart and ADCP velocities were recorded (table 1). Interestingly, the bottom track measurements showed a mean error of –0.62 cm/s, whereas the water track velocities had a mean error of zero. Normally, one would expect bottom-track velocity measurements to be more accurate than water-track velocity measurements. The reasons for this difference and for the negative "offset" for bottom track velocities should also be investigated further. Errors do not tend to increase with speed (figure 1). This result is in contrast to results from Appell and others (1988) that showed that some of the early ADCP's manufactured by RD Instruments had errors that increased with speed.

Figure 1. Graph of showing differences between tow cart velocity and ADCP measured velocity.

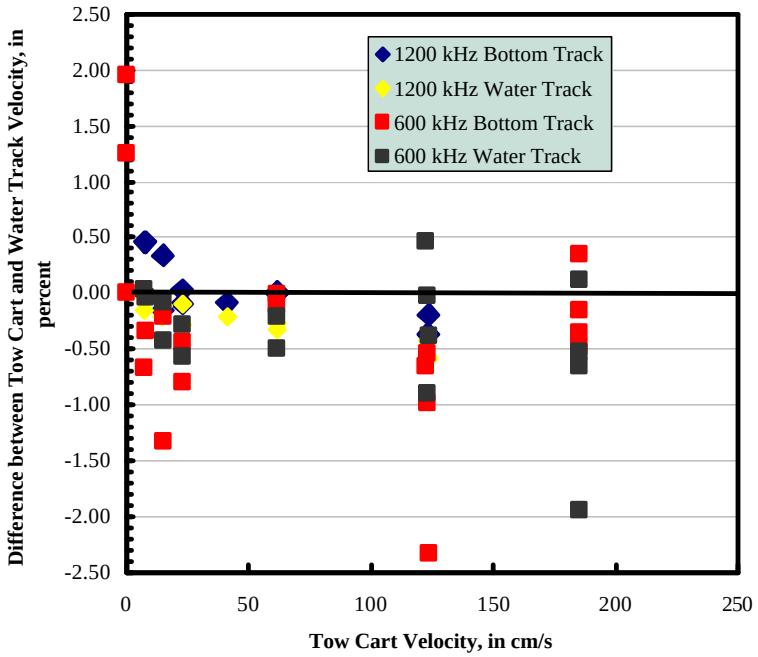

Although these results appear promising, a number of practical difficulties were encountered during these tests. First, the large amount of metal in the towing basin introduced some errors into the measurements. For data analysis, the compass heading had to be ignored and values for the heading, pitch, and roll fixed to a constant value. Although assigning a constant value for heading can be done easily in the laboratory, and in fact, heading, pitch and roll values were constant during the measurements, field measurements made with an ADCP require the use of the compass and are subject to pitch and roll changes that must be applied throughout the measurement. Second, the surfaces (bed and sidewalls) of the tow tank acoustically are quite reflective. It is likely that side-lobe interference from reflections off of the bed could account for observed variability in bottom track velocity measurements. Finally, and most importantly, the intensity of signal returned to the ADCP (referred to here as backscatter) appreciably varied in space and time. The average backscatter for one of the tow-tank measurements are shown in figure 2a. For one of the depth cells, backscatter ranges from 43 db for beam 3 to 52 db for beam 2. Backscatter for beams 3 and 4 are similar because they are in the same vertical plane. In contrast, for a typical river measurement, variation in backscatter among the 4 beams is no more than 3 db (figure 2b).

Figure 2. Graphs showing the variation in backscatter with depth for (a) tow tank measurements and (b) typical field measurements.

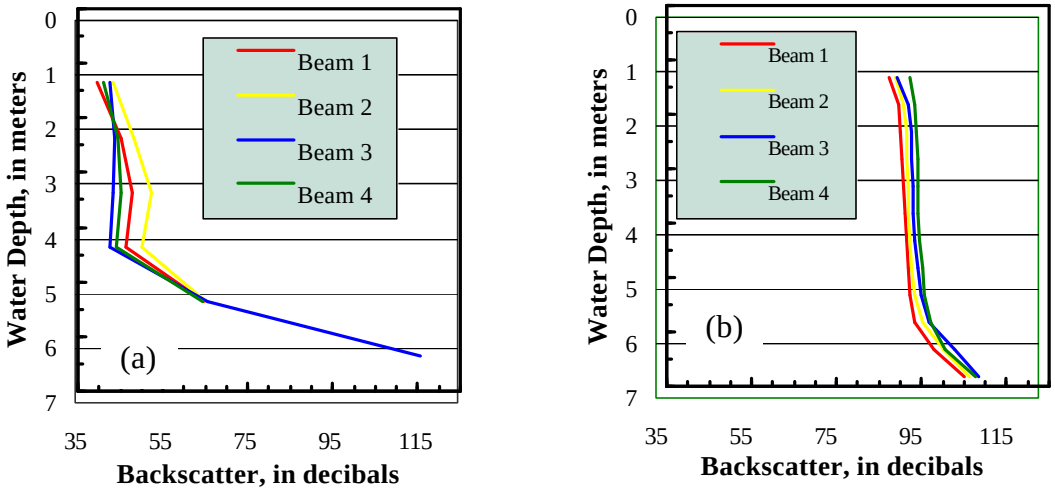

In addition, the backscatter changed appreciably between runs and with depth for a given run. For example, the average backscatter for beam 2 dropped 7 db in about 25 minutes, for measurements made in the same area of the tow tank.

Field Method for Calibrating ADCP's

The USGS is investigating use of a new method for calibration of ADCP's, originally suggested by Gary Murdock (RD Instruments, personal communication, 2002). This method requires the use of a differential global positioning system (DPGS) with sub-meter accuracy and standard software for collecting ADCP data. It is essentially a variation of the distance course method referred to above. Calibration measurements using this method should ideally be made on a lake where the currents are relatively small and there is little or no wave action. The method involves

traversing a long (400 – 800 meter) course at a constant compass heading and speed, while simultaneously recording both DGPS and ADCP data. Then a course of the same length is traversed at a heading approximately 180 degrees from the previous pass. This is repeated for a total of 4 times, (8 passes altogether), while rotating the ADCP 45 degrees between each pair of courses. Rotating the ADCP helps to insure that no directional bias is introduced by a moving bed or other unexpected problems. The ratio of the straight-line distance traveled (commonly called the made-good distance) as measured by means of bottom tracking with the ADCP and the straight-line distance traveled as measured by means of DGPS can be computed. This ratio is referred to herein as BC/GC. When BC/GC is less than 0.995, measurements made with RD Instruments' Rio Grande ADCP most likely has a negative bias error and when it is greater than 1.003 the ADCP most likely has a positive bias error. Values for BC/GC were selected based on work done by RD Instruments (G. Murdock, RD Instruments, personal communication, 2002). A value for BC/GC of 0.995 corresponds to a -0.5% error in bottom-track velocity measurements. A value for BC/GC of 1.003, corresponding to a +0.3% error in bottom-track velocity measurements, was chosen because most RD Instruments Rio Grande ADCP's with firmware 10.14 or greater will tend to under-report bottom track velocities by about 0.1% (Gary Murdock, RD Instruments, personal communication, 2002). Well-calibrated Rio Grande ADCP's should have BC/GC values of approximately 0.998 or 0.999. It is estimated that this procedure can be completed in 2 hours or less, and can be done by anyone with access to a sub-meter DGPS. This time estimate does not include setup time and the time required to drive to the lake.

The primary drawback to this technique is that the full capability of the profiler to measure discharge is not fully tested. In particular, this method primarily tests the bottom-track measurements and not water-track measurements. However, experience has shown that the major sources of bias errors are often in beam alignment errors which will be present in both water-track and bottom-track velocity measurements. Bias errors are a primary concern in using ADCP's to measure streamflow. With proper measurement techniques, random errors can often be reduced to an acceptable level by obtaining more samples (measurements). However, bias errors cannot be eliminated by this means. The above method will provide a good overall check of ADCP performance and it can be done in a cost-effective manner.

During the next 6-12 months, the USGS will document a protocol for this method and will have the protocol evaluated by various offices throughout the country. During this period, appropriate values for BC/GC will be determined for SonTek profilers. After any necessary adjustments to the protocol are made, it is likely that a policy will be implemented within the USGS in which every acoustic profiler will be calibrated using this procedure at fixed intervals in time and after any factory repairs or upgrades.

Summary

Various approaches for calibrating ADCP's have been outlined in this paper, along with brief discussions of the advantages and disadvantages of each approach. Tow tanks, in which an ADCP is towed in a towing basin at known speeds, have been used by Appell and others (1988) and Shih (2000) to calibrate ADCP's. Nystrom (2002) evaluated the ability of ADCP's to accurately measure mean velocities, turbulence intensities, and Reynold's stresses in a flume.

ADCP's and conventional methods for measuring velocity and discharge have also been compared and distance course have been used to evaluate ADCP performance. However, each of these methods have significant drawbacks, such as inadequate and non-uniform backscattering material in tow tanks, width and depth restrictions associated with use of flumes, and field calibrations are costly and often subject to relatively large uncertainties.

The USGS conducted tow tank calibration tests in a large towing basin using five ADCP's in March 13-16, 2000. Results of these tests for two ADCP's show that the mean difference between the tow cart velocity and the ADCP velocity measured was 0.21 cm/s for bottom track data and 0.23 cm/s for water track data. The mean percent difference was 0.8% for bottom track and 0.7% for water track. ADCP bottom tracking measurements made at zero cart speed showed a mean error of –0.62 cm/s. While this is still quite small, the cause for this error should be investigated further.

A new method for calibration of ADCP's is proposed in this paper. This method requires the use of a differential global positioning system (DPGS) with sub-meter accuracy and an ADCP to collect data on a course with a fixed heading. The ratio of the straight-line distance traveled (commonly called the made good distance) as measured by means of bottom tracking with the ADCP and the straight-line distance traveled as measured by means of DGPS can be computed. When this ratio is less than 0.995, measurements made with RD Instruments' Rio Grande ADCP most likely have a negative bias error and when it is greater than 1.003 this ADCP most likely has a positive bias error. It is estimated that this procedure can be completed in 2 hours or less, and can be done by anyone with access to a sub-meter DGPS (not including setup and driving time). It is believed that this technique will be useful in helping detect significant bias errors in ADCP's cost-effectively. The USGS is exploring implementation of this method nationwide.

References

Appell, G.F., Mero, T.N., Sprenke, J.J., and Schmidt, D.R. (1985) "An intercomparison of tow acoustic Doppler curren profilers." *Proc. Of Oceans '85,* New York, NY, 723-730.

Appell, G.F., Gast, J., Williams, R.G., and Bass, P.D. (1988) "Calibration of acoustic Doppler current profilers." *Proc. Of Oceans '88--Conference and Exposition October 31-November 2, 1988,* Baltimore, MD, 346-352.

Bos, W.G. (1991) "A comparison of two Doppler current profilers." *J. Oceanic Eng.*, AMS, 16, 374-381.

Lemmin, U., Rolland, T. (1997) "Acoustic velocity profiler for laboratory and field studies." *J. Hydr. Eng.*, ASCE, December 1997, 1089-1098.

Lohrmann, A., Cabrera. R., and Kraus, N.C. (1994) "Acoustic-Doppler Velocimeter (ADV) for laboratory use." *Proc. Conf. On Fundamentals and Advancements in Hydraulic Measurements and Experimentation*, Buffalo, NY, ASCE, 351-365.

Morlock, S.E. (1995) *Evaluation of Acoustic Doppler Current Profiler Measurements of River Discharge*: U.S. Geological Survey Water Resources Investigation Report 95-4218, 41 p.

Mueller, D.S. (2002) "Field Assessment of Acoustic Doppler Based Discharge Measurements." *Proc. Hydraulic Measurements & Experimental Methods 2002*, Estes Park, CO, ASCE.

Nystrom, E.A., Oberg, K.A., Rehmann, C.R. (2002) "Measurement of Turbulence with Acoustic Doppler Current Profilers - Issues and Laboratory Results." *Proc. Hydraulic Measurements & Experimental Methods 2002*, Estes Park, CO, ASCE.

Shih H. H., Payton C., Sprenke J., and Mero T. (200) "Towing Basin Speed Calibration of Acoustic Doppler Current Profiling Instruments", *Proc. 2000 Joint Conference on Water Resources Engineering and Water Resources Planning and Management*, Minneapolis, MN, ASCE.

Simpson, M. (2002) *Discharge Measurements Using a Broad-Band Acoustic Doppler Current Profiler*: U. S. Geological Survey, Open-File Report 01-01, 128 p., http://water.usgs.gov/pubs/of/ofr0101/

Simpson, M.R., and Oltmann, R.N. (1993) *Discharge measurement using an acoustic Doppler current pro?ler*: U.S. Geological Survey Water-Supply Paper 2395, 34 p.

Voulgaris, G., and Trowbridge, J.H. (1998) "Evaluation of Acoustic Doppler Velocimeter (ADV) for turbulence measurements." *J. Atmos. Oceanic Tech.*, AMS, 15, 272-289.

KNOW THE FLOW PROJECT STAGE 2
REVIEW OF AUSTRALIAN IRRIGATION METER TESTING REQUIREMENTS AND CAPABILITIES

Report No. MHL1179

NSW Department of Commerce
Manly Hydraulics Laboratory

Report No. MHL1179
DPWS Report No. 02021
MHL File No. HS6-00067
First published April 2003

Manly Hydraulics Laboratory is Quality System Certified to AS/NZS ISO 9001:1994.

Table of Contents

Appendices

List of Tables

1. Introduction

1.1 Background

Each year in its benchmarking report (ANCID 2002) the Australian National Committee on Irrigation and Drainage (ANCID) reflects on current and emerging issues facing the irrigation industry. In 2002 the issues included:

- the need to do more with less water due to the general realisation that there is less availability of water resources relative to agreed Water Entitlements together with the introduction of Transferable Water Entitlements
- water is increasing in value due to increased demand, transferable water titles and requirements for transparent full cost recovery by water providers
- inhibition of water trading despite removal of water trading barriers due to a number of factors
- transfer of state assets to community management in response to the need for greater accountability for irrigation system management
- increased water allocation to the environment for restoration of natural river ecosystems
- water quality and land salinity impacts.

These issues all contribute to increasing the need for accurate measurement of water delivery. Inaccurate measurement generates disputes over water charges and has the potential to promote wastage, increase unaccounted-for losses and undermine storage security and environmental flows.

ANCID (2002) reported that an average of 94% of supply points are metered in the 40 systems which provided data on metering. Water delivery to customers is still predominantly measured by Dethridge meters but these are gradually being phased out. The balance of water delivery is measured by a range of meter types from a range of manufacturers deployed in a range of installations. The accuracy, in service, of the diverse metering arrangements in use has not been fully assessed.

There have been two previous Know the Flow (KtF) projects. The Know the Flow Stage 1 project investigated a wide range of issues relating to metering of irrigation water. Three workshops were held during the project: two at Tatura, Victoria, and a final workshop at Manly, NSW. The testing facility at Manly Hydraulics Laboratory (MHL), which can test irrigation metering installations in simulated field conditions, was established as part of the project.

The Know the Flow website (www.ancid.org.au/ktf) was established during 2001 based on a recommendation from KtF1. The website provides a centralised database for a wide range of irrigation metering information.

ELSEVIER

Flow Measurement and Instrumentation 13 (2002) 285–289

Flow Measurement and Instrumentation

www.elsevier.com/locate/flowmeasinst

A method for comparing the performance of open channel velocity-area flow meters and critical depth flow meters

Richard W. Jones*

Hymetrics Limited, Abingdon, OX13 5NW, UK

Abstract

New technologies enable velocity measurements to be acquired continuously from a moving body of water flowing on an open channel. They provide an alternative to the well-established flow measurement methods using weirs and flumes: commonly known as the critical-depth methods. These velocity measurements must be integrated across the measurement cross-section to enable the flow rate to be calculated. Open channel flow is turbulent and therefore the measurement process needed to determine the average velocity must be complex. At present, there is little or no independent data to define the measurement performance of velocity-area techniques. The critical-depth method, however, has been thoroughly researched and its performance is well defined in the various published Hydrometry Standards. Using the critical-depth method as a benchmark, measurement uncertainty analysis is used to define performance criteria required of velocity-area methods.

1. Introduction

The direct method of measurement of flow in open channels requires i) the measurement of the mean of the velocity across the channel section and ii) the measurement of the cross-section area through which that velocity passes. The product of these two quantities is equal to the rate of flow.

The cross-section area is determined from a knowledge of the channel geometry and from a measurement of the depth of water. If the channel is man-made, this can usually be done with a measurement uncertainty of 2%.

Nomenclature

u^*	dimensionless standard uncertainty of a variable (b,h,$\bar{V}$,*etc*.) (usually expressed as a percentage)
u^*uc	combined dimensionless standard uncertainty of a variable (b,h,$\bar{V}$,*etc*.) (usually expressed as a percentage)
b	width dimension of a rectangular channel
b'	width dimension of a contracted section of a rectangular channel (flume throat)
h	depth (head) of water in a channel
h'	depth of water in a contracted section of a channel
h_C	depth of water in a contracted section of a channel at the critical condition
H	total head of water in the channel
C_D	discharge coefficient of flow through a weir or flume
Q_C	flow rate in the channel determined by the critical depth method
Q_{VA}	flow rate in a channel determined by the velocity area method#

E-mail address: rwj@hymetrics.com (R.W. Jones).

0955-5986/02/$ - see front matter © 2002 Published by Elsevier Science Ltd.
PII: S0955-5986(02)00062-6

The technical challenge is to find the mean velocity. Friction at the channel walls causes strong velocity gradients, illustrated in Fig. 1, which are unstable and migrate as vortices through the body of the flow. This causes turbulence and unsteady conditions. (Note, turbulence exists in a moving body of water even when the water surface appears tranquil.) The measurement process therefore needs to scan the cross-section while integrating and averaging the velocity components.

Technologies used for the direct method include: time-of-flight ultrasonics, pulsed Doppler sonar and electromagnetic methods. More recently, Doppler radar has been used.

Through the guidelines of [1] it is possible to define criteria for the comparison of the measurement performance of these techniques. The superior technique would be the one that minimises the uncertainty $u^*(\bar{V})$ of the mean velocity $\bar{V}$ of the turbulent profiles illustrated in Fig. 1.

2. Weirs and flumes—a benchmark technology

Direct methods can be compared as a class with the well-established critical-depth method (the basis of the weir and flume technique).

Since the 19th century it has been known that when flow passes over a weir, a unique relationship exists between the upstream water level and the flow rate, and that relationship is largely independent of the velocity profiles approaching the weir. Analysis shows that by accelerating the flow at a weir or through a flume, the velocity distortions are greatly reduced and that, for practical purposes, the velocities adopt a geometrically consistent pattern for each class of weir or flume. This is shown in Fig. 2 for a rectangular flume.

A unique relationship therefore exists between the upstream water level, the cross-section of the accelerated flow and the mean velocity in the accelerated section. This relationship is defined by the critical depth theory.

Weirs and flumes have a long history of laboratory investigation. The uncertainties of the measurement process have been carefully researched so that the ISO Standards now include procedures for the evaluation of uncertainty. These procedures can be used to establish a ‘benchmark’ for the assessment of direct velocity-area methods.

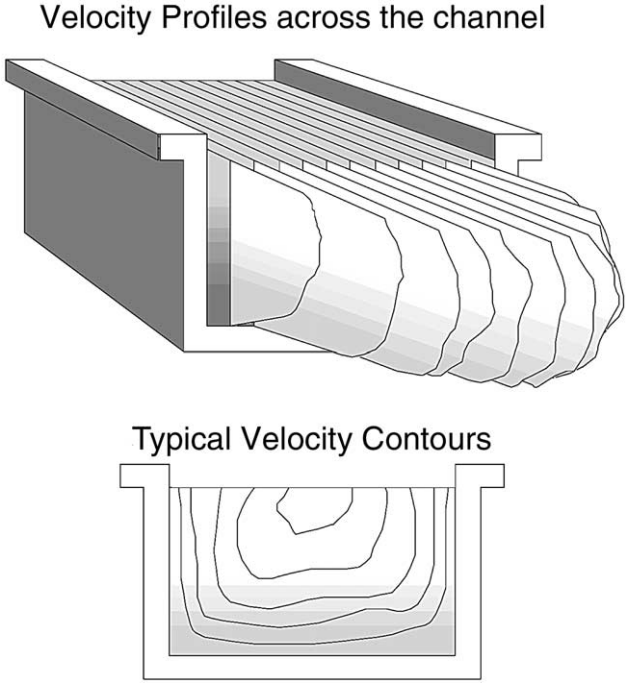

Fig. 1. Typical velocity profiles and contours

3. Measurement uncertainty

There are various rules that can be applied to any measurement process to state the quality of the results in terms of uncertainty. A flow measurement can never be exact. For example if water is controlled to flow at a constant rate, then a flow meter will exhibit a spread of measurements about a mean value. The standard deviation of this spread of measurements is, by definition, termed standard uncertainty.

The standard deviation of a set of measurements can be directly used to estimate the uncertainty of velocity or head measurements (the Type-A methods of [1]).

This would be inappropriate for measuring the channel geometry. An alternative to working with standard deviation is to define a probability distribution for a measurement process.

The GUM [1] and ISO 5168 [2] provide guidance on the application of the principles of measurement uncertainty. These documents develop the concept of standard uncertainty to include:

1. standard deviation of the mean value of a set of measurements

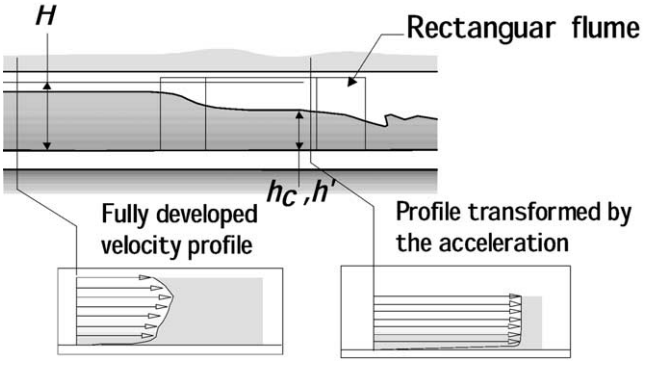

Fig. 2. Acceleration through a flume

2. probability distributions for simple measurement processes to enable the equivalent standard uncertainty values to be estimated (the Type-B methods of [1]), and
3. how to combine the uncertainties of the variables in the formula to derive flow rate for each class of weir or flume.
4. how to expand uncertainty estimations from standard values to values at the 95% confidence limit.

An analysis of flow measurement uncertainty starts with the formula used for computation.

4. Formula for the computation of flow in rectangular channels

4.1. The direct-method velocity-area equation (rectangular cross-sections)

$$Q_{VA} = b \times h \times \bar{V} \tag{1}$$

This equation defines the flow rate Q through a rectangular channel of width b and water depth h. The most problematic of these is the measurement of mean velocity $\bar{V}$ which is known to vary strongly across the channel cross-section (see Fig. 1).

4.2. The critical-depth equation (rectangular cross-sections)

This variant of the basic equation relates the mean velocity $\bar{V}$ to the change in the water surface level that occurs when the flow is accelerated in the channel. Here, the acceleration is induced by a contraction of the width of the channel (such as a long-throat flume). If the streamlines within the contraction have very little curvature, then it can be shown that $\bar{V} = \sqrt{2g(H-h')}$ where H is the total head of the flow in the channel and h' is the head of water in the contraction, refer to Fig. 2.

Thus;

$$Q_C = b' \times h' \times \sqrt{2g(H-h')}$$

where b' is the width of the rectangular channel in the contracted section.

Critical depth theory shows that for a rectangular cross-section, the head of water h' in the contraction can be reduced only to a limiting value h_C known as the critical depth which is related to the total head H by

$$h_C = \frac{2}{3}H$$

Therefore

$$Q_C = b' \times \frac{2}{3}H \times \sqrt{2g\left(\frac{1}{3}H\right)}$$

This equation is exactly equivalent to (1) with the depth and velocity terms replaced by $2H/3$ and $\sqrt{2gH/3}$ respectively.

To account for factors not included in this simplified theory, for example curvature of streamlines over a weir or the development of boundary layers in flumes, a discharge coefficient C_D is introduced. Thus, for rectangular cross-sections,

$$Q_C = C_D \times b' \times \frac{2}{3}H \times \sqrt{\frac{2g}{3}(H)}$$

This equation is usually presented in the form:

$$Q_C = \left(\frac{2}{3}\right)^{1.5} \sqrt{g} \times C_D \times b' \times H^{1.5} \tag{2}$$

For rectangular weirs, the value of C_D is determined from laboratory tests, the results of which are presented in the various ISO standards. For rectangular long-throat flumes, the value of C_D can be reliably predicted by the application of boundary-layer theory [3,4].

Note. This analysis uses the assumption that H is constant in the channel whereas in reality, it varies slightly across the approach section. The magnitude of the variation however is small compared with the mean value of H.

5. Uncertainty estimation of flow measurement

References [1] and [2] describe the relationship between the variables of Eqs. (1) and (2) and their respective measurement uncertainties. The relationships are:

$$u_C^*(Q_{VA}) = \sqrt{u^*(b)^2 + u^*(h)^2 + u^*(\bar{V})^2} \tag{3}$$

$$u_C^*(Q_C) = \sqrt{u^*(C_D)^2 + u^*(b')^2 + (1.5u^*(H))^2} \tag{4}$$

These equations show how the combined uncertainties $u_C^*(Q_{VA})$ and $u_C^*(Q_C)$ are related to the uncertainty of the variables of their respective equations $u^*(b)$,$u^*(C_D)$ etc. An error in any one of the components will induce a corresponding percentage error in Q.

Note that Eq. (4) for critical depth methods includes H to the power 1.5 which makes Q more sensitive to error in H than when used in the velocity-area Eq. (3). The sensitivity is the amount of change of Q that occurs for any given change of H, i.e. the rate of change of Q with respect to H, which is $\frac{\partial Q}{\partial H}$. From (2) this value for a rectangular flume is 1.5. Therefore, the critical depth method of flow measurement is one and a half times more sensitive to errors of head measurement than the direct methods using the velocity-area equation.

Sensitivities of the flow value with respect to errors of

b measurement are the same for velocity-area and critical depth methods. This also applies to errors in $\bar{V}$ and C_D.

6. The measurement performance of velocity-area methods compared with critical depth methods

The measurement performances of weirs and flumes are well established and documented in Standards. $u_C^*(Q_C)$ can therefore be used as the benchmark for the comparison. The condition for velocity-area methods to have better measurement performance is:

$$u_C^*(Q_{VA}) < uc^*(Q_C)$$

Using Eqs. (3) and (4)

$$u^*(b)^2 + u^*(h)^2 + u^*(\bar{V})^2 < u^*(C_D)^2 + u^*(b')^2 + (1.5u^*(H))^2 \quad (5)$$

Assuming that the same measurement methods for width and head are used throughout then it is reasonable to assume that the evaluations of uncertainty will be similar. It is therefore assumed to a first approximation that:

$$u^*(b) \doteq u^*(b')$$

$$u^*(h) \doteq u^*(H)$$

So Eq. (5) can be rewritten,

$$u_C^*(\bar{V}) < \sqrt{u^*(C_D)^2 + 1.25u^*(H)^2} \quad (6)$$

The significance of Eq. (6) is illustrated in the following example with a typical flume of throat width 0.400 m with a maximum head of water in the approach channel of 0.600 m. It is assumed that the head measurement carries an uncertainty of 0.003 m.

Fig. 3 is a graph of head measurement uncertainty and discharge coefficient uncertainty against flow rate. Flow rate and $u^*(C_D)$ have been calculated using the methods of reference [3].

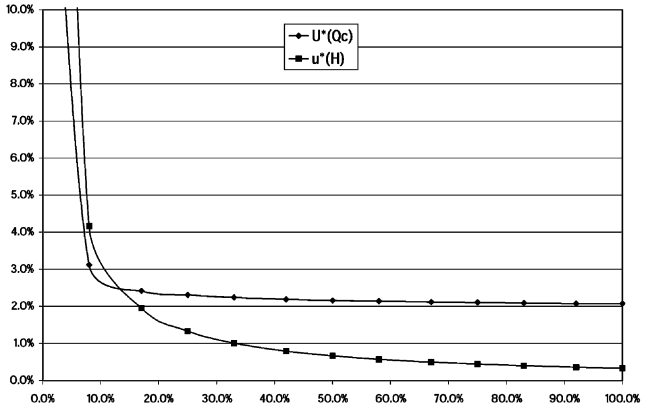

Fig. 3. Typical variation of head and discharge coefficient uncertainty with flow rate

This data is used in (6) to define the minimum criteria for $u_C^*(\bar{V})$. This is shown in Fig. 4.

Velocity-area methods able to measure $\bar{V}$ with uncertainty values below the curve would outperform weirs and flumes; those above the curve would not.

7. Discussion of velocity measurement technologies

Ideally, a velocity-area method should scan the channel cross-section rapidly to obtain a 'snapshot' of the velocity profile. Assuming that the velocities are accurate to 1%, and the ability to resolve spatially (locate velocity contours) is similarly accurate then the integration process should be able to derive the mean velocity to better than 2%.

In practice, the methods are less rigorous. This is discussed briefly below.

7.1. Electromagnetic methods [6]

An electromagnetic field is used to induce a voltage gradient across the channel which is detected by electrodes on opposite walls. The induced voltage is related to the integrated effect of the velocity components crossing a path between the electrodes.

The electrode voltage is not uniquely related to the mean velocity by a simple formula. The relationship depends on the construction of the metering system itself, the location of the electrodes relative to the water surface and other factors. To resolve this, electromagnetic meters are individually calibrated.

7.2. Doppler sonar [7]

High frequency sonar reflected from particles moving with the water cause Doppler-shifted echoes. When transmitted in short bursts, the reflections can be detected at varying distances along the sonic path to

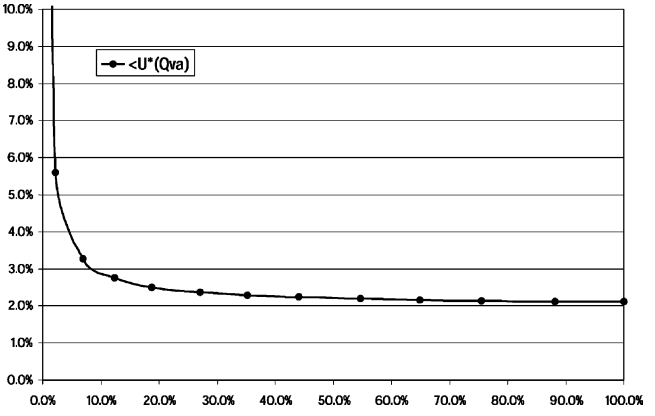

Fig. 4. Minimum criteria for velocity measurement uncertainty

define a velocity profile. There are technical problems associated with this method:

1. short pulses are needed to provide good spatial resolution, but short pulses give poor velocity resolution
2. turbulence and velocity gradients 'blur' the reflected signals
3. relationship between the reflected signal strength, the distance along the path and the particle size is unpredictable.
4. Sonar side-lobes prevent measurement along paths close to the channel walls.

Each of these factors carries a portion of uncertainty.

7.3. Transit-time Sonar [5]

Sonar transceivers are arranged to propagate ultrasonic pulses along a path across the channel angled to the direction of the flow. There is a unique relation between the following i) the propagation angle, ii) the difference between the transit times of pulses directed with and against the flow, iii) the channel width, and iv) the mean velocity of the streamlines intersecting the path. The mean channel velocity can be determined by using a large number of paths.

Unlike electromagnetic and Doppler methods, this technique provides a direct measure of mean velocity along the path. It therefore requires no calibration. The transit-time method has the potential to measure mean velocity measurements with an uncertainty order of 2%.

In practice, a small number of paths are used. Therefore assumptions are made of the velocity profiles between the paths which introduces a portion of uncertainty over and above those related to the angle, timing and distance measurements (listed above). The main difficulty lies in the application of the technique to small channels. The pulse time differential becomes very small, especially for low velocities. Path distortion can also be problematic in shallow channels.

8. Conclusions

The criterion of Eq. (6) applies to velocity measurement techniques in rectangular channels and is compared with measurements using rectangular flumes. Similar criteria apply to flume and weir types, the rectangular form being chosen as representative of all critical depth applications.

Improvements in level measurement technology are likely to reduce the value of $u(h)$ to values of the order of 0.001 m. In which case, the target performance criteria for $u_C^*(\overline{V})$ will be determined largely by the published values of $u_C^*(C_D)$: currently with measurement uncertainties of the order of 2–3%.

To compete, velocity-area methods must be capable of demonstrating velocity integration across a channel with similar levels of measurement uncertainty.

Criteria derived from this analysis present a challenge to the various velocity-area methods which, to outperform measurement using the critical depth method, must determine the value of $\overline{V}$ with a target uncertainty of between 2 and 3%.

Acknowledgements

The author wishes to thank Hymetrics Limited for permission to use the illustrations, Figs. 1, 2 and 3.

References

[1] Guide to the Expression of Uncertainty, ISO, Geneva 1995.
[2] ISO/TR 5168, 1998. Measurement of fluid flow—Evaluation of uncertainties.
[3] ISO 4359, 1983. Liquid flow measurement in open channels; Rectangular, trapezoidal and U-shaped flumes.
[4] ISO 748, 1997. Measurement of liquid flow in open channels—Velocity-area methods.
[5] ISO 6416, 1992. Measurement of liquid flow in open channels; measurement of discharge by the ultrasonic (acoustic) method.
[6] ISO 9213, 1992. Measurement of total discharge in open channels; electromagnetic method using a full-channel-width coil.
[7] ISO/TS 15769, 2000. Hydrometric determinations—Liquid flow in open channels and partly filled pipes—Guidelines for the application of Doppler-based flow measurements.

Pergamon

Phys. Chem. Earth (C), Vol. 26, No. 10–12, pp. 743–749, 2001

1464-1917/01/$ - see front matter

PII: S1464-1909(00)00106-X

Reliability and Uncertainty in Flow Measurement Techniques - Some Current Thinking

N. Whalley[1], R. S. Iredale[2] and A. F. Clare[1]

[1]Hydro-Logic Ltd, 6 Victoria Road, Mortimer, Reading, Berkshire, RG7 3SH
[2]Environment Agency, Midlands Region, Sapphire East, 550 Streetsbrook Road, Solihull, West Midlands, B91 1QT

Received 31 July 2000; accepted 27 October 2000

1 Abstract

Improvements in the quality and availability of flow measurement equipment are undoubtedly capable of enhancing the reliability and accuracy of the hydrometric data that we require. However much of the UK's hydrometric data is acquired by the tried and trusted methods that have remained the mainstay of flow monitoring for many years. Should the results provided by these established techniques always be so readily accepted given the range of assumptions on which they are based?

Current meter gauging is the principle technique used for the establishment of stage discharge relationships in the UK. Either directly for the establishment of stage-discharge relationships in open channels, indirectly for calibration of flow measurement equipment (e.g. ultrasonic Doppler velocity meters) or as a means of verification of existing flow measurement structures. Recent projects involving current meter gauging techniques have provoked much thought as to the validity of established techniques and in particular the assumptions on which they are based.

The chosen case studies highlight a number of projects where there have been questions regarding the reliability and uncertainty of the flow measurement techniques employed. The alternative approaches required to deal with such problems are also discussed.

Key words: **flow measurement; current meter gauging; flow measurement structures; calibration; stage-discharge relationship.**

2 Introduction

This paper aims to provide a brief insight into some of the issues currently of concern to those involved in hydrology and hydrometry within the UK.

The following topics are discussed:

3 Current Meter Gauging

i) Uncertainty in the performance of rotating element current meters

ii) Spin tests for performance checking of rotating element current meters

iii) Positioning of current meter in gauging section

4 Flow Measurement Structures

i) Calibration and Performance Checking

ii) Fish Movement

3 Current Meter Gauging

3.1 Uncertainty in the performance of rotating element current meters.

3.1.1 Introduction

The consistent performance of rotating element current meters is imperative to achieve good quality current meter gauging results. It is possible that bias in the gauging data due to changes in current meter performance with time will have a significant effect on the conclusions drawn from that data.

The Environment Agency has a fleet of approximately 400 current meters and undertakes of the order of 25,000 gaugings per year. The Agency is currently investigating the pre- and post-calibration performance of rotating element current meters in an attempt to gain an insight into the potential effect of variations in performance with time.

3.1.2 Analysis of calibration data

At present the Environment Agency's rotating element current meters are serviced and calibrated every two years by HR Wallingford Ltd, who are widely recognised as the leading specialists in current meter calibration in the UK.

The preliminary study was conducted using a selection of current meters and impellers provided by the Environment Agency's Midlands and North East Regional Hydrometry sections. A total of 18 meters were used for the analysis; 8 from Midlands Region and 10 from North East Region. Importantly, five of the meters provided by North East Region had not been used in the period prior to re-calibration and could therefore be used as a control set.

Correspondence to: Richard S Iredale

A range of Ott and Seba models were included in the analysis to ensure that any trends identified were not the result of a single faulty meter. Where meters were supplied with a range of impellers each meter/impeller combination was included within the analysis.

The performance of each current meter and impeller combination was assessed for each of the points in time specified below:

i) "Previous" calibration

ii) "As received" for calibration (pre-service)

"New" calibration (post-servicing)

A comparison of the relative performance of each meter/impeller combination with time was then undertaken to assess the effects of usage and servicing.

3.1.3 Results

Due to the relatively limited number of current meters on which this analysis is based the results of this study should only be taken as a preliminary indication of the extent to which the usage, servicing and calibration effect the performance of rotating element current meters.

The main results of the investigation would appear to indicate the following:

The majority of meter/impeller combinations tested exhibited a significant deviation in performance in their as received state when compared to previous calibration and post-service new calibration meter states.

At very low velocities there would appear to be a greater variation in performance with a range of negative and positive deviations.

The minimum response speed is generally greater for meters in their as received state than for meters after previous or new calibrations. Where there are exceptions to this the difference between the as received results and both the previous and new calibrations is minimal.

The degree of deviation observed for previous calibration, as received and new calibration state varies between meters and impellers.

The greatest deviations are observed at lower velocities. The deviation is most significant as the velocity approaches the minimum response speed

The preliminary results indicate that current meter performance does not deteriorate with time if they are not used. Meters that have been used exhibit degradation whilst those not used exhibit little or no change in performance.

3.2 Spin tests for performance checking of rotating element current meters

3.2.1 Introduction

The current criteria for re-calibration of a current meter are as follows:

i) at least once every two years;

ii) if the meter has been used for approaching four hundred gaugings since last calibrated;

iii) if the meter is damaged and requires significant maintenance e.g. replacement of spindle or bearings.

Although these criteria serve the purpose only the last is based on any definite indication that a meter needs re-calibrating.

Field staff will probably undertake a spin test on site at the beginning of each gauging day to see if the meter is spinning freely, the meter shaft is not bent and to listen for any bearing noise (wear). The rough and ready on-site spin test is important. However, it does not provide an objective, quantifiable, scientific basis for determining whether a current meter is within acceptable limits of its most recent current meter calibration.

In January 2000 a Consultant was commissioned by the Environment Agency to undertake an R&D Study to determine an objective and scientific basis for a spin test procedure. The purpose of the procedure is to determine if a current meter and impeller combination is within acceptable limits of the most recent calibration equation.

3.2.2 Objectives

The main objective of the R&D Project was the definition of an objective and scientific procedure for evaluating the performance of rotating impeller current meters.

Spin tests were undertaken on a representative batch of current meters and impellers in both pre- and post calibration condition. Guidelines for spin test procedure were produced and criteria developed to establish acceptable calibration limits based on evaluation of the spin test results.

3.2.3 Results

The main results of the R&D Project were as follows:

i) A simple revolution counting programme has been written that produces a *.csv file as output, this can be read into any spreadsheet.

ii) The best methodology for spinning the impeller is by blowing the impeller. For some impellers it may be difficult to produce an airstream wide enough for long enough to spin the impeller sufficiently, in which case the impeller can be spun by a blast from a hairdryer. While undertaking a spin test the current meter should be stood on end with the impeller pointing upwards. This ensures the bearings are tested evenly.

iii) The spin test start speed was taken as the revolution rate that appeared in most of the test files, or the maximum calibrated speed of the current meter – whichever was the lower. This tended to vary from meter to meter and obviously varied between impellers. The stop speed of each meter was also recorded.

iv) The simplest spin test algorithm that can be used is the time between start and stop speed. This time was significantly lower when the meters needed calibrating. Fitting an equation to the decay curve for a slowing current meter is also a possible methodology for assessing performance. It is a more complex and less clear-cut method for testing the meters.

v) The twelve meters tested were all due for calibration according to the standard criteria mentioned previously. Each meter was tested using the new spin test procedure before and after calibration. Each meter was calibrated in

the towing tank at HR Wallingford before and after being serviced. The pre and post spin tests and pre and post calibrations were available for comparison. The differences were greater for some meters than for others indicating that some meters were more in need of calibration than others.

vi) For most of the meters tested, for post calibration tests the time between start and stop speeds was within 10% of the average, whereas pre calibration tests the time was over 20% away from the average. Instruments where this difference was less may not have required re-calibration.

3.3 Positioning of current meter in gauging section

3.3.1 Introduction

BS ISO 748 (Ref. 1) provides a general specification for velocity-area methods of stream flow measurement in the UK. The document identifies a number of approved methods for the calculation of the mean velocity in each vertical and specifies the minimum number of verticals that should be used. However there is a certain amount of flexibility to allow for the range of sites and conditions over which stream flow measurements are conducted in the UK. Much of the decision making is therefore left to the discretion of the individual gauger at the time of gauging.

In 1997 a "Report on the Analysis of Current Meter Data" (Ref. 2) was produced for the Environment Agency North East Region assessing the optimum method of current meter gauging on a range of medium to large rivers in the former Yorkshire Region of the Environment Agency. The study examined the effect on gauging accuracy of i) a reduction in the number of velocity measurements taken in the vertical and ii) a reduction in the number of verticals at which measurements are made. Changes in current meter exposure time were not assessed as part of the study.

Recommendations made in earlier studies for the Yorkshire area of the Environment Agencies predecessor had led to the use of five point gauging methods for the majority of the medium and large sized gauging sites in the North East Region.

3.3.2 Analysis

Analysis was undertaken using a total of 507 five-point gaugings taken from a total of 23 gauging sites.

Number of measurements in vertical

A program was written to calculate flows from the velocity data for each sample gauging using the following methods.

- One point = 0.6d
- One point = 0.5d*0.95
- Two point = (0.2d + 0.8d)*0.5
- Three point BSI/ISO = (0.2d + (2 x 0.6d) + 0.8d)*0.25
- Three point average = (0.2d + 0.6d + 0.8d)*0.33
- Five point BSI/ISO = (surface + (3 x 0.2d) + (3 x 0.6d) + (2 x 0.8d) + bed)*0.1
- Five point average = (surface + 0.2d + 0.6d + 0.8d + bed)*0.2

Where surface = 0.1d and bed = 0.9d

Number of verticals in section

In order to assess the effect of using a reduced number of verticals a program was written that calculated flow after an iterative reduction in the number of verticals. Three different methods of reduction were used to assess the effect of a reduction in verticals over different parts of the gauging section.

- *Uniform vertical reduction* – uniform reduction in number of verticals
- *Middle outwards reduction* – reduced number of verticals in mid-channel
- *Edge inwards reduction* – reduced number of verticals at edge of section

3.3.3 Results

Summary of findings of reduction of points sampled in the vertical.

In general a reduction in the number of points in the vertical results in a small increase in error, and that this was within the random error to be expected of a current meter gauging.

The use of a greater number of points in the vertical is beneficial at low flows. This is particularly the case at sites where the flow is mainly a function of the velocity in the section i.e. the cross section area is similar at low and high flows.

Results obtained using the two-point method are at least comparable to those obtained using a greater number of points.

Percentage uncertainties obtained during the study generally compare well with those stated in BS3680 Part 3A Annex E.

Summary of findings of reduced number of verticals in section

Figure 2.1 indicates the overall increase in uncertainty for a reduction in the number of verticals in the section.

The greater the number of verticals used the greater the gauging accuracy. The relationship between the reduction in the number of verticals and the increase in error follows an exponential trend.

There would appear to be no statistical difference in the increase in uncertainty using a higher number of verticals in the mid-section than using a higher number of verticals at the edges. This is most likely due to the distribution of flow within the cross section.

comparable to those stated in BS3680, Part 3A, Annex E when there is a significant reduction (i.e. 50% or greater) in the number of verticals. However, a small reduction (i.e. 25%) in the number of verticals produced a significantly greater uncertainty than that stated in BS3680.

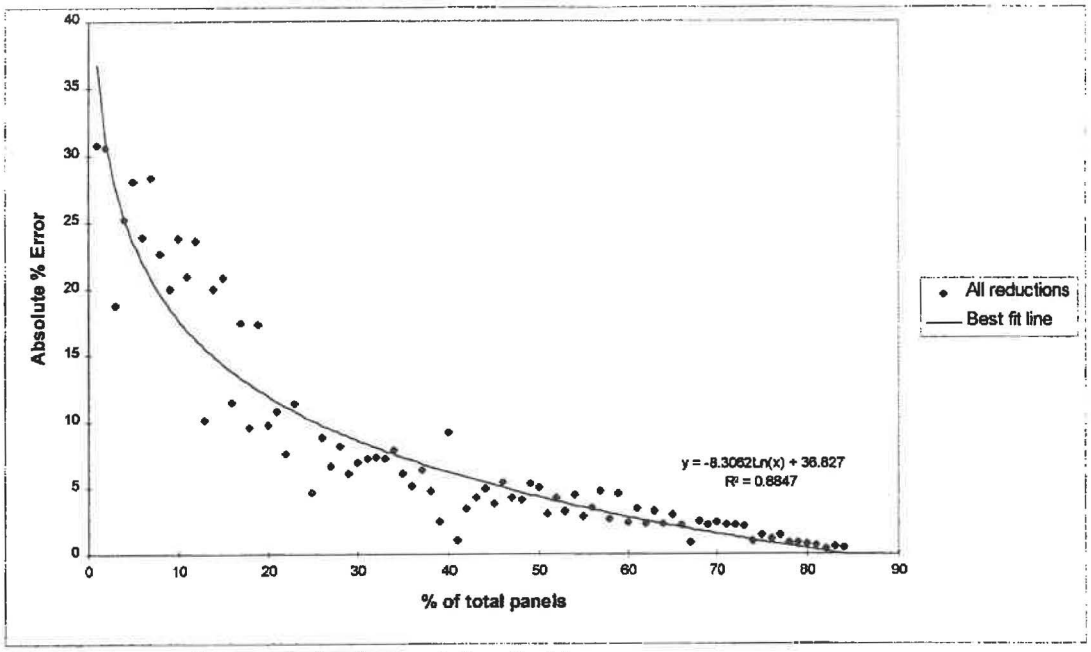

Figure 2.1 – Increase in error from vertical reduction (all methods)

4 Flow Measurement Structures

4.1 Calibration and performance checking

4.1.1 Introduction

Current meter gauging methods are widely used for the calibration and performance checking of permanent gauging stations in the UK. There is a large variation in the quantity and quality of gauging records available for different gauging stations and for different periods of their operation. A number of Environment Agency sites have relatively complete records for periods of over 30 years. However, there are also sites for which there is no available record of calibration or check gaugings.

Recent work suggests that an over-reliance on current meter gauging data at some sites may have resulted in a lack of appreciation of the underlying hydraulic principles associated with many of the standard structures used at flow measurement sites. However at other sites a total reliance on the theoretical hydraulic rating may have led to unrealistic flow prediction due to the limited range over which the equation applies or changes in site conditions that have either gone unrecorded or are not obvious without more detailed investigation.

4.1.2 Stage-discharge relationship derivation for Standard structures.

There are currently a variety of weir and flume structures used for flow measurement in UK rivers, a large number of which are covered by existing International Standards and British Standard BS3680. The general form of hydraulic equation that provides the basis for the theoretical stage discharge relationship for a horizontal weir or flume structure is:

$$Q = C_d(\sqrt{g})bH^{1.5} \quad (1)$$

Where Q = discharge in cubic metres per second (m^3/s),

C_D = coefficient of discharge,

B = cross-section width in metres (m), and

H = total hydraulic head in metres (m)

i.e. $H = h + V^2/2g$

g = acceleration due to gravity (m/s)

The use of different discharge coefficients for specific types of weirs and flumes allows the computation of a reasonably accurate rating curve that will conform to the correct hydraulic principles.

However it would appear that where sufficient gauging data is available there is a tendency for some hydrologists to derive stage-discharge relationships using the best mathematical fit to the data often with little thought given to the hydraulic reality of the control section. This can produce stage-discharge relationships that are not totally representative of the actual hydraulic conditions pertaining to the station. A feature observed on a number of stage-discharge relationships recently reviewed by the authors is an erroneous curvature of the rating curve at the extreme upper and lower ends of the range. This is a function of the least-squares curve-fitting methodology commonly employed to gain a mathematical best fit of the stage-discharge relationship to the gauging data.

Whilst BS ISO 1100-2 (Ref. 4) states that "*the stage-discharge relation must conform to the calibration measurements*" further qualification of this statement indicates that "*the rating should be hydraulically correct, and that every calibration measurement does not necessarily fit on the same rating curve*".

It is often the case that for gauging stations where a long calibration gauging record exists that numerous stage-discharge relationships have been applied to account for what are often minor trends in the data. Whilst many significant trends or steps in the data can be explained from the station history files there is often insufficient information available to provide a conclusive reasoning for less significant deviations.

When discussing the accuracy of fit of gauging data to a stage-discharge relationship it is important to remember that all flow measurements are subject to a degree of error. For the majority of current meter gauging work an error for an individual gauging of ±10% of true flow would normally be acceptable.

4.1.3 Case Study: Sprint Mill Gauging Station, River Sprint, Cumbria.

Sprint Mill Gauging Station is located on the River Sprint, Cumbria and is included within the Environment Agency's Primary River Flow Monitoring Network. The existing flat-vee crump-profile weir structure is fully conformant with BS3680 Part 4G and ISO 4367. A review of the stage-discharge relationship for Sprint Mill gauging station was recently undertaken for the North West Region of the Environment Agency. This involved examination of the existing and historical stage discharge relationships and a recommendation for the most suitable stage-discharge relationship for accurate flow estimation.

There is a relatively complete current meter gauging record at the site for the period 1969 to present. A total of three different stage-discharge relationships have been used for flow estimation since 1969, all of which appear to be derived using the best mathematical fit to the gauging data.

Detailed as-built dimensions of the structure produced from topological survey were used for the derivation of the theoretical stage-discharge relationship and to verify that the structure is BS3680 compliant.

Comparison of the theoretical stage-discharge relationship with the available current meter gauging data revealed a reasonable correlation. However a number of minor trends were identified for which no physical reason could be identified from the station history files. The main deviation from the theoretical rating occurred at stages less than 0.3mASD (Above Station Datum) and the deviation decreased with increasing stage. At stages less than 0.2mASD the associated deviation was observed to be greater than 20%.

Whilst it is possible that a variation in the relative positions of the gaugeboard and weir crest is responsible for the observed deviation it is unlikely that this accounts entirely for the gradual long term trend observed in the data. The existing gaugeboard had been installed within the two years before the inception of the project in 1998. During the detailed survey for the project undertaken in November 1999 the elevation of both the gaugeboard and weir crest were found to be consistent.

Boundary effects are also unlikely to be responsible for the overall trend in deviation as they usually restricted to within 0.06m of the zero point of the weir crest. It is possible that boundary effects are responsible for some of the deviation observed at very low stages below 0.06mASD.

For most of the record period the theoretical rating appears to provide a consistent stage-discharge relationship. The majority of gauging data falls within ±10% of the theoretical rating. The structure conforms to the specification for flat-vee weirs provided by BS3680 and there is little evidence to suggest significant change to the structure with time. Detailed examination of the latest as-built dimensions of the structure also failed to reveal any evidence for a change in the control.

There was no obvious change in the staff undertaking the gauging work and no evidence of routine gauging error. Both of the Environment Agency staff responsible for the site are aware of the trends in the gauging data but are uncertain as to the causes. Both staff are experienced hydrometrists and have been involved with the site for a significant period of time.

It was therefore recommended that the theoretical stage-discharge relationship should be applied for the entire period of record. A reassessment of the stage discharge relationship should be undertaken if any further information becomes available. A programme of multi-point current meter gauging should be undertaken to ascertain the validity of the classic velocity-depth profile and its relation to the mean velocity in the approach channel and gauging section. 4.2 Fish movement

The Environment Agency has a duty to maintain, develop and enhance freshwater and salmonid fisheries. As part of this duty the Fish Pass Technical Group are required to consent the installation of a new structure or modification to an existing structure which is likely to cause an obstruction to fish movement or effect the passage of fish. Historically the movement of salmonid fish populations has been of most importance but recent experience would suggest that there has been a significant increase in the importance given to the movement of coarse fish populations in UK rivers. This is confirmed by findings of the recent "Salmon And Freshwater Fisheries Review" (Ref. 5). Recommendation 126 states "*Anyone creating a new obstruction to the passage of any fish, or increasing or rebuilding an existing one, either in whole or in part, on any river should be required by law to install a fish pass to a design approved by the Environment Agency unless excused from doing so by the Environment Agency.*"

The positive and negative aspects of the three main approaches to fish movement and flow measurement structures are summarised in Table 1 below.

Approach	*Positives*	*Negatives*
Construction of bypass structure	Designed to suit specific site and fish population. Can be used for monitoring fish movement.	High capital works cost Possible problems with accurate measurement of low flows.
Use of supplementary fish pass e.g. baffles on flat-vee weir	Relatively cheap and cost-effective. Can be installed on existing structures.	Possible problems with accurate measurement of low flows. Use limited to specific structures e.g. flat-vee weirs
Use of non-intrusive methods e.g. time-of-flight ultrasonic and ultrasonic Doppler alternatives.	No barrier to fish movement. Relatively cheap compared to cost of new structure. Can be used in conjunction with some existing structures.	Potential barrier to certain fish e.g. shad at low frequencies but unlikely to be a problem in practice. Not suitable for all sites.

Table 1. Approaches to fish movement and flow measurement structures.

The authors were recently involved in the installation of a new flow measurement station in a relatively small chalk fed river in eastern England. The initial proposal was for a flat-vee weir to be installed in a suitable section of channel. However during the feasibility study it was established that the river included important brown trout and coarse fish populations and the Environment Agency's Fisheries Section recommended that the proposed solution should not act as a barrier to fish movement. Sensitivity of the local landowners to flooding was also a consideration.

To meet the above requirements a dual sensor ultrasonic Doppler velocity meter with stop log arrangement was proposed. Ultrasonic Doppler technology for flow monitoring in small concrete channels (<1m width) and pipes has been an established technique in the waste-water industry for a number of years. The use of the technique for flow monitoring in small natural channels is currently the subject of an Environment Agency R & D project.

The solution approved by the Environment Agency included stop logs at 0.2m elevation above the existing bed level. This was deemed acceptable given the nature of the existing fish population and the sensitivity to flooding in the area.

The approved solution of dual sensor ultrasonic Doppler velocity meter and stop log set-up has since been installed and is reported to be working successfully. The installation was undertaken at a fraction of the cost normally associated with the installation of a more conventional flow measurement structure.

5 Conclusions

5.1 Current meter gauging

1 Regular servicing of current meters between calibrations may help to prevent the observed deviation from the calibration at low velocities most likely caused by general wear and tear and accumulation of dirt.

2 To minimise the degradation in performance of rotating element current meters it is important that the existing guidelines for best practice concerning the care and checking of current meters should be closely followed at all times.

3 A National Group has been set up under the auspices of the National Hydrometric Group to look at approaches that may limit the effect of degradation in current meter performance with time. This may include calibration on a more frequent basis either based on a fixed period or linked to field exposure time or a frequent review of meter performance using a Spin Test procedure such as that developed in the current R&D Project.

4 The observed reduction in performance is likely to be of greatest significance when conducting studies concerned with low flows or at sites effected by low velocities i.e. low flow studies, calibration and performance checking of gauging stations at low flows, studies in areas of low relief.

5 The use of an increased number of verticals when current meter gauging by the two-point method provides an increase in the overall accuracy of flow estimation with a reduction in the time taken to undertake each gauging. For example the replacement of a 16 vertical five-point current meter gauging by a 20 vertical (plus 2 at edge) two-point current meter gauging compliant with BS3680 Part 3 would provide an overall time saving of 25% and an increase in accuracy of 4%. The time saving is provided by a 45% reduction for the number of points sampled compared with a 20% increase for the number of verticals. The increase in accuracy is provided by a gain in accuracy of 5% due to the increased number of verticals compared to a loss of accuracy of 1% due to the reduced number of points sampled.

6 The use of the five-point method with a minimum of 20 verticals (plus 2 at edge) may be justified at particular sites or in particular circumstances particularly where the classic velocity-depth distribution is not thought to occur.

7 In times of rapidly varying stage the use of a one-point method is recommended as it is considered that the slight reduction in accuracy due to the reduction in points sampled will be more than offset by the errors associated with gauging during variable flow conditions. Analysis confirmed the recommendations made in R & D Report

529 (Ref. 3), that 0.95 should be used as a factor for single-point measurements made at 0.5d.

5.2 Flow measurement structures

1 The use of performance checks and regular dimensional surveys to verify existing theoretical hydraulic stage-discharge relationships at standard flow measurement structures may in some cases be more appropriate than the derivation of a rating from gauging data collected as part of an ongoing calibration programme. This is most likely to be applicable for stations where the existing structure conforms to BS3680 and the stage discharge relationship is identified as stable following an initial calibration programme over the full flow range.

2 It is suggested that check gaugings and detailed dimensional survey should be undertaken following hydrological events such as flooding or extreme drought or if any other changes to the nature of the control are suspected e.g. significant channel maintenance in the vicinity of the station. Further current meter gauging during flood and drought events is also extremely useful as it reduces the need to extrapolate the stage-discharge relationship at the extremes of range where data is either limited or unavailable.

3 It is important when using hydrological software packages for the derivation of stage-discharge relationships that due consideration is given to the hydraulic and physical reality of the measurement section. This is of particular importance when assessing the stage discharge relationship for structures conforming to International and British Standards.

5.3 Overall Conclusions

1 The results provided by established techniques such as current meter gauging should not always be so readily accepted without further thought for the assumptions on which they are based.

2 Further refinement of existing methods may provide improvements in both the accuracy and consistency of essential hydrometric data. It is therefore important that sufficient resources continue to be made available for research and development of fundamental issues.

3 There is significant scope for the use of "new technologies" to provide alternative methods of flow measurement where existing methods are of limited use or do not conform to requirements. Many new technologies are already used for similar applications e.g. ultrasonic Doppler velocity meters in waste water or have been the subject of Environment Agency R & D Projects e.g. portable time-of–flight ultrasonics for calibration of gauging stations (Ref. 6).

REFERENCES

(BS ISO 1100-2: 1998). "*Measurement of liquid flow in open channels - Part 2: Determination of the stage-discharge relation*",

(BS ISO 748: 1997). "*Measurement of liquid flow in open channels - Velocity-area methods*",

(Environment Agency North East Region 1997). "*Report on the analysis of current meter data*"

(Environment Agency R & D Technical Report W189, 1999) "*Calibration of Gauging Stations Using Portable Ultrasonics*",.

(Environment Agency) R & D Report 529.

(Ministry for Agriculture Fisheries and Food, 2000) "*The Salmon and Freshwater Fisheries Review*",.

Irrigation and Drainage Systems **11:** 241–259, 1997.

Practical technologies for irrigation flow control and measurement

JOHN A. REPLOGLE
U.S. Water Conservation Laboratory, Agricultural Research Service, USDA, 4331 East Broadway, Phoenix AZ 85040, USA

Accepted 7 April 1997

Abstract. Practical technologies can encourage farmers to adopt practices that support sustainable irrigated agriculture. Important among these are convenient water measurement and control techniques. Many simple constructions or operating procedures are available that can bring considerable convenience to farmers and irrigation delivery system operators. Some are new technologies and some are improvements on older technologies. Many can be implemented with small expense. Some are superior replacements for current practices. The techniques and devices discussed included: (a) accurate and convenient zero setting for weirs and flumes (b) pressure-transducer field checks, (c) easy-to-use scales for orifice and Venturi meters, (d) flow-profile improvers to assist accurate meter operations in irrigation pipelines, (e) floor sills and wave suppressors for canals that usually flow at variable depths of flow, (f) water surface slope measurements–based on static-pressure tubes, and (g) field checks of flow velocity profiles to evaluate flow conditioning using rising-bubble techniques for flow-profile visualization. Many of the concepts are demonstrated in a summary illustration showing several items in a typical stilling well and broad-crested weir (long-throated flume) that need attention, and offers suggestions for correcting the deficiencies.

Key words: Flow measurements in canals, flumes, depth sensing, pressure transducers, flume installation errors

Introduction

Practical technologies can encourage farmers to adopt practices that support sustainable irrigated agriculture. Important among these are the availability of water management tools that include convenient water measurement and control techniques. These techniques need to be available not only to the farmers, but also to the delivery system operators that make the system responsive to the on-farm needs. Improved irrigation planning and management techniques depend heavily on accurately controlling and quantifying water deliveries. Automation places a further burden on reliable operation of primary water measuring and flow control equipment. A persistently weak link in the management and control process is the questionable reliability associated with automatic devices.

User understanding of the proper application, installation, use, and maintenance of control and measuring devices is generally poor. Reliability problems exists because much of the equipment is not easily field checked for proper functioning. Moreover, many observable clues, when they do exist, go unrecognized by inadequately trained field personnel. This paper deals with a compilation of practices and design suggestions that help the operator to know when valid measurement data or control functions are being obtained. These suggestions are intended to make these devices easier to use, easier to verify, and more economical to construct and install. Also included is a discussion of some flow conditioning ideas used in field practice for devices installed in adverse conditions. Some suggestions are qualitative in nature and point to fruitful areas of research.

Irrigation practice and design suggestions

Flume and weir zero setting

Inaccurate setting of the gage zero on weirs and flumes is a frequent source of error in discharge measurements. Flumes and weirs can be of almost any size. We will first deal with small portable sizes that usually measure flow rates less than 200 l/s.

Small portable flumes

Among conveniences that would make a flume easily portable would be eliminating the need for precise leveling. Previous work showed that long throated flumes are very forgiving. That is, they can be sloped upward slightly in the direction of flow without changing the discharge equation significantly (Replogle et al. 1987). However, the upstream depth gage must be referenced always to the elevation of the throat floor near the out-fall of the flume. Using a point on the sill crest about one-quarter of the throat length from the outlet end for the zero reference elevation is suggested. If a wall gage is used in the upstream section of the flume, then that gage is going to lose its accurate zero reference whenever the flume is not level either longitudinally or laterally. In this situation the offset stilling well is useful. With it, the water surface upstream is siphoned to the region of the zero reference along the centerline of the flume and small lateral slope and longitudinal slopes are compensated.

Another convenient field aid is to attach water trays to the top of the flume, one longitudinally and one laterally. These shallow trays are a quick substitute for a carpenter's level, and reduce the items that are needed at each site. Side wall gages marked in flow rate are also helpful. These usually

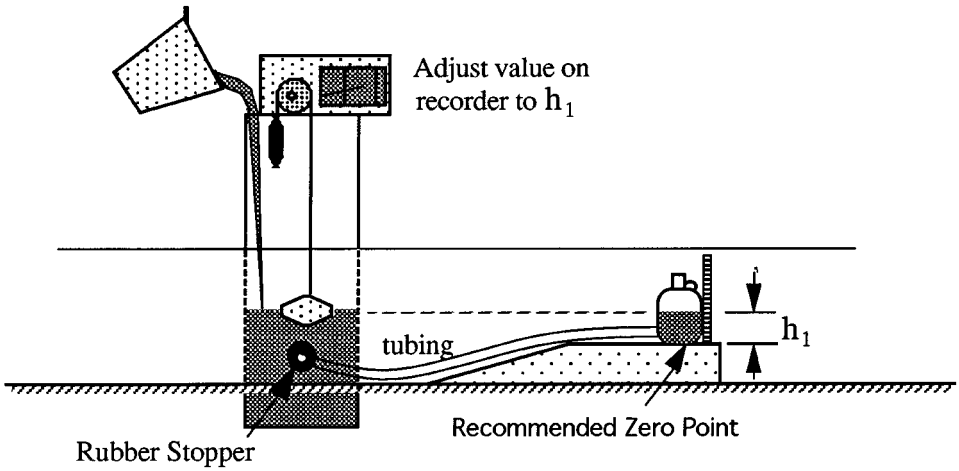

Figure 1. Method to zero-reference a flume or weir in dry channel (for both portable and permanent flumes). Use tubing and stopper to connect container to stilling well tap hole; Fill stilling well with water and allow it to fill container placed at sill zero location; Measure h_1; Adjust value on recorder to h_1.

produce readings accurate enough for irrigation purposes, and reduce the chance of using the wrong flow table or equation.

If a stilling well and a recording instrument are to be used, then convenient and accurate zero setting is again needed to properly reference the instrument. The so-called "drain-down-to-zero" method commonly found in field practice is to be avoided. It is not accurate enough for most small field channel installations because of surface tension effects (Bos et al. 1991).

A simple and accurate scheme to zero-reference a portable, or permanently installed, flume is a slightly modified version of that described in Bos et al. 1991. Referring to Figure 1, a container is connected with tubing to the stilling well hole using any water tight seal such as clay, rubber stopper, etc. Water is poured into the stilling well to activate the float and to fill the container through the attached tubing to some arbitrary depth. This depth is measured and the value is set on the recorder. The recorder should now be accurately zeroed to the flume reference point. This procedure should be adaptable to most weirs and flumes. It permits the stilling well to be unattached from a portable flume because it can be readily re-zeroed after movement. This makes the installation more convenient and flexible because the stilling well can be upstream in the channel, downstream in the channel, or at the side. Locating it in the channel usually requires less digging and disruption of the canal section.

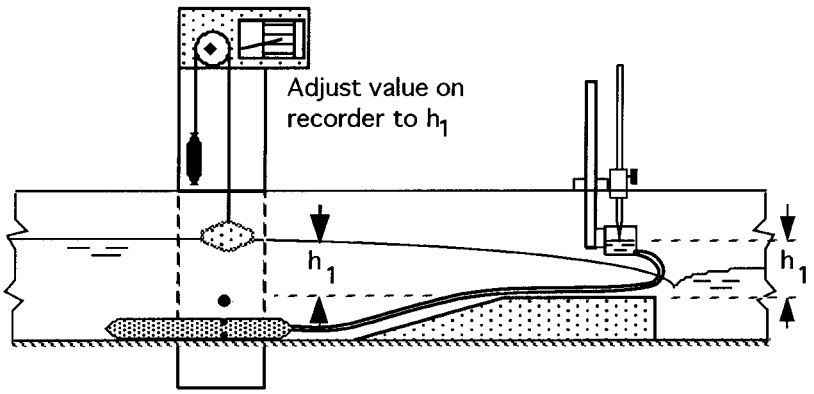

Figure 2. Method to zero-reference a flume or weir in flowing water.

For flowing water situations, a static pressure tube (see discussion below describing these tubes) is placed in the flow. The sensing holes of the static pressure tube should be placed upstream at about the same distance as the stilling well tap. The output is read with a point gage in a cup suspended above the reference elevation, Figure 2 (Bos et al. 1991). The head reading is the difference between the water surface in the cup and the top of the sill as illustrated in Figure 2. This value is set on the recorder. If possible, check another flow level to assure that mistakes are eliminated. A common mistake with chart recorders is that the technician sets the physical reading of h_1 on the chart instead of the gear-reduced chart value of h_1.

Flow conditioning in the field

Measuring devices frequently must be installed in flow situations that are less than ideal. The meter may be too close to an upstream gate or to a channel bend. Sometimes large pipes are used as outlets to secondary canals and flow meters placed in them are subject to flow profile distortions.

This occurred in some canals in Arizona using single-path ultrasonic meters. The pipe was about 0.75 m in diameter and delivered approximately 400 l/s. The flow rate readout was unstable, with fluctuations varying by about 15%. The problem appeared to be caused by slowly spiraling flow induced by the bottom jet from a partly open pipe inlet gate and a 45deg elbow. This is similar to two closely spaced pipe elbows that are not in the same plane. This causes spiral flow (ASME 1971). A successful attempt to modify the jet and cause it to cross mix so that the jet effects and the strength of the spiral flow were reduced, was accomplished by inserting a large ß-ratio orifice in the pipe, Figure 3. This consisted of an annular metal ring with the outside

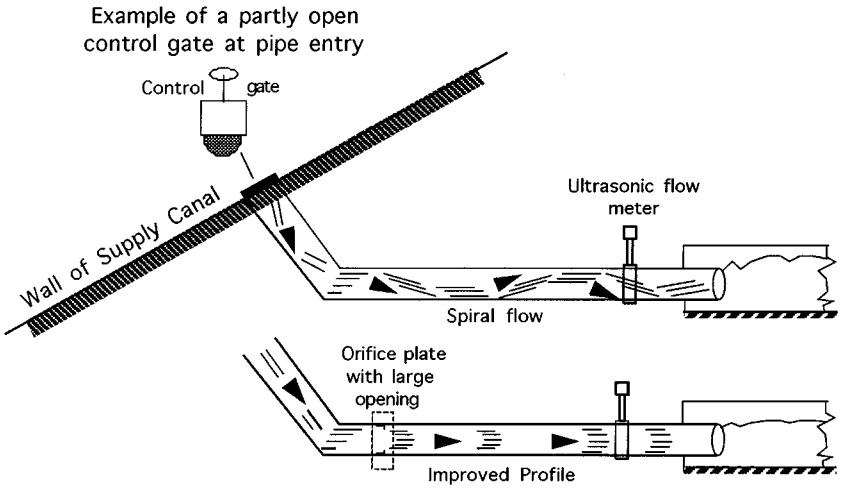

Figure 3. An orifice plate with a large opening is used to condition flow profile.

radius approximately that of the pipe and an inside diameter about 10% less, or an orifice with ß = 90%. The orifice was installed about three diameters downstream from the elbow. The slight increase in head loss was compensated by increasing the upstream gate opening. The orifice can be constructed by cutting notches from an appropriately sized piece of angle iron or aluminum and bending it to a polygon that approximates the circle. Some leakage around the ring is acceptable. For propeller meters, additional vanes projecting from the walls may be needed to further reduce spiral flow.

Wave suppression in canals

Excessive waves in irrigation canals make reading sidewall gages difficult. These waves are usually caused by a jet entry from a sluice gate or by a waterfall situation. The unstable surface can be 10 to 20 cm high and extend for tens of meters downstream. For canals that usually flow at one level, wave suppression has been achieved by constructing a roof-like structure that penetrates the flow by about 10% of the flow depth. In severe jet cases an additional floor sill, also about 10% of the flow depth in height, has been used successfully.

The length of the roof in the flow direction has not been well studied, but our field observations seem to support a length greater than two lengths of the surface wave, if that can be estimated. For a 30-cm trapezoidal canal with 1:1 side walls, flowing about 60 cm deep, at 400 l/s, a solid roof across the canal that was 60 cm long and penetrated the flow 6 cm was successful.

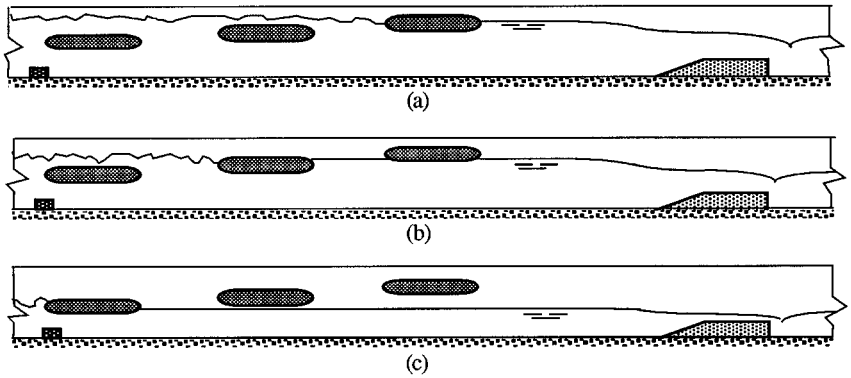

Figure 4. Wave suppressor for variable-depth flows in a canal.

To suppress waves in canals that do not always flow at the same depth, a staggered set of baffles may help. Because these will be submerged part of the time, they must have a thickness that overlaps slightly to accommodate the vertical depth of interest. To avoid obstructing the channel severely, these baffles probably should not obstruct more than about 20% of the channel at any one location. Staggering them as shown in Figure 4 should accomplish this without excessive obstruction. Rounding the upstream edges will help shed trash. Observe in the sequence of drawings in Figure 4 that the staggering is upward in the downstream direction. Note that the next baffle slightly overlaps the horizontal flow lines so that flow passing over the top of one baffle is not allowed to free-fall and start another wave. Figure 4(a), (b) and (c), illustrate the general behavior as the flow becomes less deep.

Checking a flow profile

Sometimes there is a need to inexpensively check how the velocity profile is behaving near a measuring device, and to check if measures taken to condition it have been effective. One way to obtain quick and easy results is the rising bubble method. Trickle irrigation tubing is weighted so that it will stay in a straight line across the channel of interest. pressurized air or other gas is released at a rather fast rate from the many small holes. The predominant larger bubbles rise uniformly enough to define an undisturbed water surface area between the line of injection and the predominant emergence. The smaller bubbles rise more slowly and emerge in the downstream bubble trail. One immediate observation is the symmetry of the emergence line. A ragged, nonsymmetrical line in a prismatic channel indicates velocity profile distortions.

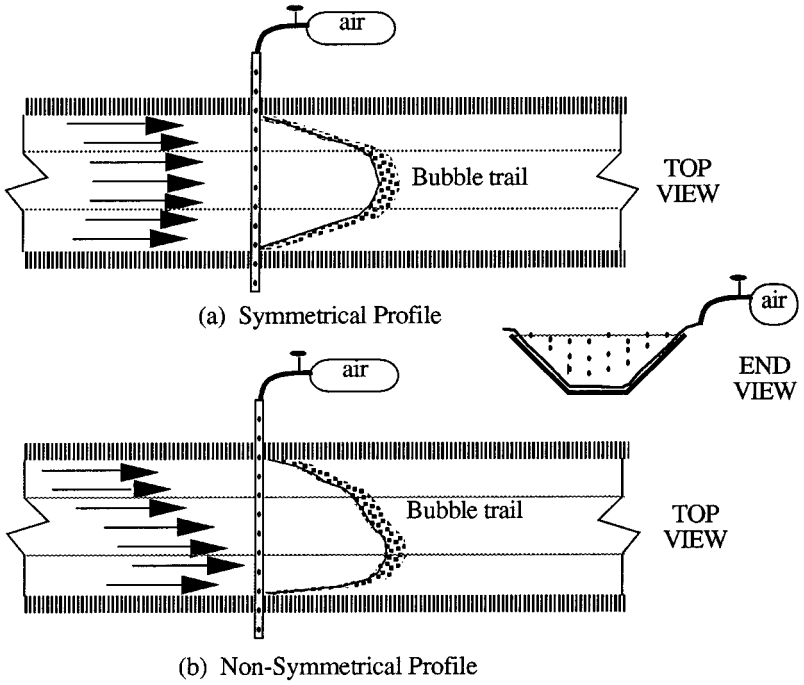

Figure 5. Air bubbles used to check velocity patterns.

Using rising bubbles as a flow measurement method

This same system can be used to measure discharge rate. The discharge is calculated quite simply by the product of the area defined by the emerging bubbles and the release line, multiplied by the rise velocity of 0.218 m/s (Herschy 1985). A limitation of this rising-bubble method is the difficulty of measuring the surface area accurately, but this method will give good discharge estimates in poorly defined earth channels, and automatically adjusts for both velocity profile and channel shape.

Differential head meters

Venturi meters and orifice meters can be made more convenient for the user if provided with a scale to indicate flow rate directly. For any given meter, a scale can be produced that the user simply uses by placing the bottom on one leg of a manometer and reading flow rate directly at the level of the other leg. No subtracting of readings and no table look-up is needed (Replogle & Wahlin 1993). The manometer level can be raised or lowered to suit the observer without changing the net differential reading, Figure 6.

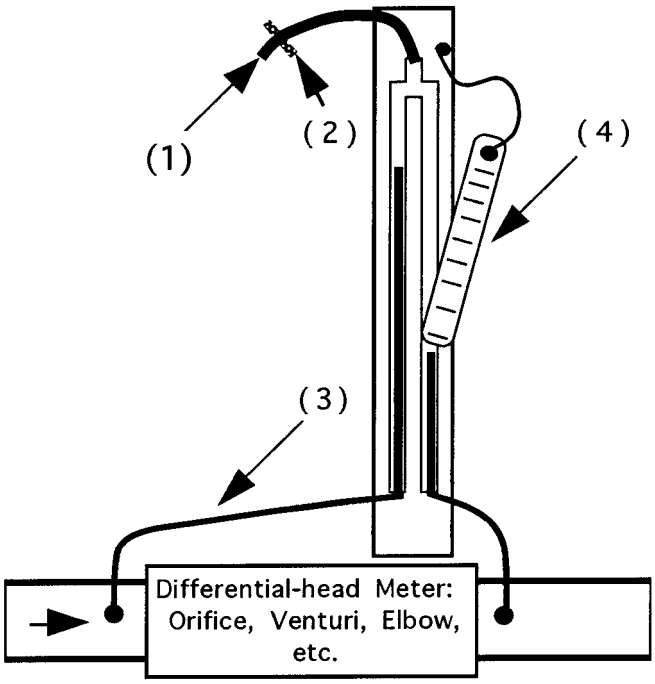

Figure 6. Differential head can indicate discharge rate directly. (1) Apply suction or pressure to adjust the differential pressure to a convenient reading level; (2) Clamp; (3) Remove bubbles in pressure tubes; (4) The scale is marked in flow-rate units.

Stilling wells

Many pressure tappings for stilling wells on weirs and flumes are poorly constructed. The instrument installed in the stilling well cannot detect and transmit accurate flow information if it senses a stilling well level that does not represent the canal level.

Stilling wells may be of limited accuracy if the connecting pipe to the stream is not installed correctly, a frequent problem in earthen channels, Figure 7. The error can be as great as plus or minus one velocity head ($\pm v^2/2g$ where v is the velocity and g is the gravitational constant). Figure 7 shows typical stilling well installations in lined and unlined channels. The third illustration in Figure 7 shows the undesirable situation with the pipe protruding into the channel flow.

The opening to the stilling well should be located in a region of low velocity flow so that the maximum velocity effect will be less than 1% of the detected head reading. For example, a flow velocity of one meter per second in the region of the pressure tap has a potential to cause up to 5 cm error

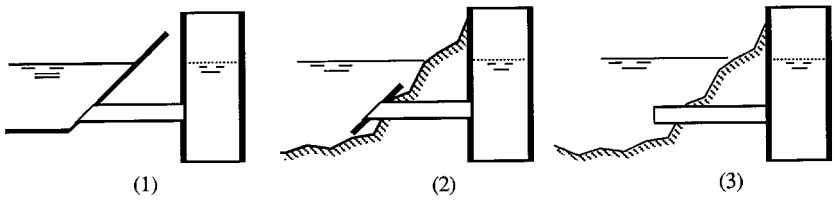

Figure 7. Stilling well installation. (1) Pipe cut smooth at channel boundary wall; (2) Pipe cut smooth at plate on channel wall; (3) Undesirable installation: pipe protrudes into channel flow.

in reading if the pipe points into the flow. A smaller, but not readily defined fraction of this error occurs when the pipe is partly pointing into or away from the flow, or has an uneven cutoff, or protrudes into the flow perpendicular to the velocity. Sometimes flush and smooth boundary-surface pipe terminations may not be practical and special measures such as the static pressure tube can salvage the situation.

Static pressure tubes

The static pressure tube can be built from simple lengths of pipe with holes drilled through the wall (Rantz 1982). To meet the criteria for good pressure detection, the wall thickness of the pipe should be greater than about twice the diameter of the holes. For example, 3 mm drilled holes in a pipe wall that is 6 mm or thicker is recommended. It is important that the holes be perpendicular to the pipe and free of burrs (Rouse 1961; Shaw 1960). If possible the holes should be drilled against a solid bar inside the pipe to prevent burrs, or other means can be devised to remove the burrs. The burrs are more important in fluctuating flows than in non-fluctuating flows, because the stilling well level reading may be biased if the fluctuating flow can move through the holes more easily in one direction than the other. Figure 8 shows some construction configurations for the static pressure tubes. In general, the idea is to have enough pipe length so that any end disturbances do not influence the pressure detection.

Figure 8 shows how a static pressure tube can be assembled from ordinary pipe and can be used to move the stilling well tap location, or to obtain good readings in an earthen channel. Note that in the illustration the horizontal pipe points downstream to lessen the chances of catching debris on the stem that could obstruct the sensing holes. These holes are subject to plugging by algal growths, snails, crayfish etc. Wrapping plastic window screen around the horizontal part of the tube of Figure 8 appears to make plugging more difficult and lengthens the periods between required maintenance while still providing accurate depth sensings with errors less than about ± 1 mm for most

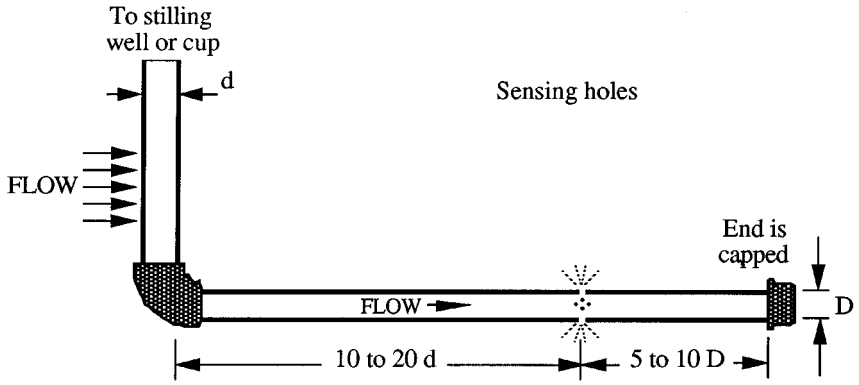

Figure 8. A suggested construction for a static pressure tube.

canal flow situations. The screen may also slow the response time, but this is usually not critical in irrigation applications.

Typically, the minimum distances between the pressure sensing holes and changes in pipe size, such as pipe fittings, attachment hardware, handles, pipe tee fittings, etc., should be from 10 to 20 pipe diameters upstream and downstream, depending on the size of pipe fitting or perpendicular handle rod or pipe. Rounded points need to have about 10 pipe diameters from the point to the sensing holes. Pipe caps should tend more toward 20 pipe diameters. This is similar to the recommendations for the standard Prandtl Pitot tube (combination impact and static tube) that has been in use for decades (ASTM 1971), with added lengths for extra disturbance factors. The number of holes can vary depending on the rapidity of response needed in the stilling well, and they do not all need to be in the same radial plane for usual applications where the flow lines are not curving. For hydrologic events, a typical recommendation is that the ratio of the area of the pipe (or openings) to the area of the stilling well should be 1:100. For irrigation this is less important because the flow rate changes are usually on a large time scale. The installation should be in a place where the direction of flow is assured. Good locations are near a wall in a straight section of channel. Laying the tube directly against a wall does not appear to compromise its function in most practical situations. The channel floor also is included in this recommendation, but is subject to sedimentation problems.

Accurate water surface elevations and water depths are some of the major hydraulic parameters needed to characterize open channel flows. Yet these are usually difficult for field crews to retrieve with any degree of precision. The surveying rod held on a choppy water surface is less than desirable.

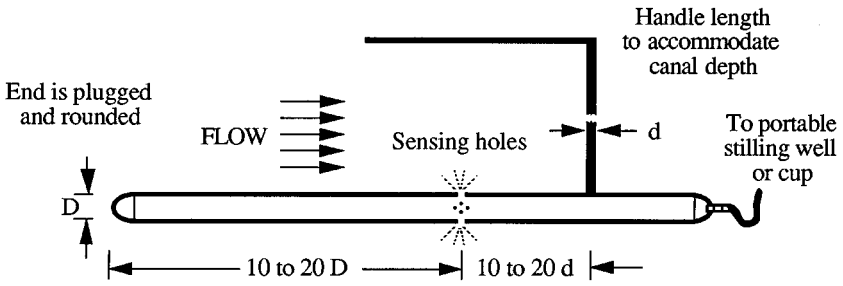

Figure 9. Portable version of static pressure tube useful for flume zeroing and channel depth measurements for accurate water surface slope determinations.

Figure 9 shows a typical portable static pressure probe that can be suspended in the flow, hung against a wall or laid on the channel floor. The precautions and dimensions previously suggested for the fixed static pressure probe apply here as well. A handle rod is usually attached so that the probe can be readily oriented into the flow direction. Usually these probes are used with attending personnel while making measurements and debris problems are corrected manually when they occur.

One or more of these probes can be used in canals to quickly and accurately determine roughness values. They provide accurate water surface determinations to an accuracy consistent to the surveyed accuracy of the hard bottoms and sidewalls of concrete canals. From this, the energy slope and hence the roughness values can be calculated.

Some depth sensing concepts and methods

The accuracy of a flow-rate measurement depends on knowledge of the true, upstream sill-referenced head on flumes, and on true differential-head across orifices. Even the less-accurate and often questionable rated-channel technique requires accurate sensing of water surface elevation relative to a reference datum. The portable static pressure tube described above can be used for this latter method.

Staff gauges. A staff gage is recommended at all depth sensing locations regardless of the attending electronic detection and transmission because it provides immediate field data validation.

Purge-bubble systems. Bubble gages, or purge bubble systems, can be used with pressure transducer detection of the pressure needed to cause slow bubbling (3 to 5 bubbles per second) from a submerged orifice. The bubbles are usually released from small tubes in the quiet water of a stilling well because the same tubes projecting into flowing water can prove to be erratic. Again,

the stilling well itself must be properly constructed to produce an accurate water depth.

A special format of the purge bubble method is the "Double-bubbler method" (Dedrick & Clemmens 1984). By mechanized, periodic valve openings, a pressure transducer senses, in turn, atmospheric pressure, then pressure from two bubble-outlet ports set a known vertical distance apart (typically 15 cm). From these three values, the response properties of the pressure transducer can be immediately re-computed to account for any drift or temperature effects. Linearity of the transducer is assumed. The output is used to accurately compute the distance to the water surface above one of the bubble outlets. This outlet elevation itself is referenced to the flume or weir crest elevation by surveying or other techniques. This allows inexpensive transducers to be used because they are in an air environment away from the corrosive effects of the water. Water surface is indicated to within $\pm$ 2 mm. A gas supply is necessary. (Commercial versions are now offered by Campbell Scientific, USA.)

Pressure transducers

Water submergible, temperature compensated pressure transducers are being used for detecting water surface elevation in large canal systems. Typically, this has meant tolerating an uncertainty greater than $\pm$3 mm to 6 mm. For small head readings, more precision is needed and the Double-Bubbler system described above can be used even with low quality pressure transducers.

A similar concept can be used to field-calibrate and field-check submerged pressure transducers. (This check mimics only one cycle of the Double-Bubbler method and does not replace it as a continuous transducer correction system.) To make submerged transducers conveniently field checkable, the device should be mounted on a rigid movable rack device with detents, or stops, at final depth and some known other depth, and in the air.

These mounting detents can be as simple as "eye" bolts and slide rod. The transducer can be read in the stilling well while:

1. in the air, where the zero pressure reading, e_0, is read;
2. at operating depth, where it should produce an output signal level, e_1, in any scale units without particular regard to span or zero setting, and
3. at a fixed distance, Δy, above or below the operating depth position, where it should indicate another output, e_2.

From these three readings the distance to the sensed water surface, h_1, can be calculated as:

$$h_1 = \frac{e_1 - e_0}{\left(\frac{e_2 - e_1}{\Delta y}\right)}$$

This can be referenced to the zero elevation of the flume, weir, or other measurement device, such as a permanently-mounted wall gage referenced

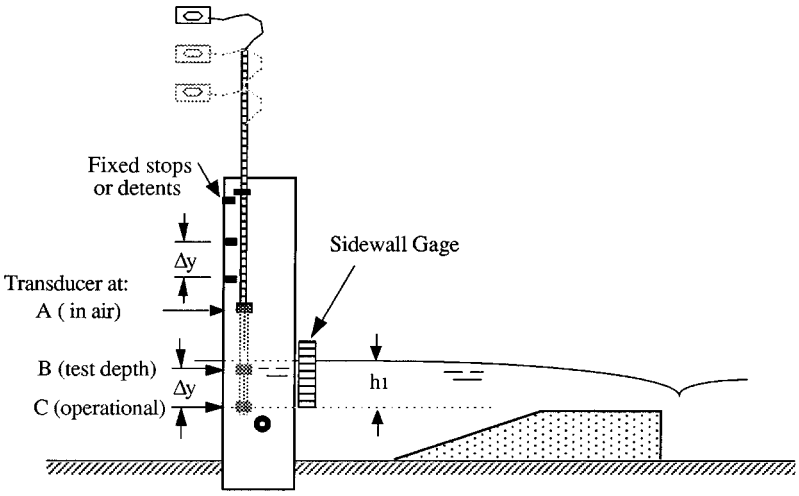

Figure 10. Pressure transducer on movable rack.

to the same elevation. Thus, the field technician can quickly verify proper function and can conveniently calibrate the pressure transducer in the field environment. For convenience of description, the final location of the transducer is at the reference elevation of the flume or weir, Figure 10. This is not necessary as long as the transducer zero offset is determined and is applied to the value of h_1 by survey or other means.

Float systems. Float operated recorders have a long history and are fairly well established. The major design feature is selecting the float diameter, usually between 15 and 30 cm for most canal observations. These are discussed in many texts (Bos 1989; Bos et al. 1991). These float recorders are frequently used for farm canal and secondary canal weirs and flumes. The operative concept is that the float needs to have a diameter that is large enough so that small displacements of the water surface can generate enough force to operate and overcome the instrument friction with an acceptable small change in float depth. This will usually require floats with diameters as large as 30 cm. Note that the float weight does not influence this operation except as it would cause more bearing friction. Thus, in concept, counter weighted solid concrete blocks could be used if they are suitably coated to reduce variable water absorption. Usually cylindrical floats serve as well or better than ball floats. Glass jugs, partly filled with rocks to assure that they stay upright, can be used. Plastic jugs are to be avoided, particularly if they can change shape and cause a zero shift. Flow totalizing can be accomplished with suitable secondary computer processing, using any of these devices.

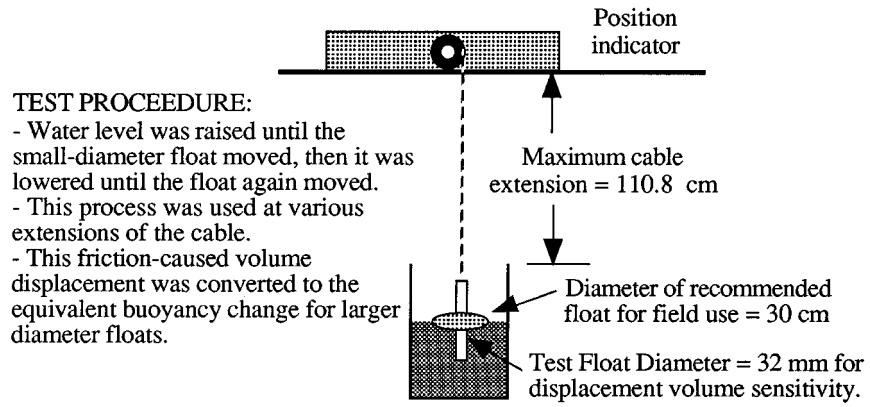

Figure 11. Testing position indicator for change in force with cable length.

Constant force position indicator used as water surface detector

Recently a machine shop instrument called a position indicator has been applied to read float positions in a stilling well. This device replaces the counterweighted flow instruments discussed above. It produces an output signal for either local reading or can be transmitted to a central headquarters by wire or radio. The device is an approximate constant-force spring that exerts a constant tension on the roll-up cable at all extensions of the cable. They were originally designed to follow hard metal surfaces in machine shop operations.

In that application, the position indication readout is controlled by the movement of the tool to which it was attached. Because it is controlled by displacement, slight changes in the tension force on the cable, more specifically, change in force with changes in cable extension, are of little significance.

When applied to stilling well floats, Figure 11, any variation in spring tension will change the relative buoyancy of the float and thus the zero reference. Thus, the position indicator becomes force-controlled because the displacement is a combination of the water surface movement and the float buoyancy change relative to the water surface. This shortcoming can be handled if the change in buoyancy causes only a small change in position. This buoyancy depends on the changes in force of the spring and friction in the device. That is, when the water surface reverses direction, the friction will cause the float to rise or sink slightly to obtain the necessary buoyancy force before it will start to move. This was evaluated for one of the devices in the manner indicated in Figure 11.

The force change varied by nearly 75%, throughout a range of extensions of the cable, Table 1. In Table 2 these force changes are translated into the buoyancy displacement error that various diameters of floats would produce

Table 1. Float diameter and buoyancy force relations.

(A)

Approx. extension cm	Rising water cm	Falling water cm	Test float Δy cm	Test float Δvolume cc	Force N
0.0	9.7	15.1	5.4	42.8	0.42
12.3	8.9	15.7	6.8	54.1	0.53
25.2	21.3	29.0	7.7	61.1	0.60
38.1	34.0	42.1	8.1	63.9	0.63
52.3	47.9	56.7	8.8	69.7	0.68
66.3	62.0	70.6	8.5	67.6	0.66
79.4	75.3	83.5	8.2	65.2	0.64
97.1	92.7	101.5	8.8	70.0	0.69
110.8	106.1	115.5	9.4	74.8	0.73

(B)

Δy needed by various float diameters for force to overcome friction

Approx. Cable ext. cm	7.5 cm Δy mm	10 cm Δy mm	15 cm Δy mm	25 cm Δy mm	30 cm Δy mm	40 cm y mm	45 cm Δy mm	55 cm Δy mm
0.0	9.4	*5.3*	2.3	1.0	*0.6*	0.4	0.3	0.2
12.3	11.8	*6.7*	3.0	1.3	*0.7*	0.5	0.3	0.2
25.2	13.4	*7.5*	3.3	1.5	*0.8*	0.5	0.4	0.3
38.1	14.0	*7.9*	3.5	1.6	*0.9*	0.6	0.4	0.3
52.3	15.3	*8.6*	3.8	1.7	*1.0*	0.6	0.4	0.3
66.3	14.8	*8.3*	3.7	1.6	*0.9*	0.6	0.4	0.3
79.4	14.3	*8.0*	3.6	1.6	*0.9*	0.6	0.4	0.3
97.1	15.3	*8.6*	3.8	1.7	*1.0*	0.6	0.4	0.3
110.8	16.4	*9.2*	4.1	1.8	*1.0*	0.7	0.5	0.3

Celesco Position Indicator, Model PT420-0050-111-1110, Serial No. A49899 SCD)

with this device. For example, Table 2 shows that a 30-cm diameter float will reduce the error to about ±1 mm or less, which is usually acceptable. A 10-cm diameter float, on the other hand, will have nearly ±9.2 mm of error, which is usually not acceptable. The general conclusion is that 20 cm to 30 cm float diameters should be used.

Canal isolation

An important concept that is often not observed in the design of secondary canals, is that if at all possible, they should be suitably isolated from the

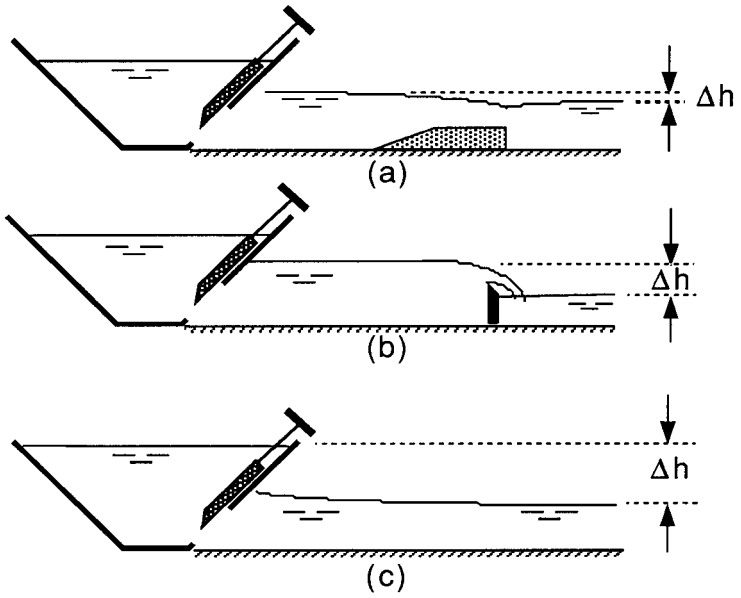

Figure 12. (a) A long-throated control such as this broad-crested weir can isolate the small canal from its source with significantly smaller head loss, Δh, than can a sharp-crested weir (b) or a free discharging orifice (c).

main canal so that unplanned changes in backwater effects in the secondary do not alter the withdrawal rate from the main canal. Several means are available to accomplish this, including steep canals, critical-flow controls (such as over-spilling sills or weirs), near the head of the secondary canals, and free-discharging orifices, also at the head of the secondary canals. Only the critical-flow controls and orifices are of interest to this discussion.

An overspilling control sill is particularly useful if it also serve as measuring device. This could be in the form of a sharp-crested weir. However, these require so much head drop that they are usually not practical, particularly in areas of flat terrain, and because of their limited maximum flow rate. If head loss must be small, a long-throated flume, including the related long-throated, broad-crested weir works well. By forcing the flow to pass critical flow control caused by an overfall, the flow rate to the secondary is nearly immediately stabilized to a constant value, and future downstream effects are isolated from causing changes in the main canal. This helps the gate operator to set the gate immediately and confidently for the desired secondary canal flow rate without concern for changes caused by increasing backwater as the secondary canal fills. Thus, both main and secondary canals benefit.

Note that long critical flow controls that exceed in length about twice the flow depth can isolate downstream effects with barely 10% to 15% drop in

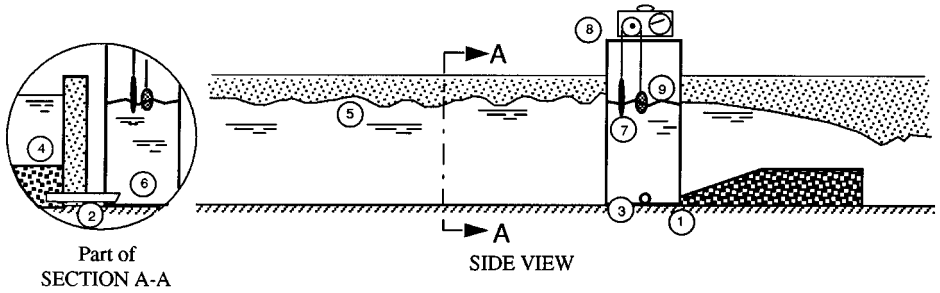

Poor Installation with many problems:

1. Stilling well is too close to ramp of broad-crested weir.
2. Stilling well tap located too close to floor of channel and is subject to sediment plugging.
3. Stilling well without sediment storage area at bottom may require frequent cleaning.
4. Stilling well pipe is reentrant into channel and is subject to velocity effects.
5. Choppy water surface in approach channel causes fluctuations in stilling well.
6. Unmatched end conditions on stilling well pipe can cause pressure bias in fluctuating flow.
7. Counterweight touches the water at high flow depths.
8. Counterweight may strike pulley wheel at low flow depths.
9. Float may be too small in diameter to achieve necessary sensitivity.
10. No wall gage to facilitate operational check of recording/transmitting instrument.

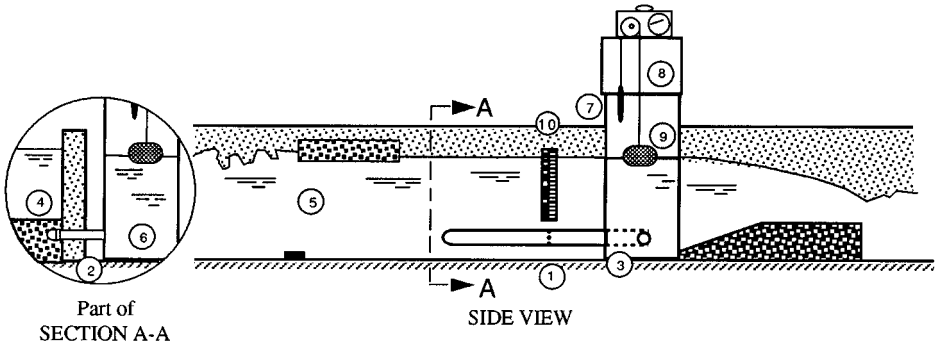

Acceptable Installation with previous problems addressed:

1. Stilling well tap moved to correct location using static pressure tube attached to wall.
2. Stilling well tap raised from floor to avoid sediment plugging.
3. Stilling well has a sediment storage area at bottom to avoid frequent cleaning.
4. Stilling well pipe no longer reentrant into channel because of static pressure tube
5. Choppy water in approach channel is reduced by surface wave suppressor and floor block.
6. Matched ends on stilling-well connecting pipe reduce pressure bias from fluctuating flow.
7. Counterweight does not touch the water at high flow depths.
8. Stilling well height increased to lengthen counterweight cable and avoid striking the pulley.
9. Float diameter increased to improve sensitivity of depth measurement
10. Wall gage (linear or direct reading) facilitates operational check of recorder/transmitter.

Figure 13. Example of how to correct poor installations of flumes.

water surface elevation, Figure 12a, while sharp crests will pass downstream effects upstream unless there is complete ventilated overfall, about 110% to 120% of weir-head depth, Figure 12b. As mentioned above, this huge water surface drop is usually not available in most irrigation projects. Free discharging orifices also isolate the secondary canal, but also at the expense of high head loss, Figure 12c.

Contrast this with flow measuring methods that do not isolate the canals, such as the rated channel method. With this method flow stage relationships are correlated, and vertical slide gate openings are used as submerged orifices with differential heads on the orifice opening. However, a secondary canal may take hours to fill to final discharge rate and flow depth. The back pressure of the secondary onto the main canal will constantly change and the operator would need to keep making minor adjustments that fluctuate both the secondary and the main. Even high technology systems, such as the one using an electromagnetic floor-mounted probe to sense channel velocity and a pressure transducer to determine flow depth and area, do not fully address the control aspects without further channel constructions. Similar problems accompany another high-tech system, the trans-channel ultrasonic techniques. Both orifice-based and the high-tech systems can be significantly improved by appropriately constructing an overfall control near the device to isolate the secondary from the main canal.

Examples of installation errors and corrections

Figure 13 illustrates a number of wrong or undesirable conditions for a long-throated flume installation. It also shows some suggested corrective measures to consider for each problem.

References

ASME (American Society of Mechanical Engineers). 1971. *Fluid meters, their theory and application.* 6th ed. Report of ASME Research Committee on Fluid Meters. American Society of Mechanical Engineers, New York, 202 p.

Bos, M.G. (Ed). 1989. *Discharge measurement structures.* Third Revised Edition. Publication 20. International Institute for Land Reclamation and Improvement/ILRI, P.O. Box 45, 6700 AA Wageningen, The Netherlands. 401 pp.

Bos, M.G., Replogle, J.A. & Clemmens, A.J. 1991. *Flow measuring flumes for open channel systems*. American Society of Agricultural Engineers. 321 pp. (Republication of Book by same title, originally by John Wiley and Sons, New York. 1984.)

Dedrick, A.R. & Clemmens, A.J. 1984. Double-bubblers coupled with pressure transducers for water level sensing. Trans. ASAE. 27(3): 779–783.

Herschy, R.W. 1985. *Streamflow measurement.* Elsevier Applied Science Publishers, London and New York. 553 pp.

Rantz, S.E. 1982. *Measurement and Computation of Streamflow: Volume 1. Measurement of Stage and Discharge.* Geological Survey Water-Supply Paper 2175. U.S. Geological

Survey, Department of Interior. United States Government Printing Office, Washington, DC. 297 pp.

Replogle, J.A., Fry, B.J. & Clemmens, A.J. 1987. Effects of non-level placement on the accuracy of long-throated flumes. Journ. of Irrigation and Drainage Engineering. ASCE. 113(4): 584–594.

Replogle, J.A. and Wahlin, B.T. 1993. Venturi meter construction for plastic irrigation pipelines. Applied Engineering in Agriculture. American Society of Agricultural Engineers. Vol. 10(No.1): 21–26.

Rouse, H. 1961. *Laboratory Instruction in the Mechanics of Fluids.* Iowa Institute of Hydraulic Research, Published by the University, Iowa City. 60 pp.

Shaw, R. 1960. The influence of hole dimensions on static pressure measurements. Journal of Fluid Mechanics 7(April): 550–564.

Calibration and Measurement

Figure 1. Example of Volume Measurement Devices

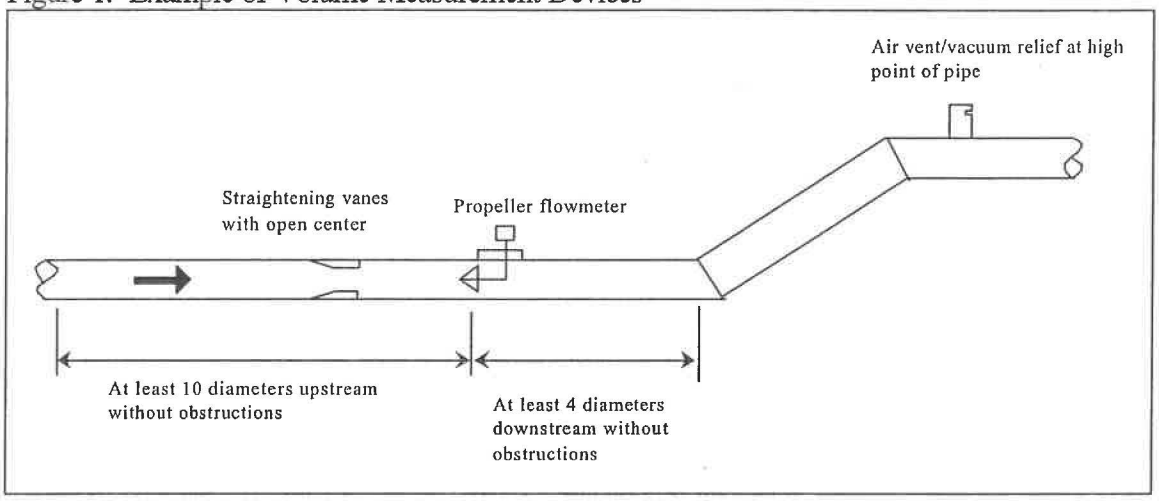

1. Propeller Meter;
2. Venturi Meters
3. Magnetic Meters
4. Acoustic Meters

These have a high level of accuracy with proper installation and periodic maintenance and calibration.

Meters	Installation	Maintenance	Calibration
Propeller Flow Meters	When ordering a meter, it is very important to know the exact wall thickness and ID of the pipe (see Figure 2) in which it is to be placed (i.e., 11.9" vs. 12"). The meter must be exactly centered in the pipelines in order to be accurate. Units are typically not accurate at low velocities. Meters should be operated at greater than 1 foot/second.	When propeller meters are placed in locations with large amounts of algae and trash, remove the trash before it gets to the meter or frequently clean the propellers. Also, sand and normal wear can cause the propeller to not spin freely, as it should. The problem may show up as a more erratic needle movement.	Calibration is typically done by sending the unit back to the manufacturer on a regular maintenance cycle and having it checked. Field checks of meters can be done using a portable acoustic meter (transit time type).
Venturi Meters	Manufacturers of the Venturi Meters should be requested to furnish the rating tables for the unit purchased. Venturi Meters are susceptible to turbulence in the pipe.	The tubes used to measure the pressure can easily become plugged so they must be checked periodically.	Field calibration can be done using an insert pitot tube or done using a portable acoustic meter (transit time type).
Magnetic Meters	Spool type magnetic (see Figure 3) meters can be very accurate even with turbulence	Low maintenance on spool meters. Insert meter sensors must be periodically	Field checks of meters can be done using a portable acoustic meter (transit time

Meters	Installation	Maintenance	Calibration
	in the pipeline. Insert magnetic meters should follow propeller meter installation guidelines.	cleaned.	type).
Acoustic Meters	Acoustic meters can be used in both pipelines and channels. Acoustic meters should follow propeller meter installation guidelines.	Transducers (see Figure 4) must be periodically cleaned. It is important to avoid multipath interference and signal bending from solar heating.	For calibration by current-meter measurement or theoretical computation, it is essential to place device in a cross section that will not change significantly. If the transducers are placed out in the channel, the triangular side areas not measured must be accounted for in the calibration.

Figure 2. Inside Diameter (ID) of the Pipe

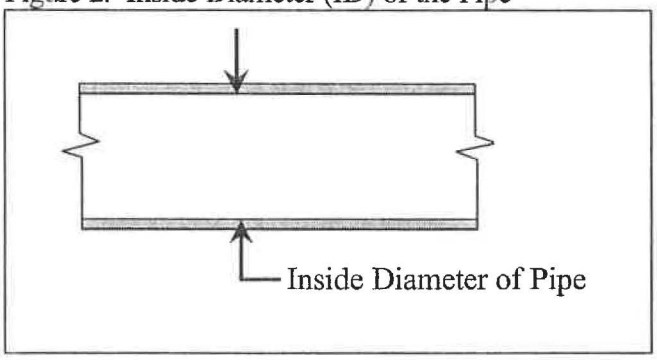

Figure 3. Magnetic Meters (Spool Type)

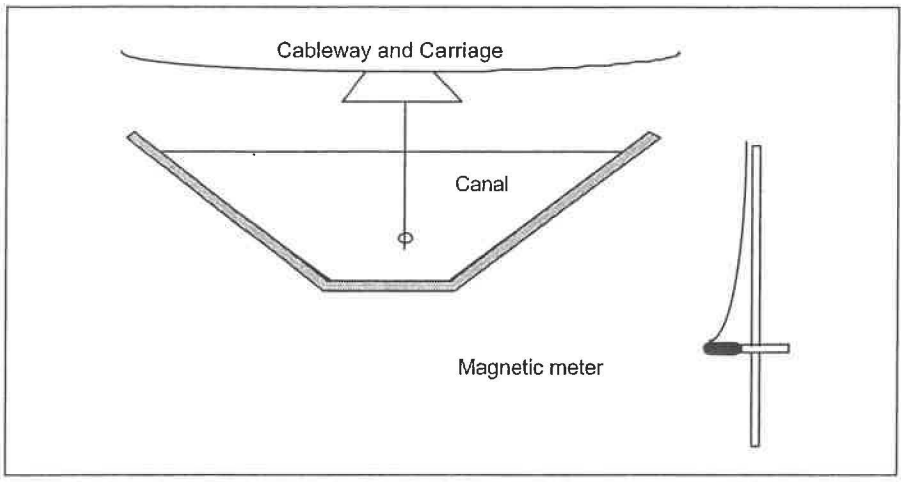

Figure 4. Acoustic Meter

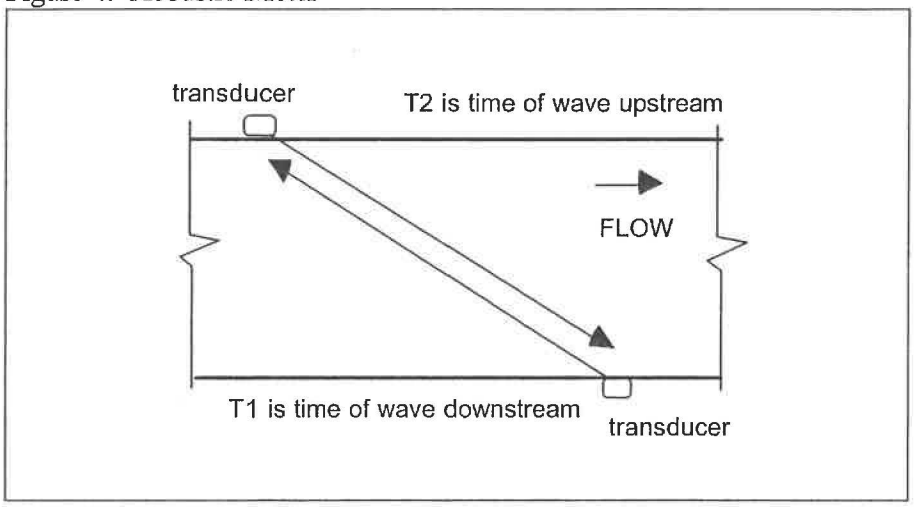

The second category includes standard flow measurement devices that measure flow rate and also require accurate measurements of delivery time to determine volumes:

1. Replogle and Parshall flumes
2. Rectangular, Trapezoidal (Cipolletti), and V-Notch weirs
3. Canal meter gates

These devices require proper installation, regular recording of flow rates and delivery times, adjustments for approach velocity in some cases, and regular maintenance and calibration for good accuracy.

Flumes, Weirs and Gates	Installation	Maintenance	Calibration
Replogle	It is essential that the entrance of	It is important to keep the	Can be calibrated with

Flumes, Weirs and Gates	Installation	Maintenance	Calibration
and Parshall Flumes	the control section of the flume be level in the direction of the flow. Water must be moving "straight" toward the flume. The flume should be located about 10 times the average channel width downstream of checks, gates, or bends in the channel. Staff gauges set too high will underestimate the actual flow rate.	stilling wells (see Figure 5) from being plugged or partially plugged. The surfaces of the flume must be kept relatively clear of moss and sediment build up. Limits of submergence should be checked at high and low-flow rates.	errors of less than 2 percent. The rating curve used for the flume can be field checked using a current meter.
Rectangular and Trapezoidal Weirs	It is important that the weir crest is horizontal or level and for the sides of the rectangular weir to be vertical, because the actual flow area of the water will not be correct. The water must be moving straight into the weir, and the face of the weir must be vertical.	It is important to keep the stilling wells from being plugged or partially plugged. Flow into and out of the weir should be as smooth as possible. Sediment accumulation below the weir crest should be removed.	Rating tables must be adjusted to account for the velocity of approach for calibration. Rating tables must be checked for the correct weir (i.e., contracted weir vs. suppressed weir). Rating tables must be adjusted for submergence or slanted conditions.
(Cipolletti), and V-Notch Weir	Is important to determine which size of notch (how many degrees) is being used so that the correct flow-rate table can be used. It is also important to determine if there are any errors in the construction of the notch. The water must be moving straight into the weir, and the face of the weir must be vertical.	Same as the rectangular and trapezoidal weirs above.	Same as the rectangular and trapezoidal weirs above.
Canal Meter Gates	1. "Zero" height (wee figure 6) of the stem is when the flow starts to leak through the gate. 2. Always pull up on shaft (by the turning wheel) before taking measurement. 3. Keep the bottom of the gate entrance clean.	Flow toward and into the structure should be as smooth as possible. Obstructions should be removed to improve the entrance conditions. Remove accumulations of sediment, because they may reduce the actual area of orifice. Debris, such as weeds, should also be removed.	Manufacturer's specifications must be followed precisely in order to obtain accurate flow rate measurements.

Flumes, Weirs and Gates	Installation	Maintenance	Calibration
	4. A change in pipe material several diameters downstream of the gate will not affect the accuracy. 5. A water level in the downstream pool is not the same as a water level measured in a whistle pipe (see Figure 7). 6. Eddies at the gate entrance will generally cause an overestimation of the flow rate. 7. The accuracy is poor if the gate is more than 70 percent open.		

Figure 5. Stilling Well

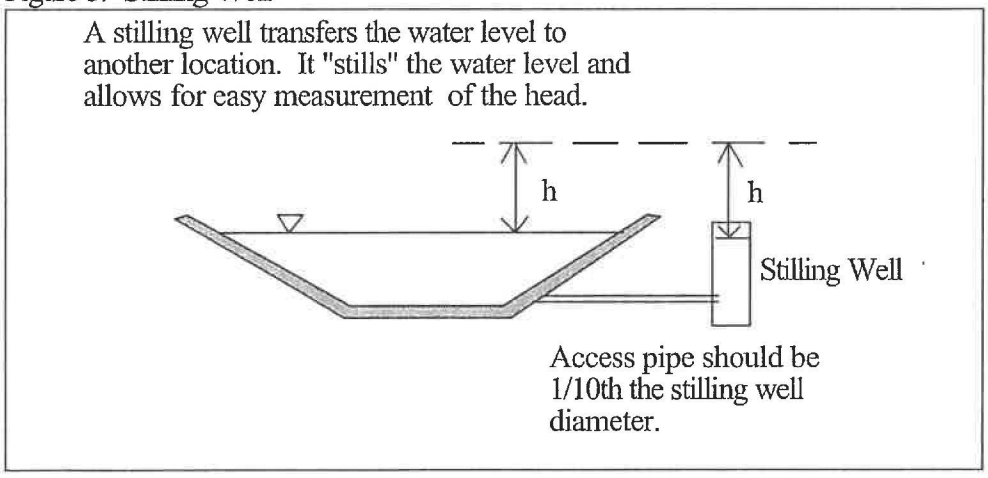

Figure 6. "Zero" Reference

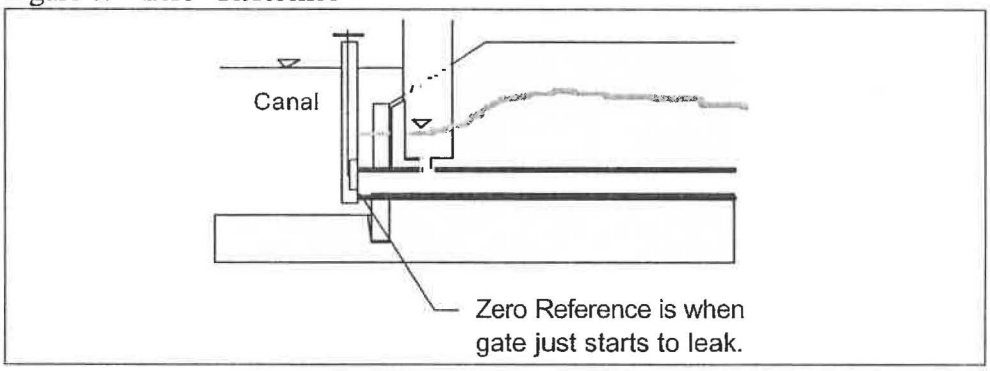

Figure 7. Whistle Pipe

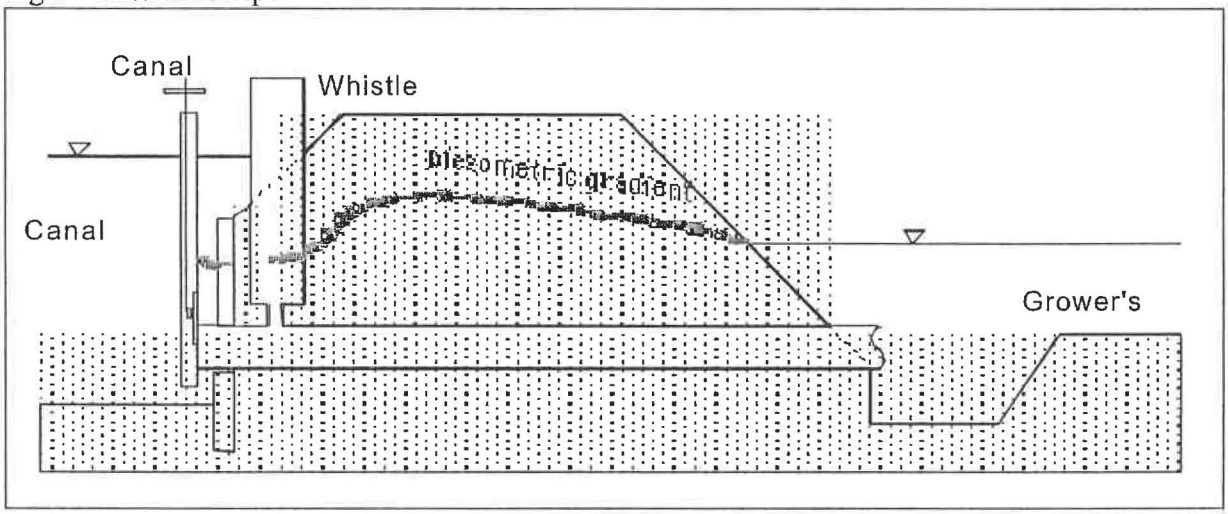

The third category includes non-standard, calibrated flow measurement devices. This category includes special measurement devices developed by a district. Typically, there are no published standard dimensions or flow tables for such devices. Consistent dimensions and installations; accurate determination of delivery time; local calibration and a verification of accuracy, based on a representative sample number of devices measured over time; and a proposed schedule for maintenance and calibration would be necessary for acceptability.

The following steps can be used to calibrate a non-standard structure:

1. Use a current meter to calibrate the non-standard structures. The individuals who will perform the current metering need to demonstrate proficiency in the required skills to perform the measurements.

2. The individuals will need to use an established site such as a calibrated Replogle flume to verify their proficiency in making good current meter readings.

3. Non-standard structures have certain requirements that must be met in order to be calibrated. If these conditions cannot be met, it is useless to spend time calibrating the structure. These required conditions include:

   a. Good entrance conditions with a low velocity.

b. If the device to be calibrated is located right next to a supply canal (within 10 feet or so), the supply canal must have a fairly constant velocity.

c. The staff gauge must be "zeroed."

d. There must be no moss build up. That is, the conditions must not change with time.

4. The recommended calibration procedure for a non-standard site that meets the above conditions is as follows:

a. A wide spread in the measured flow rate is required. At least a 2:1 ratio in the flow rates should be used to create the table.

b. A minimum of 10 values should be measured across the flow rate range.

c. Data should be plotted on a log-log scale graph. See the following figure. Such a graph is a standard option in programs such as Microsoft Excel.

Figure 8. Log-Log Plot of the Current Meter Data

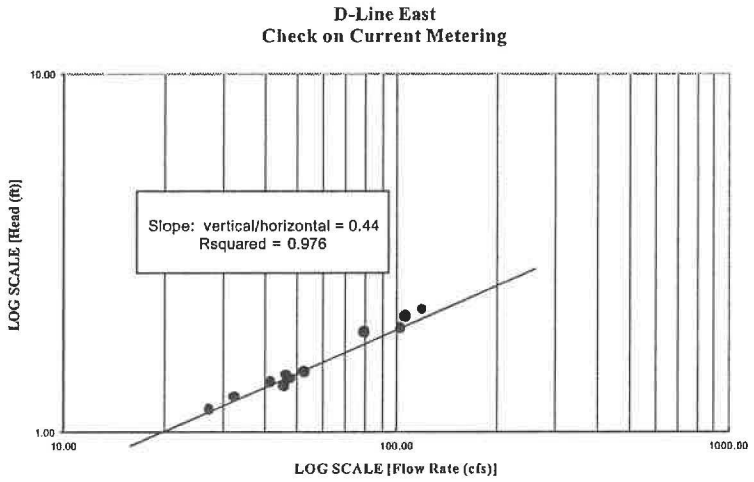

e. The data should plot out as a line (not a curve) with a slope between 0.4 and 0.67. A program such as Microsoft Excel can be used to determine the equation, and the equation should be of the form:

$H = KQ^x$
where "x" is a value between 0.4 and 0.67

f. The regression coefficient (r^2) must be better than **0.97** to assure confidence in the results.

A fourth category is using rough estimates of flow rate or volume, such as flow-rate estimates at check structures or the sum of siphon tubes (or other methods of measurement not specified here). These approaches are NOT acceptable since they do not provide a documented reasonable degree of accuracy.

For more information and support on measurement and calibration, please contact the Cal Poly Irrigation Training and Research Center at (805) 756-2434.

References:
Bureau of Reclamation Water Measurement Manual - 3rd Edition
Cal Poly Irrigation Training and Research Center - Flow Measurement (Fall 1999)

Included with the Workshop Registration Material is a CD with Flow Measurement Brochures from companies providing flow measurement equipment.

The CD was prepared by the Irrigation Training and Research Center, California Polytechnic State University, San Luis Obispo, California.

An Index of the Flow Measurement brochures on the CD follows.

Flow Measurement Brochures
Index

JBS Instruments

AquaCalc 5000
AquaCalc Accessories

Mace

AgriFlo
HVFlo

Marsh-McBirney

Flo-Mate Portable Flowmeter
Flowmeter selection guide

McCrometer

General product guide
Propeller flowmeter
Ultra Mag
V-Cone flowmeter

MGD Tech.

ADFM Velocity Profiler
ADFM brochure

Milltronics

OCM III - Open channel meter

Nortek AS

Aquadopp
Easy Q

Nusonics Inc.

Sonic Flowmeters

Nu-way

Adjust-a-Flume

Omega

FD610 Series Portable Doppler Flowmeters
Ultrasonic Flowmeters

Panametrics

LT 868 Flowmeter
PT 868 - Portable flowmeter
PT 878 - Specifications
PT 878 - Portable liquid flowmeter

Rocky Mountain Instruments (RMI)

Model 3000 - Wireless flow monitor

SonTek

ADV
Argonaut-SL

Stevens

Data Collection
- AXSYS CCR
- AXSYS
- DOT Logger
- RTU 0850
- VX 1004
- VX 1100 - Data Collection Platfoms

Water Quality Sensors
- Multi-parameter sensors
  - CS 304
  - CTD 350
  - CTDP 300
- Single parameter sensors
  - DO 100
  - EC 250
  - PH 100
  - TS 100

ThermoPolysonics

Vector DX25 - Open channel flowmeter
Vector PX20 - Portable open channel flowmeter

Unidata

Product overview
Starflow

Waterman

Doppler

Plug-and-Play Canal Automation

Main components

- Sensors, field units (RTUs), and communications - Automata, Inc.
- SCADA software – any commercial product (iFix by Intellution)
- *SacMan* software and U.S. Water Conservation Lab (USDA-ARS) control logic

General philosophy

- Low cost, reliable, proven components
- Standard protocols (e.g., MODBUS) and compatibility with other components
- Start simple and add complexity as needed
- Fast, plug-and-play installation
- Start with all control from central computer for fast installation, minimal debugging time, documentation of control actions, and on-line tuning of parameters. Control transferred to remote sites as needed.

Levels of implementation

- Remote manual control, unassisted – hardware and SCADA
- Remote manual control, assisted – add *SacMan* software for value-added manual control, including *SacMan Orders* and features from *SacMan CP*
- Local upstream level control – add *SacMan* features for implementing local water-level controllers, including *SacMan Orders* and features from *SacMan CP*
- Full automatic control – add *SacMan* features for centralized control (upstream control, volume control, downstream control – as defined by user), requiring *SacMan Orders* and *SacMan CP* (Control Program)

Additional Features

	Overall Control Strategy		
	Manual	Local	Central
Flow Monitoring	☑	☑	☑
Flow Control	☑	☑	☑
Demand Scheduling	☑	☑	☑
Incremental gate flow changes	☑		☑
Out-of-Bounds control	☑		☑
Pool Volume Mismatches	☑	☑	☑
Pool Flow Balance	☑	☑	☑
Control start-up		☑	☑
Water-Level setpoint changes		☑	☑
Alarms	☑	☑	☑

Contact: Bert Clemmens, U.S. Water Conservation Lab, 4331 E. Broadway Rd., Phoenix, AZ 85040 phone: 602 437-1702 fax: 602 437 5291 email: bclemmens@uswcl.ars.ag.gov

SACMan

Software for Automated Canal Management

SACMan CP

Canal Control Software

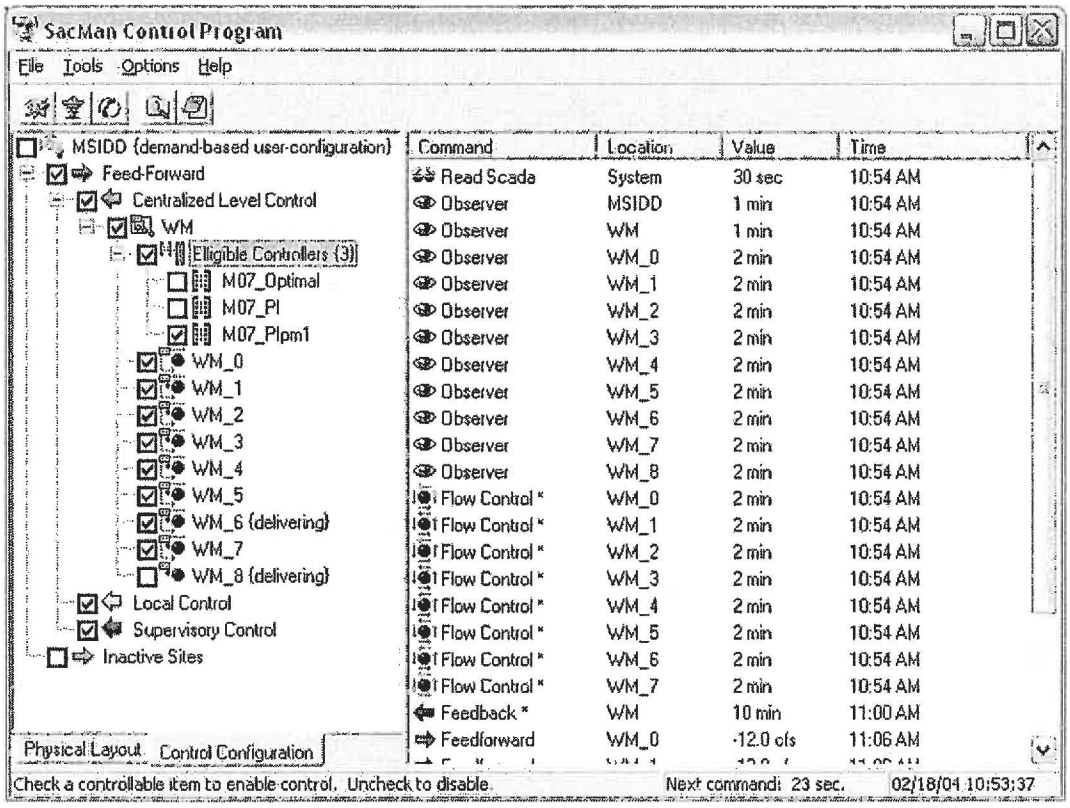

The SACMan Control Program (CP) provides monitoring and control capabilities for use in irrigation canal management by interfacing directly with commercial SCADA software (currently Intellution iFix 2.6). SACMan CP aids in supervisory control by providing diagnostic information and backup out-of-bounds control in emergency situations. Control capabilities range from local upstream level control to centralized downstream feedback control.

System Requirements

200 MHz Pentium running Windows NT 4.0, 2000, or XP Professional, 256 MB RAM, 4GB of free Hard Drive, Intellution iFix 2.6, Mouse, Keyboard.

Contact: Bert Clemmens, U.S. Water Conservation Lab, 4331 E. Broadway Rd., Phoenix, AZ 85040 phone: 602 437-1702 fax: 602 437 5291 email: bclemmens@uswcl.ars.ag.gov

SACMan
Software for Automated Canal Management

SACMan Orders

Order Entry and Scheduling Software

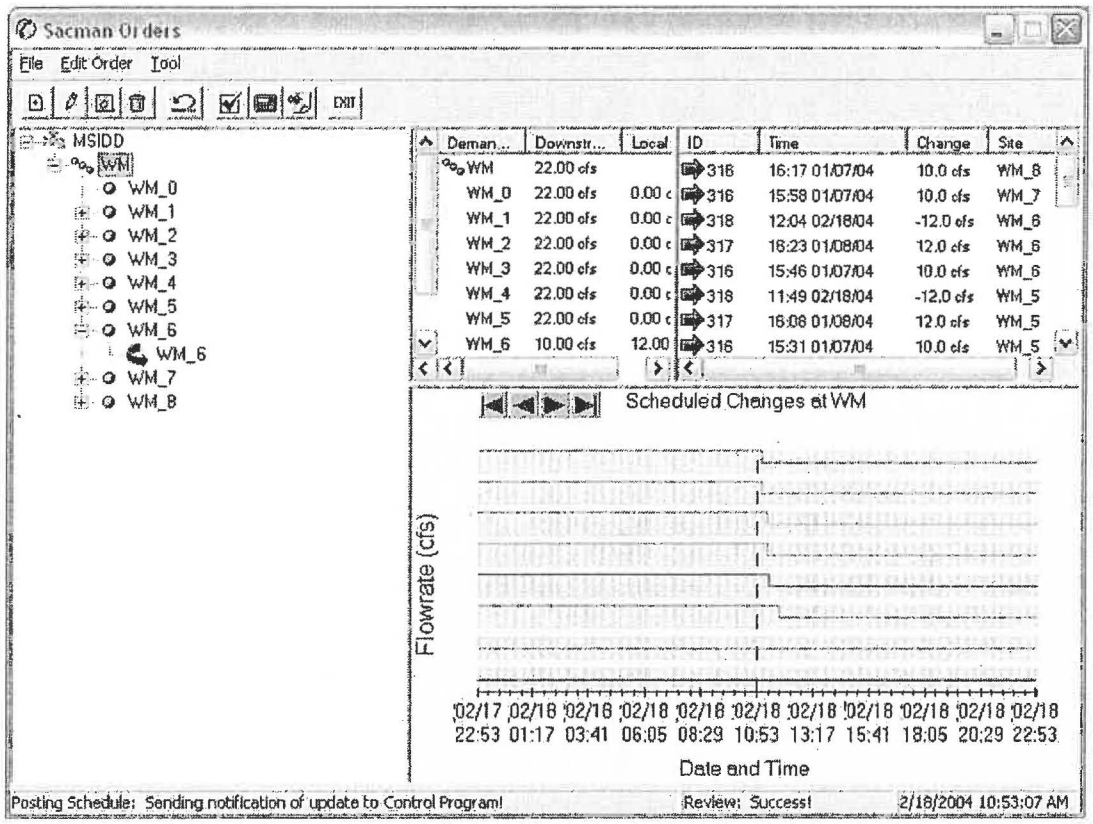

The SACMan Orders software provides order entry and scheduling capabilities for use in irrigation canal management. The software can generate printed schedules for manual/supervisory operation. Additionally, SACMan Orders can interact with SACMan CP and with commercial SCADA software (currently Intellution iFix 2.6) to automatically route scheduled delivery changes through the canal system.

System Requirements

700 MHz Pentium running Windows NT 4.0, 2000, or XP Professional, 256 MB RAM, 4GB of free Hard Drive, Intellution iFix 2.6, Mouse, Keyboard.

Contact: Bert Clemmens, U.S. Water Conservation Lab, 4331 E. Broadway Rd., Phoenix, AZ 85040 phone: 602 437-1702 fax: 602 437 5291 email: bclemmens@uswcl.ars.ag.gov

Application of Canal Automation in Central Arizona

A.J.Clemmens[1]
R. J. Strand[2]
L. Feuer[3]

ABSTRACT

The Central Arizona Irrigation and Drainage District (CAIDD) and the Maricopa Stanfield Irrigation and Drainage District (MSIDD) were constructed in the late 1980s with the promise of automatic control. All check structures on main and lateral canals were equipped with motorized gates, RTUs, radios, etc. These systems never performed as promised. District personnel were only able to acheive remote manual control operational on their main canals. In the mid 1990s, engineers from the U.S. Water Conservation Laboratory (USDA-ARS) began experimenting with canal automation on relatively small canals, yet large enough for real testing and where motorized gates were available. Through this research, ARS engineers were able to develop SacMan (Software for Automated Canal Management) in cooperation with Automata, Inc. SacMan has several levels of implementation ranging from manual control to full automatic control, including upstream level control, flow rate control, routing of known demand changes, and full downstream level control. SacMan interfaces with commercial Supervisory Control and Data Acquisition (SCADA) software, currently *iFix* by Intellution, Inc., but potentially applicable to other SCADA packages. The software was successfully tested on the WM canal of MSIDD. Sister district, CAIDD, was the first customer for this new software. Implementation started in August 2002 with manual control on 45 check structures. Various automatic control features are to be phased in over the winter of 2002-03 and expanded to their entire network (108 sites). This paper describes the features of this canal automation software and the implementation process that is taking place.

INTRODUCTION

In the spring of 2002, the Central Arizona Irrigation and Drainage District (CAIDD) experienced serious communications problems with their narrowband UHF radio communications. These radios were used to communicate between

---

[1] Laboratory Director, U.S. Water Conservation Laboratory, USDA-ARS, 4331 E. Broadway Rd., Phoenix, AZ 85040 bclemmens@uswcl.ars.ag.gov
[2] Electrical Engineer, U.S. Water Conservation Laboratory, USDA-ARS, 4331 E. Broadway Rd., Phoenix, AZ 85040 bstrand@uswcl.ars.ag.gov
[3] President, Automata, Inc., 104 New Mohawk Rd. Suite A, Nevada City, CA 95959-3261 automata@automata-inc.com

their central computer SCADA system and the RTUs at their canal gates. The lack of communication resulted in canal operators driving the canals to control check gates, something they had not done for more than a decade. Complaints rose and the district board had to make a decision. While a new radio frequency and recrystalled radios would have solved the problem in the short run, their system was somewhat out of date and would likely need replacing soon anyway. So the district's Board of Directors decided to purchase a new canal automation system that used more up-to-date technology and had significant potential for upgrading water delivery service and performance.

In late June 2002, CAIDD purchased the SacMan canal automation system from Automata, Inc. This system was developed through a Cooperative Research and Development Agreement between ARS at the U.S. Water Conservation Laboratory and Automata, Inc. The system was field tested on the WM lateral canal of the Maricopa Stanfield Irrigation and Drainage District (MSIDD). CAIDD and MSIDD are sister districts designed by the same consulting firm and constructed at about the same time. They started with the same canal automation equipment, used the same SCADA software, and made similar adaptations to the original systems.

The Automata hardware for 45 sites was delivered over a three week period from late August to early September. The new hardware and software were installed and the main canals were again controlled remotely by the end of September – less than 6 weeks after the first equipment arrived and less than a month after all equipment was received.

The purpose of this paper is to discuss the evolution of canal automation in these two districts, and to describe the SacMan canal automation system and how it is being adapted to operation of these two districts.

THE SACMAN CANAL AUTOMATION SYSTEM

The canal automation system available through Automata, Inc. includes three main components: Automata hardware, a Supervisory Control and Data Acquisition (SCADA) system, and special canal control software. The hardware includes the Automata "Mini" that serves as the RTU, Automata water level sensors, and a new Automata gate position sensor. The SCADA system currently used is *iFix* by Intellution, Inc. The special canal control software, SacMan (Software for Automated Canal Management) was develop by the Agricultural Research Service (ARS), U.S. Water Conservation Laboratory. These three components are described below.

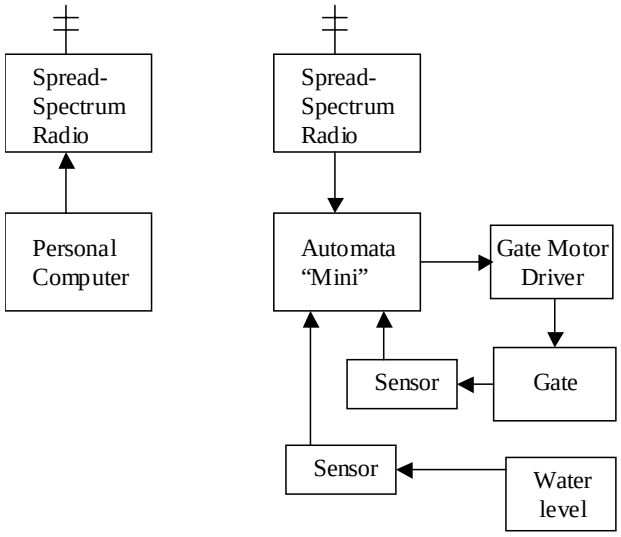

Figure 1. Hardware for SACMAN canal automation control system.

Hardware

The hardware for this system consists of water level and gate position sensors, RTUs, gate motor drivers, gate motors, spread-spectrum radios, and a personal computer, as shown in Figure 1.

The Automata "Mini" has a 10-bit processor for analog to digital conversion. For this application, it is set up for 1 digital input, 2 digital outputs, and 4 analog inputs. Any commercially available water level sensor can be used: as long as its range (e.g., 4-20 ma) is compatible with the analog input of the "Mini" (as ordered).

We developed a new gate position sensor that includes two sensors, one for absolute position and one for relative position. A rigid gear rack, attached to the gate along its centerline, passes through the gate position sensor enclosure. The gear rack rotates a gear that drives two position sensors: a potentiometer that gives absolute gate position to within 0.004 ft or 1.2 mm (based on a 4 ft span divided into 2^{10} or 1024 parts) and an optical encoder that gives relative gate position to within 0.003 ft or 0.9 mm regardless of span (based on diameter of gear). This interval can be cut in half with additional programming, but this does not seem to be needed at this time. In principle, any gate position sensor can be used. However, control of gate position change with a pulse-based optical encoder has proven easier and more reliable than driving the gate to a position with a continuous position sensor.

Automata has standard circuits for controlling gate motors. The circuit boards generally need to be set up to fit the particular gate motor housing being used, or packaged separately.

Communication between the RTUs and the computer is through 900 MHz spread-spectrum radios with ModBus protocol. These radios have a reliable range of about 5 miles but require line of site. Repeater sites are used to cover larger distance. Any "Mini" can be set up as both a local RTU and a repeater, at the same time.

Firmware

The “Mini” uses a 10-bit PIK microprocessor. Codes sent from *iFix* are used to request sensor information, change register values, and carry out functions. The “Mini” is programmed to accept signals in ModBus protocol. In the current application, a request for a change in gate position is sent as a binary signal. The first bit is a sign bit, which indicates up or down movement. The other seven bits represent the amount of gate movement (two’s complement). After this value is placed in a register, the relays are set to start moving the gate in the proper direction. For each count on the pulse counter, the register is decremented by one. When it reads zero, the gate motor is stopped. Run-on has never been more than one pulse. A timer limits overrun in the event of sensor failure. The absolute position sensor provides a check, and a backup, if the optical encoder fails. Use of this sensor for gate control has not yet been programmed. Adaptation of this system to gates without position sensors is discussed later.

SCADA Software

iFix by Intellution, Inc. is the SCADA package currently being used. The canal is set up for supervisory control in a standard manner. The *iFix* communication drivers are used to communication with the field sites through ModBus protocol over the spread-spectrum radios. Information from field sites is processed through a series of calculation blocks to yield information that is directly useful to the operator – for example, transducer voltage is converted to a depth and then the depth is adjusted for the location of the sensor to yield canal water depth.

iFix monitors canal water levels every minute and stores these values in a database. Standard *iFix* displays are used to graph the current water levels, flow rates, and gate positions for each check structure. In addition, the water level and flow setpoints are added to the display. These displays can be customized to suit the users’ needs. The canal operator can always manipulate gates manually, even when various automatic features are active. Database information and control actions taken are automatically archived for future evaluation.

The above functions are generally available with most commercial SCADA packages. However, not all are capable of the interface required for this canal automation system. SacMan and its interface to *iFix* is described next.

SacMan Software

SacMan monitors the canal by reading the *iFix* database through propriatary database calls, as shown in Figure 2. Based on this information, it determines whether control actions are needed. If a change in gate position is needed, SacMan writes a command to the *iFix* database. This “write” command prompts

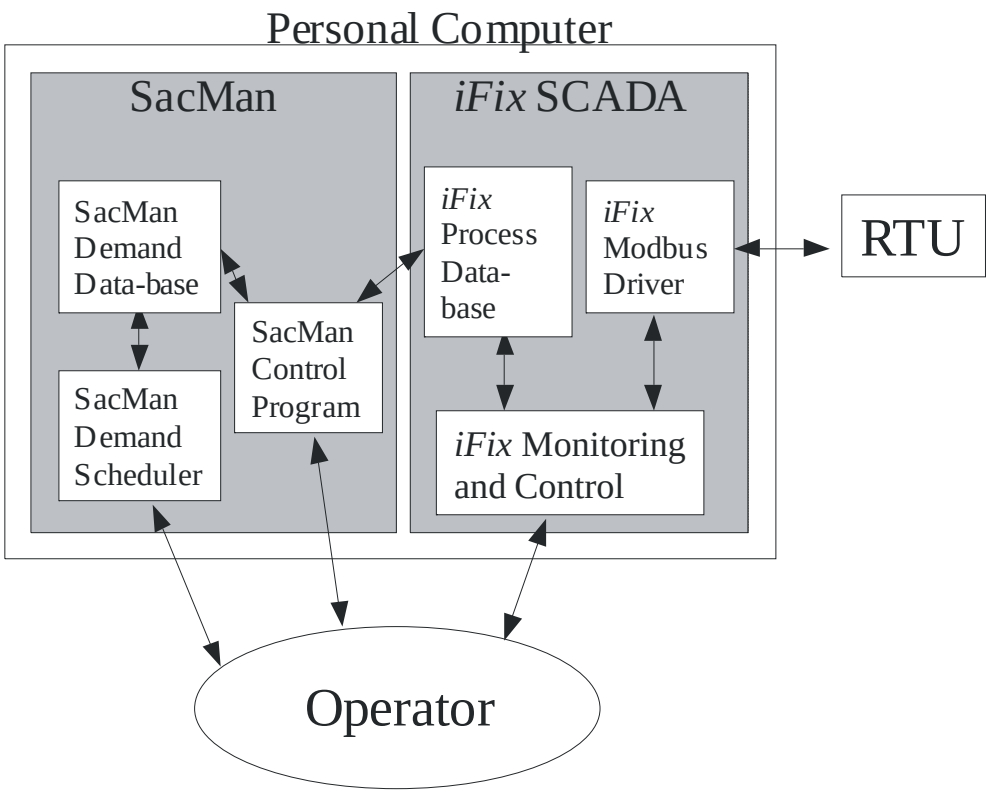

Figure 2. Layout of SACMAN canal automation control system software.

iFix to take action. *iFix* interprets the information that was written by SacMan and sends a command to one or more gates through the ModBus driver. These actions are archived for future evaluation. A schematic of the interface between the operator, *iFix* and SacMan is shown in Figure 2.

SacMan has three different levels of implementation: Manual control, local upstream water-level control, and centralized control, including downstream water-level control. Currently all control functions are performed at the central computer, except actual gate position changes, even though some of the control functions use local control logic. Centralized operations allow operators to monitor these processes and to provide archived data on control actions, which is useful in diagnosing the cause of problems.

Within these three main categories, there are various features that can be implemented. For standard manual control or upstream level control, no other features are required. Operators can add various features as they become familiar with SacMan. The first useful feature is the ability to increment or decrement the flow by an operator specified discharge. The second is the ability to set and maintain the flow rate at a particular structure, particularly canal headgates.

A series of alarms are available to alert the operator to any unusual circumstances, particularly when the canal is under automatic control. An out-of-bounds controller is available for sensing excessively high or low canal water levels. When such a conditions exists, an alarm is given and control reverts to automatic-upstream level control to protect the canal from failure. This mode is available even for manual control.

Another feature, the ability to route water orders through the canal system, requires a special user interface to SacMan. With this interface, the operator specifies the location, time, date and flow change (start, stop, or change). SacMan keeps track of the water being delivered throughout the system and computes the timing of check gate flow changes to accommodate the changes in demand. This can either be implemented by the operator or automatically by SacMan.

With multiple changes taking place, it is sometimes difficult for operators to keep track of flows within the system. If water orders are entered into the SacMan demand scheduler, SacMan will display the sum of the demands downstream from any check structure. This can then be compared to the actual flow rates. The operator can then get a quick sense of whether or not canal flows are in balance, even when under automatic control.

Pool volume is an important pool property and is used directly in many control schemes. The rate of change of pool volume is related to the mismatch between inflow and outflow, and thus is a measure of flow rate errors. This flow-rate error can be used by operators to adjust canal flows.

It has been shown that automatic control methods can become unstable if started suddenly. To avoid such problems, SacMan has a smooth start-up procedure. It assumes that the initial water levels are the water level setpoints and gradually adjusts them to the real set points. This ability to vary setpoints also allows the operator to schedule in the volume needed to raise canal water levels.

The SacMan options and features described above are summarized in Table 1.

APPLICATION AT MSIDD

The SacMan control system has been implemented on the WM canal at the Maricopa Stanfield Irrigation and Drainage District (MSIDD). The WM canal is a lateral canal with a capacity of 90 cfs (2.5 m^3/s). It was originally supplied with motorized gates. Relay boards, built by Automata, were installed in each gate motor. “Level-tel” water level sensors were installed in existing stilling wells along the upstream side of the gate frame. Automata’s new gate position sensors were also installed.

Table 1. SacMan control options and features.

Additional options and features	Overall (Feedback) Control Strategy		
	Manual Control	Local level control (upstream control)	Centralized level control (primarily far downstream control)
No other features	Okay	Okay, but requires manual control of headgate	Not allowed.
Flow control	At canal headgate (manually set value and/or adjusted with feedforward) (essentially requires gate position sensors)	At canal headgate (manually set value and/or adjusted with feedforward) (essentially requires gate position sensors)	Required at all gates (essentially requires gate position sensors)
Demand Scheduling (Feedforward control)	At any gate (one-time flow change or change in headgate flow setpoint)	At canal headgate (one-time flow change or change in flow setpoint)	At any gate (changes flow setpoint)
Incremental gate flow changes (manual control)	At any gate	At canal headgate	At any gate
Out-of-Bounds control	At any check gate	n.a.	At any check gate
Information on pool volume mismatches	Available	Available (but not useful)	Available (but currently not used)
Information on pool flow balance (downstream demands)	Available (essentially requires gate position sensors)	Available (essentially requires gate position sensors)	Available (but currently not used) (essentially requires gate position sensors)
Control start-up	n.a.	Available (ramps water level setpoints)	Available (ramps water level setpoints, requires feedforward?)
Scheduling of water level setpoint changes	n.a.	Available (does not require feedforward)	Available (requires feedforward?)
Alarms	Available	Available	Available

The feedback control logic used in this application is described by Clemmens and Schuurmans (2003). Application to ASCE test canal 1, which is based on the WM canal, is described in Clemmens and Wahlin (2003). The control logic converts water level errors into flow rate changes at each gate. SacMan determines the gate position change needed to achieve that flow control change and sends a gate position change to *iFIX*. The current control system determines new flow

setpoints for each check structure every 10 minutes. Gate position changes to achieve that flow rate at each check structure are performed every 2 minutes. If a large number of sites are being controlled, the flow control function may best be accomplished locally, depending on the complexity of the flow calculations.

Field Testing

The system was initially tested in the fall of 1999. Since then, we have converted from Automata's older RTU to the "Mini," the ModBus protocol was programmed into the "Mini" and Automata's base station firmware, we switched from FM to spread-spectrum radios, and the SACMAN software was totally reworked. These conversions were completed in the summer of 2001. Field studies were conducted in the fall of 2001 and the spring/summer of 2002. Some of these results were presented by Clemmens et al. (2002).

Most of the features in Table 1 have been implemented and tested. The remaining items have been implemented and will be tested in early 2003.

MSIDD is not currently considering upgrading their SCADA system, but will likely start replacing RTUs and radios in the near future.

IMPLEMNTATION AT CAIDD

As discussed in the introduction, CAIDD had lost reliable radio communication and decided to abandon their existing system and replace the RTUs, radios and SCADA software. The district decided to purchase the SacMan canal automation system from Automata, Inc. The plan was to convert all sites over the first year and to phase in various levels of automatic control. In the summer of 2002, 45 sites were upgraded, with the remaining sites to be upgraded early in 2003 (new budget year). As of February 2003, 102 sites were under manual supervisory control. The district expects to automate 108 out of roughly 130 potential sites.

CAIDD wanted the new system slightly customized and to mimic the operation of their old system. More specifically they wanted screens to display water levels along certain segments of each canal. Special commands were provided to allow operators to increment or decrement the flow at any control structure. This required a calibration factor in the software for each gate, since no gate position sensors are currently used at CAIDD. The gate calibration factor relates the gate-motor excitation time to approximate change in flow rate. Using this approach, the canal is operated with only water-level sensors at each check structure. Special routines were written to allow easy calibration of water level sensors and gate movement.

CAIDD opted for the manual system level (minimum capability), to get started. To fully automate or provide any of the flow calculation for the various flow control modes, gate position sensors will have to be added. Software and/or

hardware can be upgraded independently as required. Plans will be made in the near future for implementing various automatic control features. CAIDD is particularly interested in automatic controls for their main canals.

DISCUSSION

We have demonstrated that the SacMan control system is capable of controlling water levels in an irrigation canal. The basic components are working satisfactorily within a commercial SCADA package. The Automata hardware and firmware in the field is also performing as expected. Refinements are needed to make this system more failsafe so that it can run essentially unsupervised.

The SacMan control logic has been developed in a flexible manner so that a variety of control objectives can be attained. More details on the control approach can be found in Clemmens et al. (2002), Clemmens et al. (1997), and Clemmens and Schuurmans (2003).

Application to CAIDD poses many control challenges. Automatic upstream water-level controllers pass all errors in flow to the tail end of the canal. If there is no storage there, the last users get either too much or too little, or the excess is spilled. At CAIDD and MSIDD, only small infrequent spills are tolerated. Under manual control, this also happens, but with manually controlled check gates, some of the error in flow gets distributed to users all along the canal. SacMan currently provides information on flow and volume errors to assist the manual operator in adjusting canal inflow to minimize these problems.

Downstream water-level feedback control eliminates the problem of excesses and shortages. However it is recognized that sloping canal systems cannot automatically respond to large demand changes regardless of the control logic (i.e., open canals cannot perform like closed pipelines). Major flow changes need to be routed through the canal. With SacMan, this can be done manually by the operator or automatically by SacMan itself.

The downstream control logic moves errors in flow to the upstream end of the canal, adjusting the headgate flow to get the canal flows and volumes into balance. However, on many large canals, the headgate flow is not continuously adjustable. CAIDD receives water from the Central Arizona Project (CAWCD), which can only be changed twice per day. Here, what was a downstream control logic has to be adjusted to a more central control logic, taking this upstream constraint into account. SacMan's flexible approach to control can make this happen. Further, information on flow and volume mismatches provided by SacMan help a manual-control operator in deciding how much water to order from CAWCD.

REFERENCES

Bautista, E., A.J. Clemmens, and T.S. Strelkoff. 2002. Routing demand changes with volume compensation: an update. p. 367-376. In Proceedings, USCID/EWRI Conference on Energy Climate and Water – Issues and Opportunities for Irrigation and Drainage, San Luis Obispo, CA 10-13 July.

Clemmens, A. J., E. Bautista, and R. J. Strand. 1997. Canal automation pilot project, Phase I Report, WCL Report #22, U.S. Water Conservation Laboratory, Phoenix, AZ.

Clemmens, A. J., E. Bautista, R. J. Strand, and B. T. Wahlin. 2001. Canal automation pilot project: Phase II Report. *WCL Report 24*. U.S. Water Conservation Lab., Phoenix, AZ

Clemmens, A. J. and J. Schuurmans. 2003. Simple optimal downstream feedback canal controllers: Theory. *J. of Irrigation and Drainage Engineering*. Accepted.

Clemmens, A.J., Strand, R.J., Feuer, L. and Wahlin, B.T. 2002. Canal Automation system demonstration at MSIDD. p. 497-506 In Proceedings, USCID/EWRI Conference on Energy Climate and Water – Issues and Opportunities for Irrigation and Drainage, San Luis Obispo, CA 10-13 July.

Clemmens, A. J. and B. T. Wahlin. 2003. Simple optimal downstream feedback canal controllers: ASCE test case results. *J. of Irrigation and Drainage Engineering*. Submitted.

Delft Hydraulics 2000. SOBEK flow module technical reference guide, version 2.2, Delft, The Netherlands.

ROUTING DEMAND CHANGES WITH VOLUME COMPENSATION: AN UPDATE

Eduardo Bautista[1]
Albert J. Clemmens
Theodor S. Strelkoff

ABSTRACT

Using the gate-stroking method, this paper shows that a complex open-channel flow feedforward control problem can be treated as a series of linearly additive single flow-change control problems. A key element of this approach is determining the initial conditions for each single flow-change problem. An inadequate choice of initial conditions will result in under or overestimation of the canal storage volume change needed for the new steady-state conditions. These findings provide support to a simple feedforward control scheme based on volume compensation and time delay. An example is used to demonstrate that the simple scheduling approach is nearly as effective in controlling water levels as the complex gate-stroking approach.

INTRODUCTION

Bautista and Clemmens (1998) proposed a simple method for routing known demand changes through an open-channel water delivery system (the feedforward control problem) using the concept of volume compensation. Volume compensation refers to the volume of water that needs to be added or removed from a canal pool in going from an assumed initial steady-state to a desired new steady-state condition. That volume is delivered through a small number of step changes in inflow rate. The magnitude of those changes depends on estimates of the time needed for the flow changes to travel the length of the channel (the travel delay time τ). A key problem of volume compensation is determining this delay, and thus, the timing of the inflow changes.

Simulation studies have demonstrated the application of the volume-compensating feedforward control method to specific water delivery systems (Bautista and Clemmens, 1998; Bautista and Clemmens, 1999a). Additional research is needed to generalize those results and to identify limitations of the method. A recent study used gate-stroking (Wylie, 1969) and volume compensation to examine the characteristics of feedforward control solutions for single-pool canals of uniform geometry (Bautista et al, 2002). The gate-stroking

---

[1] Respectively, Research Hydraulic Engineer, Director, and Research Hydraulic Engineer. USDA-ARS U.S. Water Conservation Laboratory, 4331 E. Broadway Rd., Phoenix AZ 85040.

method solves the governing equations of unsteady open-channel flow inversely in space. The study considered a wide range of canal geometries and flow configurations. The gate-stroking method can fail to find a solution or can produce a solution requiring discharges exceeding the canal capacity or flow reversal under conditions where the time needed to supply the canal volume change is small relative to the disturbance wave travel time. Volume compensation offers a solution under those conditions and the resulting water level control is satisfactory. There are also conditions under which upstream flow changes travel with little attenuation and, therefore, the inflow hydrograph computed by gate-stroking nearly matches the desired outflow hydrograph. Under those conditions, a volume-compensating schedule can be easily identified and will produce water level control comparable to that obtained with gate-stroking.

Bautista and Clemmens (1998) outlined a volume-compensation strategy for multi-pool canal systems subject to multiple changes, but provided no justification for the approach. Recent tests, not reported here, with canal systems subject to multiple flow changes have resulted in adequate control for some demand changes but less adequate for others, suggesting problems with the original approach. The purpose of this paper therefore is to reexamine the basic concept used and to refine the method.

MULTI-POOL SYSTEMS: ADDITIVITY OF SOLUTIONS

The volume-compensating feedforward control method for multi-pool systems suggested by Bautista and Clemmens (1998) treats the multiple flow change problem as a series of linearly additive single flow change problems. Because the governing equations of unsteady open-channel flow are nonlinear, one can not expect this assumption to hold in general. This section analyzes the linearity of feedforward control solutions, using the full Saint Venant equations (the gate-stroking method) under a specific set of flow conditions. Determining conditions under which gate-stroking solutions are additive should suggest conditions under which the feedforward control problem can be treated as a linear problem.

This analysis uses one of the test cases proposed by the ASCE Task Committee on Canal Control Algorithms (Clemmens et al, 1998), ASCE Test Canal 2, Scenario 2. Canal characteristics and test details are given in Table 1. The canal is 28 km long and relatively flat. The canal's geometry, together with the specified flow conditions, results in a low Froude number for all pools. All pools are entirely in backwater for the initial flow conditions. This means that disturbances can travel up and down the canal for a long time and, thus, flow levels can oscillate for a long time. In a previous study, a finite-difference gate-stroking model for multiple pools (Bautista et al. 1997) was used to compute a feedforward flow schedule for this test case and was shown to produce satisfactory water level control (Bautista and Clemmens, 1999b). In this paper,

rather than processing all demand changes simultaneously as was done in that reference, each flow change was processed individually, as is described next.

Table 1. ASCE Canal Control Test Case 2-2: geometric[§] and flow data

Pool	Pool Length (km)	Pool Bottom Width (m)	Pool Target Downstream Depth (m)	Initial Pool Inflow (m^3/s)	Initial Offtake Flow (m^3/s)	Offtake Flow Change (m^3/s)
1	7.0	7.0	2.1	2.7	0.2	1.5
2	3.0	7.0	2.1	2.5	0.3	1.5
3	3.0	7.0	2.1	2.2	0.2	2.5
4	4.0	6.0	1.9	2.0	0.3	
5	4.0	6.0	1.9	1.7	0.2	
6	3.0	5.0	1.7	1.5	0.3	0.5
7	2.0	5.0	1.7	1.2	0.2	1.0
8	2.0	0.6	1.7	1.0[‡]	0.3	4.0

[§] For all pools, bottom slope = 0.0001, side-slope = 1.5, and Manning n = 0.02

[‡] Flow past the canal's tail end is 0.7 m^3/s.

In the example, flows change at six of the eight turnouts three hours after the beginning of the test[2]. Since all demand changes take place at the same time, it is clear that the change in the most-downstream pool has to be routed first (i.e., requires the earliest change in inflow at the head of the canal). Initial conditions for that sub-problem are, simply, the time-zero initial conditions (discharges and levels). The second demand change to be routed is that originating in the penultimate pool, 7. Assuming a new steady-state as a result of the demand change in pool 8, initial flows for this second sub-problem are the sum of the initial flows and the demand change for the first sub-problem (a flow increase of 4.0 m^3/s in all pools). Initial water levels depend on these flows and the prescribed downstream target level. The same logic can be applied to determine the initial conditions of all remaining flow changes.

Solutions were combined for each check structure by adding all *flow increment* hydrographs for that particular check structure to its time-zero initial discharge. As an example, for the head gate, the time-zero initial discharge is 2.7 m^3/s (table 1). Since six individual offtake flow changes need to be processed, six different hydrographs are computed for the head gate. The flow increment hydrograph

---

[2] The Test Case originally requires changes to occur two hours after the beginning of the test (Clemmens et al., 1998). This time was modified to allow the initial flow changes at the head gate to occur at a time greater than time zero.

resulting from each demand change is the difference between the gate-stroking solution and the initial conditions for that particular sub-problem. Since demand changes at a location do not affect check flows downstream from that location (once unsteadiness caused by the change has dissipated), the number of flow increment hydrographs that needs to be combined decreases as the check is located farther downstream. For example, for the check structure between pools 6 and 7, the combined hydrograph is simply the solution to the individual demand change in pool 8 plus the flow increment hydrograph due to the change in 7.

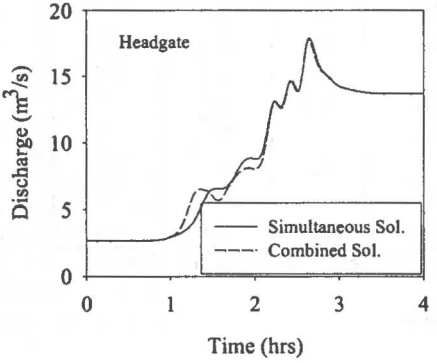

Figure 1. Gate-stroking inflow hydrographs for ASCE Test Case 2-2: simultaneous and combined solutions

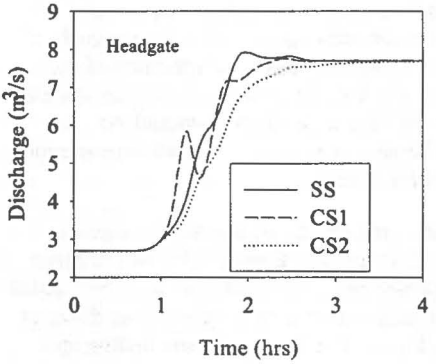

Figure 2. Gate-stroking inflow hydrographs for two offtake flow change problem: simultaneous (SS) combined (CS1, CS2) solutions

Figure 1 compares the linearly combined and nonlinear simultaneous solutions obtained for the head gate. The solutions are nearly in agreement for most of the hydrograph. The mismatch in the initial part of the hydrograph suggests that the difference is related to the demand change or changes at downstream pools, since those changes would require the earliest flow changes at the head gate.

To understand the above mismatch, gate-stroking solutions were developed for a simpler problem, consisting of the demand changes in pools 7 and 8 only. Two different combination solutions (CS1, CS2) for the head-gate are shown in Figure 2, along with the simultaneous solution (SS). Solution CS1 is based on the same assumption used in the preceding analysis, namely that in processing the demand change in pool 7, prior changes (i.e., the change from pool 8) have reached steady-sate conditions. In contrast, solution CS2 assumes that the prior change in pool 8 has not taken place. That change is larger than the initial canal flow so it is likely that the resulting steady state will not be reached until after the change in

pool 7 takes place. Because initial conditions are difficult to identify, the same initial conditions used to process the change in pool 8 were applied to process the demand change in pool 7. In comparison with the hydrograph from the simultaneous solution (SS), the CS1 hydrograph shows a large flow rate increase and then a large decrease. Those oscillations are not present in the CS2 hydrograph and, the hydrograph's shape is closer to the simultaneous solution. Notice however that the volume of water delivered to the canal with CS2 is less than that delivered by the simultaneous solution (the volume can be calculated by integration of the hydrograph with respect to time). This volume mismatch should cause water levels to temporarily deviate from their target value. Clearly, the steady conditions assumed by the original approach, CS1, result in an incorrect estimation of the transient response, however they do account more accurately for the needed volume change (the resulting volume is in close agreement with the volume delivered by the simultaneous solution hydrograph).

Determining the initial of conditions of each sub-problem is easy for the Test Case and the order in which each demand change needs to be routed is evident. If the demand changes take place at different times, determining the order in which they need to be routed, and the resulting impact on initial conditions of subsequent flow changes, is less obvious. This problem was solved as follows: individual gate-stroking solutions were generated for a set of demand changes (with changes in the pools at different times) using the time-zero initial conditions for each individual sub-problem. The solution requiring the earliest flow change at the head gate was then assumed the first to be routed. The final conditions resulting from this first demand change were then used to define new initial conditions for the remaining set of demand changes, from which the next demand change to be routed was identified. The process was continued until all demand changes were processed. This approach was applied to modified versions of the Test Case, with demand changes taking place at different times. Results of these tests, which are not presented here, again showed reasonable agreement between the hydrographs computed by routing all changes simultaneously and those computed by routing the changes individually and then combining them.

These results show that the complex feedforward control problem, consisting of multiple pools and flow changes, is somewhat linear. Difficulties in applying this approach are likely to be encountered when dealing with very large flow rate changes, as such changes would result in long-lasting unsteady flow. In such cases, one could consider interpolation, to estimate a more representative set of initial conditions for a given flow change. While that approach may reflect better the dynamics of the transient, it will not satisfy its volume compensation requirements. The simpler and more consistent approach is to assume that each individually routed demand change completely defines the initial conditions for the next change.

SIMPLE VOLUME COMPENSATION SOLUTION

A volume-compensating feedforward control schedule for a single demand change in a single-pool canal can be obtained by dividing the pool's volume change ΔV by the travel delay τ (Bautista and Clemmens, 1998; Bautista et al. 2002):

$$\Delta Q_1 = \frac{\Delta V}{\tau} \tag{1}$$

ΔQ_1 represents the flow rate change at the upstream check structure. The desired final steady-state check discharge, Q_f, is the sum of the initial steady-state check discharge, Q_0, and the demand change, Δq_d. Depending on the value of τ, $Q_0 + \Delta Q_1$ may not match Q_f. Therefore, a second check-flow change, ΔQ_2, will likely be needed to adjust the check discharge to Q_f.

$$\Delta Q_2 = \Delta q_d - \Delta Q_1 \tag{2}$$

For the range of conditions examined in Bautista et al (2002), suggested bounds for τ are:

$$\tau_{DW} \le \tau \le \tau_{\Delta V} \tag{3}$$

τ_{DW} is a delay estimate based on dynamic wave theory,

$$\tau_{DW} = \frac{L}{v_0 + c_0} \tag{4}$$

where L is the canal length, v_0 the average flow velocity under the initial flow conditions, and c_0 average celerity under the initial flow conditions. τ_V in (3) is a delay based on the time needed to supply ΔV at a rate equal to the demand change:

$$\tau_{\Delta V} = \frac{\Delta V}{\Delta q_d} \tag{5}$$

In cases where the wave introduced by upstream flow changes travels with little attenuation, τ_V can also be interpreted as a kinematic shock travel time. With τ in (1) given by (5), $\Delta Q_2 = 0$.

Bautista and Clemmens (1988) computed τ using kinematic and dynamic wave theory. That approach requires estimates of the pool length affected by backwater for the given flow conditions. When applied to the Test Case, this approach proved inappropriate as it yielded discharge changes at the check structures

greater than the canal capacity as a result of very small delay values. A simpler and more conservative approach was used here, by using (5) as the delay. As noted, this reduced the inflow schedule to a single change,

$$\Delta Q = \Delta q_d \tag{6}$$

and, more importantly, bounded the magnitude of the check-flow change.

If the canal has multiple pools and a single demand change occurs in pool *J*, then a schedule of inflow changes needs to be computed for all check structures upstream from pool *J*. The schedule of check *J* (pool *J*'s upstream check) is a function of pool *J* only. For pool *J-1*, the schedule is a function of the sum of volume changes and accumulated delays of pools *J-1* and J. For *j*-th check structure, the expression for the discharge change is (Bautista and Clemmens, 1998):

$$\Delta Q_j = \frac{\sum_{k=j}^{J} \Delta V_k}{\sum_{k=j}^{J} \Delta \tau_k} \tag{7}$$

This equation applies to the general case in which τ in (1) is obtained by any reasonable procedure. In such case, the timing for ΔQ_1 for structure j is given by:

$$t(\Delta Q_1) = t_d - \sum_{k=j}^{J} \Delta \tau_k \tag{8}$$

while the timing for the second check-flow change, $t(\Delta Q_2)$, is the demand change time, t_d. If the delays are given by (5), then application of (7) yields simply Δq_d (Eq. 6) while $\Delta Q_2 = 0$. For a canal subject to multiple demand changes, each change has to be processed separately. The resulting time sequence of ΔQ_js then defines the feedforward control schedule for check structure *j*.

Bautista and Clemmens (1998) applied this approach to situations with multiple demand changes by assuming that a pool's flow was equal to the time zero discharge plus all demand changes ordered prior to the time of the requested Δq_d. Only demand changes in the pool being processed or in pools downstream from it were included in this sum. That approach was modified to properly identify the initial conditions that need to be used to process each individual demand change, as discussed in the previous section. However, instead of using gate-stroking solutions, accumulated delays (the denominator of (7)) were used to determine the order in which individual demand changes needed to be routed.

The head-gate inflow hydrograph obtained with this method is shown in Figure 3 along with the hydrograph obtained via gate-stroking. It should be noted that the

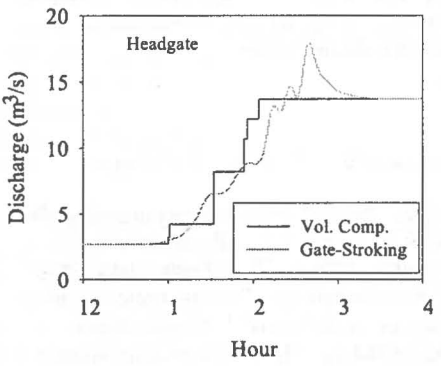

Figure 3. Volume-compensating and gate-stroking inflow schedules

final steady-state conditions of the test case are close to the canal's maximum discharge capacity (Clemmens et al., 1998) and, therefore, the gate-stroking solution exceeds temporarily that maximum value.

Water level control produced with the gate-stroking and volume-compensation feedforward control schedules are shown in Figures 4. These results were computed with the unsteady flow simulation model CanalCAD (Holly and Parrish, 1995). The simulator used the control schedules to determine check flow rate setpoints as a function of time and internally computed a gate position for the new flow setpoint. Flow through the gravity offtakes varied in response to water level fluctuations in the canal.

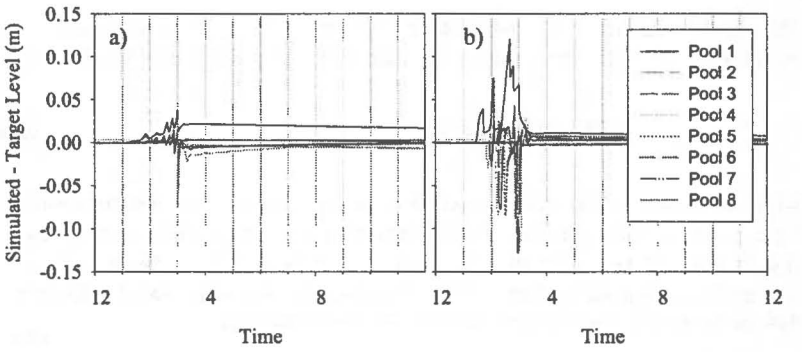

Figure 4. Difference between simulated and target water levels with a) gate-stroking and b) volume-compensating feedforward control schedules

Three things are evident from Figure 4. First, water-level deviations were much larger with the simple approach (Figure 4b) than with gate-stroking (Figure 4a). Second, despite these large deviations, near-steady-state conditions were achieved shortly after the time at which the offtake flow changes occur. Lastly, in both cases the deviations were small relative to the target levels (Table 1).

Table 2. Maximum Absolute Error (MAE) and Integrated Average Error (IAE) for test case, from simulation with gate-stroking and volume compensating solutions

	Pool 1	Pool 2	Pool 3	Pool 4	Pool 5	Pool 6	Pool 7	Pool 8
Gate-Stroking								
MAE	1.8%	0.8%	1.5%	0.4%	0.4%	0.7%	1.1%	4.5%
IAE	0.8%	0.2%	0.1%	0.1%	0.1%	0.1%	0.1%	0.3%
Volume-Compensation								
MAE	5.7%	4.0%	3.7%	4.4%	4.4%	5.2%	7.6%	7.2%
IAE	0.6%	0.1%	0.2%	0.1%	0.1%	0.3%	0.2%	0.2%

Two performance measures recommended by the ASCE Task Committee on Canal Control Algorithms (Clemmens et al, 1998) were computed for these tests. The Maximum Absolute Error (MAE) is a measure of the maximum water level deviation relative to the target. The Integrated Average Error is a measure of the average absolute error relative to the target. Results are summarized in Table 2. The MAE for the simple feedforward control is as much as ten times greater than with gate-stroking, however these errors are short lived and have little impact on the average performance. The average error for all pools with both feedforward control methods is less than 1% of the target level.

CONCLUSIONS

For the example presented, similar gate-stroking results were obtained by processing all demand changes simultaneously and by treating the problem as a linear combination of single-flow change problems. The analysis assumed a succession of steady states and, thus, differences in results were due to unsteady flow effects not accounted for in defining initial conditions for individual flow change problems. Results show that even under conditions where strong unsteady effects would persist for long times, reasonable results can be obtained by assuming that each demand change creates a new set of steady initial conditions for the next flow change to be routed. Such an approach also assures volume compensation. It has been previously shown that a simple feedforward control method based on volume compensation can produce reasonable water level control in single-pool canals subject to a single demand change. A strategy was developed to apply the volume compensation method to multiple-pool canals subject to multiple flow changes. The resulting water level control over the test period was, on the average, comparable to that obtained with gate-stroking. This

suggests that the proposed volume compensation approach is both practical and effective.

REFERENCES

Bautista, E., A. J. Clemmens, and T. S. Strelkoff. 1997. Comparison of numerical procedures for gate stroking. *J. Irrig. and Drain. Eng.* 123(2):129-136.

Bautista, E. and A. J. Clemmens. 1998. An open-loop control scheme for open-channel flow. p. 1852-1857. In *Int. Conf. on Water Resources Engineering Proceedings*, Memphis, TN. Aug. 3-7, 1998.

Bautista, E. and A. J. Clemmens. 1999a. Computerized anticipatory control of irrigation delivery systems. p. 359-373. In *Proc. USCID Workshop on Modernization of Irrigation Water Delivery Systems*, Scottsdale, AZ. Oct. 17-21, 1999.

Bautista, E. and A. J. Clemmens. 1999b. Response to the ASCE Task Committee Test Cases to Open-loop Control Measures. *J. Irrig. and Drain. Eng.* 125(4): 179-188.

Bautista, E., T. S. Strelkoff, and A. J. Clemmens. 2002. General characteristics of solutions to the open-channel flow feedforward control problem. *J. Irr & Drain. Eng.* (Submitted)

Clemmens, A.J., T.F. Kacerek, B. Grawitz, and W. Schuurmans. 1998. Test cases for canal control algorithms. J. Irr & Drain. Eng. 124(1): 23-30.

Holly Jr., F.M. and J.B. Parrish. 1995. CanalCAD: Dynamic flow simulation in irrigation canals with automatic gate control. Iowa Institute of Hydraulic Research. Iowa City, Iowa.

Wylie, E.B. 1969. Control of transient free-surface flow. *J. Hyd Div. ASCE.* 95(HYD1): 347-361.

General Characteristics of Solutions to the Open-Channel Flow, Feedforward Control Problem

E. Bautista, A.M.ASCE[1]; T. S. Strelkoff, M.ASCE[2]; and A. J. Clemmens, M.ASCE[3]

Abstract: A dimensionless formulation of the open-channel flow equations was used to study the feedforward control problem for single-pool canals. Feedforward inflow schedules were computed for specified downstream demands using a gate-stroking model. The analysis was conducted for various design and operational conditions. Differences in the shape of the computed inflow hydrographs are largely related to the volume change resulting from the transient, the time needed to supply this volume, and the time needed by the inflow perturbation to travel down the canal. The gate-stroking method will fail to produce a solution or the solution will demand extreme and unrealistic inflow variations if the time needed to supply the canal volume change is much greater than the travel time of the upstream flow change. As an alternative, a simple feedforward-control flow schedule can be developed based on this volume change and a reasonable delay estimate. This volume compensating schedule can deliver the requested flow change and keep water levels reasonably close to the target under the range of conditions tested.

DOI: 10.1061/(ASCE)0733-9437(2003)129:2(129)

CE Database subject headings: Open channel flow; Flow control; Canals.

Introduction

Development of practical feedforward control strategies that can be applied to a wide range of canal systems and the design of canals that are amenable to feedforward control actions require a thorough understanding of the control characteristics of canals as a function of their physical characteristics and the range of demands imposed on them. Wylie (1969) developed a solution to feedforward control problems, which he named gate-stroking, by solving the governing equations of open-channel flow inversely in space. Chevereau (1991) studied the effect of channel length on the shape of input hydrographs computed with a finite-difference gate-stroking model. Deltour (1992) examined the pool volume changes as a function of changes in flow rate and the target downstream depth (water level setpoint). He developed a series of diagrams for a specific pool that illustrates how pool volume must be adjusted to reach a new steady-state flow under either upstream or downstream control. Using a dimensionless formulation of the de Saint Venant equations, Strelkoff et al. (1998) examined the response of canals to upstream perturbations as a function of canal geometry and downstream boundary conditions. With the nondimensional formulation, a large range of dimensioned canals can be studied with a single simulation. The study concluded that the shape of the backwater curve is relatively constant for a given dimensionless downstream target depth and channel length (i.e., insensitive to variations in dimensionless bottom width, side slope, and Froude number). Further, they also determined that the downstream boundary condition (e.g., weir, underflow gate, etc.) and backwater depth had a significant impact on how fast an upstream disturbance travels downstream. Bautista et al. (1996) presented a limited analysis of the general features of gate-stroking solutions for single-pool canal systems. That study suggested that the Froude number under the initial flow conditions was an important factor influencing the shape of the computed hydrograph.

This paper extends Bautista's et al. (1996) analysis of the feedforward control characteristics of canals. The study analyzes the interaction among various design variables on the gate-stroking solutions. Given the limitations of the gate-stroking method, the paper also examines the behavior of downstream water levels when subjected to a simpler feedforward control strategy. The objective is to identify general conditions under which simple anticipatory canal control strategies will yield reasonable control and conditions under which more sophisticated approaches may be required.

Approach

The first part of this paper analyzes the general behavior of inverse (gate-stroking) solutions as a function of canal physical characteristics. The second part compares the effectiveness of the water level control produced by the gate-stroking solution and by a simple feedforward control action based on a simple delay.

Inverse calculations were carried out with an implicit nonlinear finite-difference gate-stroking model (Bautista et al. 1997). Simulations of the response to these hydrographs were computed with the unsteady flow model CanalCAD (Holly and Parrish 1995). Both the finite-difference gate-stroking model and CanalCAD solve the governing equations based on the four-point Pre-

[1]USDA-ARS U.S. Water Conservation Laboratory, 4331 E. Broadway Rd., Phoenix, AZ 85040.

[2]Research Hydraulic Engineer, USDA-ARS U.S. Water Conservation Laboratory, 4331 E. Broadway Rd., Phoenix, AZ 85040.

[3]Director, USDA-ARS U.S. Water Conservation Laboratory, 4331 E. Broadway Rd., Phoenix, AZ 85040.

Note. Discussion open until September 1, 2003. Separate discussions must be submitted for individual papers. To extend the closing date by one month, a written request must be filed with the ASCE Managing Editor. The manuscript for this paper was submitted for review and possible publication on November 20, 2001; approved on February 28, 2002. This paper is part of the ***Journal of Irrigation and Drainage Engineering***, Vol. 129, No. 2, April 1, 2003. ©ASCE, ISSN 0733-9437/2003/2-129–137/$18.00.

issman finite-difference scheme. A time weighting factor of 0.7 was used in both sets of calculations.

To generalize results, inverse calculations were carried out with the governing equations expressed in dimensionless form. Equations were nondimensionalized using the system of variables proposed by Strelkoff and Clemmens (1998)

$$A^* = \frac{A}{Y_R^2}; \quad Q^* = \frac{Q}{Q_R}; \quad x^* = \frac{x}{X_R}; \quad t^* = \frac{t}{T_R} \tag{1}$$

where A=flow area; Q=discharge; x=distance along the channel; t=time; Y_R=reference length for all transverse canal dimensions; Q_R=reference discharge; X_R=reference length for longitudinal dimensions; and T_R=reference time. The asterisk denotes the dimensionless counterpart of a dimensioned variable. The canal's design flow Q_n (or some other convenient flow value) is used to define Y_R and Q_R. Reference depth Y_R is set equal to normal depth (y_n) for Q_n. Thus, y_n^*, the dimensionless normal depth at the design flow, is equal to unity. The dimensionless area at normal depth or aspect ratio, A_n^*, serves to define Q_R in terms of the design flow

$$A_n^* = \frac{A_n}{Y_R^2} \tag{2}$$

$$Q_R = \frac{Q_n}{A_n^*} \tag{3}$$

If the channel is trapezoidal, $A_n^* = b^* + z$, with b^* the dimensionless bottom width (b/Y_R) and z the side slope (horizontal/vertical). It follows from Eq. (3) that $Q_n^* = A_n^*$ and that the dimensionless normal velocity at design flow $v_n^* = 1$. Reference length in the direction of flow X_R is given by

$$X_R = \frac{Y_R}{S_{0_R}} \tag{4}$$

where S_{0_R}=bottom slope at a reference section; and X_R serves to define the dimensionless canal length $L^* = L/X_R$. A dimensionless formulation of the de Saint Venant equations that is similar in appearance to the dimensional formulation can be obtained by requiring that

$$\frac{X_R Y_R^2}{T_R Q_R} = 1 \tag{5}$$

where T_R=reference time. This relationship serves to define the value of T_R. The dimensionless expressions for the governing equations are then

$$\frac{\partial Q^*}{\partial x^*} + \frac{\partial A^*}{\partial t^*} + q_0^* = 0 \tag{6}$$

$$\frac{1}{g^*}\left[\frac{\partial Q^*}{\partial t^*} + \frac{\partial}{\partial x^*}\left(\frac{Q^{*2}}{A^*}\right) + u_0^* q_0^*\right] + A^*\left[\frac{\partial h^*}{\partial x^*} + \frac{Q^{*2} n^{*2}}{c_u^{*2} A^{*2} R^{*4/3}}\right] = 0 \tag{7}$$

where g^* and c_u^*=dimensionless parameters; h^*=dimensionless water surface elevation; R^*=dimensionless hydraulic radius; q_0^*=dimensionless lateral outflow per unit length; u_0^*=dimensionless longitudinal velocity component of the lateral flow; and n^*=relative Manning n, $n^* = n/n_R$ with n_R the Manning n at a representative canal section. In a uniform canal, n^* (and $S_0^* = S_0/S_{0_R}$) is equal to unity. Expressions for g^* and c_u^* are the following:

Table 1. Hypothetical Dimensioned Channel Characteristics as Function of F_n for Channel with $b^*=5$, $z=1.5$, $Y_R=1.5$ m, and $n=0.018$

F_n	g^*	Q_n (m^3/s)	S_{0_R}	X_R (m)	T_R (h)
0.1	123.1	5.1	3.3E-05	45,737	36.74
0.15	54.7	7.6	7.4E-05	20,327	10.89
0.2	30.8	10.1	1.3E-04	11,434	4.59
0.3	13.7	15.2	3.0E-04	5,082	1.36
0.4	7.7	20.2	5.2E-04	2,859	0.57
0.5	4.9	25.3	8.2E-04	1,829	0.29
0.6	3.4	30.3	1.2E-03	1,270	0.17
0.7	2.5	35.4	1.6E-03	933	0.11
0.8	1.9	40.5	2.1E-03	715	0.07
0.9	1.5	45.5	2.7E-03	565	0.05

$$g^* = \frac{1}{F_n^2\left(\frac{A_n^*}{B_n^*}\right)} \tag{8}$$

$$c_u^* = \frac{1}{R_n^{*2/3}} \tag{9}$$

where F_n=Froude number; B_n^*=dimensionless top width; and R_n^*=dimensionless hydraulic radius with the subscript n denoting in all cases normal depth conditions for the design flow. Standard unsteady flow models based on dimensional governing equations similar in form to Eqs. (6) and (7) can be nondimensionalized by replacing the gravitational constant g with g^* and the units factor for the Manning equation c_u with c_u^*. Expressions for other variables in Eqs. (6) and (7) are provided by Strelkoff and Clemmens (1998). A family of hydraulically similar canals is defined by the particular combination of geometric variables, b^*, z, and dimensionless canal length (L^*) and F_n.

Note that from the definition of wave celerity c (Henderson 1966)

$$c = \sqrt{g\frac{A}{B}} \tag{10}$$

the celerity at normal depth for the design flow, c_n, is the same for all canals with the same aspect ratio. In Eq. (10), B represents the top width. Its dimensionless counterpart, c_n^*, is simply the inverse of F_n

$$c_n^* = \frac{c_n}{v_n} = \frac{1}{F_n} \tag{11}$$

Gate-Stroking Solutions

Effect of Froude Number F_n

The analysis is restricted to single-pool canals of uniform cross section and slope. The effect of variable F_n on the gate-stroking solutions is analyzed first for canals with dimensionless characteristics $b^*=5$, $z=1.5$, and $L^*=1.0$. The impact of b^*, z, and L^* will be examined later. With this choice of b^* and z, A_n^* and Q_n^* are both equal to 6.5 [Eq. (3) and comment following]. For illustration purposes, hypothetical dimensioned channels (Strelkoff and Clemmens 1998) were computed by assuming $Y_R=1.5$ m and $n=0.018$ (Table 1). The dimensioned channels have identical

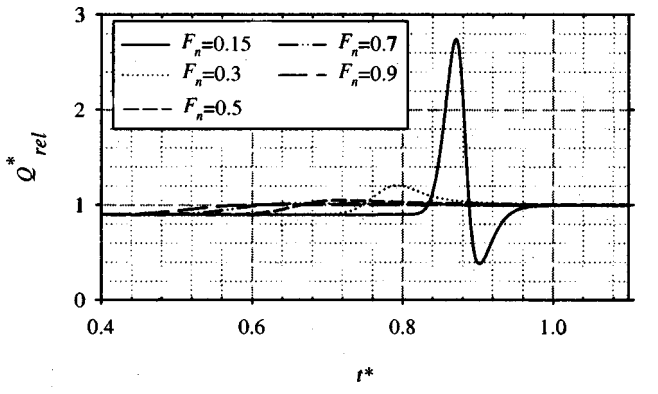

Fig. 1. Variation in gate-stroking solutions with F_n ($L^*=1$, $b^*=5$, $z=1.5$, $y^*_{st}=1.25$)

cross sections at normal depth (area, top width, wetted perimeter, etc.) but differ in length, slope, design capacity, etc. as a function of F_n.

The example seeks to route a single stepwise change in downstream demand ΔQ^*_d in a channel that is initially under steady state, while keeping the downstream water depth y^* at the setpoint $y^*_{st}=1.25$ (1.25 times the design flow normal depth). Initial inflow Q^*_o is 90% of Q^*_n (5.85); ΔQ^*_d is 10% of Q^*_n (0.65); and the time at which the demand change takes place, t^*_d, is 1.0. In the following paragraphs, the subscript *o* denotes the value of the variable under the initial flow conditions. To facilitate the discussion, results are presented in terms of relative discharge Q^*_{rel}, which is related to Q^* as follows:

$$Q^*_{\text{rel}}=\frac{Q^*}{A^*_n}=\frac{Q}{Q_n} \tag{12}$$

Therefore, the initial and final relative inflow Q^*_{rel} are 0.9 and 1.0, respectively.

Numerical experiments were conducted to determine an appropriate combination of spatial and temporal increments, Δx^* and Δt^*, respectively, in the finite difference solutions. Nearly identical results were obtained with $\Delta x^*\leqslant 0.025$ and, thus, 0.025 was used as the space increment in all subsequent calculations. Δt^* was determined by enforcing a dimensionless Courant condition close to 1, based on the selected Δx^* and F_n (and thus c^*_n) to minimize numerical damping effects on the solution.

For the proposed flow conditions, the desired outflow hydrograph becomes physically more difficult to produce as F_n decreases, requiring more extreme variations in the computed inflow hydrograph (Fig. 1). Peak upstream Q^*_{rel} at $F_n=0.15$ is nearly three times the canal capacity, which is an unacceptable solution in practice. For $F_n<0.15$, no solution could be found as the execution was terminated due to the calculation of negative A^* values. This implies that for $F_n<0.15$, inflow cannot be varied in any way to produce the desired output. Peak inflow decreases rapidly with increasing F_n and is nearly equal to the desired final demand for $F_n\geqslant 0.5$. Results also indicate that the transient needs to be initiated ever earlier, in dimensionless time, with increasing F_n. If the duration of the gate-stroking computed transient (which will be denoted by τ^*_{GS}) is defined as the time between the initial upstream flow change and the time at which the demand change occurs, then from Fig. 1, τ^*_{GS} is about 2.9 times greater for $F_n=0.9$ than for $F_n=0.15$ (Table 2).

It is useful to analyze the role of F_n in determining the solutions of Fig. 1. Initial conditions used to solve Eqs. (6) and (7) are nearly the same for each value of F_n, and boundary conditions are exactly the same. Thus, differences in the computed hydrographs can be attributed mostly to the parameter g^* in Eq. (8). g^* increases as $1/F_n^2$, and this magnifies the relative contribution of the local and convective acceleration terms in Eq. (7).

Table 2. Volume Change and Delay Characteristics of Computed Transient for Selected Values of F_n

	F_n				
Variable	0.15	0.3	0.5	0.7	0.9
	(a) Dimensionless values				
τ^*_{GS}	0.19	0.29	0.40	0.50	0.56
V^*_o	6.93	6.90	6.83	6.71	6.54
ΔV^*	0.29	0.29	0.30	0.30	0.32
$\tau^*_{\Delta V}$	0.44	0.44	0.45	0.47	0.49
$\overline{y^*_o}$	1.05	1.05	1.04	1.03	1.00
$\overline{v^*_o}$	0.84	0.85	0.86	0.87	0.90
$\overline{c^*_o}$	6.82	3.40	2.03	1.44	1.11
τ^*_{DW}	0.13	0.24	0.35	0.43	0.50
$\tau^*_{\Delta V}/\tau^*_{DW}$	3.37	1.89	1.31	1.08	0.99
	(b) Dimensional values				
$\tau_{\Delta V}$ (h)	4.79	0.60	0.13	0.05	0.03
τ_{DW} (h)	1.42	0.32	0.10	0.05	0.03

The role of F_n can be analyzed also in terms of volume changes needed to produce the transient, the time needed to supply this volume, and the time needed for the perturbation to travel down the canal. Because F_n has little influence on the shape of the dimensionless, steady-state water surface depth and velocity profiles, ΔV^*, the dimensionless volume change from the initial steady state to the final steady state, varies slightly with F_n (ΔV^* represents in all cases close to 4% of the initial volume V^*_o) (Table 2). If ΔQ^*_d is used to supply ΔV^*, then the dimensionless time needed to supply that change is $\tau^*_{\Delta V}$

$$\tau^*_{\Delta V}=\frac{\Delta V^*}{\Delta Q^*_d} \tag{13}$$

This estimate assumes the canal outflow remains constant up to $t^*=t^*_d$. Because ΔQ^*_d is a constant (0.65), F_n has little influence also on $\tau^*_{\Delta V}$ (Table 2). F_n has an important effect on the travel time, however. An estimate of the minimum dimensionless time needed by the leading edge of the flow perturbation to travel down the canal is τ^*_{DW}

$$\tau^*_{DW}=\frac{L^*}{\overline{v^*_o}+\overline{c^*_o}} \tag{14}$$

where $\overline{v^*_o}$ and $\overline{c^*_o}$, respectively, are average dimensionless velocity and celerity under the initial flow conditions. Their sum is the average dimensionless dynamic wave velocity. $\overline{v^*_o}$ is nearly constant with F_n, but $\overline{c^*_o}$ varies essentially with $1/F_n$. (The values in Table 2 were computed based on $\overline{y^*_o}$, the average, dimensionless, initial depth of flow.) Therefore, τ^*_{DW} is about 3.8 times greater at $F_n=0.9$ than at $F_n=0.15$ (Table 2).

If $\tau^*_{\Delta V}>\tau^*_{DW}$, as occurs at lower values of F_n, then discharge can be increased to supply ΔV^* within the time required by the inflow perturbation to travel. Under those conditions, flow must be accelerated and subsequently decelerated to keep the water level at the downstream end of the canal constant. However, if the ratio $\tau^*_{\Delta V}/\tau^*_{DW}$ is close to 1, as occurs at high values of F_n, then ΔQ^*_d can supply the needed ΔV^* in about the same time required

Table 3. Hypothetical Dimensioned Channel, and Dimensionless Volume Change and Delay Characteristics of Computed Transient as Function of b^* for Channels with $F_n=0.15$ and $F_n=0.5$ ($L^*=1$, $z=1.5$): Dimensioned Channels Computed with $Y_R=1.5$ m, and $n=0.018$

	$F_n=0.15$			$F_n=0.5$		
	b^*			b^*		
Variable	2.5	5	10	2.5	5	10
F_R^2	0.016	0.018	0.020	0.182	0.203	0.221
g^*	61.11	54.70	50.24	5.50	4.92	4.52
Q_n (m^3/s)	4.42	7.59	14.00	14.72	25.29	46.68
S_{O_R} ($\times 10^{-4}$)	0.80	0.89	0.97	8.87	9.91	10.8
X_R (m)	18,785	16,814	15,444	1,692	1,513	1,390
T_R (h)	10.63	9.01	7.93	0.29	0.24	0.21
ΔV^*	0.19	0.29	0.48	0.19	0.3	0.49
$\tau^*_{\Delta V}$	0.47	0.44	0.41	0.48	0.45	0.43
τ^*_{DW}	0.09	0.11	0.12	0.35	0.35	0.35
$\tau^*_{\Delta V}/\tau^*_{DW}$	5.21	4.21	3.59	1.39	1.31	1.24

for the perturbation to travel down the canal and flow rate does not need to be increased beyond ΔQ_d^*. In summary, for a given flow geometric configuration (L^*, b^*, z, and y_{st}^*), as F_n increases, the transient goes from being limited by the volume change to being limited by the dynamic characteristics of the canal.

It is helpful to review these relationships in dimensional form. With ΔV^* nearly constant, differences in actual ΔV as a function of F_n are essentially explained by differences in the scaling factor X_R (Table 1), which varies with $1/F_n^2$. Thus, volume change is nearly 36 times greater at $F_n=0.15$ than at $F_n=0.9$. At the same time, the flow rate available to supply this volume change decreases with decreasing F_n (Table 1). As a result, it takes almost 216 times longer to supply this volume at $F_n=0.15$ than at $F_n=0.9$ (Table 2).

Table 4. Hypothetical Dimensioned Channel, and Dimensionless Volume Change and Delay Characteristics of Computed Transient as Function of z for Channels with $F_n=0.15$ and $F_n=0.5$ ($L^*=1$, $b^*=5$): Dimensioned Channels Computed with $Y_R=1.5$ m, and $n=0.018$.

	$F_n=0.15$			$F_n=0.5$		
	z			z		
Variable	0	1	2	0	1	2
F_R^2	0.023	0.019	0.018	0.250	0.214	0.194
g^*	44.44	51.85	57.14	4.00	4.67	5.14
Q_n (m^3/s)	6.47	7.19	7.99	21.58	23.97	26.64
S_{O_R}($\times 10^{-4}$)	0.98	0.84	0.76	10.87	9.32	8.46
X_R (m)	15,330	17,886	19,711	1,380	1,610	1,774
T_R (h)	7.40	9.33	10.79	0.20	0.25	0.29
ΔV^*	0.20	0.26	0.32	0.21	0.27	0.32
$\tau^*_{\Delta V}$	0.40	0.43	0.45	0.42	0.44	0.46
τ^*_{DW}	0.13	0.11	0.10	0.34	0.31	0.28
$\tau^*_{\Delta V}/\tau^*_{DW}$	3.09	3.84	4.55	1.22	1.45	1.67

Effect of Dimensionless Bottom Width b* and Side Slope z

Tables 3 and 4 show the hypothetical dimensioned channel for two values of F_n(0.15,0.5) as a function of, respectively, dimensionless bottom width and canal side slope. The range of b^* and z values considered is typical of real canals. While b^* and z are transverse scale factors, they also affect the longitudinal, time, and flow rate scale of the problem. As the channel widens with other dimensionless design and operational variables held constant ($L^*=1$ and $y_{st}^*=1.25$), the desired downstream outflow hydrograph becomes easier to produce (Fig. 2). Note that in this figure as in Fig. 3, the left axis represents the scale for $F_n=0.15$ while the right axis is the scale for the $F_n=0.5$ curves. Even though ΔV^* increases by 2.5 times in the range of b^* studied, $\tau^*_{\Delta V}$ decreases (as a result of increasing design capacity) while τ^*_{DW} increases, at $F_n=0.15$, or decreases slightly, at $F_n=0.5$ (Table 3). In contrast, increasing z makes control more difficult (Fig. 3). In this case, $\tau^*_{\Delta V}$ increases (the capacity increase is insufficient to offset the volume change) while τ^*_{DW} decreases at either F_n value (Table 4). Differences in computed hydrograph shapes are more modest for varying z than for varying b^* within the typical range of interest.

Effect of Dimensionless Length L*

Figs. 4 and 5 illustrate the effect of L^* on the gate-stroking solutions for two values of F_n, 0.15 and 0.5 (with $b^*=5$ and $z=1.5$) with $y_{st}^*=1.25$, as in the initial example. For $F_n=0.5$ and $L^*>2$, inflow variations had to be initiated earlier than $t^*=0$ to complete the transient by $t_d^*=1.0$, hence the negative values in the time axis of Fig. 5. For each F_n, there is a range of L^* over which a solution can be obtained. (For $F_n=0.15$, no solution can be obtained if L^* is greater than about 1.25 while for $F_n=0.5$, solutions can be obtained up to approximately $L^*=5.0$.) Within that range, the desired transient is more difficult to produce with increasing L^*, a logical result given that the dimensionless volume that needs to be added to the pool and $\tau^*_{\Delta V}$ also increase (Table 5). Notice however that the relationship between $\tau^*_{\Delta V}/\tau^*_{DW}$ and L^* is different depending on F_n. Therefore, by itself, the ratio $\tau^*_{\Delta V}/\tau^*_{DW}$ does not indicate whether substantial acceleration of flow will be required for a desired change in demand.

Although wave diffusion increases with L^*, the duration of the gate-stroking transient τ^*_{GS} (defined in an earlier section) varies almost in proportion to L^*. This suggests that the upstream inflow perturbation could, perhaps, attenuate rapidly and then travel at nearly constant speed, i.e. as a kinematic wave (Henderson 1966; Fenton et al. 1999). This theory was tested by computing values of ν^*_{KW}, the dimensionless kinematic wave velocity, and the resulting travel time estimates $\tau^*_{KW}=L^*/\nu^*_{KW}$ as a function of L^* for the average initial depth conditions (Table 5). ν^*_{KW} is given by

$$\nu^*_{KW}=\frac{dx^*}{dt^*}=\frac{1}{B^*}\frac{dQ^*}{dy^*} \tag{15}$$

Given in the same table are estimates of τ^*_{GS} (derived from Figs. 4 and 5). ν_{KW} increases only slightly with L^* but the resulting travel time τ^*_{KW} is much greater than τ^*_{GS}, over 4.3 times at $F_n=0.15$ and over 1.8 times at $F_n=0.5$. Consequently, and because a closer relationship exists between τ^*_{GS} and τ^*_{DW}, one would have to conclude that the inflow perturbation does not behave like a kinematic wave, especially in the lower F_n range.

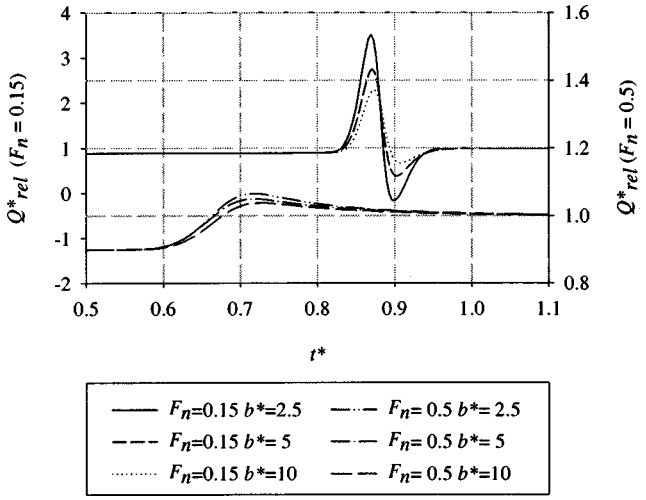

Fig. 2. Variation in gate-stroking solutions with b^* for $F_n = 0.15$ and 0.5 ($L^* = 1$, $z = 1.5$, $y^*_{st} = 1.25$)

Effect of Downstream Water Depth Setpoint y^*_{st}

The effect of increasing y^*_{st} on the gate-stroking solutions was investigated also, using two values of F_n (0.15 and 0.5) and with $b^* = 5$, $z = 1.5$, and $L^* = 1$. For $F_n = 0.15$, increasing y^*_{st} from 1 (normal depth at design capacity) to 25% above normal depth reduces ΔV^* by 10% (Table 6); consequently, peak Q^*_{rel} decreases by over 30% (Fig. 6). While ΔV^* continues to decrease as y^*_{st} increases, substantial increases in y^*_{st} are needed to force peak Q^*_{rel} close to canal capacity. Increasing y^*_{st} also reduces τ^*_{GS} (the transient's duration) (Fig. 6), even though τ^*_{DW} remains nearly constant (Table 6). Results computed at the higher value of F_n show a similar variation in ΔV^* with y^*_{st} (Table 6). However, because small inflow changes are already required at $y^*_{st} = 1.0$, increasing y^*_{st} only has a slight impact on peak Q^*_{rel} (Fig. 7). Similarly, the effect on the transient's duration is minimal. In Fig. 7, for the gate-stroking hydrographs computed at $y^*_{st} = 1.75$ and 2.0, inflow rate during the transient never exceeds final Q^*_{rel} and this value is reached only after $t^* = 1.5$ (that is, after the final downstream outflow conditions have been achieved). In these cases, the ratio $\tau^*_{\Delta V}/\tau^*_{DW}$ is less than 1 (Table 6), so the only limitation to producing the desired demand change is the velocity at which the perturbation can travel down the canal.

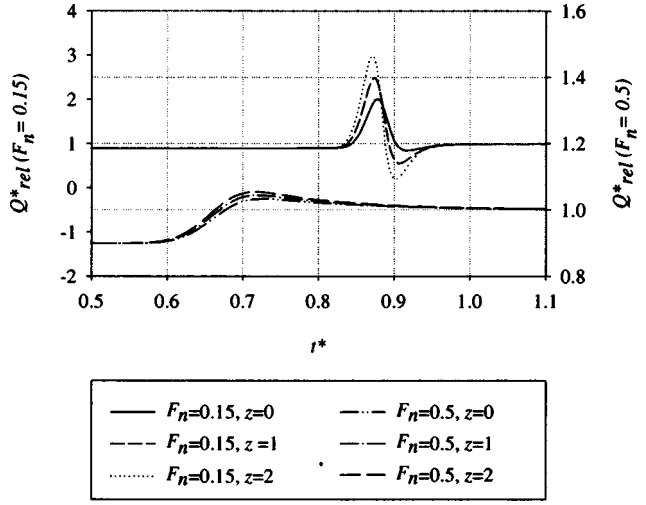

Fig. 3. Variation in gate-stroking solutions with z for $F_n = 0.15$ and 0.5 ($L^* = 1$, $b^* = 5$, $y^*_{st} = 1.25$)

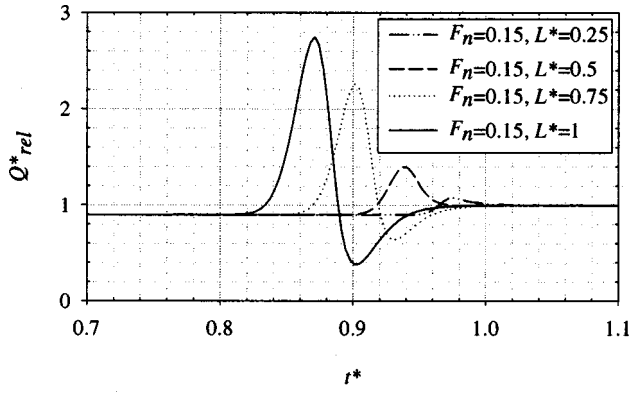

Fig. 4. Variation in gate-stroking solutions with L^* at $F_n = 0.15$ ($b^* = 5$, $z = 1.5$, $y^*_{st} = 1.25$)

Forward Solutions

Simulations were conducted with CanalCAD to test the gate-stroking solutions presented in Fig. 1. Since CanalCAD does not allow the user to modify the values of g and c_u, calculations were carried out in dimensional form, using the hypothetical dimensioned channel data (Table 1). Results were subsequently nondimensionalized. Simulations used the gate-stroking solution as an upstream boundary condition. The downstream boundary condition consisted of a vertical sluice gate at a fixed position. The gate opening was determined assuming free flow based on the gate width $b^*(5)$, $Q^*_o(5.85)$, and the given y^*_{st} value (1.25). A gravity offtake just upstream from the check structure was used to simulate the demand change. The offtake was initially closed and was opened at $t^* = 1$ to deliver ΔQ^*_d. The constant offtake opening was calculated internally by the simulator based on the desired depth upstream from the offtake, y^*_{st}, and a constant depth downstream from the offtake equal to half normal depth. The operational scenario represented by this gate and turnout combination is realistic although results cannot be fully generalized because of the specific gate and turnout hydraulic relationships used in CanalCAD.

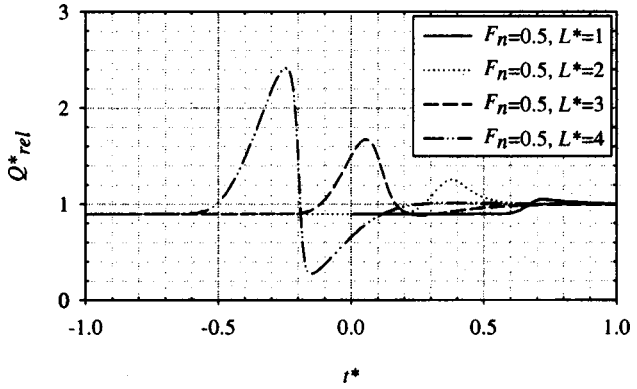

Fig. 5. Variation in gate-stroking solutions with L^* at $F_n = 0.5$ ($b^* = 5$, $z = 1.5$, $y^*_{st} = 1.25$)

Table 5. Dimensionless Volume Change and Delay Characteristics of Computed Transient as Function of F_n and L^*

	$F_n=0.15$				$F_n=0.5$			
	L^*				L^*			
Variable	0.25	0.50	0.75	1.00	1	2	3	4
ΔV^*	0.02	0.09	0.18	0.29	0.30	0.75	1.21	1.67
$\tau^*_{\Delta V}$	0.04	0.14	0.28	0.44	0.45	1.16	1.86	2.56
y^*_0	1.18	1.12	1.08	1.05	1.04	0.99	0.98	0.97
τ^*_{DW}	0.03	0.06	0.10	0.13	0.35	0.69	1.03	1.38
$\tau^*_{\Delta V}/\tau^*_{DW}$	1.12	2.10	2.85	3.37	1.31	1.68	1.80	1.86
ν^*_{KW}	1.01	1.09	1.15	1.20	1.22	1.31	1.34	1.36
τ^*_{KW}	0.25	0.46	0.65	0.83	0.82	1.53	2.23	2.94
τ^*_{GS}	0.06	0.11	0.15	0.19	0.40	0.80	1.20	1.60

The time variation in downstream water depth deviations, $y^*(t^*)-y^*_{st}$ is illustrated in Fig. 8. The desired initial steady-state flow conditions could not be matched due to round-off errors. These errors were slight in most cases but increased abruptly at $F_n=0.9$. While the gate-stroking solutions were unable to keep the downstream depth perfectly stable throughout the transient, control was excellent, with peak deviations not exceeding 0.03 (less than 3% of normal depth), and results improved as F_n decreased. Note that the inability of the gate-stroking solution to precisely produce the desired transient is due to theoretical limitations of the gate-stroking concept (Fenton et al. 1999; Bautista et al. 1997) and round-off errors of both the inverse and forward solutions.

The results presented in previous sections showed how the dimensionless design and operational variables interact to determine the shape of the gate-stroking solution. For a given demand change, some conditions require substantial inflow acceleration and deceleration; for other conditions, inflow changes essentially need to match the demand change, but with the upstream change applied at a time $t^*_d-\tau^*$ (where τ^* is a delay). Canal operators commonly use this latter approach irrespective of canal geometry and flow conditions, with the delay determined from experience. Of interest, then, is to determine a reasonable value for the delay and to examine the performance of this simple feedforward control strategy flow under a variety of flow conditions.

One alternative for determining the delay is Eq. (13). With this choice, a the simple feedforward inflow schedule is given by

$$\Delta Q^*_1(t^*_1)=\Delta Q^*_d; \quad t^*_1=t^*_d-\tau^*_{\Delta V} \tag{16}$$

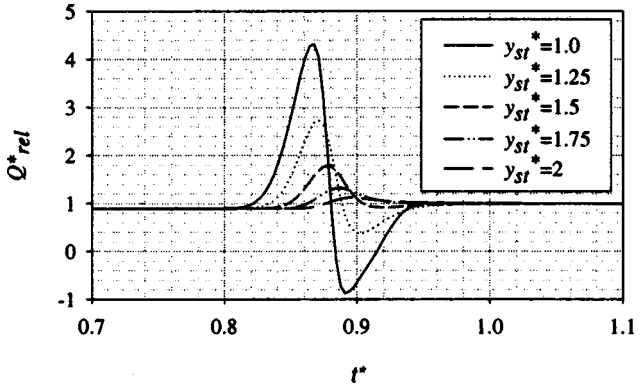

Fig. 6. Variation in gate-stroking solutions with y^*_{st} at $F_n=0.15$ ($L^*=1$, $b^*=5$, $z=1.5$)

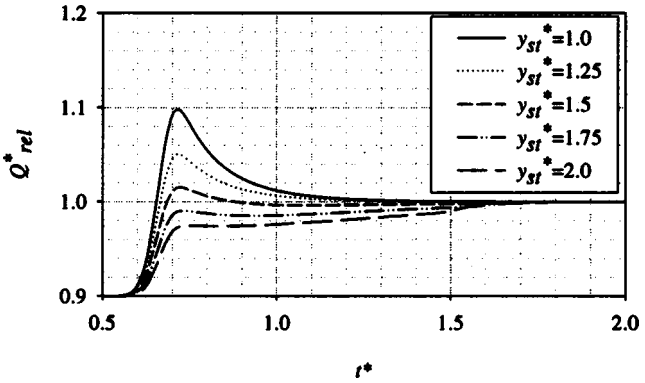

Fig. 7. Variation in gate-stroking solutions with y^*_{st} at $F_n=0.5$ ($L^*=1$, $b^*=5$, $z=1.5$)

This approach can be referred to as volume compensation, because it explicitly accounts for the pool volume storage change needed for the new steady-state condition. Volume compensation is one of the principles behind the dynamic regulation canal control method (Deltour 1992). Note that this compensating volume is supplied also by the gate-stroking solutions. Feedforward schedules were developed using Eq. (16), the ΔV^* and $\tau^*_{\Delta V}$ values of Table 2, and the specified ΔQ^*_d. Simulations were conducted with the same downstream boundary condition and offtake configuration as before. Depth deviations obtained with this feedforward control strategy (Fig. 9) were only slightly larger than those obtained with the gate-stroking solutions (Fig. 8). More important, reasonable results were obtained even for $F_n=0.15$, conditions under which the gate-stroking solution required significant acceleration and deceleration of flow.

In Fig. 9, all deviations are positive. This implies that most of the volume change needed for the new steady-state, has been stored in the pool by the time the offtake is opened. Further reductions in the downstream water depth deviations seem possible, therefore, by using the same compensating volume ΔV^* but with a smaller delay τ^*, i.e., by timing the upstream inflow change so that the downstream flow rate change occurs before the bulk of the volume change has been added to the pool. A reasonably small choice for τ^* is τ^*_{DW}. The resulting feedforward schedule consists then of two upstream flow changes

$$\Delta Q^*_1(t^*_1)=\frac{\Delta V^*}{\tau^*_{DW}}; \quad t^*_1=t^*_d-\tau^*_{DW}$$
$$\Delta Q^*_2(t^*_2)=\Delta Q^*_d-\Delta Q^*_1; \quad t^*_2=t^*_d \tag{17}$$

The second change is needed to match the inflow with the sum of the initial inflow and the demand flow change. Volume compensating schedules were developed with Eq. (17) for the same

Table 6. Dimensionless Volume Change and Delay Characteristics of Computed Transient as Function of F_n and y^*_{st}

	$F_n=0.15$					$F_n=0.5$				
	y^*_{st}					y^*_{st}				
Variable	1.00	1.25	1.50	1.75	2.00	1.00	1.25	1.50	1.75	2.00
ΔV^*	0.33	0.29	0.23	0.17	0.12	0.36	0.29	0.23	0.16	0.10
$\tau^*_{\Delta V}$	0.51	0.44	0.35	0.27	0.19	0.55	0.45	0.35	0.24	0.16
τ^*_{DW}	0.13	0.13	0.13	0.12	0.12	0.34	0.35	0.35	0.35	0.34
$\tau^*_{\Delta V}/\tau^*_{DW}$	3.83	3.37	2.80	2.19	1.62	1.59	1.31	1.00	0.70	0.47

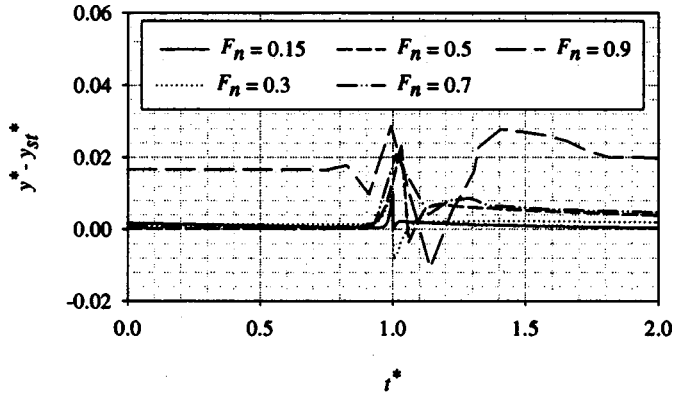

Fig. 8. Simulated downstream $y^* - y_{st}^*$ computed with gate-stroking solutions of Fig. 1

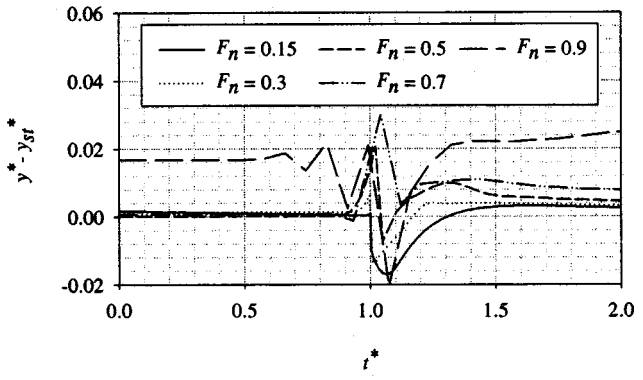

Fig. 10. Simulated water level errors computed with volume compensating feedforward schedule and delay τ_{DW}^*

flow conditions as before, using the τ_{DW}^* values of Table 2. Water level deviations were mostly negative at lower F_n values, indicating that τ_{DW}^* underestimates the delay under those conditions (Fig. 10). Slightly better results were obtained at higher values of F_n, even though τ_{DW}^* and $\tau_{\Delta V}^*$ are very similar under those conditions (Table 2). This suggests the volume compensating approach is fairly sensitive at high Froude numbers. Despite these limitations, these results along with those obtained with Eq. (16) show that a feedforward strategy based on volume compensation will perform adequately if the delay is within $\tau_{DW}^* \leqslant \tau^* \leqslant \tau_{\Delta V}^*$, for cases in which $\tau_{DW}^* < \tau_{\Delta V}^*$. Tests not presented here suggest that in the alternative case, $\tau_{DW}^* < \tau_{\Delta V}^*$ (e.g., the solution computed for $F_n = 0.5$ and $y_{st}^* = 1.75$ in Table 6), better water level control would be obtained with τ_{DW}^* as the delay. It is worth noting that in a previous study, two of the authors (Bautista and Clemmens 1999) proposed computing a delay for feedforward control based on a combination of τ_{DW}, computed for the pool section under backwater influence, and τ_{KW} [see text preceding Eq. (16)], applied to the section not affected by backwater. Results presented herein suggest that approach, besides being more complex, could severely overestimate the wave travel time, particularly at very low Froude numbers and when flow is close to normal.

Additional simulation tests were conducted with one of the examples shown in Fig. 5, a canal with design $F_n = 0.5$ and $L^* = 4.0$. As shown in Fig. 5, the gate-stroking solution for this case requires large acceleration and deceleration of flow. Simulations used first the gate-stroking solution, and then the volume compensating schedule with delay $\tau_{\Delta V}^*$. Peak downstream water depth deviation computed with the gate-stroking solution for $L^* = 4$ (Fig. 11) is only slightly larger than that obtained for the same F_n value but with $L^* = 1$ (Fig. 8). Thus, the gate-stroking method continued to produce reasonable results under these more extreme flow change conditions. In contrast, peak depth deviation computed with the volume compensating schedules at $L^* = 4$ (Fig. 1) is about 1.6 times greater than the corresponding results obtained at $L^* = 1$ (Fig. 9). Clearly, the effectiveness of the volume compensating decreases with increasing channel length although results may still be adequate for field applications. As in Fig. 9, deviations obtained with the volume compensating schedule are all positive, meaning that control can be further improved through the choice of a smaller delay.

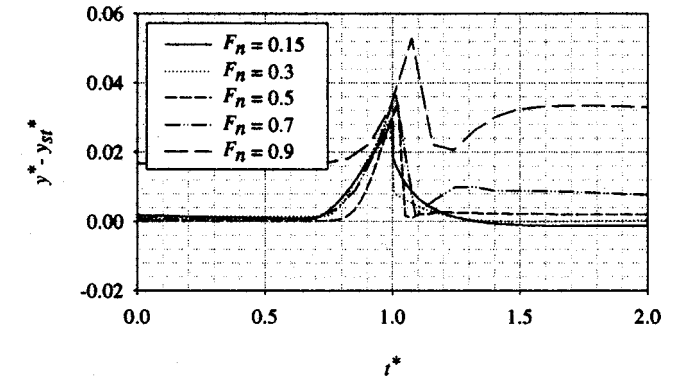

Fig. 9. Simulated water level errors computed with volume compensating feedforward schedule and delay $\tau_{\Delta V}^*$

Discussion

Gate-stroking is a restrictive method, because it requires downstream depth to vary in a prespecified manner. It is also a poorly-posed problem (Cunge et al. 1980). As a result, solutions are very sensitive to the physical characteristics of canals. Despite these limitations, the above presented analysis provides us with insights about the feedforward control problem.

Clearly, accounting for the change in pool storage needed for the new steady state is critical, independently of canal characteristics. Both the gate-stroking method and the proposed simple scheme account for this change and are nearly as effective. For a given F_n, gate-stroking solutions become more extreme with increasing L^* and decreasing setpoint, i.e., as supply time becomes greater relative to travel time. These are also conditions under which control with the simple volume-compensating feedforward scheme degrades. While the resulting downstream water level deviations are more extreme, they are still small relative to the setpoint and would not endanger the canal. Also, while unsteady conditions persist for longer times than with gate-stroking, the deviations would only have a slight effect on the accuracy of deliveries. Thus, the degradation in water level control would not offset the benefit less extreme inflow fluctuations which are potentially required with the gate-stroking solution. The analysis also shows that time at which gate-stroking inflow changes need to be initiated are generally bound by simple travel time estimates, τ_{DW} and $\tau_{\Delta V}$. Thus, simple scheduling approach can be developed in accordance with these bounds.

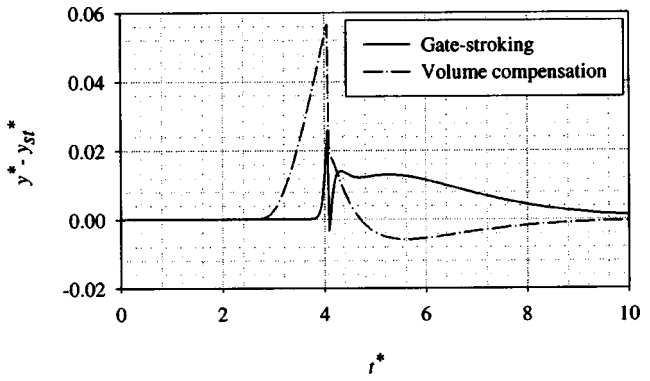

Fig. 11. Simulated water level errors computed with the gate-stroking solution and volume compensating schedule for a canal with $F_n=0.5$ and $L^*=4.0$ ($b^*=5$, $z=1.5$, $y_{st}^*=1.25$)

The analysis presented herein applies to single pool canals of uniform cross section subject to a single demand change. Real irrigation delivery systems consist of networks of canals, with pools of irregular slope and cross section, and multiple flow changes. A canal scheduling algorithm based on volume compensation for complex delivery systems has been proposed (Bautista and Clemmens 1999) and is currently being further developed.

Conclusions

Differences in the shape of inflow hydrographs computed with the gate-stroking method can be explained in terms of volume changes resulting from the transient, the time needed to supply this volume, and the time needed by the inflow perturbation to travel down the canal. Severe inflow fluctuations are needed when the ratio between the supply and travel time is relatively large, that is when the supply rate limits the desired flow change. This relationship is Froude number dependent and, therefore, it is difficult to determine whether significant flow increases will be needed to produce a desired downstream flow change from that ratio alone.

A feedforward control strategy based on volume compensation performed nearly as well as the gate-stroking method under the range of conditions studied. The method is simple as it requires at most two discrete flow rate changes and not continuous flow variations as with gate-stroking, and the magnitude of required flow changes can be bound. Thus, the method represents a practical feedforward control strategy. Reasonable bounds for the delay in the volume compensating method are the time needed to supply the volume change and the travel time computed from dynamic wave theory. Within this range, errors in the delay estimation will result in moderate deviations over relatively long times at lower values of the flow's Froude number, and larger but shorter-lived deviations at higher Froude values.

Notation

The following symbols are used in this paper:

A = flow area;
A_n = flow area at normal depth for the design flow (aspect ratio);
B = top width;
b = bottom width;
c = celerity;
c_o^* = average dimensionless celerity under the initial flow conditions;
c_u = units parameter in the Manning resistance equation;
c_u^* = parameter in the dimensionless momentum equation;
F_n = Froude number at normal depth for the design flow;
g = gravitational constant;
g^* = parameter in the dimensionless momentum equation;
h = water surface elevation;
L = channel length;
n = Manning n;
Q = flow rate;
Q_n = design flow rate;
Q_R = reference flow rate;
Q_{rel}^* = relative flow rate;
q_0 = lateral flow per unit length;
R_n = hydraulic radius at normal depth for the design flow;
S_0 = channel bottom slope;
S_{0_R} = reference slope;
T_R = reference time;
t = time;
t_d = time for the demand flow rate change;
v_o^* = average dimensionless flow velocity under the initial flow conditions;
X_R = reference length along the channel;
x = length along the channel;
Y_R = reference tranverse length;
y = flow depth;
y_{st} = water depth setpoint;
y_o^* = dimensionless average depth of flow under the initial flow conditions;
z = canal side slope;
ΔQ_d = demand flow rate change;
Δx^* = dimensionless space increment in the finite difference solution;
Δt^* = dimensionless time increment in the finite difference solution;
ΔV = volume change between the initial and final steady-state flow rate;
τ = delay;
τ_{DW} = dynamic wave delay;
τ_{GS} = duration of the gate-stroking transient; and
$\tau_{\Delta V}$ = time needed to supply ΔV.

Superscript

$*$ = dimensionless counterpart of a dimensioned variable.

References

Bautista, E., and Clemmens, A. J. (1999). "Computerized anticipatory control of irrigation delivery systems." *Proc., Workshop on Modernization of Irrigation Water Delivery Systems*, U.S. Committee on Irrigation and Drainage (USCID), Scottsdale, Ariz., 359–373.

Bautista, E., Clemmens, A. J., and Strelkoff, T. S. (1996). "Characterization of canal operations under ideal anticipatory control." *Proc., North American Water and Environment Congress and Destructive Water*, ASCE, Reston, VA, 1,887–1,892.

Bautista, E., Clemmens, A. J., and Strelkoff, T. S. (1997). "Comparison of numerical procedures for gate stroking." *J. Irrig. Drain. Eng.*, 123(2), 129–136.

Chevereau, G. (1991). ''Contribution a L'Etude de la Regulation dans les Systemes Hydrauliques a Surface Libre.'' Doctoral thesis, Institut National Polytechnique de Grenoble, Grenoble, France (in French).

Cunge, J. A., Holly, F. M., and Verwey, A. (1980). *Practical aspects of computational river hydraulics*, Pittman, London.

Deltour, J. L. (1992). ''Application de l'Automatique Numerique a la Regulation des Canaux.'' Doctoral thesis, Institut National Polytechnique de Grenoble, Grenoble, France (in French).

Fenton, J. D., Oakes, A. M., and Aughton, D. J. (1999). ''On the nature of waves in canals and gate stroking and control.'' *Proc., Workshop on Modernization of Irrigation Water Delivery Systems*, U.S. Committee on Irrigation and Drainage (USCID), Scottsdale, Ariz., 343–357.

Henderson, F. M. (1966). *Open-channel flow*, Macmillan, New York.

Holly, F. M., and Parrish, J. B. (1995). *CanalCAD: Dynamic flow simulation in irrigation canals with automatic gate control*, Iowa Institute of Hydraulic Research, Iowa City, Iowa.

Strelkoff, T. S., and Clemmens, A. J. (1998). ''Nondimensional expression of unsteady canal flow.'' *J. Irrig. Drain. Eng.*, 124(1), 59–62.

Strelkoff, T. S., Deltour, J. L., Burt, C. M., Clemmens, A. J., and Baume, J. P. (1998). ''Influence of canal geometry and dynamics on controllability.'' *J. Irrig. Drain. Eng.*, 124(1), 16–22.

Wylie, E. B. (1969). ''Control of transient free surface flow.'' *J. Hydraul. Div., Am. Soc. Civ. Eng.*, 95(1), 347–361.

ADVANCES IN THE OPERATION OF IRRIGATION WATER DELIVERY SYSTEMS

Albert J. Clemmens
Director
U.S. Water Conservation Laboratory
USDA – Agricultural Research Service
4331 E. Broadway
Phoenix, AZ 85040 USA
1-602-379-4356 x269
1-602-379-4355 Fax
bclemmens@uswcl.ars.ag.gov
www.uswcl.ars.ag.gov/

ABSTRACT

The amount of flexibility provided by irrigation water delivery systems and their ability to supply the needed flows can have a large impact on the performance of farm irrigation systems. The last two decades have seen a gradual shift in the attitudes and practices of irrigation water purveyors – from supply-oriented water retailers to demand-oriented service providers. Yet even where water ordering and operational philosophy are more demand orientated, significant improvements in operations and water control are still possible. Improved delivery service and performance are possible with a comprehensive water control strategy, including some aspects of canal automation. This paper discusses the progress that has been made on the theory and application of canal automation, the limitations imposed by the physical system, and future directions in the improvement of irrigation water delivery systems.

INTRODUCTION

In the western United States a number of factors have come together to place significant pressure on irrigation districts to improve their operations. Over the past several decades, available water supplies have become fully or even over-allocated. During drought years, junior water right holders have found themselves with little or no water available. This reached near crisis proportions in central California in the early 1990s. Some agricultural water users along the Colorado River are facing the possibility of reduced water supplies as other users with established water right begin to use their share. Environmental uses of water in the Pacific Northwest, particularly associated with restoring Salmon habitat, threaten to drastically reduce water available for other uses. Native American Indian water right claims pose a dilemma for the Federal Government, since such claims come on top of fully allocated supplies.

In many parts of the western U.S., water rights are held by irrigation districts, with no strict regulation of water use by individual land owners. Within this context, irrigation districts are being asked to more accurately document their water use and to develop water conservation plans. The intent is to improve the measurement and control of water delivered to users. Where water is inexpensive, farmers have little incentive to conserve, while the irrigation district is still accountable for all water delivered. In contrast, for some parts of Arizona water rights are tied to individual land owners, with water use reported and regulated by farms. Irrigation districts must accurately report water delivered to these farms. Losses within the irrigation district are limited to 10%, with additional losses charged against users' water allocation.

Increasing use of pressurized irrigation to improve irrigation performance in areas that have traditionally used surface irrigation pose an interesting problem for irrigation delivery system operations. Pressurized systems are less forgiving of canal system limitations. Over the last decade, the Columbia Basin project has seem distribution system performance drop by 10% due to the conversion to pressurized systems (i.e., spills have increased by 10% of the supply), somewhat reducing the positive benefits of pressurized irrigation.

Over the last two decades, agricultural production has faced an increasingly competitive market with significant international competition. Growers have been forced to tighten their belts to achieve more efficient production. Poor delivery service is simply becoming unacceptable to growers, particularly where water is expensive or supplies are unreliable. While many irrigation districts have worked hard to improve operations and service, there is still much more improvement that can and probably needs to occur.

Fortunately, a great deal has been learned regarding the operation and automation of canal delivery systems over the last decade that should help irrigation districts improve their service and operations. Also, the cost of remote and automatic controls has come down substantially, in many cases by an order of magnitude over the last decade. The purpose of this paper is to discuss what has been learned about delivery system operations and how that knowledge can be applied in practice today.

NEED FOR FLEXIBILITY

It has been a challenge to define the amount of flexibility needed for a particular delivery system. Generally, the delivery and the farm irrigation systems are developed in concert with one another, that is the farm system is designed to accommodate the limitations of the delivery system. Thus the farm irrigation system is made to work under the constraints of the delivery system. However, this can severely restrict changes in on-farm irrigation systems and their ability to adapt to new crops and markets. These become lost opportunities, which are extremely difficult to place a monetary value on. Where farmers can influence their water delivery systems, the two can evolve together. Resistance to change makes this a slow process.

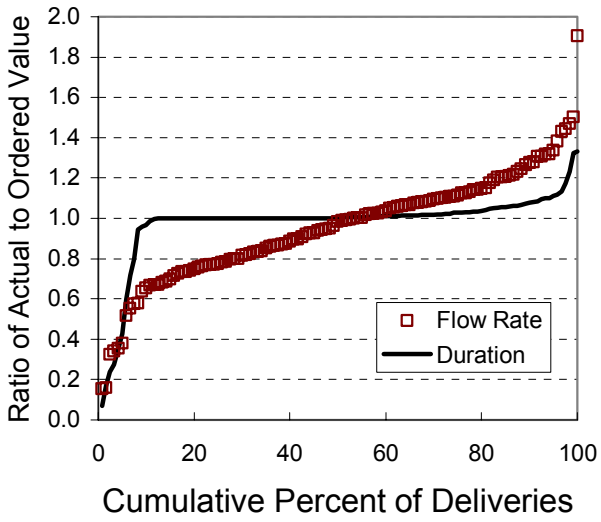

Figure 1. Data on water deliveries on two lateral canals (from Palmer et al. 1991).

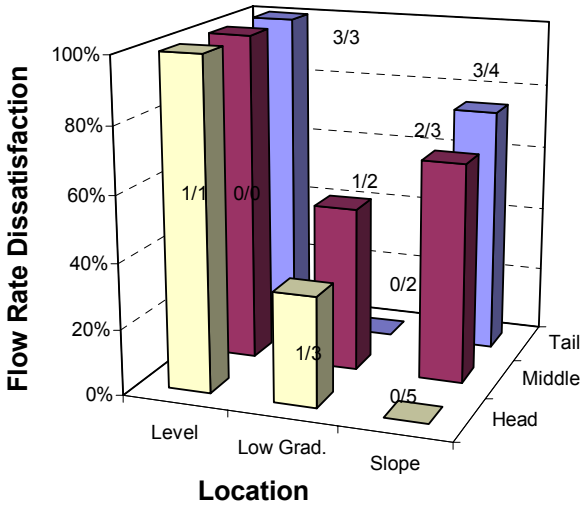

Figure 2. Results of farmer survey from Clemmens et al. (2000).

Any number of metrics or performance parameters can be used to evaluate the performance of an irrigation water delivery system. From a hydrologic standpoint, water resources agencies are interested in water diverted, water consumed, and the ultimate destination of water not consumed. A variety of metrics have been proposed for such views (Bos 1997). A number of studies have evaluated delivery performance. Figure 1 shows variations in the flow rate delivered to users from one such study (Palmer et al (1991). Determining appropriate or acceptable values for these metrics has still been subjective. An alternate approach is to survey farmers regarding their satisfaction with the delivery system. Farmers' satisfaction with flow rate fluctuation from a farmer survey (Clemmens et al. 2000) is shown in Figure 2. Within any water delivery system, you will always find water users that are dissatisfied with the delivery service, for example because of system constraints, special needs that are not met, etc.

DELIVERY SYSTEM LIMITATIONS

Irrigation water delivery systems have both physical and operational limitations that preclude them from providing perfect service to all users. It is only recently that we have begun to quantify delivery system physical limitations and their influence on operating rules and level of service. Sloping canal system response is limited by the time required for waves to travel through the canal and by the dispersion of those waves as shown in Figure 3. Canal pool and structure properties (e.g., cross-sectional area) also influence canal response. Strelkoff et al. (1998) provide an approach to evaluating these limitations for canals from an operational standpoint. Pipeline systems have less problems associated with delays, but are often more constrained by capacity and by the rate and magnitude of flow changes. This paper will focus primarily on open-channel water delivery systems, since these pose a more difficult and significant problem.

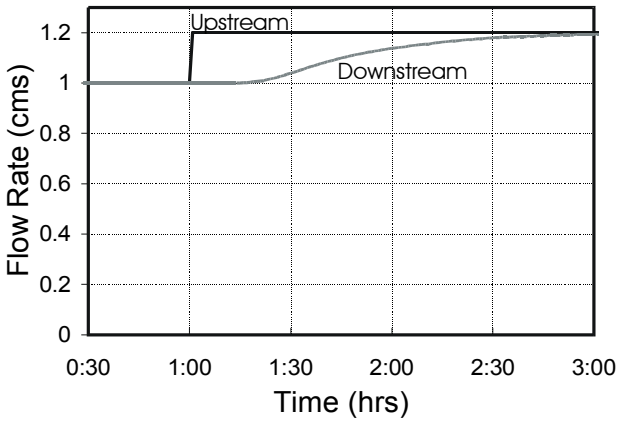

Figure 3. Flow rate dispersion for a canal.

For most open-channel irrigation water delivery systems, all or most of the control structures are operated manually by canal operators who visit the sites. Remote monitoring and control, for example with Supervisory Control And Data Acquisition (SCADA) systems, are often applied to large main canals, but seldom to secondary or lateral canals. Lamacq (1997) simulated the manual operation of a lateral canal for an irrigation district and showed that even if operated perfectly according to the operating rules, water delivery service to the users was imperfect. Such imperfect service reflects the inability of manual operators to visit the sites frequently enough to overcome flow transients (i.e., wave time delays and dispersion).

WATER CONTROL CONCEPTS

In simple terms, the control of water within a delivery system centers on **control of flow rate** and **control of volume** at various points within the system, particularly at delivery points. For any part of the system, inflow equals outflow plus change in storage volume over time. Most canal-operating schemes focus on these two concepts of flow and volume balances in one form or another. While these concepts are simple in theory, they are often difficult to apply in practice. For sloping canals, changes in flow rate and/or resistance to flow result in changes in pool volume that may not be considered by operators (Figure 4). Changes in pool water levels upstream from control structures also changes pool volumes. ***Operators are easily fooled by the time delays, wave dispersion, and pool volume changes that occur within a system***.

Flow rates set at check and offtake structures are never exact. These flow-rate errors tend to accumulate within the system. For effective, modern operations, some form of feedback, either manual or automatic, is needed to remove these errors. Improved water measurement and accounting are an important aspect of effective water control. "***To Measure is to Know***!"

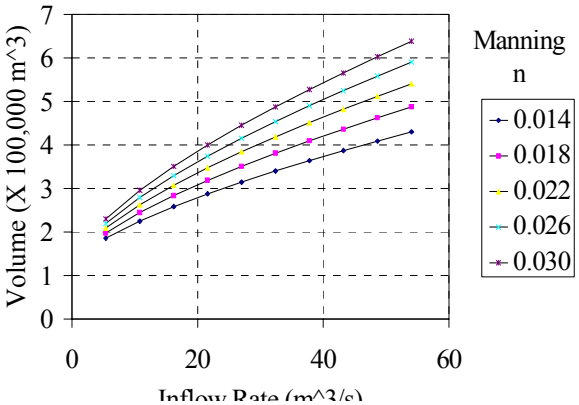

Figure 4. Canal pool volume variations.

Check and offtake structure properties influence how flow changes are divided at a bifurcation. They influence pool volume (e.g., if the downstream level changes) and the speed at which upstream changes are felt downstream (see Strelkoff et al. 1998 for examples). Thus, structure hydraulics also influence the response of the system and have an influence on the effectiveness of both manual and automatic controls.

Manual Operations: A vast majority of canal systems are operated manually, with varying degrees of success. The main job of canal operators is to route flow changes through the canal system. This is a time-consuming, tedious task. Water in open canals flows according to the laws of physics and not necessarily the desire of canal operators. The work involves considerable judgment and experience because of transients (time delays and wave dispersion). This judgment can be improved with a better understanding of canal hydraulics — i.e., "training" (Johnston and Robertson 1990).

For manually operated systems with gates (or combined weirs and gates) as control structures, increases in flow are nearly always routed from the canal head to the offtake being changed. The operator starts flow into the canal, travels to the next gate downstream, and waits for the change in flow to arrive. Since the wave arrives gradually, judgement is required to know when to adjust the check gate. Figure 5 shows what happens to the flow rate to the offtake and downstream canal while the water level stabilizes. This type of offtake hydrograph is not uncommon.

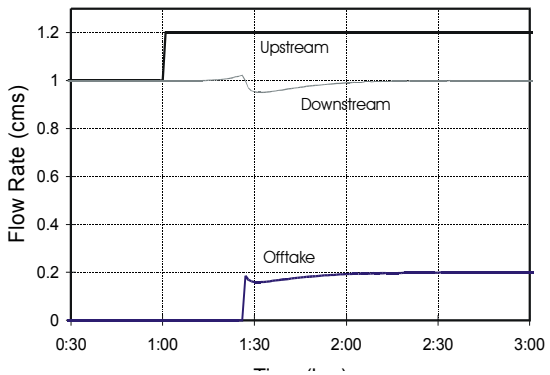

Figure 5. Impact of flow dispersion on downstream flows.

The operator proceeds downstream changing each gate in turn until the offtake is opened. Now the operator must return to the canal head and repeat the setting of gates with the assumption that flows have stabilized. Adjustments are made to correct for errors made during the first pass. If the inflow to the canal is set wrong, the actual canal inflow and the desired outflow cannot balance. To achieve a balance, the headgate must be adjusted and the process starts over. The routing of flow changes through the canal is considered open-loop or feed-forward control. The process of making adjustments until the canal is in balance is considered closed-loop or feedback control. A common practice is to deliver a greater flow change than needed to satisfy changes in demand. Experience suggests that this "carriage" water is useful for supplying the pool volume changes associated with the change in flow rate. Unfortunately, this carriage water is often left in the canal long after the transient period, resulting in high canal water levels and/or wasted water.

A single operator has difficulty controlling a canal where changes are taking place at many locations at once. For large canals, it has become practical to control gates remotely from a centralized location. SCADA systems replace local canal operators with supervisory control operators. One of the main advantages of supervisory control operations is that the operator can see what is occurring on the entire canal simultaneously. SCADA systems typically provide operators with remote canal water levels, gate positions, flow rates, etc. Like local canal operators, supervisory control operators also have difficulty dealing with canal transients. Control decisions are often only made after flows have stabilized -- a change and wait approach. Judgement and experience can improve performance. Automated systems, discussed below, can be designed to take transients into account so that control actions do not have to wait for the flows to stabilize.

SUCCESSFUL AND UNSUCCESSFUL CANAL CONTROL CONCEPTS

Methods currently in use for the automatic control of irrigation canals are summarized by Rogers and Goussard (1998). Malaterre et al. (1998) summarize the canal control algorithms that have been proposed.

Dynamic Regulation: One of the more insightful approaches to canal operations is dynamic regulation, developed for the Canal de Provence in southern France. The scheme estimates future demands, observes water levels within the system, and determines changes in flow rate at the head of canal needed to restore volumes. Pool volumes as a function of flow rate and stage are known. Flows between pools are adjusted by automatic gates that try to maintain a constant difference in water levels between pools. Water is pumped from the canals into water towers for pressurizing sprinkler irrigation systems. Thus the canals really serve as reservoirs, and are quite different from the gravity flow systems typical of much of the world. Other systems built by the French and operated in a similar way also tend to have large storage volumes – i.e., canals are not designed as efficient sections for transmission of water, as is typical in most irrigation projects. This is primarily an open-loop control system, with some local feedback components.

Central Arizona Project: Another interesting approach is that used to control the Central Arizona Project. Their control approach is to determine the desired conditions for some future time, and then gate settings are changed so that when the transients die down, the system will be at the desired steady state. The system attempts to maintain constant pool volumes, and thus pool water levels change with flow rate. The system seems to work well and is useful, particularly when considering the constraints imposed by lift station pumps. However, it is not responsive to changes in demand and the staff has to continuously calibrate gate coefficients and canal roughness parameters. This is an open-loop system without feedback control. Gate stroking was originally proposed (discussed below), but proved too difficult to implement.

Gate Stroking: Wiley (1969) first proposed a method for numerically computing, with the method of characteristics, the timing and amount of upstream flow changes to satisfy downstream changes in demand. This method has come to be known as gate stroking. It is a form of open-loop feedforward control. The U.S. Bureau of Reclamation (Falvey and Lunig 1979) developed software to implement Wiley's method. Several attempts have been made to implement this in practice and they have all been unsuccessful. Several finite-

difference approaches (e.g., Preissman scheme) to the gate-stroking problem have also been attempted. Bautista et al. (1997) summarize these methods and present an improved method. However, research suggests that any gate-stroking method will be difficult to use because of hydraulic limitations and constraints. The numerical procedures often produce upstream inflow hydrographs that oscillate significantly or are not physically possible (e.g., negative flows). Bautista and Clemmens (1999) developed a simplified gate-stroking method that is based solely on changes in pool volume and pool delay times. The effectiveness of the method was demonstrated with the ASCE test cases. This method is presented in more detail below.

Feedback Control: There have been several attempts at applying a series of local feedback controllers on irrigation canals. ELFLO (Rogers et al. 1995) has been applied to several canals. Its performance has been mixed. While it seems to work well during some flow conditions, at high flows operators just shut the system off and operate it manually. There were also several unsuccessful attempts at applying the CARDD feedback control technique on lateral canals in western Canada. A modified form of Zimbelman's feedback control method was attempted at the Maricopa-Stanfield Irrigation and Drainage District (MSIDD) in central Arizona. The system designers were not able to make this control system functional (Clemmens et al. 1994).

Local versus Centralized Control: An important issue for water-level feedback on canals with many pools is whether to use local, feedback controllers (e.g., ELFLO or BIVAL) or more centralized controllers. A series of local water-level feedback controllers (downstream or upstream) on canals with many pools can perform poorly due to the interaction among pools. Schuurmans (1992) proposed decoupling as a means of improving performance of these controllers. Local downstream control schemes are typically not set up to handle simultaneous routing of demand changes, which is a more centralized function. Centralized controllers are very complex and appear to the operator as a black box. There is a strong reluctance to actually implement some of these controllers because of their complexity and because they are not intuitive.

Lessons Learned: A clear lesson from dynamic regulation, CAP, and gate stroking is that successful open-loop canal control can be developed by understanding the canal pool volume relationships under steady-state conditions. These methods require a "change and wait" approach – that is, make a change, wait and see what happens, then adjust. These methods are not responsive to unforeseen changes, errors in flow setting, etc. Feedback control can account for these difficulties. However, past attempts at feedback control have been not been particularly successful. One of the main difficulties in the application of feedback control has been a lack of understanding of how canal properties influence the control system. We can apply to feedback control some of the lessons learned from successful open-loop control methods.

Feedback control methods for downstream control of canals generally use deviations from desired or target water levels as the indicator that a correction needs to be made. The idea is that if the water level is at the target value, then the flow through check and offtake gates will be correct. If the canal is at steady state at the target water level, a change in water level can only occur if the inflow to the canal does not match the outflow. The idea of feedback control is to correct the inflow to match the outflow, with water level deviation as the indicator of success. The relationship between rate of change of water level and the inflow - outflow mismatch is related to the pool volume relationships. This can be expressed mathematically as

$$Q_{in} - Q_{out} = \frac{\Delta V}{\Delta t} = A\frac{\Delta h}{\Delta t} \qquad \textbf{(1)}$$

where Q = flow rate, V = volume, h = water surface elevation, t = time, and A = surface area of the portion of the canal pool that is under backwater. This equation is only appropriate when there is a relationship between water level at the downstream end of the pool and pool volume. This occurs when the pool is under backwater. For pools entirely or partially under backwater, the backwater surface area, A, changes slowly with discharge and with water depth. Thus, A can be assumed constant over a range of conditions. If the pool is at normal depth or below, then A changes rather rapidly with depth and discharge and the relationship defined in equation 1 is not very useful. This change of conditions when a pool is no longer under backwater is probably why ELFLO systems were shut off at high flow rates, that is, normal depth was approached and the controller tuning parameters were no longer appropriate.

Integrator-Delay Model: Schuurmans et al. (1995) propose an approximate model of canal response (integrator-delay model) based on two simple canal pool properties: the disturbance wave time delay and the water surface area of the pool portion influenced by backwater from the control structure. A canal pool can

be thought of as having two parts: a part under normal depth where waves are transmitted and a part under backwater that essentially acts like a reservoir (Figure 6). A step inflow change results in a delay as the wave travels along the uniform-flow section followed by a constant rate of change of backwater pool volume, and thus level. Assuming that the backwater area is constant for a given set-point depth, the rate of rise of the water level is then related to the mismatch in flow rate, as in equation 1. These two properties, delay time and backwater pool area, can be computed from their equations, determined from observation of canal properties, or computed with unsteady-flow simulation. Delay times can also be determined from the kinematic wave equation for the uniform-flow portion. These two integrator-delay model properties can be used to develop feedback controllers. For pools affected by backwater over their entire length, the above-described model assumes no time delays. In this case, the backwater pool area is the only feedback controller design variable. However, reflection waves may be present for these types of pools, which must be handled with filters. Design of filters requires knowledge of pool frequency response. Most pools have either a significant time delay or reflection waves, but seldom will they have both. The integrator-delay model has been shown to accurately describe canal pool properties for controller design by Schuurmans et al. (1999) and Clemmens et al. (1997).

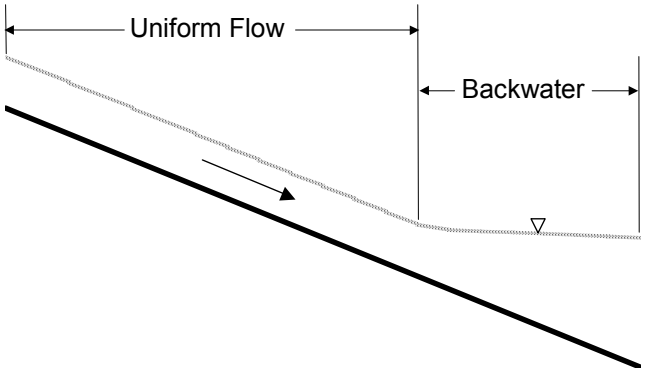

Figure 6. Canal pool for Integrator-delay model.

Decoupling of canal pools: The interaction between canal pools can be minimized by separating canal pool hydraulic response from gate hydraulic response. This can be accomplished by designing the feedback and feedforward control algorithms to determine needed changes in flow at each check structure. A separate flow-control function is used to maintain flow between pools, thus effectively removing hydraulic interactions, or decoupling. This has the added advantage that feedback, feedforward and manual control can be combined since they all send the same type of signal to the flow controller. Most of the more advance control algorithms assume flow-rate control at these structures.

NEW CANAL AUTOMATION SYSTEMS – WHAT DOES THE FUTURE HOLD?

Studies of canal automation potential have demonstrated that pool properties limit what can be accomplished with feedback alone (Strelkoff et al. 1998). Routing of major flow changes is still required for most canal systems. Only minor flow changes and corrections due to errors can be effectively handled with feedback alone. In one study, feedback control could only handle flow changes representing 5% of capacity without unacceptable deviations in water levels (Clemmens et al., 1997). Applications of open-loop routing of flow changes have been successful, but without feedback control they overly constrain the flexibility needed for modern operations. This suggests that effective canal automation strategies must include both open-loop routing of known or scheduled flow changes and closed-loop feedback control of downstream water levels. A centralized control strategy is necessary to make canal automation truly effective.

SCADA systems are becoming more and more popular among irrigation districts because of their advantages in controlling large canals. With the improvements in personal computers (PCs), commercial grade SCADA systems are now available for PCs. Further, Remote Terminal Units (RTUs) and other electronic devices have become less and less expensive. This has opened up SCADA technology to smaller irrigation districts and potentially to smaller canals. SCADA control of canal networks may become practical in the near future.

USWCL Control Scheme: The staff at the U.S. Water Conservation Laboratory (USWCL) has developed a control scheme that is based on the integration of automatic controls with existing, manual operations. It allows one to take a more systematic approach to canal automation. It uses the simple volume-time delay relationships discussed above to develop controller components and attempts to maintain simplicity and understandability. It has three components:

1. open-loop control of flow rate and volume based on hydraulic routing,
2. closed-loop control of (distant) downstream water levels, and
3. local closed-loop control of check-structure flow rate based on 1 and 2.

Routing of flow changes is required because many canals have insufficient storage to provide adequate control with downstream feedback control alone. Feedback control of downstream water levels is necessary, even when demand changes are made by routing, since flow rates set at check structures always contain errors and since routing is never perfect. Check structure flow rate control allows feedback, feedforward and manual controls to be easily combined. The automatic control does not have to be shut off to make manual changes. The general scheme for one pool is shown in Figure 7.

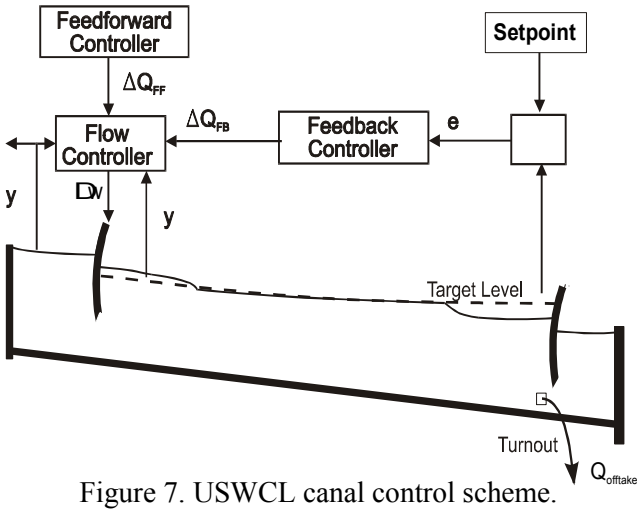

Figure 7. USWCL canal control scheme.

Routing of Scheduled Flow Changes: Bautista and Clemmens (1999) developed a simplified routing scheme based on required volume changes and kinematic and dynamic wave velocities. The approach is outlined in Figure 8. It starts with determining the change in volume required, ΔV, to go from the initial steady flow rate, Qi, to the final steady flow rate, Qf, resulting from a requested flow change, Δq. Next the travel time for a wave to go from the upstream end to the downstream end of the pool is determined, Δτ. The initial change in flow rate upstream, ΔQ(t1), is computed as the needed change in volume, ΔV, divided by the travel time, Δτ. This change in flow rate may be different from the requested flow change. In this case, a second flow change, ΔQ(t2), is made upstream so that inflow and outflow balance. The assumption behind this method is that if the correct volume is applied and inflow matches outflow, the pool will eventually stabilize itself with the correct volume and flow rates. Simulation studies performed suggest that this is the case.

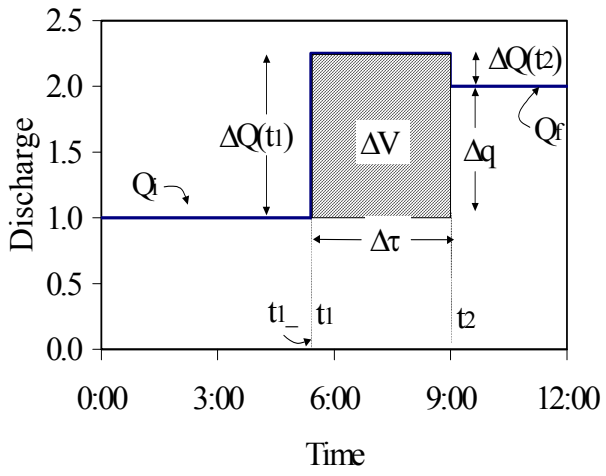

Figure 8. Simple open-loop routing method.

For multiple pools, the volumes and delay times are summed from downstream to upstream. The cumulative volume is divided by the cumulative delay time to arrive at the flow change for each structure. If multiple flow changes are desired, flow changes are computed for each change. These incremental changes are then overlapped. In order to implement this method, pool volumes must be determined for various combinations of 1) flow rate, 2) downstream set-point level, and 3) Manning n, as shown in Figure 4. Volume as a function of these variables can be determined from computed backwater curves and canal geometry, or from simulation with steady hydraulic models (e.g., HEC-RAS). Delay times are computed from the kinematic wave equations for the pool portion under uniform flow and ½ the dynamic wave travel time for the pool portion that is under backwater.

Feedback Control of Downstream Water Levels: Clemmens and Schuurmans (1999) proposed a new downstream-water-level-control method where a variety of controllers with different levels of complexity can be designed, ranging from a series of simple proportional-integral controllers to a fully centralized controller. The design procedures are based on the simple properties of the integrator-delay model. Simulation studies have shown that these controllers can be very effective (Clemmens et al. 1997, Bautista and Clemmens 1999, and Clemmens and Wahlin 1999).

Implementation: The wide-spread implementation of canal automation depends upon it being integrated with the overall operation of the district. Several research projects are ongoing to provide the needed integration. A pilot project on canal automation was initiated by the Salt River Project (SRP). Under this pilot project, the USWCL canal automation scheme will be tested in real time. During Phase I, completed in March 1997, simulation tests were run to determine whether the automatic control system (Figure 7) could handle typical SRP control situations on the upper Arizona Canal (Clemmens et al. 1997). An example of the performance of these controllers is shown in Figure 9 for one of their tests. This test is typical of their daily changes,

where multiple flow changes were routed through the system. Water levels stayed well within acceptable limits. Routed flow changes can be seen as square waves, with feedback control actions shown as deviations from these square waves. This phase was very successful and the control system is now being installed on SRP's SCADA system during Phase II, scheduled for completion in April 2000. Real time testing has been postponed pending SRP's conversion to a PC-based SCADA system.

A cooperative research and development agreement was established between the U.S. Water Conservation Laboratory and Automata, Inc. to jointly develop a canal automation product line based on the USWCL control scheme. The intent is to develop a system that is "*plug-and-play*" so that canal automation systems can be purchased off-the-shelf without the need for extensive research and development that has been common for most automation applications. Initial testing of Automata's system is being done on MSIDD's WM canal. Strand et al. (1999) present the details of this system. The system is being implemented with a PC-based commercial SCADA package called FIX Dynamics, developed by Intellution Inc., Norwoood, MA, USA. Available PC-based SCADA packages are set up to handle local feedback control only. No structure is provided for centralized logic. The USWCL control system program was written in C++ to run parallel with FIX in the Windows NT environment. The control program can access FIX data, send commands to FIX to move gates or collect data, and special windows can be imbedded within FIX display windows to provide real-time manual control functions. Radios are used to communicate from the central computer base station to RTUs located at each check structure. Automata's RTUs were programmed to retrieve water levels, gate positions, battery voltage, etc. and to change gate position. A new gate position sensor was developed to provide both absolute position and precise differential position. With the new gate position sensor, driver, and firmware, gate positions can be adjusted to within 1 mm, and possibly to within ½ mm with additional firmware, if needed.

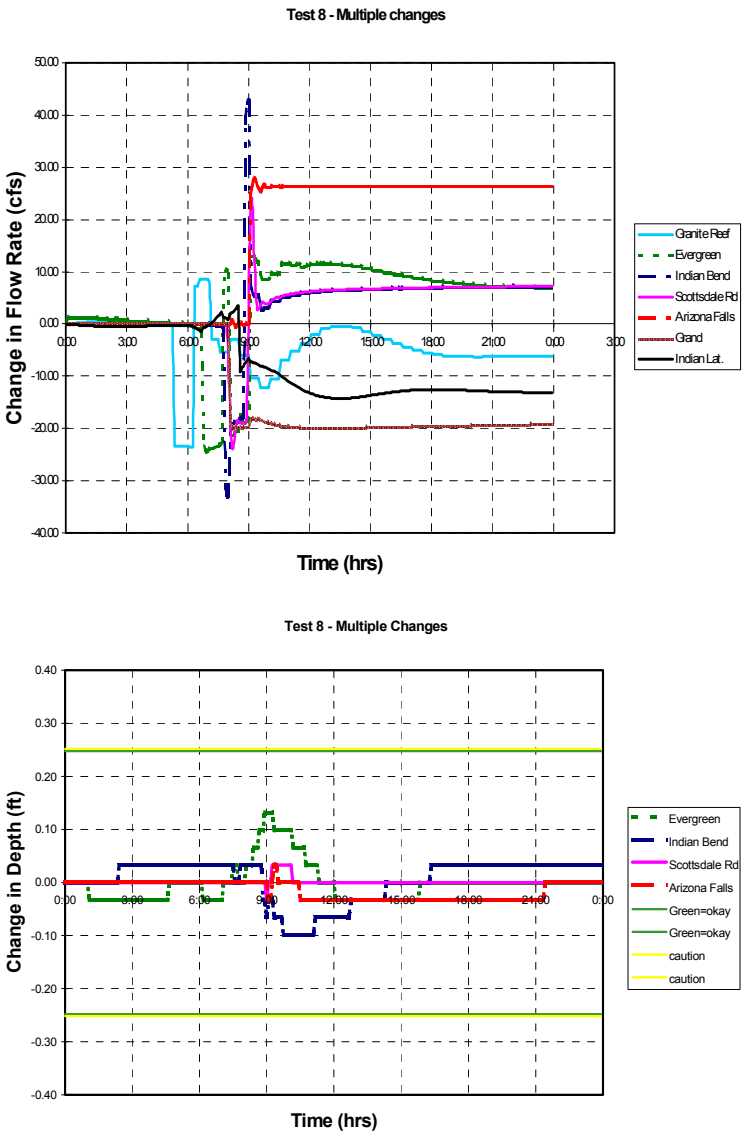

Figure 9. Simulation results for test 8 for the Salt River Project's upper Arizona Canal.

An event queue is used to keep track of both the feedforward routing of scheduled flow (demand) changes and the feedback cycles for both downstream water level and check gate flow control. This later function may be eventually moved to the check gate RTUs. In addition to routing flow changes, the system is being programmed to handle the routing of volume changes needed to alter the downstream water level setpoint. This routing of setpoint changes is an effective method for startup of the feedback routines. If all canal pools are far from their setpoint values at startup, the feedback control signals could be extreme and the system could become unstable. In the proposed startup procedures, the initial water levels are used as the starting setpoints and they are scheduled to change gradually over some reasonable period of time.

This system was made operational on the WM canal in October 1999 for initial testing. Results for one of these tests are shown in Figure 10 for the first 5 pools (MW-0 is the headgate and no water was flowing past WM-5). Not all the features of the control system were included at this time, resulting in slow movement of the setpoint to the target depth (the lower of the two lines on WM-1 through WM-5). (And we discovered an error in our estimated delay times). Some refinements are currently being programmed and additional testing is planned for the 2000 irrigation season.

The intent of this control system is easy adaption to any canal. Some engineering work is required to define canal pool and structure properties and to develop controller constants, but this should be minimal. Once the programming is completed, a user should be able to define a particular canal and implement this automation system with a minimum of customization. If possible, we will implement the system from MSIDD on SRP's Arizona Canal. If these two efforts are successful, canal automation may quickly become a useful and available tool for improvement of irrigation water delivery system operations.

Figure 10. Output screen from application of USWCL Canal Automation Scheme on MSIDD's WM canal, October 19, 1999.

SUMMARY

The key features of canal pools have been identified. These are

- for open loop routing:
  - change in pool volume for a change in flow or target level
  - delay times: kinematic wave time for normal depth part and ½ dynamic wave time for backwater part
- for closed-loop feedback:
  - pool backwater surface area.
  - delay times for normal depth part of pools: kinematic wave time or from analysis

These canal pool features have been used to develop effective methods for feedforward routing of scheduled flow and volume changes and for feedback control of downstream water levels. These control components have been extensively tested with simulation and have shown good performance, subject to the physical limitations imposed by the canal properties.

A canal automation system is under development that utilizes these control components and integrates them into an effective control system. Once developed, this control system should be easily applied to a wide variety of irrigation canals with minimal effort.

REFERENCES

Bautista, E., Clemmens, A.J. and Strelkoff, T.S. (1997) Comparison of numerical procedures for gate stroking. *J. Irrigation and Drainage Engineering* 123(2):129-136.

Bautista, E. and Clemmens, A. J. (1999) Computerized anticipatory control of irrigation delivery systems. p. 359-373 In *Proc. USCID Workshop on Modernization of Irrigation Water Delivery Systems*, Scottsdale, AZ. Oct. 17-21, 1999.

Bos, M.G. (1997) Performance indicators for irrigation and drainage. *Irrig. and Drain. Syst*. 11(2):119-137.

Clemmens, A.J., Bautista, E. and Strand, R.J. (1997) *Canal Automation Pilot Project*. Phase I Report prepared for the Salt River Project. WCL Report #22, U.S. Water Cons. Lab., Phx, AZ.

Clemmens, A. J., Dedrick, A. R., Clyma, W., and Ware, R. E. (2000) MSIDD on-farm system performance. *Irrigation and Drainage Systems* . (In press).

Clemmens, A. J. and Schuurmans, J. (1999) A class of optimal feedback canal controllers, including proportional-integral as a limiting case. p. 423-437 In *Proc. USCID Workshop on Modernization of Irrigation Water Delivery Systems*, Scottsdale, AZ. Oct. 17-21, 1999.

Clemmens, A.J., Sloan, G. and Schuurmans, J. (1994) Canal control needs: example. *J. Irrigation and Drainage Engineering* 120:6:1067-1085.

Clemmens, A. J. and Wahlin, B. T. (1999) Performance of various proportional-integral feedback canal controllers for ASCE test cases. p. 501-516 In *Proc. USCID Workshop on Modernization of Irrigation Water Delivery Systems*, Scottsdale, AZ. Oct. 17-21, 1999.

Favley, H.T. and Lunig, P.C. (1979) *Gate Stroking*. Report REC-ERC 79-7, U.S. Bureau of Reclamation, Denver, CO.

Johnston, W.R. and Robertson, J.B. (ed.) (1990) *Management, Operation and Maintenance of Irrigation and Drainage Systems*. Manual #57. ASCE, Reston, VI

Lamacq, S. (1997) *Coordination between Water Supply and Demands in Irrigated Systems. Scenarios, Systems and People*. PhD thesis, ENGREF, Montpelier, France.

Malaterre, P.O, Rogers, D.C. and Schuurmans, J. (1998) Classification of Canal Control Algorithms, *J. Irrigation and Drainage Engineering*, 124(1):3-10.

Palmer, J.D., Clemmens, A.J., Dedrick, A.R., Replogle, J.A. and Clyma, W. (1991) Delivery system performance case study: Wellton-Mohawk Irrigation and Drainage District, USA *Irrigation and Drainage Systems* 5:89-109.

Rogers, D.C. , Ehler, D.G., Falver, H.T., Serfozo, E.A., Voorheis, P., Johansen, , R.P., Arrington, R.M., Rossi, L.J. (1995) *Canal Systems Automation Manual*. Volume 2. U.S. Bureau of Reclamation, Denver, CO.

Rogers, D.C. and Goussard, J. (1998) Canal Control Algorithms Currently in Use. *J. Irrigation and Drainage Engineering*, 124(1):11-15.

Schuurmans, J. (1992) *Controller design for a regional downstream controlled canal*. Report No. A668, Lab. For Measurement and Control, Delft Univ. of Technology. Delft, The Netherlands.

Schuurmans, J., Bosgra, O.H., and Brouwer, R. (1995) Open-channel flow model for controller design. *Applied Mathematical Modeling*. 19: 525-530.

Schuurmans, J., Clemmens, A. J., Dijkstra, S., Ahmed, R. H., Bosgra, O. H., and Brouwer, R. (1999) Modeling of irrigation and drainage canals for control purposes. *J. Irrigation and Drainage Engineering* 125(6):338-344.

Strand, R. J., Clemmens, A. J., Feuer, L., and Sloan, G. (1999) Application of PC-based canal automation system at the Maricopa-Stanfield Irrigation and Drainage District. p. 327-341 In *Proc. USCID Workshop on Modernization of Irrigation Water Delivery Systems*, Scottsdale, AZ. Oct. 17-21, 1999.

Strelkoff, T.S., Deltour, J.L., Burt, C.M., Clemmens, A.J. and Baume, J. P. (1998) Influence of canal geometry and dynamics on controllability. *J. Irrigation and Drainage Engineering*, 124(1):16-22.

Wiley, E.B. (1969) Control of transient free-surface flow. *J. Hydraulics Div., ASCE*, 95(HYD1):347-361.

Published in Irrigation Australia 2000, Melbourne, Australia, May, 2000– pg 31-40.